Durham E-Theses

An investigation of the plasma polymerisation of organic compounds and its relationship with surface photopolyherisation

Ward, Richard James

A thesis entitled

AN INVESTIGATION OF THE PLASMA
POLYMERISATION OF ORGANIC COMPOUNDS
AND ITS RELATIONSHIP WITH
SURFACE PHOTOPOLYMERISATION

by

Richard James Ward, B.Sc. Hons. (Dunelm)

A candidate for the degree of Doctor of Philosophy

Graduate Society,
University of Durham

September   1989

i

The work described in this thesis was carried out at the university of Durham between October 1986 and September 1989. It is the original work of the author, except where acknowledged by reference, and has not been submitted for any other degree.

Some of the work described in this thesis has formed all or part of the following publications :

"Surface Photopolymerisation as a Model for Plasma Polymerisation"

H.S.Munro and R.J.Ward

Proc 9th Int. Symp. Plasma Chem., (1989)

"The Synthesis and XPS Characterisation of Iodine Containing Plasma Polymers"

H.S.Munro, R.J.Ward and E.Khor

J. Polym. Sci., Polym. Chem. Ed., In press, 1989

ABSTRACT

Plasma polymers of perfluorobenzene (PFB), perfluorotoluene (PFT), perfluorocyclohexane, perfluorocyclohexene, benzene, naphthalene and N-vinyl pyrrolidinone (NVP) were prepared and analysed by XPS and SIMS. The analysis suggested that polymers derived from perfluoroaromatic monomers consisted of aromatic and other cyclic structures linked by very short alkyl chains, while those derived from perfluorocyclohexane and perfluorocyclohexene were much more aliphatic in nature and contained fewer aromatic and other ring structures. PFB, PFT and NVP were found to produce surface photopolymers, similar to their plasma polymers, suggesting that the polymerisation proceeds via an excited state mechanism. The photopolymerisation of NVP was found to be either a one or two photon process depending on the conditions used, and an approximate lifetime was found for a polymerising gas phase species. Plasma mass spectroscopy also suggested that neutral species were largely responsible for the plasma polymerisation of PFB, but that ionic species were important in the plasma polymerisation of benzene. Considerable gas phase interaction was observed in a mixed benzene/PFB plasma. Plasma polymers containing a high concentration of -COOH were formed from a variety of carboxylic acids, by using low power and high flow rate conditions, but methyl methacrylate and acetic acid did not retain their carboxylate groups under similar conditions. Iodine was incorporated into a plasma polymer by copolymerising benzene and iodobenzene, but not at a sufficiently high concentration to prevent oxygen plasma etching. Plasma polymerisation of allyl iodide produced a polymer containing I_3^- ions.

ACKNOWLEDGEMENTS

CONTENTS

Appendix

CHAPTER 1

AN INTRODUCTION TO PLASMA POLYMERISATION AND SURFACE PHOTOPOLYMERISATION

1.1 PLASMAS

1.1.1 Introduction

A plasma is defined as a wholly or partially ionised gas, and is sometimes referred to as the fourth state of matter. A plasma generally consists of molecules, atoms and ions in both ground and excited states (including metastable states), and electrons, such that the concentration of positively and negatively charged species results in close to overall electrical neutrality. Plasmas occur in nature and in the laboratory in many different forms which can be characterised by their electron density and their average electron energy[1] (see figure 1.1). Examples of naturally occurring plasmas include stars, such as the sun, interplanetary space and the aurora borealis. In the laboratory plasmas may be produced by electrical discharges, electron beams or lasers.

Plasmas can be divided into two types known as hot or cold plasmas. In a hot, or equilibrium, plasma the electron temperature is roughly equal to the gas temperature, which must be very high in order for this to occur. This class of plasma can be used in metallurgy for reducing metallic ores and slag to the base metal[2] and in the analysis of materials by ICP OES (inductively coupled plasma optical emission spectrophotometry) or ICPMS[3] (inductively coupled plasma mass spectroscopy). In the high temperature of the plasma most materials are reduced to their constituent atoms, whose optical emission or mass spectra are taken in order to give an elemental analysis. Hot plasmas are also used in attempts to produce controlled nuclear fusion for use as a power source.

PLASMAS FOUND IN NATURE AND IN THE LABORATORY
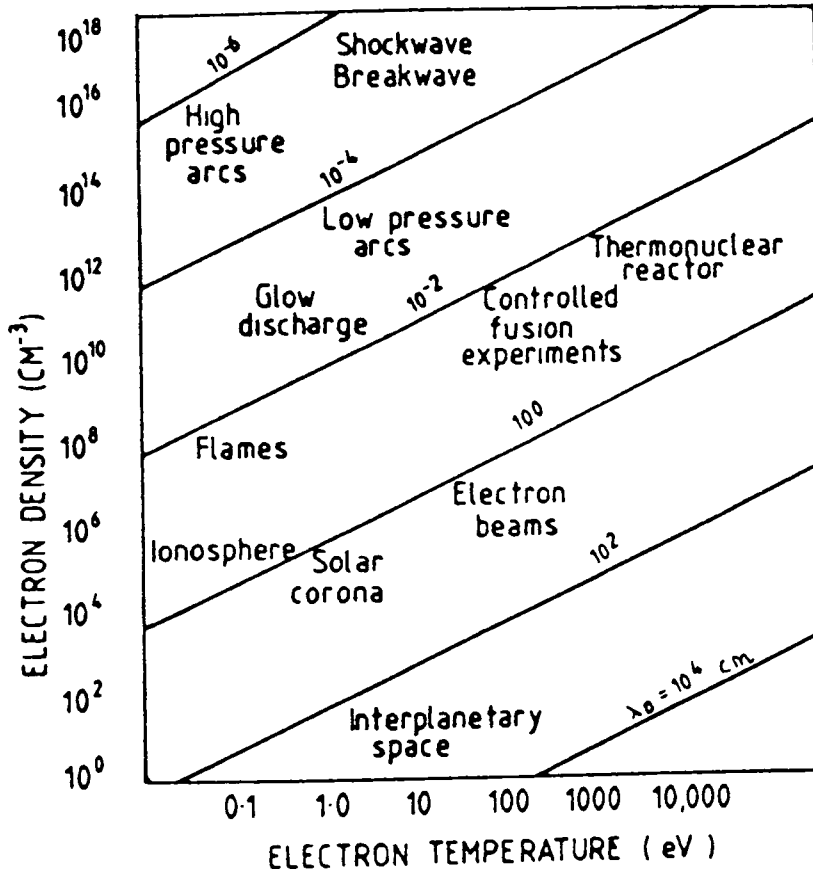
Figure 1.1 Characterisation of plasmas by their electron temperatures and electron densities

Cold, or non-equilibrium, plasmas generally have electron temperatures much higher than the temperature of the ions and molecules in the gas, typically by about 2 orders of magnitude. Cold plasmas can be formed in the laboratory by means of a gas discharge. Early investigations of gas discharges were carried out in the 18th and 19th centuries. The discovery of the induction coil by Ruhmkorff[4] led to investigations of cathode rays emitted from discharge tubes by Crookes (1879) and others.

3

In 1897 Thomson showed that cathode rays were consisted of electrons, and by the early 1900's it had been established by Townsend[5] and others that conductivity in electrical discharges resulted from ionisation in gas discharges by collision. The word "plasma" was coined by Langmuir in 1928 to denote the state of ionised gases formed in an electric discharge[6]. Cold plasmas often produce visible emission from excited species in the plasma, causing them to be sometimes known as glow discharges.

Cold plasmas have found use chemically in several areas:

(i) Synthetic Organic/Organometallic Chemistry

The energies available in a plasma are considerably greater than in conventional chemical reactions[7], and so reaction pathways not normally available can be exploited. All organic compounds undergo some reaction in a glow discharge but the product mixture may be complex, and percentage yields may be low. Best results are obtained by avoiding high electron energies and elevated temperatures, which reduces the damage done to the molecules. Most of the work in this area has been done by Suhr and coworkers[8].

(ii) Surface Modification

This can be achieved in a number of ways:

(a) Surface grafting[9]. A polymer is exposed to a plasma in order to create reactive sites which can be used to initiate a conventional free radical polymerisation on the surface. For example the wettability[10] and flame retardancy[11]of fibres can be improved by this method.

4

(b) Inert plasmas, such as argon, may be used to cross-link polymer surfaces by direct and radiative energy transfer. This can be used for example to improve the adhesive bonding of polymers[12]

(c) Direct chemical modification of surfaces may be achieved using more reactive gases. For example an oxygen plasma may be used to increase the wettability of a surface[13], while CF_4 plasmas can make a surface hydrophobic[14]. Ammonia plasmas may be used to incorporate nitrogen into a surface[15].

(d) Etching of polymeric materials can be achieved by using oxygen or halocarbon plasmas under more severe conditions, or for longer periods of time. This is of particular use in the removal of resist materials in the electronics industry[16].

(iii) Polymerisation and Film Deposition

(a) Plasma Polymerisation. Polymer formation occurs when almost any organic compound is subjected to a glow discharge[17]. The polymer is generally different from any conventional polymer and forms as a thin film on any surface in contact with the plasma. It is with plasma polymerisation that most of the work in this thesis is concerned.

(b) Inorganic materials such as silicon[18] and metals[19] may be deposited as thin films from organosilicon or organometallic plasmas. This is sometimes called plasma induced chemical vapour deposition, and is of use particularly in the electronics industry.

(c) A plasma may be used to initiate a conventional polymerisation reaction in a solid or liquid monomer which is

5

either in contact with the plasma or with reactive species generated by it[20]. This is known as plasma induced polymerisation.

1.1.2 Fundamental Aspects of Plasmas

For a plasma to exhibit approximate electrical neutrality the dimensions of the discharged gas must be greater than the Debye length[1] (λ_D) which defines the distance over which a charge imbalance may exist. This is given in equation 1.1.

$$\lambda_D = \left(\frac{E_0 kT_e}{ne^2} \right)^{1/2} \qquad\qquad 1.1$$

where E_0 = the permittivity of free space
k = the Boltzmann constant
T_e = the electron temperature
n = the electron density
and e = the charge on the electron

For a plasma to ignite an initial ionisation event must occur, either naturally from background radiation such as cosmic rays, or artificially, e.g. from a spark generator, or through dielectric breakdown of the gas if the applied electric field is sufficiently strong. Electrons produced from this ionisation are accelerated by the applied electric field and collide with other molecules in either elastic or inelastic collisions. Inelastic collisions by electrons with high energies causes further ionisation and produces a chain reaction which sustains the plasma. If the energy of the electron is too low to cause ionisation of the molecule, rotational, vibrational or electronic excitation may occur. The amount of energy electrons possess depends on their mean free path[21]. If the pressure of the gas is

too high the mean free path is too low and electrons have not

accumulated enough energy to cause ionisation before a collision.

If the pressure is too low the mean free path is too long and gas

collisions are unimportant. This results in a typical working

pressure range for plasma chemistry of 0.05-10 torr.

The average velocity ($\bar{c}$) of an electron between collisions

is given by equation 1.2[22].

$$\bar{c} = \left(\frac{Me^2E\lambda}{m^3} \right)^{1/4} \qquad\qquad 1.2$$

where M = the mass of the heavier particle
       e = the electron charge
       E = the electric field
       λ = the mean free path
  and m = the mass of the electron

Expressions describing the electron energy distribution in

terms of energy input, discharge dimensions and gas pressure lead

to a Maxwellian distribution[23] of electron energies as shown in

figure 1.2. Such numerical solutions are only possible for simple

systems, but electron energy distributions can be analysed

directly by probe measurements[24] or by direct electron

sampling[25]. The average electron energies in most plasmas are

well below the ionisation energies of most molecules, which are

generally of the order of about 10 eV. Since only a few electrons

possess sufficient energy to cause ionisation, the ion

concentration is low (typically 10^{-4} to 10^{-7} cm^{-3}), with neutral

species predominating in a non-equilibrium plasma. Much of the

chemistry of a plasma may therefore be connected not with

ionisation, but with excitation, which requires electrons of

lower energy. Typical bond energies of organic compounds are in

the range of 2-8 eV (see table 1.1). Since electrons in a plasma
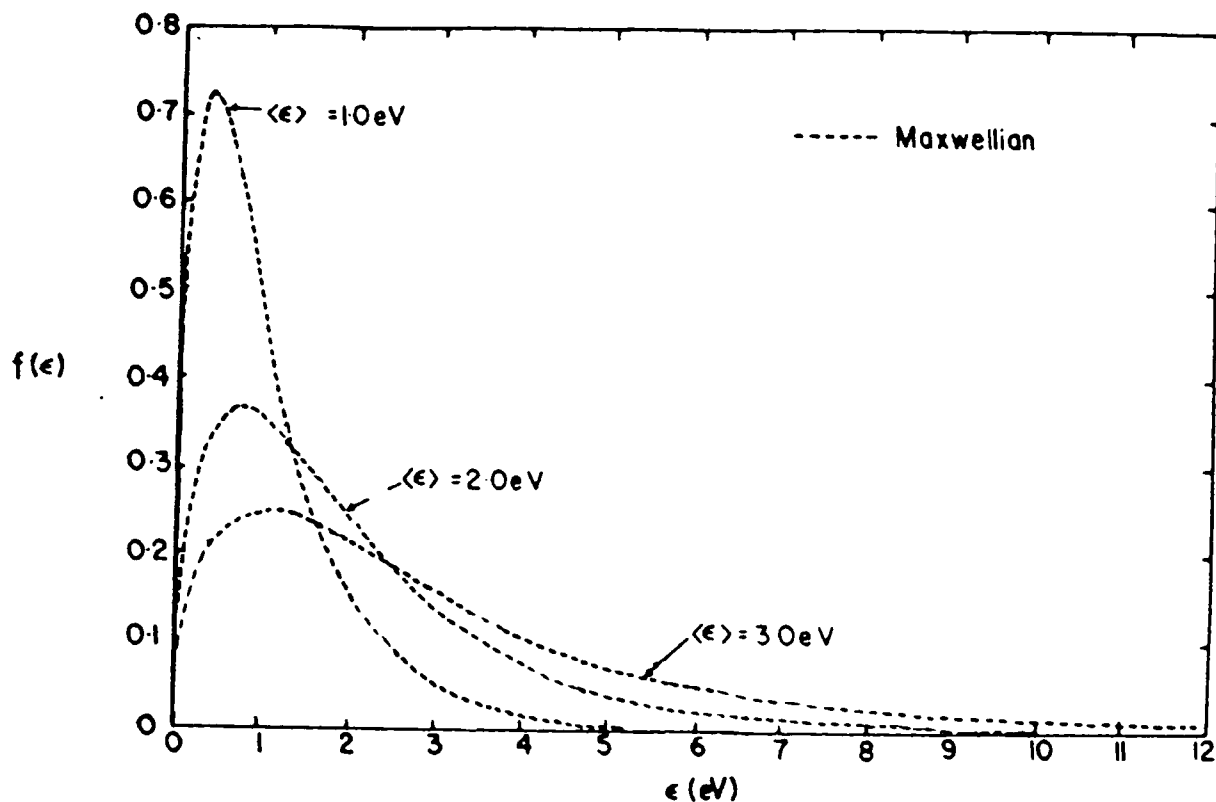
Figure 1.2 Maxwellian energy distributions of electrons in an inert gas

Table 1.1 Some typical bond energies for organic compounds (eV)

C-H	4.3	C=O	8.0
C-F	4.4	C-N	2.9
C-C	3.4	C=C	6.1

may possess energies of up to 20 eV or more, there is sufficient energy in a plasma to break any chemical bond.

De-excitation of various excited species results in the emission of electromagnetic radiation at wavelengths ranging from the microwave to the vacuum ultra-violet region of the spectrum. The emission in the visible part of the spectrum gives a plasma

its characteristically coloured glow. The most intense emission is often in the UV/vacuum UV region[26], which may cause additional excitation or ionisation in the plasma or in substrates, such as polymers, in contact with the plasma.

The reactive species in a plasma resulting from ionisation, fragmentation and excitation processes caused by electron impact (and to a lesser extent photon absorption) include positive and negative ions, neutral species, atoms, metastables and free radicals, in ground or excited states. This means that the number of reactions that may occur is very large, even for a simple plasma such as oxygen[1] (see table 1.2). In a plasma of an organic compound the variety of reactions which may occur is much greater still and may include elimination[27], isomerisation[28], dimerisation[29] and oligomerisation[30] reactions, as well as polymer formation on any surfaces in contact with the plasma.

1.1.3 Plasma Techniques

In general there are three main areas in which the conditions of a glow discharge can be varied; the electrical power source, the coupling mechanism of the electrical power to the plasma, and what can loosely be termed the plasma environment. This is illustrated schematically in figure 1.3.

The electrical power supply may either be D.C. or A.C. with A.C. frequencies ranging from 50 Hz through RF frequencies (13.56 MHz is commonly used) up to microwave frequencies. The effect of frequency on the deposition rate of an ethane plasma has shown that there are a number of different effects related to the

Table 1.2 Elementary Reactions Occurring in an Oxygen Plasma

I Ionization

1. $e + O_2 \rightarrow O_2^+ + 2e$
2. $e + O \rightarrow O^+ + 2e$

II Dissociative ionization

3. $e + O_2 \rightarrow O^+ + O + 2e$

III Dissociative attachment

4. $e + O_2 \rightarrow O^- + O$
5. $e + O_2 \rightarrow O^- + O^+ + e$

IV Dissociation

6. $e + O_2 \rightarrow 2O + e$

V Metastable formation

7. $e + O_2 \rightarrow O_2(^1\Delta_g) + e$

VI Charge transfer

8. $O^+ + O_2 \rightarrow O_2^+ + O$
9. $O_2^+ + O \rightarrow O^+ + O_2$
10. $O_2^+ + O_2 \rightarrow O_2^+ + O$
11. $O_2^+ + 2O_2 \rightarrow O_4^+ + O_2$
12. $O^- + O_2 \rightarrow O_2^- + O$
13. $O^- + O_3 \rightarrow O_3^- + O$
14. $O^- + 2O_2 \rightarrow O_4^- + O_2$
15. $O_2^- + O \rightarrow O^- + O_2$
16. $O_2^- + O_2 \rightarrow O_2^- + O$
17. $O_2^- + O_3 \rightarrow O_3^- + O_2$
18. $O_2^- + 2O_2 \rightarrow O_4^- + O_2$
19. $O_3^- + O_2 \rightarrow O_2^- + O_3$
20. $O_4^- + O \rightarrow O_2^- + O_2$
21. $O_4^+ + O_2 \rightarrow O_2^+ + 2O_2$

VII Detachment

22. $O^- + O \rightarrow O_2 + e$
23. $O^- + O_2 \rightarrow O + O_2 + e$
24. $O^- + O_2(^1\Delta_g) \rightarrow O_3 + e$
25. $O_2^- + O \rightarrow O_3 + e$
26. $O_2^- + O_2 \rightarrow 2O_2 + e$
27. $O_2^- + O_2(^1\Delta_g) \rightarrow 2O_2 + e$

VIII Electron-ion recombination

28. $$e + \begin{Bmatrix} O^+ \\ O_2^+ \\ O_3^+ \\ O_4^+ \end{Bmatrix} \rightarrow \begin{Bmatrix} O \\ 2O \\ O+O_2 \\ 2O_2 \end{Bmatrix}$$

IX Ion-ion recombination

29. $$\begin{Bmatrix} O^- \\ O_2^- \\ O_3^- \\ O_4^- \end{Bmatrix} + \begin{Bmatrix} O^+ \\ O_2^+ \\ O_3^+ \\ O_4^+ \end{Bmatrix} \rightarrow \begin{Bmatrix} O \\ O_2 \end{Bmatrix}$$

X Atom recombination

30. $2O + O_2 \rightarrow 2O_2$
31. $3O + O \rightarrow O_2$
32. $O + O_2 \rightarrow \tfrac{1}{2}O_3$
33. $O + O_3 \rightarrow 2O_2$
34. $O \xrightarrow{\text{wall}} \tfrac{1}{2}O_2$

ELECTRICAL POWER – COUPLING MECHANISM – PLASMA ENVIRONMENT

```
 DC    ⎫              ⎫   CURRENT
 AC    ⎬  RESISTIVE   ⎬   PRESSURE
 RF    ⎭  CAPACITIVE  ⎭   GAS FLOW AND TEMPERATURE
MICROWAVE  INDUCTIVE      REACTANT PHASES
                          ELECTRIC AND MAGNETIC
                                    FIELDS
```
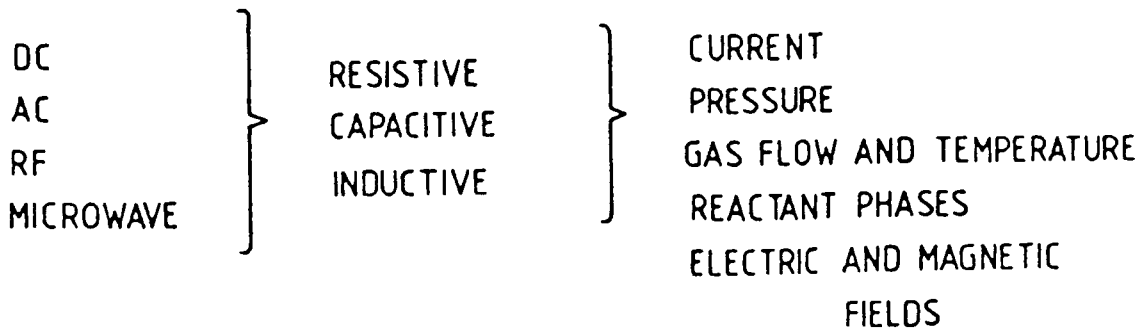
Figure 1.3 Elements of a glow discharge experiment

frequency used[31] (see the introduction to chapter 6 for a fuller description).

The coupling mechanism may be either direct (resistive) or indirect. For direct coupling the electrodes are placed inside the plasma chamber, and the discharge initiated between them. Indirect coupling may be either capacitive, in which the electrodes are placed externally to the chamber, or inductive, in which a copper coil is wound around the outside of the chamber. Direct coupling produces the highest polymer deposition rates, but problems may be caused by polymer deposition on the electrodes. Indirect coupling eliminates this problem, but may only be used at A.C. frequencies of greater than 1 MHz[8]. Microwave plasmas may also be excited inductively using tuned cavities.

The operating pressures for typical plasmas vary from 0.05 to 10 torr for reasons stated earlier, although higher pressure plasmas can be sustained by using very high powers. Powers used

may vary from 0.1 watts up to a few kilowatts, but are normally in the range of 1-150 watts. With powers of less than a watt plasmas may be difficult to sustain, but a low average power level can be achieved by using pulsed RF power. If the power level is very high, or if the power is concentrated into a small volume, the gas temperature may become very high and some form of cooling system may be necessary. Cooling is often necessary for the electrodes in D.C. discharges and for microwave cavities.

Electrical or magnetic fields are sometimes applied to perturb a plasma (possible because of the presence of charged species). This may be used for example to investigate the role played by ions in plasma polymerisation by comparing the polymer formation on a biased electrode with that on a floating substrate[32].

1.1.4 Plasma Diagnostics

There are a number of techniques available which can be used to obtain direct information concerning species present in a plasma. As mentioned previously, probe methods can be used to obtain electron energy distributions[24]. This is an intrusive technique, since the probe is inserted directly into the plasma, and so might perturb it.

Optical emission spectrophotometry (OES) is an example of a technique which is non-intrusive and so does not affect the plasma[33]. The infra-red, visible and ultra-violet radiation emitted by a plasma is characteristic of individual species within the plasma, and can be used to identify the presence of

those particular species[34]. While this is useful in showing the presence of some species it cannot give a complete picture of the composition of a plasma, since only excited states which relax by photon emission can be monitored. Also, it is only semi-quantitative since the intensity of emission from a species is not directly proportional to its concentration. This arises from problems in determining probabilities for excitation and emission under a particular mode of excitation for the species under examination.

Laser induced fluorescence (LIF) can be used to examine the ground states of some species, particularly for radicals and ions of small species, such as the CF_2 radical[35]. LIF, like OES, has its limitations since the species to be detected must fluoresce with a reasonable quantum efficiency. This is often not the case with larger polyatomic molecules which can return to their ground state non-radiatively, or dissociate from the excited state.

Infra-red absorption has been used to monitor species in a plasma[36]. This can be used to monitor a wider range of species than OES but is less sensitive, requiring either a high concentration of absorbing species or a long optical path length.

Mass spectrometry can be used to examine both ionic and neutral species in a plasma[37,38], through a small hole connecting the plasma chamber to a mass spectrometer. This is an intrusive technique, but can monitor all species present in a plasma with sufficient lifetime to reach the detector. More information about this technique can be found in chapter 3.

1.2 PLASMA POLYMERISATION

Plasma polymer formation occurs when organic vapour is injected into an inert gas plasma, or when a plasma is ignited in an organic vapour, usually taking the form of a thin film deposited on all surfaces in contact with the plasma. Polymer formation in a glow discharge has been known for many years[39], although the first polymers were thought of as unwanted by-products of the discharge experiment[40]. Conventional monomers such as vinyl compounds may be used for plasma polymerisation, but no such polymerisable structure is necessary and almost all organic compounds can give rise to polymer formation. Unlike a conventional polymer, a plasma polymer contains no regular repeat unit, but consists of a random, highly cross-linked organic network containing a large number of trapped free radicals. The polymer film is often strongly adherent to the surface on which it is deposited, but its highly cross-linked nature makes it very rigid, which causes it to become brittle and flake off if the film thickness is too great. The high degree of cross-linking also causes plasma polymers to be insoluble in most or all solvents. The number of radicals in a plasma polymer is dependent on the degree of unsaturation of the monomer used, as highly unsaturated monomers such as acetylene and aromatic species tend to polymerise through difunctional reactive intermediates, while saturated monomers generally polymerise through monofunctional species which give rise to fewer radicals in a plasma polymer. These two mechanisms are represented as cycles 2 and 1 respectively in the rapid step growth mechanism proposed by Yasuda for plasma polymerisation[17] (figure 1.4). The activated

$M_i\cdot + M \longrightarrow M_i\text{-}M\cdot$

$M_i\cdot \longleftarrow M_i\cdot + \cdot M_j \longrightarrow M_i\text{-}M_j$

$M_i\cdot$

$\cdot M_k\text{-}M_i \longleftarrow +$

Cross-cycle reaction

$M_i \text{-}\!\!\sqrt{}$

Plasma excitation

$\cdot M_k\cdot$

$\cdot M_k\cdot \longleftarrow \cdot M_k\cdot + M \longrightarrow \cdot M_k\text{-}M\cdot$

$\cdot M_k\cdot + \cdot M_j\cdot \longrightarrow \cdot M_k\text{-}M_j\cdot$

Cycle II
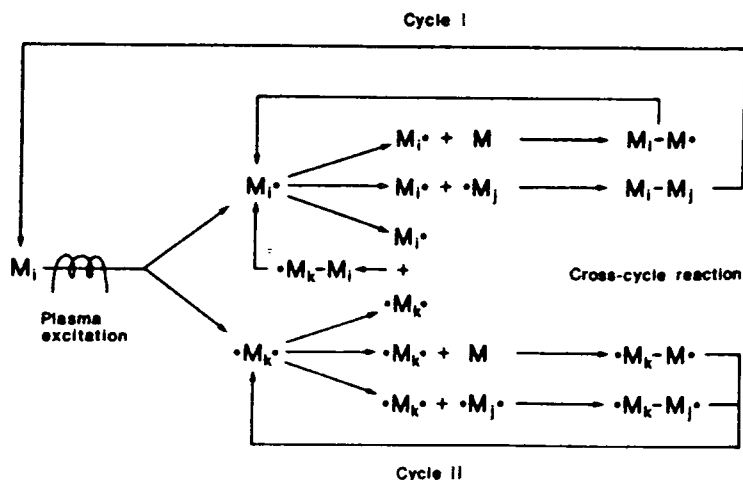
Figure 1.4 Proposed rapid step growth mechanism for plasma polymerisation

species may be either radicals or ions or both.

The final product of plasma polymerisation is determined by an equilibrium between the competing processes of polymerisation and ablation[41], illustrated schematically in figure 1.5. Ablation is particularly important in fluorocarbon plasmas, due to the reactive nature of fluorine species. In the extreme case, the fluorine content of a CF_4 plasma is sufficient for the rate of ablation to exceed that of polymerisation, and no film is formed[42]. The addition of hydrogen to a CF_4 plasma can however be sufficient to alter the equilibrium in favour of polymerisation, and produce a plasma polymer[42].

Polymer formation is very dependent on the plasma conditions used, particularly on the power (W) and monomer flow rate (F). For a given monomer the polymer deposition rate is observed to vary with the parameter W/F as shown in figure 1.6[43]. When the W/F ratio is low there is insufficient power to cause the monomer
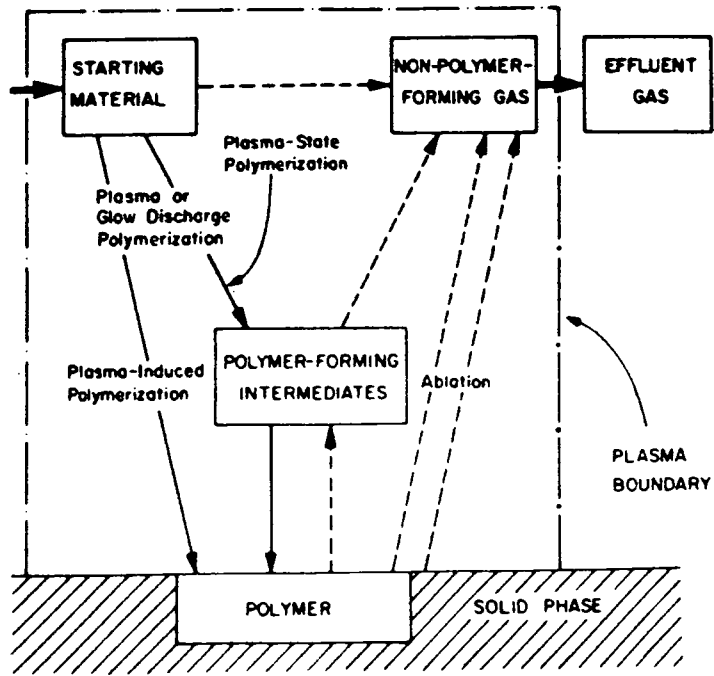
Figure 1.5 Competitive ablation and polymerisation in a plasma, showing the formation of gas phase products
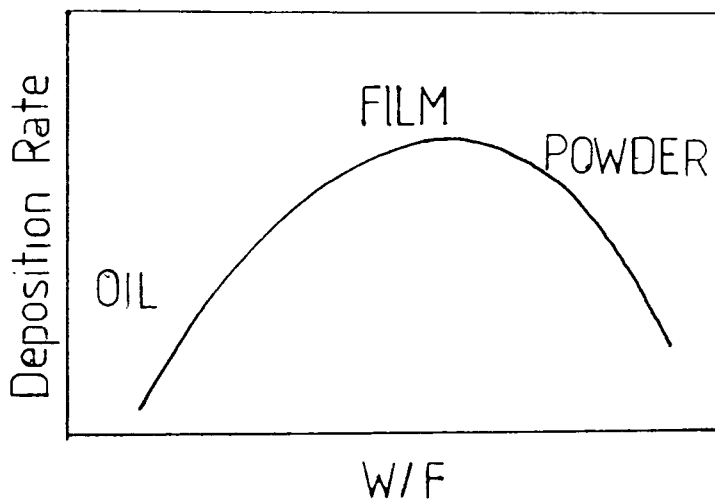
Figure 1.6 The variation of polymer deposition rate on W/F

to polymerise to a great extent, so the deposition rate is low and the polymer is of low molecular weight and oily. As the W/F ratio is increased the deposition rate increases and polymer films are formed, but when the ratio is very high there is a monomer deficiency, and so the polymerisation rate can no longer keep pace with the increasing ablation rate. The product in this case is often a powder as the polymer formation may take place rapidly in the gas phase. The chemical nature of the polymer also depends on W/F, as an increasing amount of power available per unit monomer is likely to cause an increasing disruption of the monomer structure. The deposition rates of different monomers of similar chemical composition can be related in a similar way using the composite parameter W/FM, where M is the molecular mass of the monomer.

The nature and distribution of the polymer also depends on the geometrical size and shape of the plasma reactor[44]. For this reason any comparisons between plasma polymers are difficult to make unless the same or identical apparatus is used. The nature of a polymer deposited in different regions of the same reactor may also vary[45], so to compare different plasma polymers samples must always be taken from the same position in the reactor.

Plasma polymerisation represents a simple, one-step method for depositing thin polymeric films. This leads to potential applications as resist materials[46] in the electronics industry. The inertness and insulating qualities of plasma polymers makes them useful as protective coatings (e.g. for electronic devices[47] and KBr optical windows[48], insulating films[49], and thin film capacitors[50]. The good adhesion of plasma polymers to substrates

enables them to be used in improving the adhesion qualities of other materials (e.g. platinum and teflon or steel and polythene) that do not normally adhere to each other, by coating both surfaces with a plasma polymer[51]. Other properties can be inferred by using specific monomers. For example plasma polymers of fluorocarbons can be used to produce very hydrophobic, low friction coatings[52], while those of other compounds such as N-vinyl pyrrolidone can produce very hydrophilic films, and have been used for example in improving the comfort of contact lenses[53]. Nitrogen and silicon containing plasma polymers have been considered as semi-permeable membranes[54], and organotin plasma polymers have been proposed as gas sensor devices[55]. There are also a number of possible biomedical applications[56], especially for silicon and fluorine containing plasma polymers. These include the providing of a more biocompatable surface for implants into the body, the forming of a barrier film to prevent the diffusion of small molecules to a substrate or to control the rate of drug release, and the forming of a surface suitable for immobilising biomolecules or other chemical compounds.

There are a number of problems associated with some applications of plasma polymers. One is the fact that many plasma polymers experience ageing as atmospheric oxygen reacts with free radicals in the surface, causing changes in the surface properties. A second problem is that the mechanisms of plasma polymerisation and the influence of various factors such as power, flow rate and reactor design are not fully understood, so it is not always possible to predict the nature of a plasma

18

polymer and to prepare polymers with specific properties. A third problem is that the process is difficult and expensive to do on a large industrial scale, so plasma polymerisation is more applicable to smaller, high value applications.

1.3 SURFACE PHOTOPOLYMERISATION

1.3.1 Introduction to surface photopolymers

Photochemistry using ultra violet light is a commonly used technique in synthetic organic and inorganic chemistry. The energies available in a photochemical reaction are higher than those for thermal reactions, thus enabling new reaction pathways to be exploited, although photochemical energies are lower than those available in a plasma. Molecules absorbing UV radiation are excited to an electronically excited state, which may decay via chemical reaction, often involving free radicals.

Photochemistry is frequently used to initiate polymerisation reactions in the solid or liquid phase, by creating free radicals on which polymer chains can grow. This can be achieved either directly or through the use of photo-initiators. Early investigations into low pressure gas phase photopolymerisation were carried out by Melville[57] on methyl methacrylate and by Gee[58] on butadiene. During the 1960's a number of studies showed that thin surface films could be formed from the vapour phase by photochemical means for a variety of monomers including butadiene[59], styrene[60], divinyl benzene[61], acrolein[61], tetrafluoroethylene[62] and acrylonitrile[60]. These monomers all possess double bonds which might be expected to lead to polymer

formation, but it was found that some other compounds such as benzene[63], cyclohexanol, phenol and other aromatic compounds[64] can also surface photopolymerise. In the case of benzene no polymer is formed using wavelengths of greater than 200 nm, which can only access the first singlet excited state, but surface photopolymerisation occurs at lower wavelengths (vacuum UV radiation) where higher excited states can be accessed. Organnometallic and inorganic compounds (e.g. diethyl zinc[65] and tungsten hexafluoride[66]) may also be used to deposit metallic films in a process known as photochemical vapour deposition, in a manner similar to plasma induced chemical vapour deposition.

Unlike plasma polymerisation though, not all organic compounds can form surface photopolymers. One reason for this is the requirement for a monomer to possess an excited state of suitable energy to absorb the UV radiation. Suitable excited states occur in alkenes, aromatics and carboyl compounds, but not in many saturated compounds, which can therefore not undergo photochemical reaction. Also, many compounds that do have vapour phase photochemistries do not polymerise, but undergo various isomerisation, decomposition or cycloaddition reactions instead.

Surface photopolymers form as thin films on any surface exposed to UV radiation of the appropriate wavelength, and in contact with the monomer vapour. Patterned deposition can be achieved by putting a mask over part of the substrate to shield it from the UV light[67], although in some cases polymerising species form in the gas phase with long enough lifetimes to deposit in the dark areas[68]. In some cases the polymer is

20

essentially the same as one produced by conventional means (e.g. methyl methacrylate - see chapter 4), but it is more common for there to be structural differences from the monomer or from the conventional polymer (if one exists). An example of this is the presence of CF_3 groups in a surface photopolymer of tetrafluoroethylene[62]. Like plasma polymers, surface photopolymers tend to be cross-linked and adhere strongly to the substrate.

The similarity between the surface photopolymers and plasma polymers of N-vinyl pyrrolidinone[69], perfluorobenzene and benzene/perfluorobenzene copolymers[70], shown by XPS analysis and contact angle measurements, was noted by Munro and Till and it was suggested that the polymers formed by these two processes were essentially the same materials. It was therefore proposed that like surface photopolymerisation, plasma polymerisation must proceed primarily through excited state chemistry and that surface photopolymerisation could be used as a simplified model for plasma polymerisation. This concept is further explored in this thesis.

Applications for surface photopolymers have been less well explored than for plasma polymers, but the similarity between the two means that the possible applications are much the same. Surface photopolymers have been considered for use as capacitors[71] and positive and negative resists[67]. Surface photopolymerisation has also been examined as a method for depositing a film of material with anti-blood clotting behaviour[72], a property that may also be possessed by some plasma polymers[73].

1.3.2. Light Sources

The most common type of light source used for photochemical work is the resonance arc lamp, in which a low pressure gas or vapour is excited in an electric discharge producing visible and ultra-violet light. The light is emitted as a series of resonance lines of particular wavelengths, and although for most gases many such resonances exist it is common for just one or two lines to dominate the emission spectrum.

Photochemistry at wavelengths above 200 nm is usually carried out using a medium pressure mercury arc lamp. The most intense emission line from this type of lamp occurs at 254 nm, although there is also significant UV emission at 297 and 365 nm as well as some in the visible and infra-red regions.

The region below 200 nm is known as the vacuum ultra violet, since radiation of these wavelengths is strongly absorbed by oxygen in the air. Mercury arc lamps may also be used for vacuum ultra violet work, since they possess a significant resonance line at 185 nm (especially if a low pressure mercury arc lamp is used), but there are also a number of other gases which can be used to give resonance lines at other wavelengths. Some of these are listed on table 1.3[74]. The gases used are sometimes diluted by helium in order to increase the intensity of the resonance lines[74a] by reducing self absorption and increasing the physical size of the discharge, although under some conditions this may have the opposite effect[75].

Table 1.3 Resonance Line Sources for Photochemical Work in the Vacuum UV Region

Gas	Principal Emission (nm)	Gas	Principal Emission (nm)
Mercury	185	Krypton	124
Nitrogen	174		116
	149	Hydrogen	121
Xenon	147	Argon	105, 107
Chlorine	139	Neon	74
Oxygen	130	Helium	58

The lamps described above generally use gas pressures of the order of about 1 torr. If higher pressures (e.g. 200 torr) are used the resonance lines broaden and form a continuous emission which can be used as a light source over a range of a few tens of nanometres, although the intensity at any one wavelength is much less than for a resonance line from a low pressure lamp. Continua for the rare gases are shown in table 1.4[76].

Table 1.4 Rare Gas Continua

Gas	Useful Range (Å)	Optimum Pressure (torr)
Helium	580-1100	40-55
Neon	740-1000	>60
Argon	1050-1550	150-250
Krypton	1250-1800	>200
Xenon	1480-2000	>200

The choice of window material for a photochemical experiment is also very important. Pyrex cuts out wavelengths below about 290 nm and so is unsuitable for most photochemical work. Suitable window materials for use in the conventional and vacuum ultra violet are listed on table 1.5[77].

Table 1.5 Window Materials for Photochemical Work

Material	Cut-off Wavelength (nm)
Pyrex	290
Quartz	180
Fused Silica*	160
Calcium Fluoride	122
Magnesium Fluoride	115
Lithium Fluoride	105

*Known commercially as Suprasil or Spectrosil B

Quartz is most commonly used for experiments in the conventional ultra-violet since it is transparent above 200 nm, strong and relatively cheap. Vacuum UV experiments at 185 nm generally require suprasil windows, while lower wavelengths require calcium, magnesium or lithium fluoride. Lithium fluoride has the lowest cut-off wavelength but it is water soluble and degrades easily. All of the window materials generally show poor transmission characteristics for about 10-20 nm above the cut off point. For photolysis below about 105 nm (i.e. helium, neon and possibly argon radiation) a windowless discharge[78] must be used.

24

The added difficulty of this experiment means that photopolymerisation experiments have not been carried out below this wavelength. The ionisation energies of most organic molecules are of the order of about 10 eV, which corresponds to about 120 nm, so if the reaction is to be restricted to excited state chemistry a calcium fluoride or suprasil window must be used for vacuum ultra violet work.

An alternative light source which has become available in recent years is the UV laser. Lasers are fairly commonly used in the photodeposition of metals[79], but less interest has been shown in the formation of surface photopolymers. An argon ion laser of 257.2 nm was however used by Tsao and Erlich[80] to form a surface photopolymer of methyl methacrylate. Advantages of using a laser as a light source include the fact that it is monochromatic, enabling the effect of wavelength to be studied, and that it can be focused onto a small area of the substrate to produce patterned deposition. It is also possible to get very high intensity UV radiation, although this is not always an advantage since it may cause polymer to be ablated.

Polymers can also be produced from the gas phase using multi-photon absorption from infra-red lasers[81]. Very high intensity infra-red light causes molecules to absorb many photons of light which gives them energies comparable to those obtainable using UV irradiation. A disadvantage of this technique however, is that the energy available to each molecule cannot be accurately determined.

1.4 ANALYTICAL TECHNIQUES FOR PLASMA POLYMERS AND SURFACE PHOTOPOLYMERS

1.4.1 Introduction

The techniques used to study plasma polymers and surface photopolymers can be divided into two groups: those used to study the bulk properties, and those used to characterise the surface of the film. The most important of these methods of analysis are listed on table 1.6.

Table 1.6 Analytical techniques used to study plasma polymers and surface photopolymers

A.   Bulk Properties

Elemental Analysis

Electron Spin Resonance (ESR)

Solid State NMR

Infra-Red Spectroscopy

Differential Scanning Calorimetry

Pyrolysis Gas Chromatography

B.   Surface Properties

Contact Angle Measurement

Microscopic Studies

Reflectance Infra-Red

X-Ray Photoelectron Spectroscopy (XPS)

Secondary Ion Mass Spectroscopy (SIMS)

Many of the bulk analytical techniques are difficult to apply to a polymer deposited as a thin film, since the amount of

polymer is very small compared with the amount of substrate. In the case of plasma polymers deposition can be extended for a long period of time, allowing sufficient polymer to be collected (it flakes off the walls of the reactor when the film is very thick), for bulk analysis. Surface photopolymers generally deposit much more slowly, so it is generally not possible to collect sufficient for bulk analysis. Transmission infra-red analysis can be achieved for a thin film by depositing it on a KBr window.

Surface analysis is generally easier to apply to plasma polymers and surface photopolymers, but it can not necessarily be assumed that the surface properties are the same as those of the bulk. In fact the initial surface characteristics of plasma polymers are generally considered to be much the same as those of the bulk, but after the polymer has been exposed to air surface oxidation occurs, producing a surface with a higher oxygen content than the bulk of the polymer. However since plasma and surface photopolymers are usually prepared for their surface properties, analysis of the surface is often more applicable than that of the bulk properties.

1.4.2 Bulk Analysis
a) Elemental Analysis

The composition of plasma polymers as determined by elemental analysis generally shows a deficiency of most elements in the polymer with respect to carbon, compared with the elemental ratios for the monomer[82,83], with halogens being particularly vulnerable to elimination[83]. The high carbon content is evidence of the highly cross-linked nature of plasma polymers.

A small amount of oxygen contamination is usually observed, either from contamination or from reaction with atmospheric oxygen.

b) Electron Spin Resonance (ESR)

ESR detects the presence of unpaired electrons in a sample, and so can be used to examine the trapped free radicals in a plasma polymer[84]. It has been found that the highest concentrations of free radicals occur in plasma polymers of highly unsaturated starting materials, while those from saturated monomers contain comparatively few free radicals. The fact that films with high free radical contents oxidise the most quickly shows that free radicals are responsible for this oxidation.

c) Solid State NMR

The highly insoluble nature of plasma polymers means that NMR analysis cannot be carried out in the solution state. Solid state NMR is possible however if sufficient polymer is produced, but even with magic angle spinning and cross polarisation techniques employed the peaks are generally very broad. The main reason for this is that plasma polymers tend to contain a large number of similar but non-identical chemical environments. ^{13}C NMR analysis has been carried out on the plasma polymers of ethane, ethylene and acetylene plasma polymers, and showed the presence of $=CH_2$, CH, CH_2, CH_3 and quaternary carbon groups in varying concentrations[85]. If plasma polymers are prepared from ^{13}C isotopically labelled materials, solid state ^{13}C NMR can identify which chemical environments in the polymer correspond to

which carbon atoms in the monomer. This has been used to show
that in the plasma polymerisation of toluene some methyl
carbon atoms become unsaturated, while some ring carbon atoms
become saturated[86].

d) Differential Scanning Calorimetry

This has been used to show that plasma polymers have no
phase transition point where decomposition starts to occur, but
that there is a very gradual decomposition of the polymer with
increasing temperature[87]. This reflects the good thermal
stability of plasma polymers and has been taken as evidence for
the cross-linked nature of the plasma polymer. Similar results
have also been obtained for a surface photopolymer of
butadiene[62].

e) Pyrolysis Gas Chromatography

Pyrolysis gas chromatography has been used to investigate
the structure of a number of hydrocarbon plasma polymers[88]. All
were found to be highly branched and cross-linked, partially
unsaturated and to contain short alkyl chains and aromatic rings.
The degree of branching and cross-linking was found to be
considerably higher in powders formed from very high power
plasmas. Pyrolysis GC mass spectroscopy has been used to show a
similar structure for a toluene plasma polymer[89], and in
conjunction with isotopic labelling gave evidence for partially
carbon atom scrambling between the methyl and ring carbons. The
advantage of using GC mass spectroscopy is that each peak in the
gas chromatogram can be firmly identified while the gas
chromatography is taking place.

f) Infra-Red Spectroscopy

Infra-red may be used for either a bulk or surface analysis depending on whether transmission or reflectance infra-red is used, although even reflectance infra-red analyses a sample to a greater depth than other surface techniques such as XPS or SIMS. Infra-red is a commonly used method for analysing plasma polymers, and has been by far the most common technique applied to surface photopolymers. This is because most of the past work on surface photopolymerisation was carried out in the 1960's and early 1970's when other forms of surface analysis were not available.

The infra-red spectra of plasma and surface photopolymers often have much in common with the spectrum of the monomer or the conventional polymer, but sharp peaks become broader and less well defined. This is due to the large variety of similar chemical environments and high degree of cross-linking in these polymers. The effect is particularly pronounced in plasma polymers produced at very high power. Figure 1.7 shows the infra-red spectra of plasma polymers of N-vinyl pyrrolidinone (NVP) prepared using high and low power plasmas, in comparison with the spectrum of the monomer[90]. The broadening can be clearly seen in the spectra of the plasma polymers, especially for the one prepared using a power of 50 watts. Infra-red analysis can also detect the presence of new functional groups not present in the monomer, observed as new peaks in the spectrum. An example of this can be seen in the 50 watt plasma polymer of NVP, in which a peak that is not present in the spectrum of the monomer is observed at about 2200 cm^{-1}. This could correspond to C≡N, C≡C or
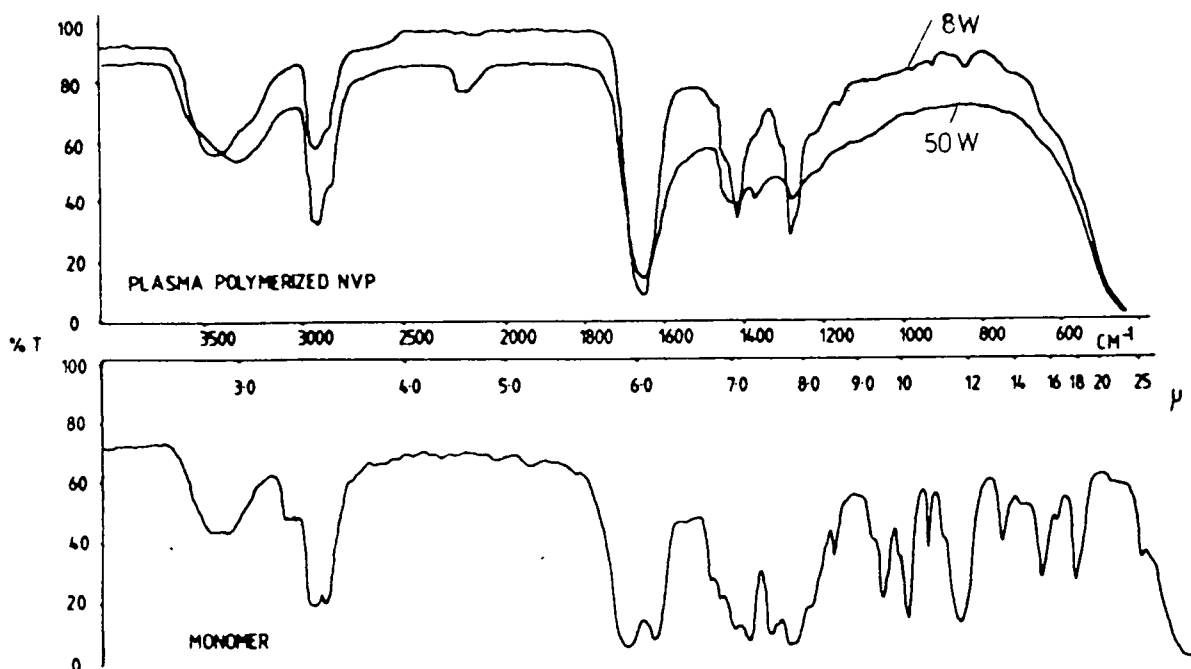
Figure 1.7 Infra-red spectra of NVP plasma polymerised at 8 and 50 watts compared with the spectrum of the monomer

N=C=O groups, none of which are present in the monomer.

The disappearance of certain peaks upon polymerisation may give an indication as to the polymerisation mechanism. In the case of NVP, the C=C peak at 1620 cm^{-1} in the spectrum of the monomer is lost upon plasma polymerisation (especially at 8 watts), suggesting that the polymerisation proceeds largely through the opening of the double bond.

The oxidation of a plasma polymer upon ageing can be followed by infra-red analysis[91]. This is achieved by monitoring the growth of peaks associated with oxygen functionalities, particularly the C=O and O-H peaks at about 1700 and 3500 cm^{-1} respectively.

31

1.4.3 Surface Analysis

a) Contact Angle Measurement

The contact angle is the angle that the surface of a small drop of liquid (usually distilled water) makes with the surface of the material it is on, and gives an indication of the surface energy of the material. A polar surface, such as a polymer containing a high level of oxygen functionalities, with high free energy gives a very low contact angle with water, while a low energy, non polar surface, (e.g. fluorocarbon) gives a high contact angle. Depending on the choice of monomer and the conditions used plasma polymers and surface photopolymers can be prepared with contact angles ranging from zero[90] to almost 180°[62,92], although very high contact angles are likely to be due to surface roughness as well as low surface energy. Measurement of the contact angle therefore provides a quick and cheap method of obtaining some information about the nature of a polymer surface which may be directly related to the desired properties of the surface. It can not however provide any detail about the chemical composition of the surface.

b) Electron Microscopy

This can be used to study the surface morphology of a deposited polymer film. Plasma polymers have been examined by electron microscopy[93], and generally show fairly smooth, pin-hole free surfaces, although polymers formed under high power and low flow rate conditions may be rougher. Electron microscopy can be very useful in examining the patterned deposition of a surface photopolymer, particularly if a laser is used as a UV light

source in the deposition to produce very fine patterns[80].

c) X-Ray Photoelectron Spectroscopy (XPS)

Also known as ESCA (Electron Spectroscopy for Chemical Analysis), this was first applied to plasma polymers by Clark and co-workers in the 1970's[94] and has since become a standard analytical technique for plasma polymers. Samples are analysed by measuring the kinetic energies of electrons ejected from core levels of atoms in the surface of the sample using monochromatic X-rays. The binding energy of the electron can then be calculated using equation 1.3.

$$BE = h\nu - KE \qquad 1.3$$

where BE = binding energy of the electron
$h\nu$ = energy of the incident x-rays
and KE = measured kinetic energy of the electron

Each atomic core level of each element has a particular binding energy, so by comparing the number of electrons observed at various binding energies (together with a knowledge of the appropriate sensitivity factors) a semi-quantitative elemental analysis of the surface can be carried out (accurate to about ± 5%). This can be achieved for all elements except for hydrogen, since this does not possess any core level electrons.

The electronic charge on an atom has an influence on the precise energies of the core levels, so the presence of charged species and electron withdrawing or donating substituents on an atom can be observed as a chemical shift. This enables a functional group analysis to be made, particularly by examining the C_{1s} core level, although substituent groups that are not

electron withdrawing may not be detected (e.g. all carbon-hydrogen groups occur at the same binding energy). Functional group analysis is particularly useful for fluorine and oxygen containing polymers, since the high electronegativities of these elements produce large chemical shifts in the C_{1s} spectrum.

The presence of a shake up satellite, which appears as a small peak at slightly higher binding energy than the direct photoionisation peak, is indicative of aromatic or other short range unsaturation. This arises from the loss of kinetic energy from a photoelectron as it causes a valence electron to be promoted into a higher energy orbital (e.g. $\pi-\pi^*$ for aromatics).

XPS is surface sensitive to a depth of approximately 50Å, due to the short mean free path of an electron in a solid material. The exact depth of sample examined can however be varied to allow a certain amount of depth profiling. This can be achieved by changing the electron take-off angle, so that an electron has to travel through more of the sample to escape from a given depth, or by examining two different core levels of the same element (e.g. O_{1s} and O_{2s}), the electrons of which have different kinetic energies and hence different mean free paths, or by using X-rays sources of two different energies.

XPS is generally a very useful technique for standard analysis of most plasma polymers and surface photopolymers, and is the principal method of analysis used in this thesis. It has the major drawback however that little information can be obtained about hydrocarbon polymers. Also, as for all forms of surface analysis, the sample must be clean since a very small layer of contamination on the surface can obscure the signal from

the sample.

d) Secondary Ion Mass Spectroscopy (SIMS)

SIMS is a relatively new technique which has not yet been much used to study plasma polymers or surface photopolymers, although its application to conventional polymers has become established[95]. An beam of ions or fast atoms is used to ablate ionic fragments from the polymer surface which are analysed in a mass spectrometer. For polymer samples the static mode is usually employed, in which a very low ion current is used and the ion beam is rastered across the surface of the sample. This is to avoid sampling any of the surface which might have already been damaged by the ion beam. Depth profiling can be achieved using the dynamic mode in which a high ion current is used and the beam remains focused in one place. This causes the sample at that point to be etched away and the variation of the spectrum obtained with time corresponds to a depth profile of the sample. This has been used to measure the thickness of a vinyl ferrocene plasma polymer, by measuring the time taken for the peak due to iron to disappear[96]. Since the ion beam can be focussed into a very small area, SIMS can also be used to take spectra from different parts of a sample and so build up a lateral image of the surface.

Although little work has yet been done on the analysis of plasma polymers and surface photopolymers by SIMS[90,97] it has the potential of providing much structural information. Although SIMS spectra of unknown materials can be difficult to interpret, a considerable amount of information can be gained by comparison

with the spectra of known conventional polymers. The information gained by SIMS analysis tends to be complimentary to, rather than alternative to, XPS analysis.

REFERENCES

1. A.T.Bell in "Techniques and Applications of Plasma Chemistry", Eds. J.R.Hollahan and A.T.Bell, Wiley, New York, (1974), Chapter 1.

2. K.Upudhya, Trans. Ind. Ins. Met., 38, 472, (1985)

3. A.C.Gray, Spectrochim. Acta., 40B, 1525, (1985)

4. S.C.Brown in "Gaseous Electronics", Vol 1, Eds. M.N.Hirsh and H.J.Hoskan, Academic Press, New York, (1978)

5. J.S.Townsend, Phil. Mag., 8, 733, (1904)

6. L.Tonks and I.Langmuir, Phys. Rev., 33, 195, (1929)

7. H.Suhr, Plasma Chem. Plasma Processing, 3, 1, (1983)

8. H.Suhr in ref. 1, chapter 3.

9a. C.I.Simonescu and F.Denes, Cellulose Chem. Technol., 14, 285, (1980)

  b. A.E.Pavlath and K.E.Lee, J. Macromol. Sci. Chem., A10, 579, (1976)

10. M.M.Millard, K.S.Lee and A.E.Pavlath, Text. Res. J., 42, 307, (1972)

11. D.M.Soignet, R.J.Berni and R.R.Banerito, J. Appl. Polym. Sci., 20, 2483, (1976)

12. M.M.Millard and A.E.Pavlath, Text. Res. J., 42, 460, (1972)

13. P.M.Tricolo and J.D.Andrade, J. Biomed. Mater. Res., 17, 129, (1983)

14. M.Strobel, S.Corn, L.S.Lyon and G.A.Korba, J. Polym. Sci., Polym. Chem. Ed., 23, 1125, (1985)

15. L.T.Nguyen, N.H.Sung and N.P.Suh, J. Polym. Sci., Polym. Chem. Ed., 18, 541, (1980)

16. R.W.Kirk, "Applications of Plasma Technology to the Fabrication of Semiconductor Devices" in ref. 1

17. H.Yasuda, "Plasma Polymerisation", Academic Press, London, (1985)

18. J.R.Hollahan and R.S.Rosler in "Thin Film Processes", Eds. J.Vossen and W.Kern, Academic Press, New York, (1979)

19. C.Oehr and H.Suhr, Appl. Phys., A45, 151, (1988)

20. Y.Osada, M.Hashidzume, E.Tsuchida and A.T.Bell, Nature, 286, 693, (1980)

21. F.Kaufman in "Chemical Reactions in Electrical Discharges", Ed. R.F.Gould, ACS, Advances in Chemistry Series 80, Washington D.C., (1969), chapter 3

22. J.M.Meek and J.D.Craggs, "Electrical Breakdown of Gases", Wiley, Chichester, (1978), chapter 1

23. W.L.Fite in ref 21, chapter 1

24. P.Brassem and F.J.M.J.Massen, Spectrochimica Acta, 29B, 203, (1974)

25. D.T.Clark and A.Dilks in, "Characterisation of Metal and Polymer Surfaces", chapter 2, Vol.2, Ed. L.H.Lee, Academic Press, New York, (1977)

26. D.T.Clark and A.Dilks, J. Polym. Sci., Polym. Chem. Ed., 18, 1233, (1980)

27. Y.I.Shmykov, S.N.Shorin, A.L.Suris, N.L.Volodon, V.T.Dyatlov, Y.V.Irzinger and A.M.Tukhvatullin, Khim. Vys. Energ., 11, 371, (1977)

28. H.Suhr and U.Schücker, Synthesis, 431, (1970)

29. C.Boelhouwer and H.I.Waterman, Research (London), 9, 5511, (1956)

30. I.Platzner and P.Marcus, Int. J. Mass Spectrom. Ion. Phys., 41, 241, (1982)

31. M.Shen and A.T.Bell in "Plasma Polymerisation", ACS Symp. Series 108, Washington D.C., (1979), chapter 1.

32. R.D'Agostino, F.Cramarossa and F.Illuzzi, J. Appl. Phys., 61, 2754, (1987)

33. R.A.Gottscho and T.A.Miller, Pure Appl. Chem., 56, 189, (1984)

34. H.S.Munro and C.Till, J. Polym. Sci., Polym. Chem. Ed., 24, 279, (1986)

35a. S.Pang and S.R.J.Brueck in "Laser Diagnostics and Photochemical Processing for Semiconductor Devices", Eds. R.M.Osgood, S.R.J.Brueck and H.R.Schlossberg, North Holland, New York, (1983)

   b. P.J.Hargis Jr. and M.J.Kushner, Appl. Phys. Lett., 40, 779, (1982)

36a. H.Sakai, P.Hansen, M.Esplin, R.Johansson, M.Peltola and J.Strong, Appl. Opt., 21, 228, (1982)

  b. H.U.Poll, D.Hinze and H.Schlemm, Appl. Spec., 36, 445, (1982)

37. M.J.Vasile and G.Smolinsky, Int. J. Mass Spectrom. Ion Phys., 12, 133, (1973)

38. M.J.Vasile and G.Smolinsky, J. Phys. Chem., 81, 2605, (1977)

39. J.Goodman, J. Polym. Sci., Lett. Ed., 44, 144, (1960)

40a. P.De Wilde, Ber., 7, 352, (1874)

  b P.Thenard, Compt. Rend., 78, 218, (1874)

41. H.Yasuda and T.Hsu, Surf. Sci., 76, 232, (1978)

42. E.Kay, Invited Paper, Int. Round Table Plasma Polym. Treat., IUPAC Symp. Plasma Chem., (1977)

43. H.Yasuda and T.Hirotsu, J.Polym. Sci., Polym. Chem. Ed., 16, 743, (1976)

44. Y.S.Yeh, I.N.Shyy and H.Yasuda, ACS Polym. Mater. Sci. Eng., 56, 141, (1987)

45. D.F.O'Kane and D.W.Rice, J. Macromol. Sci. Chem., A10, 567, (1976)

46. M.Hori, H.Yamada, T.Yoneda, S.Morita and S.Hattori, J. Electrochem. Soc., 134, 707, (1985)

47. W.D.Freitag, H.Yasuda and A.K.Sharma, Org. Coat. Appl. Polym. Sci. Proc., 47, 449, (1982)

48a. B.L.Weigand, Govt. Rep. Announce. (U.S.), 75, 179, (1975)

  b. T.Wydeven and C.C.Johnson, Polym. Prep. Am. Chem. Soc., Div, Polym. Chem., 21, 62, (1980)

49. M.Kobale and H.Pachonik, Ger. Patent, 2,105,003, (1972)

50. J.C.Dubois, Fr. Patent, 2,379,889, (1978)

51. N.Inagaki and H.Yasuda, J. Appl. Polym. Sci., 26, 3333, (1981)

52. M.M.Millard and A.E.Pavlath, J. Macromol. Sci., Chem. Ed., A10, 579, (1976)

53. M.Kuriaki, M.Hasebe, Y.Miwa and Y.Mizutani, Kobunshi Ronbunshu, 42, 11, 841, (1985). (Chem. Abs. 104 155917u)

54a. H.Yasuda, Appl. Polym. Symp., 22, 241, (1973)

   b. J.Sakata, M.Hirai, I.Tajima and M.Yamamoto, ACS Polym. Mater. Sci. Eng., 56, 802, (1987)

55. N.Inagaki and Y.Hashimoto, ACS Polym. Mater. Sci. Eng., 56, 515, (1987)

56. A.S.Hoffman, ACS Polym. Mater. Sci. Eng., 56, 699, (1987)

57. H.W.Melville, Proc. Roy. Soc. A, 163, 511, (1937)

58. G.Gee, Trans. Faraday Soc., 34, 712, (1938)

59. I.Haller and R.Srinivasan, J. Chem. Phys., 40, 1992, (1964)

60. A.N.Wright, Postprints of Soc. Plastics Engineers Regional Technical Conference, Ellensville, New York, (1967), p.110

61. L.V.Gregor and H.L.McGee, Proc. Fifth Annual Electron beam Symp. (Alloyd Corp.) p.211, Cambridge, Mass. (1963)

62. A.N.Wright, Nature, 215, 935, (1967)

63a. J.E.Wilson and W.A.Noyes Jr., J. Am. Chem. Soc., 63, 3025, (1941)

   b. H.R.Ward and U.Wishnok, J. Am. Chem. Soc., 90, 5333, (1968)

64. A.Christopher and A.N.Wright, J. Appl. Polym. Sci., 16, 1057, (1772)

65. R.R.Krchnavek, H.H.Gilgen, J.C.Chen, P.S.Shaw, T.J.Licata and R.M.Osgood, J. Vac. Sci. Technol., B5, 20, (1987)

66. M.Toyama, H.Itoh and T.Moriya, Jap. J. Appl. Phys., 25, 688, (1986)

67. C.O.Kunz, P.C.Long and A.N.Wright, Polymer Eng. and Sci., 12, 209, (1972)

68. H.S.Munro and G.R.Eyre, Unpublished data

69. H.S.Munro, ACS Polym. Mater. Sci. Eng., 56, 318, (1987)

70. H.S.Munro and C.Till, J. Polym. Sci., Polym. Chem. Ed., 26, 2873, (1988)

71. A.N.Wright in "Polymer Surfaces", Eds. D.T.Clark and W.J.Feast, Wiley, (1978)

72. A.N.Wright, U.S. Patent 3,677,800 (1972)

73. P.L.Kronick and M.E.Schafer, U.S. Govt. Res. Develop. Rep., 70, 42, (1970)

74a. H.Okabe, J. Opt. Soc. Amer., 54, 478, (1963)

  b. D.Davis and W.Braun, Appl. Optics, 7, 2071, (1968)

75.   E.W.Schlag and F.J.Comes, J. Opt. Soc. Amer., 50, 866, (1960)

76.   J.A.R.Samson in "Techniques of Vacuum Ultra Violet Spectroscopy", Wiley, New York, (1967), chapter 5

77.   J.A.R.Samson, ref 76, chapter 6

78.   R.R.Smardzewski, Appl. Spectroscopy, 31, 332, (1977)

79.   D.J.Erlich, R.M.Osgood and T.F.Deutsch, J. Vac. Sci. Technol., 21, 23, (1982)

80.   J.Y.Tsao and D.J.Erlich, Appl. Phys. Lett., 42, 997, (1983)

81.   J.Pola, V.Chvalovsky, E.A.Volnina and L.E.Guselnikov, J. Organomet. Chem., 341, C13, (1988)

82.   H.Yasuda, M.O.Bumgarner, H.C.Marsh and N.Morosoff, J. Polym. Sci., Polym. Chem. Ed., 14, 195, (1976)

83.   A.R.Westwood, Eur. Polym. J. 7, 377, (1971)

84.   N.Morosoff, B.Crist, M.Bumgarner, T.Hsu and H.Yasuda, J. Macromol. Sci. Chem., A10, 451, (1976)

85.   A.Dilks, S.Kaplan and A.VanLaekan, J. Polym. Sci., Polym. Chem. Ed., 19, 2987, (1981)

86.   S.Kaplan and A.Dilks, J. Polym. Sci., Polym. Chem. Ed., 21, 1819, (1983)

87.   L.F.Thomson and K.J.Mayhan, J. Appl. Polym. Sci., 16, 2991, (1972)

88.   M.Seeger, R.J.Gritter, J.M.Tibbet, M.Shen and A.T.Bell, J. Polym. Sci., Polym. Chem. Ed., 15, 1403, (1977)

89.   S.Kaplan, A.Dilks and R.Crandall, J. Polym. Sci., Polym. Chem. Ed., 24, 1173, (1986)

90.   C.Till, Ph.D. Thesis, Durham, (1986)

91.   H.Yasuda, H.C.Marsh, M.O.Bumgarner and N.Morosoff, J. Appl. Polym. Sci., 19, 2845, (1975)

92.   M.Klausner and I.H.Loh, ACS Polym Mater Sci Eng, 56, 227, (1987)

93. M.Niinomi, H.Kobayashi, A.T.Bell and M.Shen, J. Appl. Phys., 44, 4317, (1973)

94a. D.T.Clark and D.Shuttleworth, J. Polym. Sci., Polym. Chem. Ed., 16, 1093, (1978)

  b. D.T.Clark, A.Dilks and D.Shuttleworth in "Polymer Surfaces", Eds. D.T.Clark and W.J.Feast, Wiley, London, (1978)

95. A.Brown and J.C.Vickerman, Surf. Interface Anal., 8, 75, (1986)

96. M.R.Ross, Diss. Abstr. Int. B, 42, 2357, (1981)

97. J.Amouroux and S.Thomas, Int. Symp. Plasma Chem., 7, 1261, (1985)

CHAPTER 2

PLASMA POLYMERISATION AND SURFACE PHOTOPOLYMERISATION OF
PERFLUOROAROMATIC AND OTHER CYCLIC PERFLUORO COMPOUNDS.
XPS ANS SIMS ANALYSIS

2.1 INTRODUCTION

There has been a considerable amount of previous investigation into the plasma polymerisation of aromatic compounds. Polymers were noticed as by-products when the chemistries of benzene, toluene and other aromatic compounds in electric discharges were being investigated in the 1950's and 60's[1,2]. Plasma polymers of a series of fluorinated benzenes, ranging from monofluorobenzene through to perfluorobenzene, and also the perfluoro derivatives of cyclohexane, cyclohexene and cyclohexadienes were made by Clark et. al. in the 1970's and early 80's[3a-i]. These could be studied using XPS since the fluorine atom is very electronegative and so induces different chemical shifts in different fluorocarbon environments. The XPS showed considerable alteration in structure from the starting monomers, including the production of considerable amounts of CF_2 and CF_3 groups. Plasma polymers of perfluorotoluene have been reported by Inagaki[4], Gil'man et.al.[5] and Kaplan and Dilks[6]. As for perfluorobenzene, the polymer was found to contain CF, CF_2, CF_3 and $C-CF_n$ groups by XPS, while a ^{13}C NMR investigation by Kaplan and Dilks showed partial unsaturation of the plasma polymer. A pyrolysis GC mass spectral study of plasma polymerised toluene using isotopic labelling[6] showed evidence for carbon atom scrambling between the methyl group and the aromatic ring and led to the proposal of a tropylium cation intermediate. Solid state ^{13}C NMR evidence of partial saturation of the ring carbon atoms in a toluene plasma polymer[7] led to a proposed structure for the toluene plasma polymer (figure 2.1). As the NMR spectra ofthe polymers of toluene and perfluorotoluene were very similar,

44
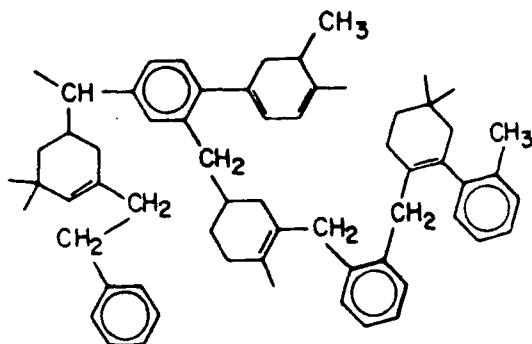
<u>Figure</u> <u>2.1</u> Proposed structure for plasma polymerised toluene

an identical but perfluorinated structure was proposed for the perfluorotoluene plasma polymer.

More recently, Munro and Till have shown that a surface photopolymer of perfluorobenzene can be formed using non-ionising radiation[8], and appears by XPS to be essentially the same as the plasma polymer. This suggests that in this case excited states are primarily responsible for the plasma polymerisation and ion chemistry need not be involved. Surface photopolymerisation of benzene has been known since the 1960's and earlier [9a-c], and a reaction scheme was proposed by Ward and Wishnok[10] involving excitation to the S_3 state followed by collapse to a vibrationally excited ground state S_{0v}. Fulvene and cis- and trans-1,3-hexadien-5-yne were formed as volatile products in the photolysis, and fulvene has also been observed as a volatile

45

product of a benzene plasma[11].

In this chapter plasma polymers of perfluorobenzene (PFB) and perfluorotoluene (PFT) produced under a range of conditions, are analysed by XPS and Secondary ion mass spectroscopy (SIMS). They are also compared with the plasma polymers of benzene, naphthalene, perfluorocyclohexane and perfluorocyclohexene. Although these and other plasma polymers have previously been analysed by XPS, SIMS been little used, except for detecting the presence of tin atoms in a plasma polymer of dibutyltin acetate[12] and, in the dynamic mode, for measuring the thickness of a plasma polymer of vinyl ferrocene[13]. No attempt has been made to investigate the structure of a plasma polymer using SIMS, although it has been used to detect the difference between high and low flow rate plasma and surface photopolymers of N-vinyl pyrrolidinone[14]. The technique should, however, be capable of providing a considerable amount of information about the structure of these materials, although interpretation of the spectra is not always easy. In this case information is gained from static SIMS spectra by comparison with electron impact mass spectra.

The surface photopolymerisation of PFT is also investigated in order to determine whether it, like PFB can produce a material similar to the plasma polymer, and what wavelength of light is required. Photopolymers of PFT and PFB are analysed by XPS and compared with the corresponding plasma polymers.
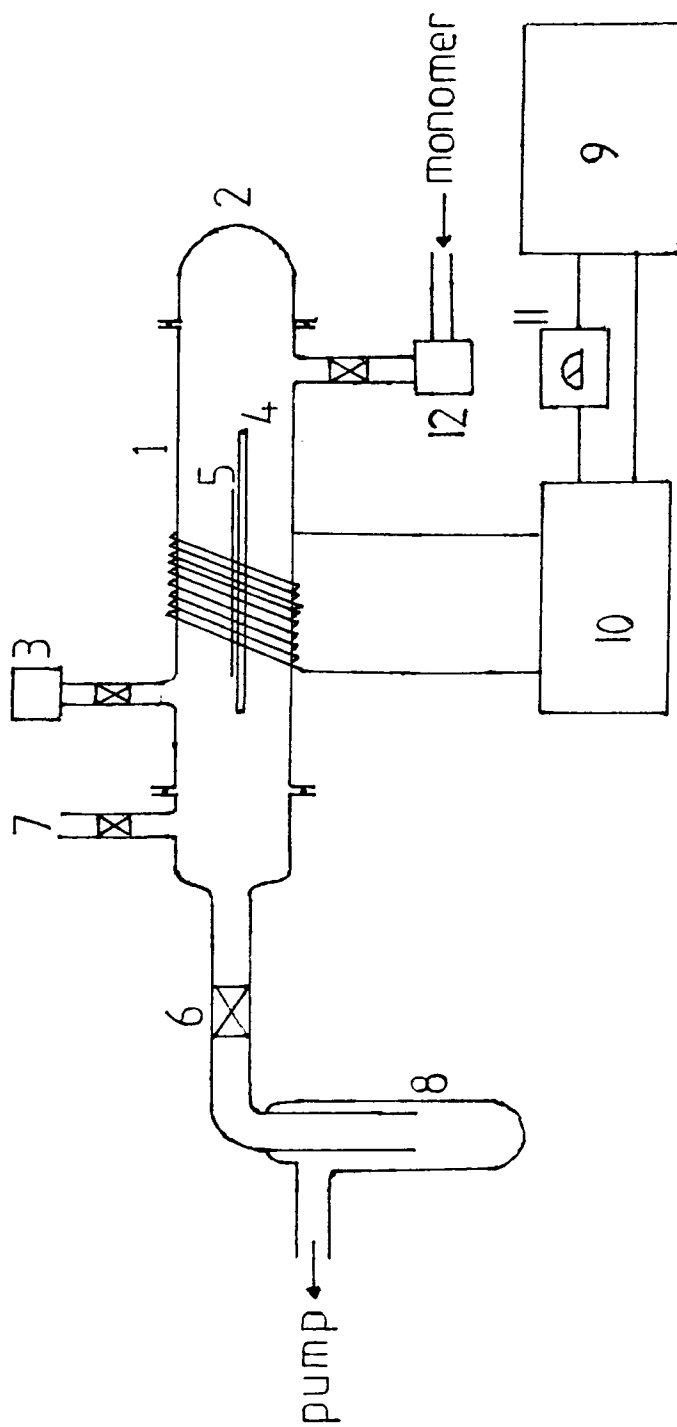
2.2 EXPERIMENTAL

2.2.1 Plasma polymerisation

Plasma polymerisations were carried out in a tubular pyrex reactor inserted into an all glass, grease free vacuum line (figure 2.2). Flanged joints and the cold trap were sealed with Viton O rings whilst all other connections were made with Cajon ultra torr couplings. Vacuum taps were sealed with PTFE stoppers. The apparatus was pumped down to a base pressure of about 3×10^{-2} torr using an Edwards ED2M2 mechanical rotary pump. Pressure measurements were made using a Pirani thermocouple gauge.

Before each deposition involving a new monomer the reactor and end caps were cleaned with a hard nylon brush using acetone, water, detergent and scouring powder, rinsed with water and acetone and baked in an oven. Any residual detergent or polymer was removed after assembly using a 50 watt oxygen plasma.

At the start of each experiment the leak rate of the vacuum line was tested by closing off the pumping and measuring the rise in pressure over a period of time. (A high leak rate can cause an unacceptable amount of oxygen incorporation into the polymer film during polymerisation). If the leak rate was low, monomer vapour was let into the reactor through an Edwards needle valve to the desired pressure, and the monomer flow rate was measured. This was achieved by closing off the pumping and monitoring the rate of increase of pressure due to the flow of monomer into the reactor. All plasma polymerisation experiments were carried out with a dynamic flow of monomer through the apparatus, i.e. the reactor was open to the pumping system during the experiment.

The RF power supplied by a 13.56 MHz RF generator was

Figure 2.2 Experimental configuration for plasma polymerisation, showing vacuum line, RF generator and associated equipment.

KEY

1) Reactor
2) End cap
3) Pirani head

4) Glass slide
5) Substrate
6) Young's tap
7) Air inlet
8) Cold trap

9) RF generator
10) Matching network
11) Power meter
12) Needle valve

48

inductively coupled to the reactor through an externally wound copper coil via an L-C matching network as shown in figure 2.2. A DIAWA SW110A meter was used to measure the RF power and standing wave ratio (the ratio of total power generated / power going into the plasma). The plasma was balanced by adjusting the matching network to give the minimum standing wave ratio (optimum value = 1). Polymerisation typically took 5-10 minutes and the polymer was collected on aluminium foil placed on a glass slide in the reactor.

All monomers were supplied by Aldrich and degassed using alternate freeze thaw cycles before use.

2.2.2 Photopolymerisation

Vacuum UV photopolymerisation experiments were carried out in a pyrex, grease free vacuum line, divided into 2 sections by a window mounted between metal flanges using Viton O rings as seals (figure 2.3). Each side was pumped down to a base pressure of 3×10^{-2} torr using an Edwards ED2M2 pump and the pressure measured by a Pirani thermocouple gauge. An RF coil was wound around the apparatus on the right hand side of the window, and this was used to produce a 50 W nitrogen plasma which acted as a source of UV radiation. Monomer vapour was bled into the left hand part of the apparatus through a needle valve, the leak rate and flow rate being measured in the same way as for plasma polymerisation. Polymer was collected on an aluminium foil substrate placed next to the window. Typical irradiation time was about 2 hours. The window was cleaned after each run using a 100 W oxygen plasma, and its UV spectrum was taken to check that any polymer had been

removed. Calcium fluoride, suprasil and quartz, transparent above 120nm, 160nm, and 180nm respectively, were used as window materials.

For photopolymerisation at 185nm a Hanovia low pressure mercury arc lamp was used with the apparatus shown in figure 2.4. The jackets separating the UV source from the reaction chamber were made of suprasil, and the spaces between them flushed with nitrogen in order to prevent absorption of the 185nm radiation. Monomer was introduced to the chamber and irradiated for a period of about 2 hours. Polymer was collected on an aluminium foil substrate placed in a holder on a glass slide and positioned in the chamber close to the light source.

2.2.3 Analysis

XPS analyses were carried out by Kratos ES 300 or ES 200 spectrometers in fixed retardation mode using Mg $Ka_{1,2}$ X-rays (96W) of 1253.6 eV energy, and a take off angle of 35°. Samples were mounted on a 3-sided probe tip measuring approximately 17mm by 8mm, using double sided Scotch adhesive tape. C_{1s} component peak positions were assigned by reference to the experimentally determined binding energies of the various functionalities in standard samples[3c] and are constant to within ± 0.3 eV.

SIMS spectra were run in the static mode using a modified VG SIMSLAB spectrometer with a quadropole analyser, employing 2 KeV argon ions with a total ion dose of $2x10^{12}$ per sample.

TOF SIMS spectra were run on a Kratos TOF SIMS spectrometer using a gallium liquid metal ion source giving 10kV

ions with an ion current of 200 picoamps.

2.2.4 Calculation of Flow Rate and Leak Rate

Working in the vacuum range, i.e. the range used for plasma and surface photopolymerisations, gases and vapours can be considered to behave ideally, and therefore to obey the ideal gas law:

$$PV = nRT \qquad\qquad 2.1$$

        where P = pressure
              V = volume of reactor
              n = number of moles of gas
              R = gas constant
        and   T = temperature (K)

Based on this, the flow rate can be calculated from the rate of pressure increase in the system when the pumping is closed off.

$$\text{flow rate} = \frac{dn}{dt} = \frac{dP}{dt}\frac{V}{RT} \quad \text{mol sec}^{-1} \qquad 2.2$$

At STP 1 mole of gas occupies 22414 cm^3. Converting the time to minutes, and the volume to litres, this leads to equation 2.3.

$$\text{flow rate} = 74.4 \ V \ \frac{dP}{dt} \quad cm^3 \text{STP/min} \qquad 2.3$$

Leak rates can be calculated using the same formula. For accurate measurement of flow rates the leak rate should be subtracted from the measured flow rate, but since the leak rates were always very small compared with the flow rates they were considered to be negligible.
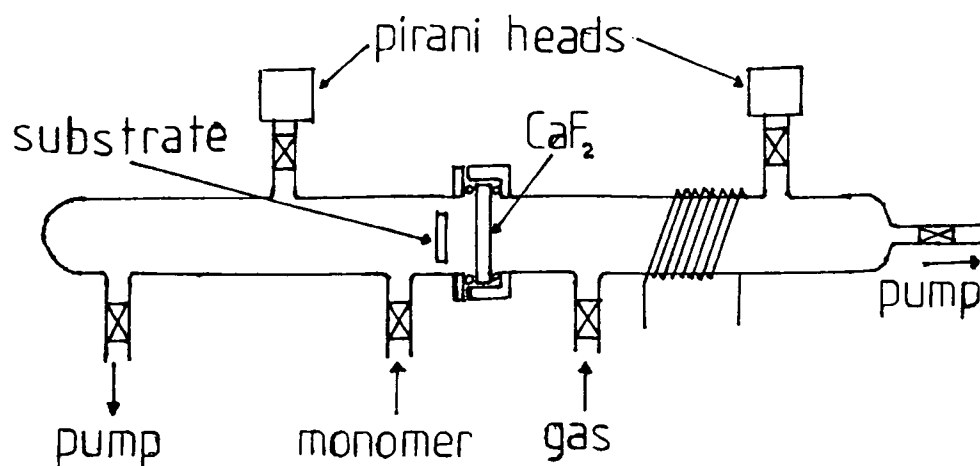

51

Figure 2.3 Photopolymerisation apparatus using a nitrogen plasma as a light source
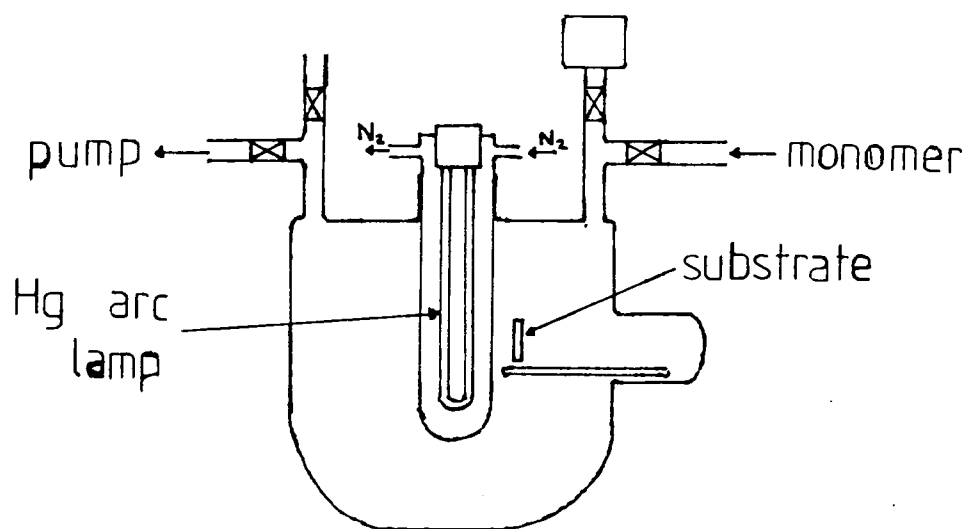

Figure 2.4 Photopolymerisation apparatus for experiments using 185nm UV radiation

2.3 RESULTS AND DISCUSSION

2.3.1 XPS of Perfluorobenzene (PFB) and Perfluorotoluene (PFT) Plasma Polymers

Typical C_{1s} core level spectra for PFT plasma polymers are shown in figure 2.5. Figure 2.5(a) shows a polymer obtained under high flow rate (1.9 cm^3/min) and low power (6W) conditions, while figure 2.5(b) is of a material made using a low flow rate (0.73 cm^3/min) and higher power (15W). The binding energies[3] and relative intensities the component peaks are shown in table 1. It can be seen that in both cases CF and CF_3 groups have been lost during polymerisation, while C-CFn and CF_2 groups have been created. The greatest changes occur in the high W/F polymer, which is as expected since there is more power available per unit monomer in this case and so more structural rearrangement might be anticipated. This is seen most clearly when comparing the relative amounts of CF, $CF-CF_n$ and CF_2. The $\pi-\pi^*$ peak is a shake-

Table 2.1 C_{1s} component peaks of PFT Plasma polymers

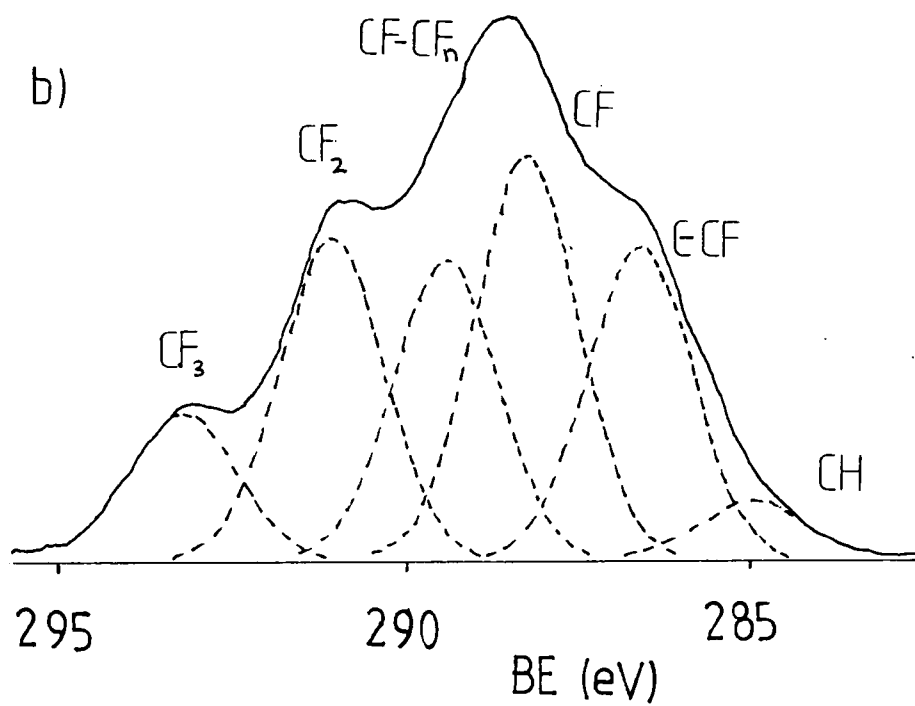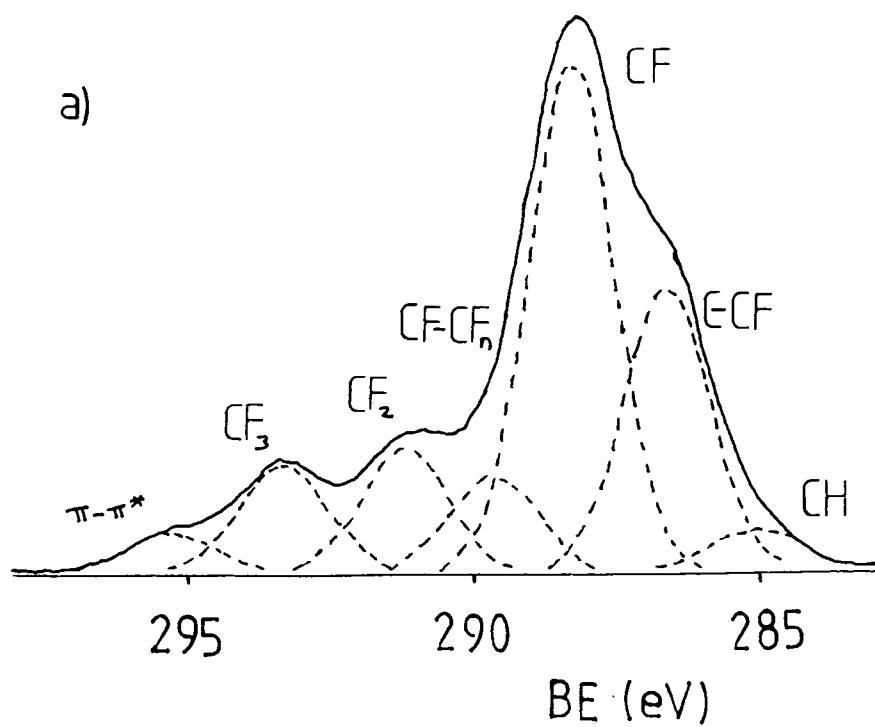| Component Peak	Binding Energy (eV)	% Contribution to C_{1s}		
		PFT[a] Monomer	High W/F Polymer	Low W/F Polymer
CH	285.0	0	3	3
$\underline{C}-CF_n$	286.6	17	24	21
CF	288.3	71	44	27
$\underline{C}F-CF_n$	289.5	0	8	20
Total CF		71	52	47
CF_2	291.2	0	11	22
CF_3	293.3	17	9	10
$\pi-\pi^*$	295.2	?	3	0.4

[a]theoretical values

53

Figure 2.5 C_{1s} core level spectra of PFT plasma polymers
(a) low W/F polymer
(b) high W/F polymer

up satellite and indicates the presence of aromatic functionality. Although it is non-quantitative, the larger shake up in the low W/F polymer suggests that more of the aromatic nature of the PFT has been retained than in the high W/F polymer. Graphs showing the changes in composition of the C_{1s} core level with respect to power and flow rate are shown in figures 2.6(a) and 2.6(b) respectively.

The F_{1s} core level spectra showed only a single peak in all cases, as the range of chemical shifts for the different fluorine environments is very low. Area ratios of the F_{1s} and C_{1s} core levels show that the F:C stoichiometry for the low W/F polymer was 0.93:1, and for the high W/F polymer was 1.16:1. This compares with a value of 1.14:1 for PFT, and shows that fluorine is lost at low W/F, but not at high W/F. This explains the larger amount of C-CF$_n$ found in the C_{1s} spectrum of the low W/F polymer. It appears therefore, that at low W/F polymerisation involves loss of fluorine and retention of aromatic structure, while at high W/F fluorine is retained and polymerisation occurs through rearrangement and opening of aromatic rings.

In all cases the O_{1s} core level showed a small peak corresponding to an O:C ratio of approximately 0.03:1. This contamination could arise from a small leak of air into the vacuum line during polymerisation, or from reaction of atmospheric oxygen with trapped free radicals in the surface of the polymer prior to analysis.

a)

PFT Plasma Polymers
power dependence at constant flow rate

b)

PFT PLASMA POLYMERS
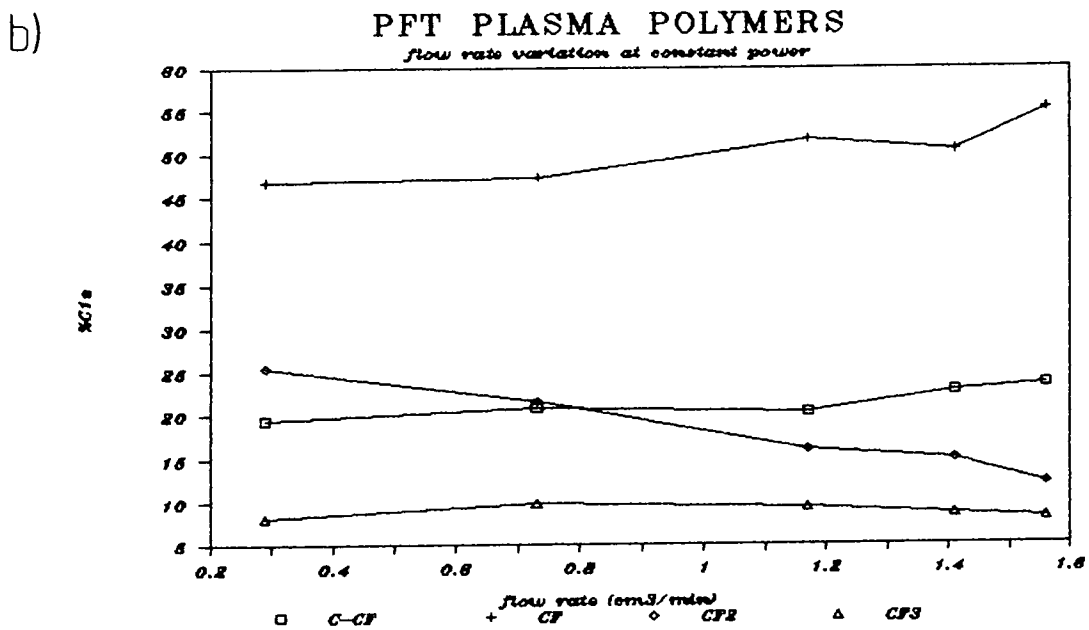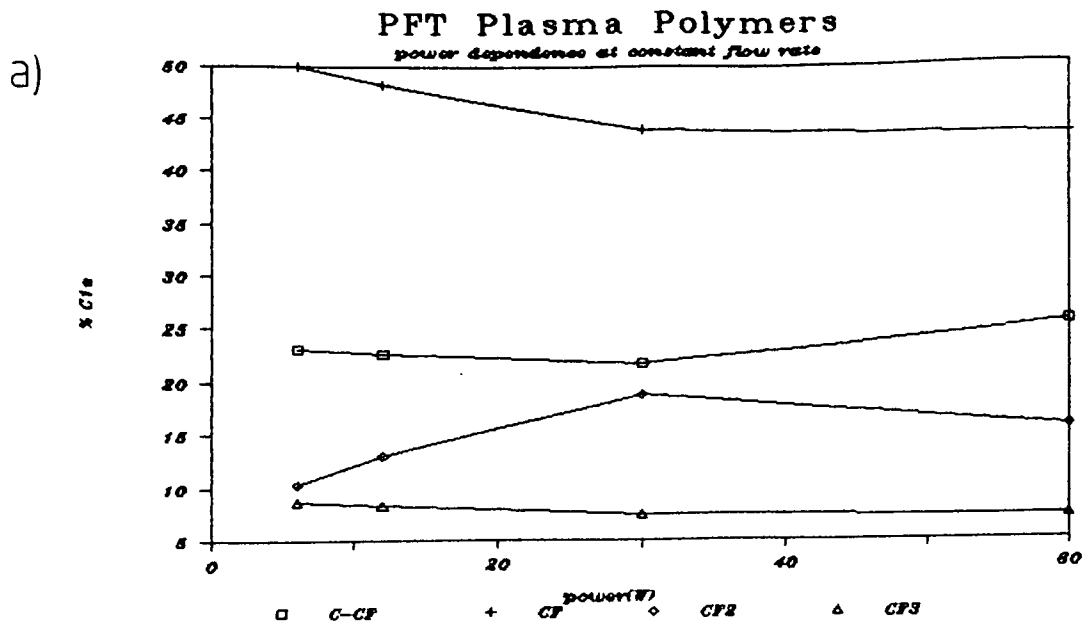### flow rate variation at constant power

Figure 2.6 Variations in composition of PFT plasma polymers with (a) power and (b) flow rate
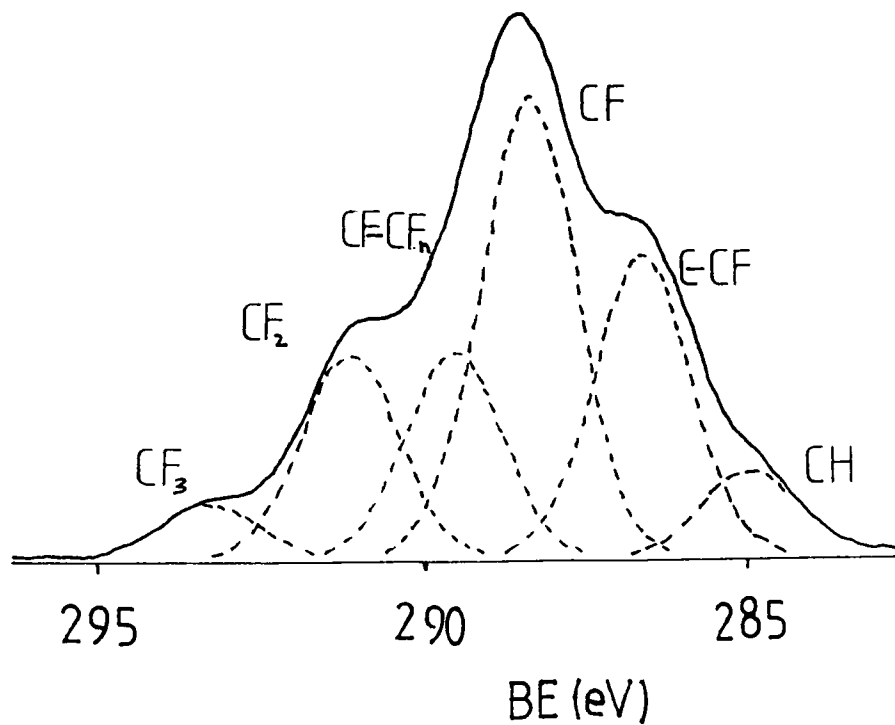
56

Figure 2.7(a) C_{1s} spectrum of a PFB plasma polymer
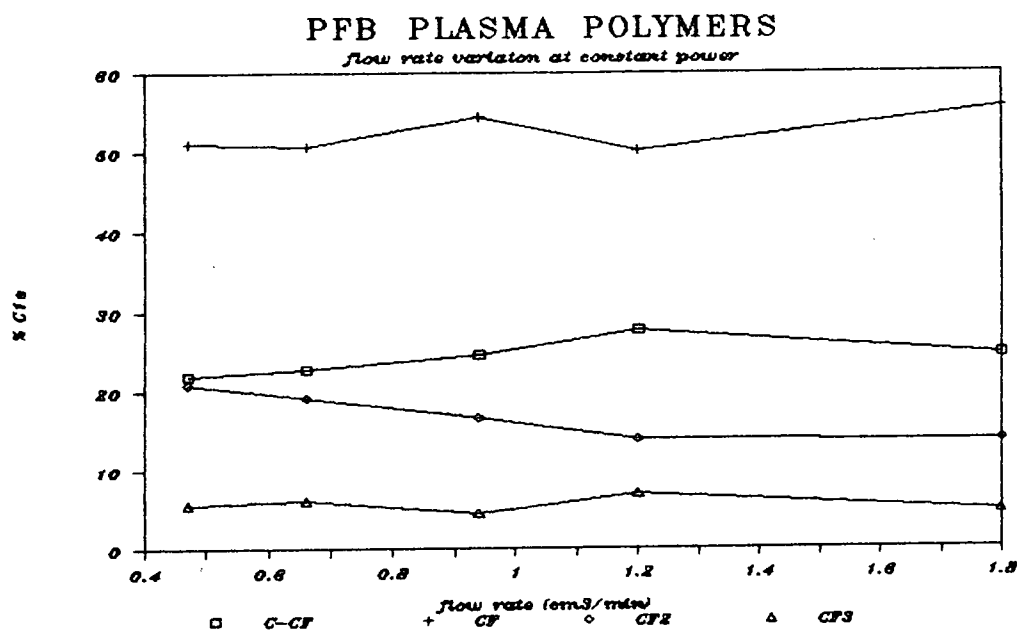
Figure 2.7(b) Variation in composition of PFB plasma polymers
flow rate at constant power (15W)

A small amount of hydrocarbon contamination was also shown by the peak at 285 eV in the C_{1s} core level spectra. This could be due to three effects: (i) a small amount of hydrocarbon present in the plasma reactor, (ii) contamination while sample was transferred to the spectrometer, or (iii) the formation of an overlayer during analysis in the spectrometer[3g], caused by hydrocarbon boiling off the X-ray cap and window.

The C_{1s} core level spectrum of a typical PFB plasma polymer (power = 15W, flow rate = 0.7 cm^3/min) is shown in figure 2.7(a). This is generally similar to the PFT plasma polymers except that there is less CF_3 and more CF, as might be expected from the monomer structure. The variation of the composition of the C_{1s} envelope with flow rate is shown in figure 7(b). The same sort of trends are observed as for PFT plasma polymers, but the actual changes are generally smaller.

2.3.2 SIMS analysis of PFB and PFT plasma polymers

The positive ion static SIMS spectrum of a PFB plasma polymer is shown in figure 2.8. Like the XPS, the positive ion SIMS shows evidence of some hydrocarbon contamination. This can be observed in the peak at 15 (CH_3^+) and in the clusters of peaks at 29-30 ($C_2H_{5-6}^+$), 39-43 ($C_3H_{3-7}^+$) and 53-57 ($C_4H_{5-9}^+$). These all correspond to peaks not present in the mass spectra of perfluorocarbons[15] and so can be taken to be indicative of the presence of hydrocarbon.
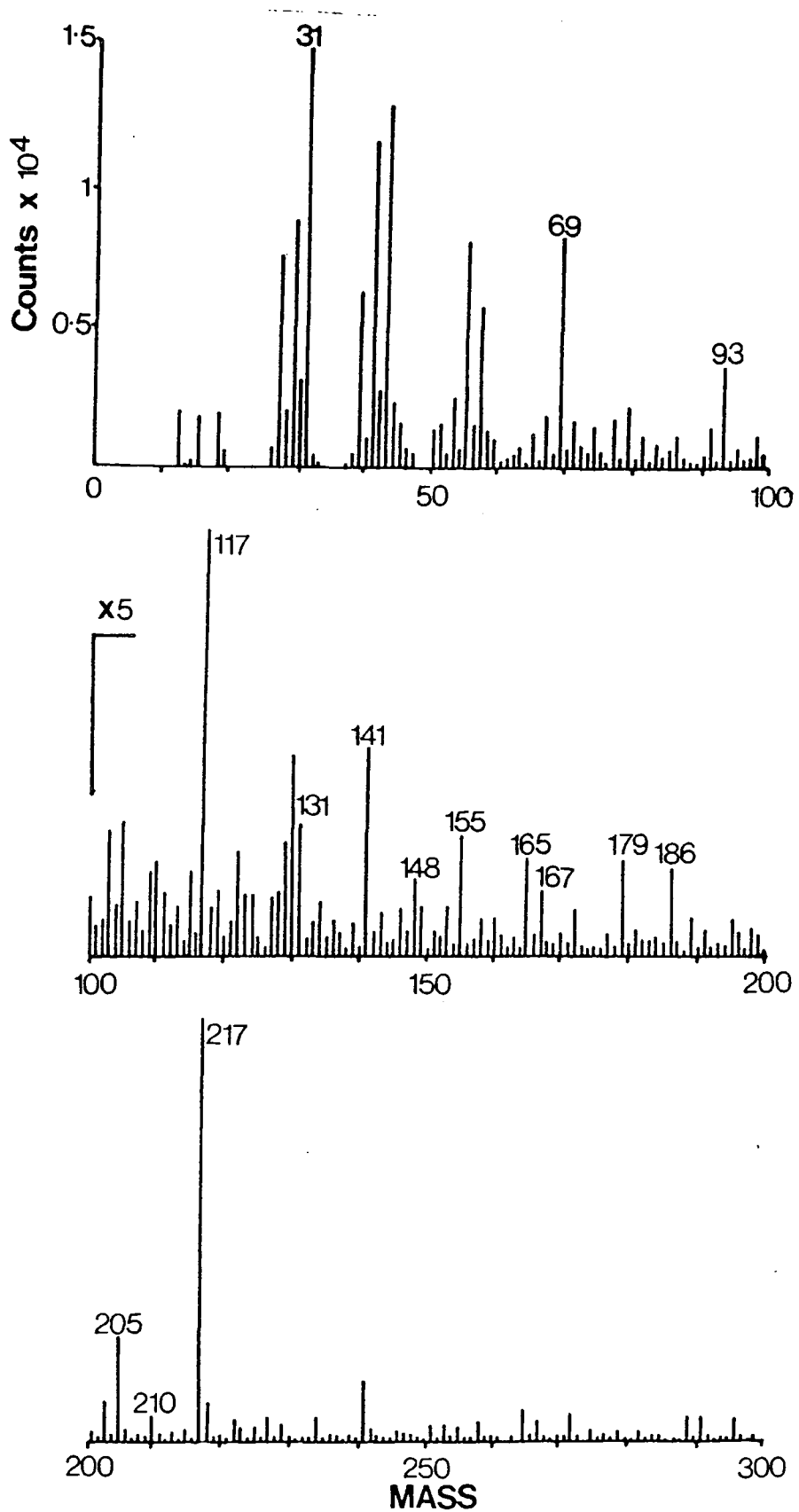
Figure 2.8 Positive ion static SIMS spectrum of a PFB plasma polymer

Table 2.2 <u>Assignments of Peaks in the Positive SIMS spectrum of</u>
<u>PP-PFB</u>

<u>A.M.U.</u>	<u>Assignment</u>	<u>Present in the E.I. MS of :-</u>
217	C7F7+	Perfluorinated Alkyl Benzenes (not Styrene)
210	C8F6+	Perfluorostyrene
205	C6F7+	Perfluoro 1,3, hexadiene
186	C6F6+	Perfluorobenzene, toluene and xylenes.
179	C7F5+	Perfluoro Alkyl Benzenes (inc. styrene).
167	C6F5+	Perfluoro Alkyl Benzenes (not styrene).
165	C9F3+	Perfluoronaphthalene and Biphenyl.
155	C5F5+	Perfluoro 1,3, hexadiene.
148	C6F4+	Perfluoro Alkyl Benzenes.
141	C7F3+	Perfluoroxylenes and styrene.
131	C3F5+	Perfluorocyclohexanes (not observed in aromatics)
117	C5F3+	Most perfluoroaromatics.
93	C3F3+	Common to all perfluorocarbons.
69	CF3+	Common to all perfluorocarbons.
31	CF+	Common to all perfluorocarbons.

The main fluorocarbon peaks below 220 a.m.u. are tabulated in table 2.2. The assignment of structural features from which the observed ions might originate has been accomplished by comparison with the electron impact mass spectra of fluorocarbons[15]. Although there may be differences in the fragmentation mechanisms between electron impact and the ion impact of SIMS, this may serve as a reasonable guide to the fluorocarbon groups present. The positive ion SIMS spectrum of PTFE[16] is basically similar to the electron impact mass spectrum of linear perfluoroalkanes, although it may contain some extra peaks of low intensities. No quantitative data can be obtained from the relative heights of the individual peaks in the SIMS spectrum, as factors such as matrix effects and sample charging can have a large influence on the peak intensities obtained, although there have been some attempts to obtain qualitative SIMS data, for example in a range of copolymer systems[17].

The peaks at 31, 69 and 93 a.m.u. correspond to the ions CF^+, CF_3^+, and $C_3F_3^+$, which are present in the mass spectra of all perfluorocarbons. Peaks at 186 (which could be assigned to the molecular ion of PFB), 167, 155 and 117 a.m.u. are all present in the electron impact mass spectrum of PFB. Peaks at 217 (which is particularly intense), 179, 148 and 141 a.m.u. are not present in the mass spectrum of PFB but are characteristic of perfluorinated alkyl benzenes. Other peaks at 210, 205, 165 and 131 a.m.u. are found in the mass spectra of perfluorostyrene, perfluoro 1,3 hexadiene, perfluoronaphthalene / biphenyl and perfluorocyclohexane respectively. There is no evidence for any perfluoroalkyl aliphatic chains in the plasma polymer.

There are a number of low intensity peaks at masses of greater than 220 a.m.u., corresponding to larger fragments from the polymer. These are more difficult to assign to any particular structure, although the peaks at 272, 253, 241 and 203 a.m.u. are characteristic of perfluoronaphthalene, and the peak at 267 a.m.u. is present in the mass spectra of perfluoroalkylbenzenes.

The negative ion SIMS spectrum of the PFB plasma polymer was dominated by the peak at 19 a.m.u. which was due to F^-. A series of peaks of diminishing intensity corresponding to C_n^- at 12, 24, 36, 48, 60 and 72 a.m.u. for n = 1-6 and C_nF^- for n = 1-6 at 31, 43, 55, 67, 79 and 91 a.m.u. were also observed. The lack of any peaks at higher molecular mass makes the negative ion data much less informative than that from the positive ions.

From the positive ion SIMS data it can be proposed that the PFB plasma polymer is composed mainly of cyclic structures (mainly aromatic with some cyclohexane, cyclohexene and cyclohexadiene) linked together by short perfluoroalkyl chains (probably no more than one carbon atom long in most cases). This is very similar to the structure proposed by Kaplan and Dilks for plasma polymerised toluene, when perfluorinated (see figure 2.1). One difference however is the presence of some naphthalene groups in the PFB plasma polymer, as indicated by the SIMS analysis.

Time of flight (TOF) SIMS analysis of a perfluorobenzene plasma polymer showed no peaks at higher mass than had been found in the spectra obtained using a quadrupole analyser. This lack of high mass fragments may be indicative of extensive cross-linking.

A series of five PFB plasma polymers made using a power of

15 watts and flow rates varying from 0.45 to 1.8 cm^3/min (the same sets of conditions as used in producing the polymers examined by XPS), were analysed using static SIMS. All gave spectra identical (apart from minor variations in individual peak intensities) to the example given above. Therefore it can be concluded that the basic structural aspects of plasma polymerised PFB are the same, no matter what flow rate conditions are used in the plasma. Differences observed in the XPS spectra of these polymers must be due to changes only in the relative abundances of the various structural features in the polymer (e.g. more aromatic groups in a high flow rate polymer, more saturated rings in a low flow rate polymer).

A similar series of PFT plasma polymers formed at 15 watts and with flow rates ranging from 0.3 to 1.55 cm^3/min were also analysed by SIMS. As for the PFB plasma polymers, no changes were observed in the SIMS spectra between any of these samples, despite differences in the corresponding XPS spectra. In fact the PFT SIMS spectra were identical to those from the PFB polymers, suggesting that plasma polymers of PFT and PFB are essentially the same material. The mechanism for the formation of the polymer is therefore probably the same in each case, with the $-CF_3$ group not playing a major role, and may be a general mechanism for the plasma polymerisation of aromatic compounds.
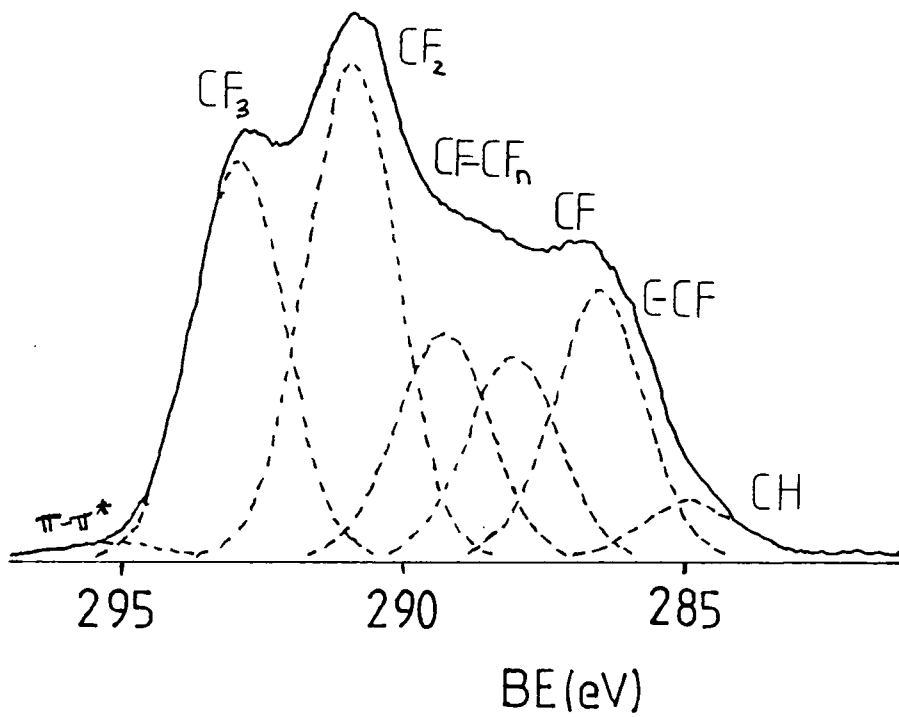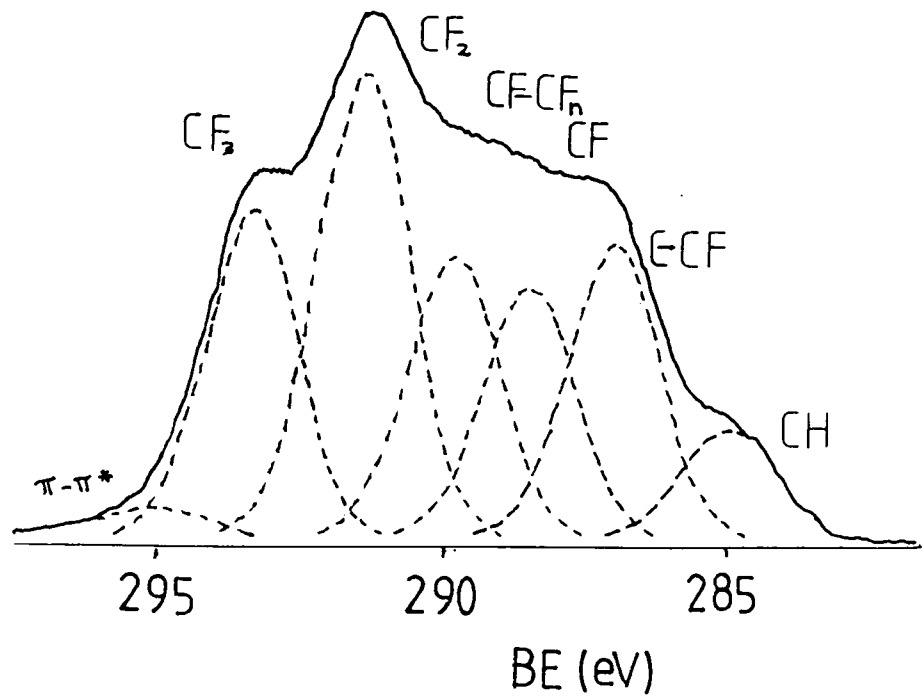
Figure 2.9 XPS C_{1s} spectra of plasma polymers of
(a) perfluorocyclohexene and (b) perfluorocyclohexane

2.3.3 Perfluorocyclohexane and Perfluorocyclohexene Plasma Polymers

Plasma polymers of perfluorocyclohexane and perfluorocyclohexene were prepared using a power of 15 watts, monomer pressure of 0.1 torr and a flow rate of 0.6 cm^3/min, and were analysed using XPS and positive and negative ion static SIMS. The results are compared with those for a perfluorobenzene plasma polymer.

The XPS C_{1s} core level spectra of the two polymers are shown in figure 2.9. It can be seen that the two are broadly similar to each other, but significantly different from the spectrum of the PFB polymer formed under similar conditions, shown in figure 2.7(a). Comparisons between the XPS spectra of these polymers and that of PFB are presented in table 2.3.

Table 2.3 Comparison of XPS analyses of plasma polymers of perfluorobenzene, perfluorocyclohexene and perfluorocyclohexane

		Perfluoro benzene	Perfluoro cyclohexene	Perfluoro cyclohexane
F:C Ratio		0.92	1.40	1.60
	CH	6	6	3
	C-CF	25	17	17
%				
	CF	35	14	13
of	$CF-CF_n$	15	16	14
	CF_2	15	26	31
C_{1s}	CF_3	4	19	25
	$\pi-\pi^*$ shake up	2	2	1

As might be expected from the composition of the monomers, the plasma polymers of perfluorocyclohexene and perfluorocyclohexane contain a considerably higher ratio of fluorine to carbon than does plasma polymerised PFB. This is manifested in the C_{1s} core level spectra in the form of much larger peaks corresponding to CF_2 and CF_3 groups, which suggests that there is much more aliphatic character to these plasma polymers. The CF peak (which includes aromatic CF groups) and the C-CF peak are considerably smaller in both cases than for the PFB plasma polymer, again suggesting less aromatic nature. The presence of a $\pi-\pi^*$ shake up satellite, however, does indicate that there is some aromaticity in all the polymers, although the $\pi-\pi^*$ peak intensity is not a reliable quantitative measure. The perfluorocyclohexane plasma polymer is generally slightly more aliphatic in character than that of perfluorocyclohexene, as would be expected from the structures of the monomers. All these plasma polymers are basically similar to those reported by Clark and Shuttleworth[3c,d].

The positive ion static SIMS spectrum of the plasma polymer of perfluorocyclohexane is shown in figure 2.10. It is basically fairly similar to the SIMS spectrum of the PFB plasma polymer shown in figure 2.8, but there are some differences. The most obvious one is the presence of considerably more high mass fragments than in the PFB spectrum. This may indicate less cross-linking in the perfluorocyclohexane plasma polymer, but it could also be caused by differences in operating conditions used in the SIMS experiment. There is no peak in the SIMS spectrum of plasma polymerised perfluorocyclohexane at 186 a.m.u. corresponding to
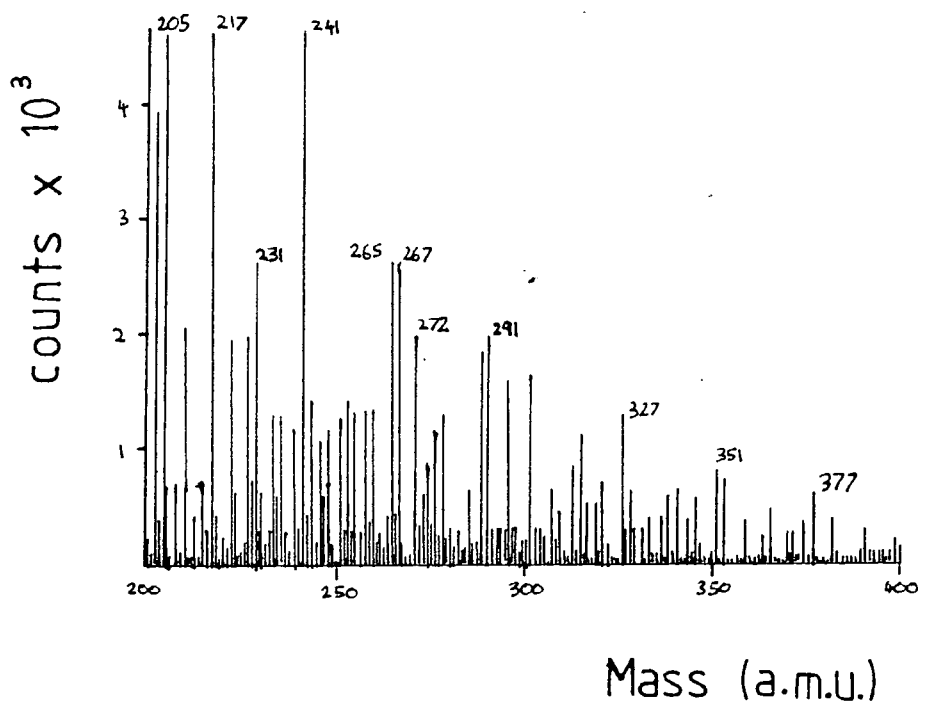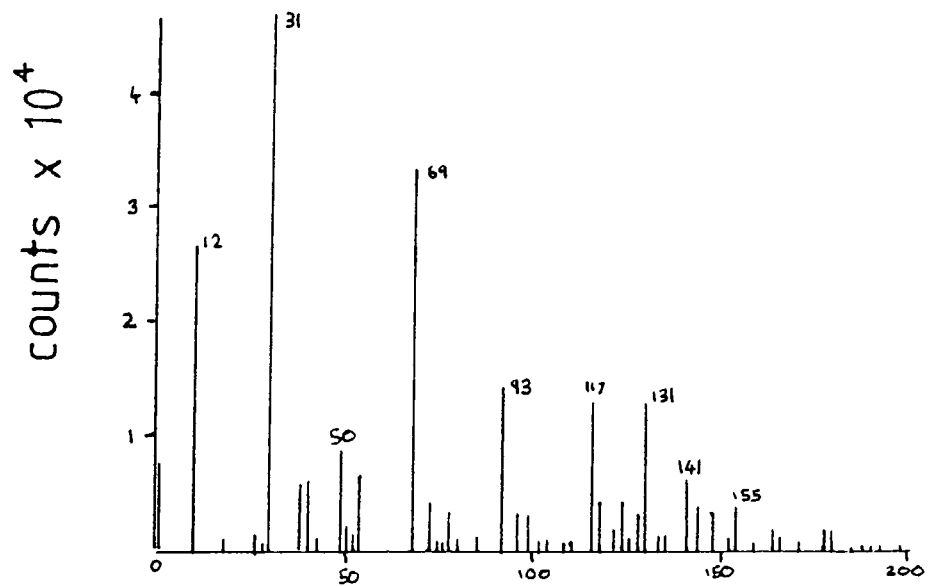
Figure 2.10 Positive ion SIMS spectrum of plasma polymerised perfluorocyclohexane

perfluorobenzene, and the intensities of peaks at 217, 179 and
167 a.m.u. arising from perfluoroalkylbenzene type structures,
are low compared to the spectrum from the PFB plasma polymer,
suggesting less aromatic character. A new peak is present at
231 a.m.u. corresponding to a $C_5F_9^+$ ion which is present in the
electron impact mass spectra of perfluorocyclohexanes. The peaks
from perfluoronaphthalene at 272, 241 and 203 a.m.u. are present
with comparatively high intensities, as is the peak at 205 a.m.u.
from perfluoro 1,3 cyclohexadiene. On the basis of this, it would
appear that the plasma polymer of perfluorocyclohexane is similar
to that of PFB, with a large number of cyclic structures. However
there seems to be fewer aromatic rings, and more saturated or
partially saturated ring systems.

The negative ion SIMS spectrum was dominated by the peak at
19 a.m.u. corresponding to the F^- ion. Unlike the negative ion
spectrum of the PFB plasma polymer, however, there were a number
of peaks in the range 100-200 a.m.u. (figure 2.11) which could
yield some structural information. The major peaks are tabulated
in table 2.4

Table 2.4 Major peaks in the negative ion SIMS spectrum of plasma
        polymerised perfluorocyclohexane

A.M.U.	Assignment	A.M.U.	Assignment
117	$C_5F_3^-$	155	$C_5F_5^-$
119	$C_2F_5^-$	169	$C_3F_7^-$
131	$C_3F_5^-$	181	$C_4F_7^-$
141	$C_7F_3^-$	193	$C_5F_7^-$
143	$C_4F_5^-$		
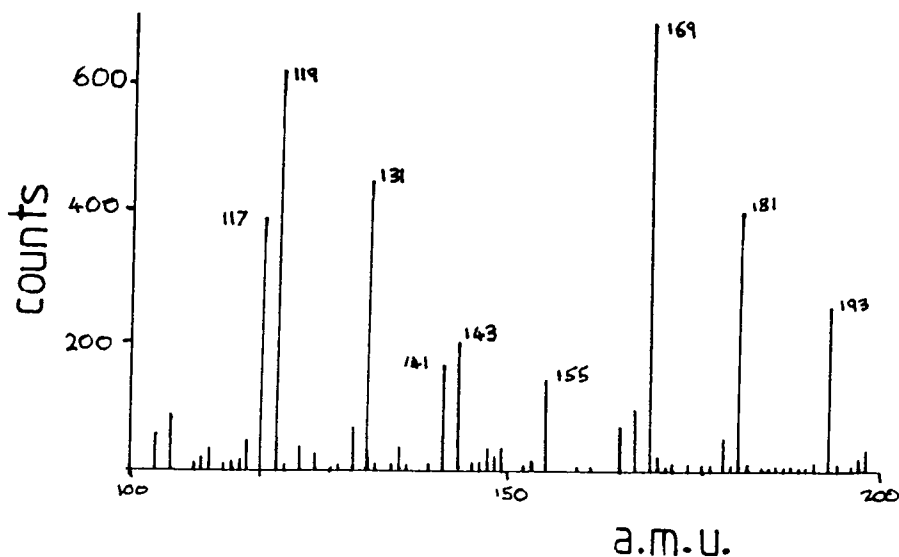
<u>Figure 2.11</u> Negative Ion SIMS spectrum of plasma polymerised perfluorocyclohexane

All of the ions listed in table 2.4 are also present in the negative ion SIMS spectrum of PTFE (figure 2.12b), although the peaks at 117, 141, 143 and 145 a.m.u. are present in considerably higher relative intensities. These are the peaks containing the higher ratios of carbon to fluorine, so their incresed intensities probably represent the presence of unsaturated structural features. Peaks at 119, 131, 169, 181 and 193 a.m.u. are all intense in the spectrum of PTFE and represent saturated aliphatic fluorocarbon. The perfluorocyclohexane plasma polymer therefore contains a considerable amount of aliphatic structure in addition to the aromatic and alicyclic structures found in the positive ion SIMS. The structure of the polymer is therefore considerably more aliphatic in character than is that of plasma polymerised PFB.
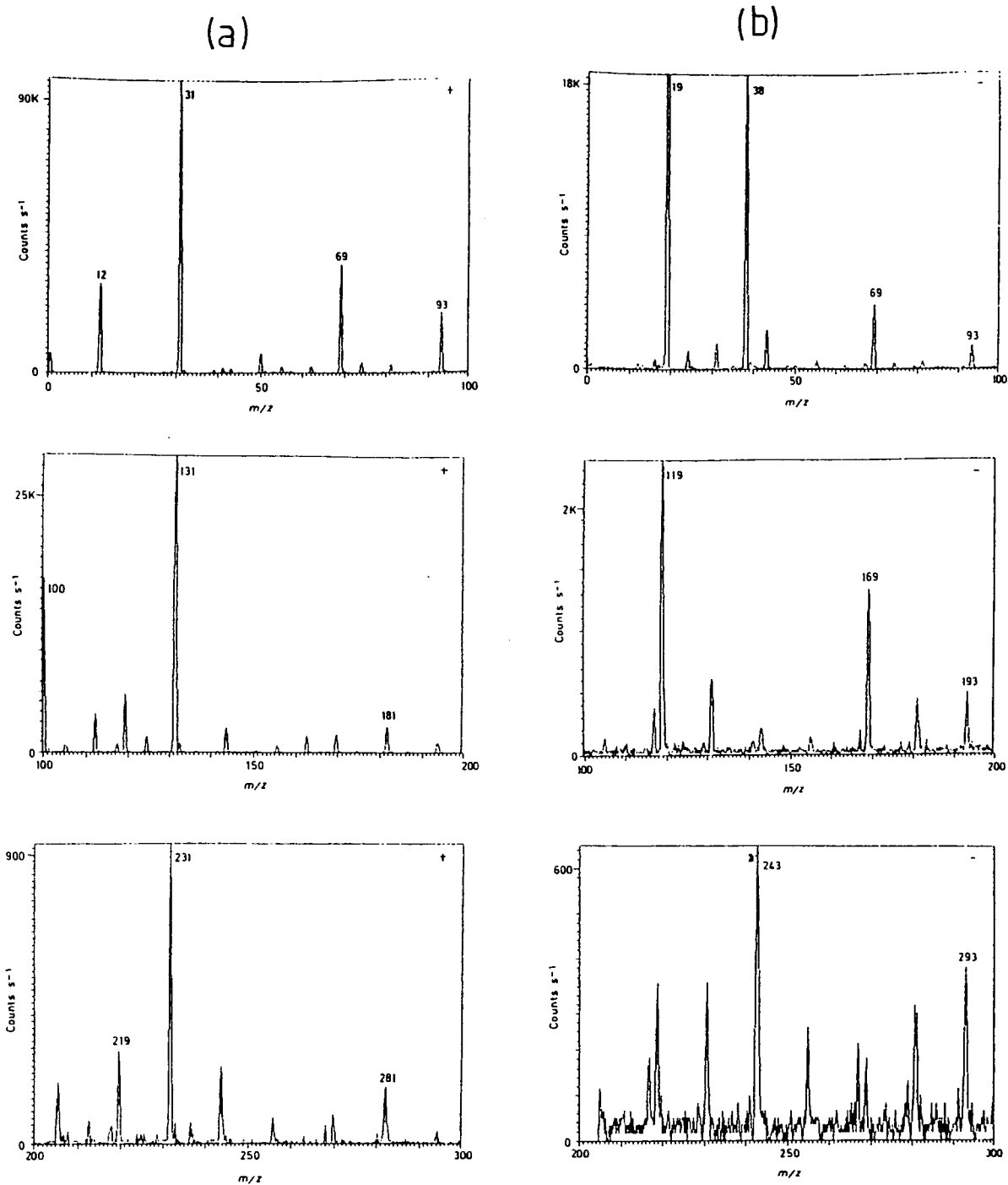
Figure 2.12 SIMS spectra of PTFE[16]. (a) Positive Ion
(b) Negative Ion

70

Another plasma polymer of **perfluorocyclohexane**, made under similar conditions, was examined by SIMS, with a time of flight analyser (TOF SIMS). The positive ion spectrum was similar to that found using the quadrupole analyser, but also contains significant peaks at 119, 143, 181 and 243 a.m.u.. These peaks are all present in the positive ion SIMS spectrum of poly (tetrafluoroethylene) (PTFE), (figure 2.12a), and are therefore indicative of aliphatic type structures.

The difference between this spectrum and that obtained with the quadrupole analyser is possibly due to slight differences in the conditions used in forming the plasma polymers. If this is so then plasma conditions used have a considerably greater effect on the SIMS spectra of perfluorocyclohexane plasma polymers than on those of perfluorobenzene or perfluorotoluene.
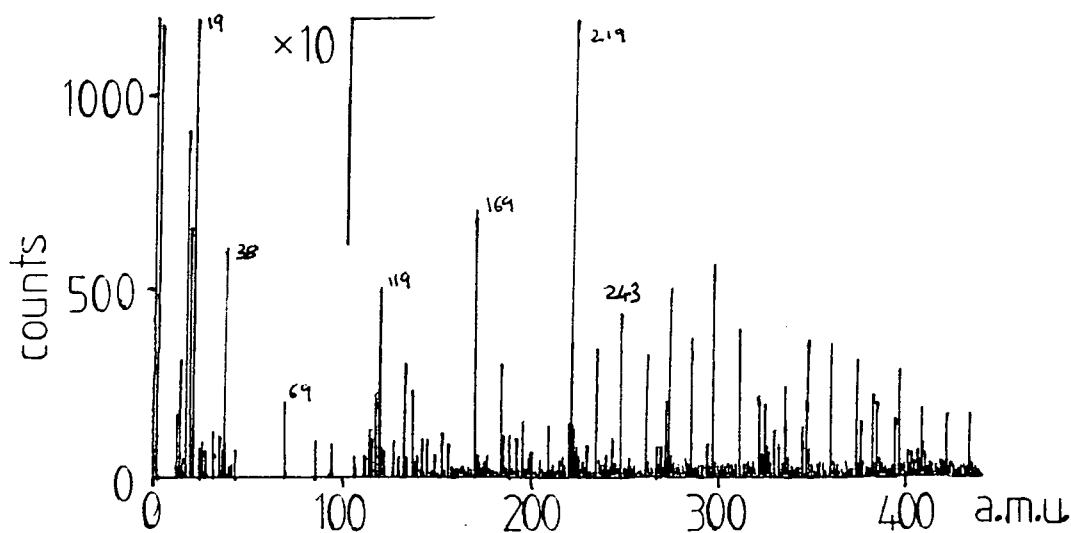
Figure 2.13 Negative ion TOF SIMS spectrum of plasma polymerised perfluorocyclohexane

The negative ion TOF SIMS spectrum (figure 2.13) contained many high mass peaks up to a mass of greater than 800 a.m.u.. The spectrum is very similar to the negative ion SIMS spectrum of PTFE (figure 2.12 b), and must therefore indicate a very large amount of aliphatic fluorocarbon. The presence of fragments of high mass is suggestive of a comparatively low degree of cross-linking. Combining the data from the positive and negative ion TOF SIMS spectra, it can be proposed that the plasma polymer is basically aliphatic perfluorocarbon, with a comparatively low degree of crosslinking, but also contains aromatic, cyclohexene, cyclohexane and naphthalene type cyclic structures. The TOF SIMS spectra are fairly similar to those obtained from a plasma polymer of n-perfluorohexane[18], suggesting that this may be fairly typical of plasma polymers of aliphatic perfluorocarbons.

The positive SIMS spectrum of the perfluorocyclohexene plasma polymer obtained using a quadrupole analyser, was similar to that of perfluorocyclohexane below 200 a.m.u. but contained little information above this point. Differences include the presence of a peak at 119 a.m.u. ($C_2F_5^+$) due to aliphatic fluorocarbon, and a small peak at 143 a.m.u. which is present in the mass spectra of perfluoroalkynes, 1,3 dienes, cyclohexenes and cyclohexanes. There was a very small peak at 186 a.m.u. corresponding to perfluorobenzene. The lack of higher mass peaks could be indicative of a more crosslinked structure, but is more likely to be simply a function of the operating conditions used. In the negative SIMS the only peaks present were at 12, 19, 24, 31 and 38 a.m.u. corresponding to C^-, F^-, C_2^-, CF^- and F_2^-. Again, the lack of information at higher mass is likely to be a

72

function of operating conditions.

TOF SIMS spectra of the perfluorocyclohexene plasma polymer contained considerably more information. Both the positive and negative ion spectra are almost identical to that of the perfluorocyclohexane apart from minor variations in peak intensity. The positive ion spectrum shows masses over 400 a.m.u. and the negative ion spectrum shows peaks up to 600 a.m.u., suggesting that the polymer is not very tightly crosslinked. The perfluorocyclohexene plasma polymer is therefore very similar to that of perfluorocyclohexane in general structure, but comparison with the data obtained from XPS would suggest that it probably contains a slightly higher percentage of aromatic and other unsaturated groups, and slightly less aliphatic fluorocarbon.

2.3.4 SIMS Analysis of Plasma Polymerised Benzene and Naphthalene

A plasma polymer of benzene was prepared using a power of 15 watts, a pressure of 0.1 torr and a flow rate of 1.5 cm^3/min, and analysed using static SIMS with a quadrupole analyser. The positive ion spectrum is shown in figure 2.14. Figure 2.15 shows a positive ion SIMS spectrum of polystyrene, and comparison of this with the spectrum of the plasma polymer shows that they are virtually identical. It is not likely however, that a benzene plasma polymer is identical to polystyrene. Plasma polymers generally have a random, highly crosslinked structure, unlike the regular repeat units found in conventional polymers. Like other plasma polymers, and unlike polystyrene, the benzene plasma

73
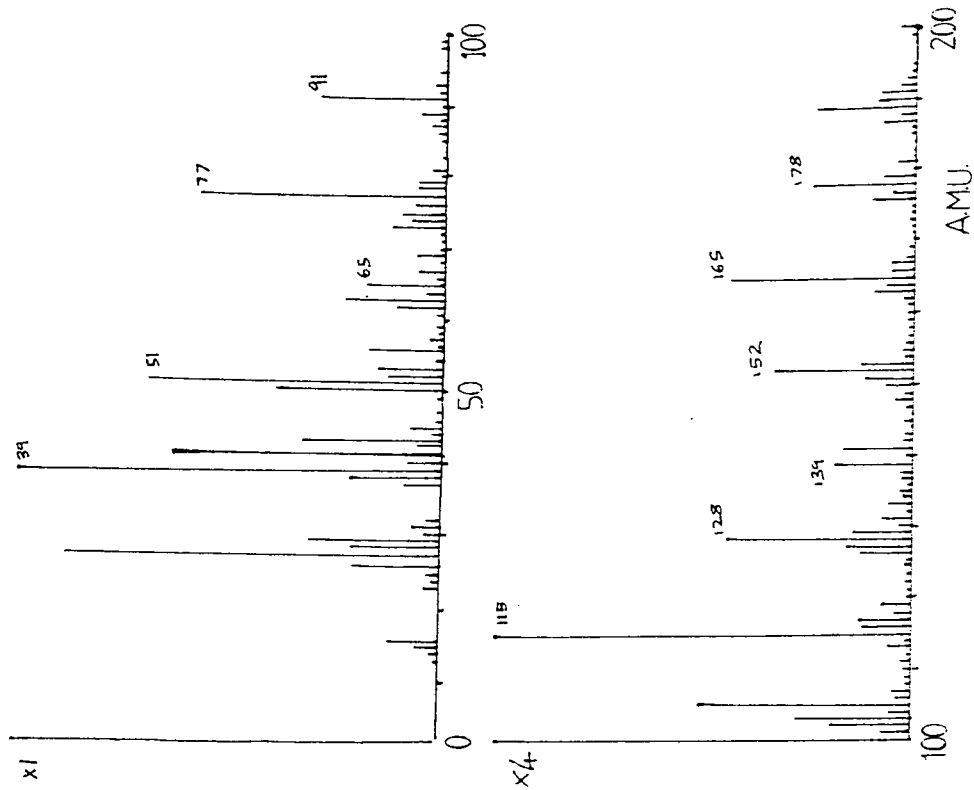
Figure 2.14 Positive Ion SIMS spectrum of plasma polymerised benzene
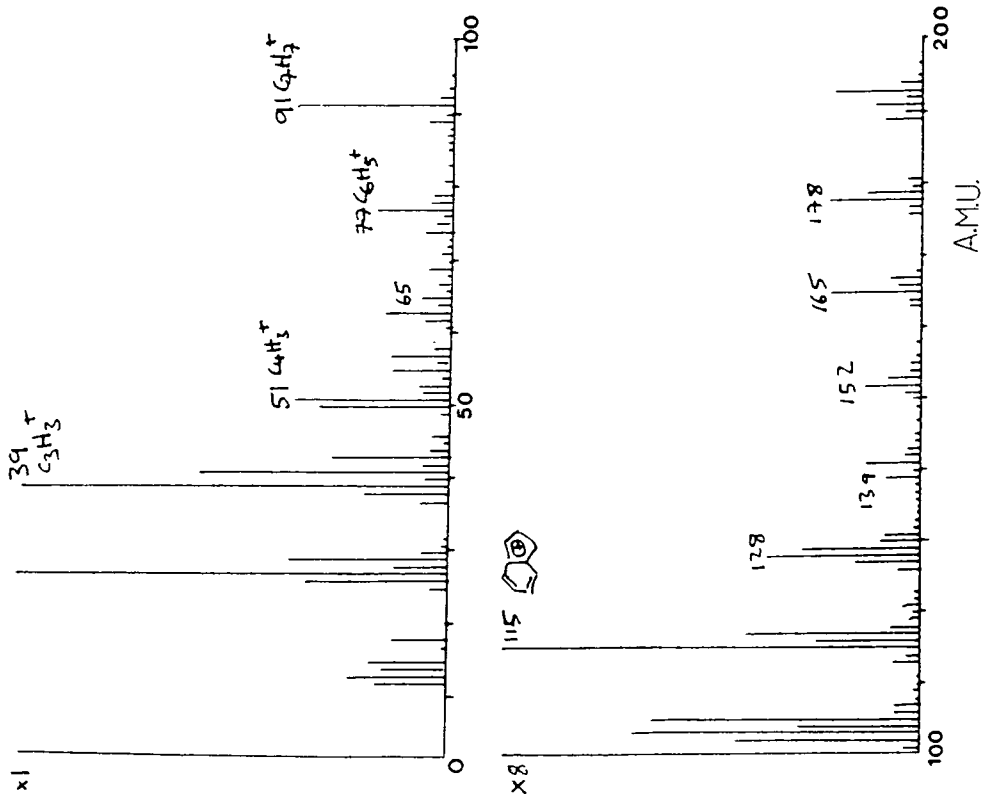
Figure 2.15 Positive Ion SIMS spectrum of polystyrene

polymer is brown coloured, oxidises rapidly in air (due to trapped free radicals), and is insoluble in organic solvents. The most likely structure for plasma polymerised benzene consists of aromatic rings and other cyclic structures joined by short alkyl chains; i.e. similar to the structure proposed for perfluorobenzene and perfluorotoluene plasma polymers, and by Kaplan and Dilks for plasma polymerised toluene[7]. The SIMS spectrum obtained is probably typical of all polymers with alkyl benzene type structures. This demonstrates that SIMS can not be relied upon to give unique "fingerprint" spectra for all materials.

The positive ion SIMS spectrum of plasma polymerised naphthalene is shown in figure 2.16. This is quite unlike the
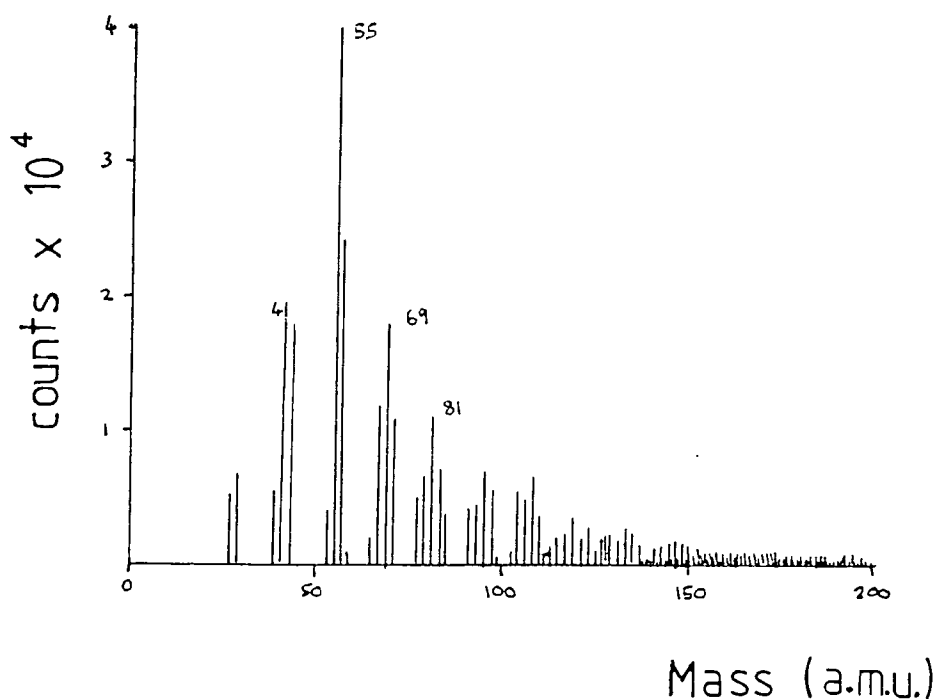
Figure 2.16 Positive ion SIMS spectrum of plasma polymerised naphthalene

75

spectra for plasma polymerised benzene and polystyrene, and is also not the same as the positive ion SIMS spectrum of poly 2-vinyl naphthalene (which is similar to that of polystyrene). Above about 100 a.m.u. peaks are observed at almost all masses of odd number (even numbered hydrocarbon masses are free radicals and hence less stable), suggesting a wide range of saturated and unsaturated hydrocarbon environments. The low intensities of these peaks may be indicative of a high degree of cross-linking.

2.3.5 Surface Photopolymerisation of Perfluorotoluene

Munro and Till[8] produced a surface photopolymer of perfluorobenzene, very similar to the plasma polymer, using an argon plasma as a source of vacuum ultra violet radiation, and calcium fluoride (cuts out wavelengths below 120 nm) as a window material. Since the plasma polymers of perfluorotoluene (PFT) and PFB have been shown to be very similar, attempts were made to repeat this experiment with PFT. Little or no polymer was found in these experiments, although a very small amount of fluorocarbon, in a sufficient range of environments to be different from adsorbed monomer, was detected by XPS in some cases. This might suggest that perfluorotoluene forms a vacuum UV photopolymer much less readily than perfluorobenzene, but similar experiments with PFB also produced little or no polymer. However, when these experiments were repeated using a nitrogen plasma as a light source instead of an argon plasma, surface photopolymers were formed from both PFB and PFT.

The explanation for this can be found by considering the

wavelengths of UV light emitted by argon and nitrogen plasmas[19].
The main emission lines from an argon plasma in the vacuum UV
region occur at 104.8 and 106.6 nm, below the cut off wavelength
of the calcium fluoride window (120 nm), and there is no emission
in the range 120-200 nm from a pure argon plasma at low pressure.
The main nitrogen emission lines consist of two doublets at 149.3
and 149.5 nm, and at 174.3 and 174.5 nm. These are wavelengths
that are transmitted through the calcium fluoride window, and
hence photopolymers formed with a nitrogen plasma but not with an
argon plasma. The formation of photopolymers in the original
experiments with PFB by Munro and Till, and to a lesser extent in
the experiments above, must be due to a leak of air into the
argon plasma. This would cause emission from nitrogen and oxygen
which could penetrate the calcium fluoride and so enable the PFB
to photopolymerise.

The C_{1s} XPS spectrum of a typical surface photopolymer of
PFT formed using a nitrogen plasma, calcium fluoride window and a
monomer vapour pressure of 0.2 torr, is shown in figure 2.17. It
can be seen that there is a significant component peak at 285 eV
(17.5% of the C_{1s}) corresponding to hydrocarbon contamination.
The source of this becomes clear when the Al_{2p} core level region
is examined, and found to contain a small peak arising from the
aluminium foil substrate. Although cleaned beforehand in a 100
watt oxygen plasma, it was not usually possible to remove all the
hydrocarbon contamination on the surface of the foil. Since the
PFT photopolymer is thin enough for the XPS to reveal the foil,
then the hydrocarbon is also revealed. A signal is also seen in
the O_{1s} region arising from aluminium oxide at the foil surface.
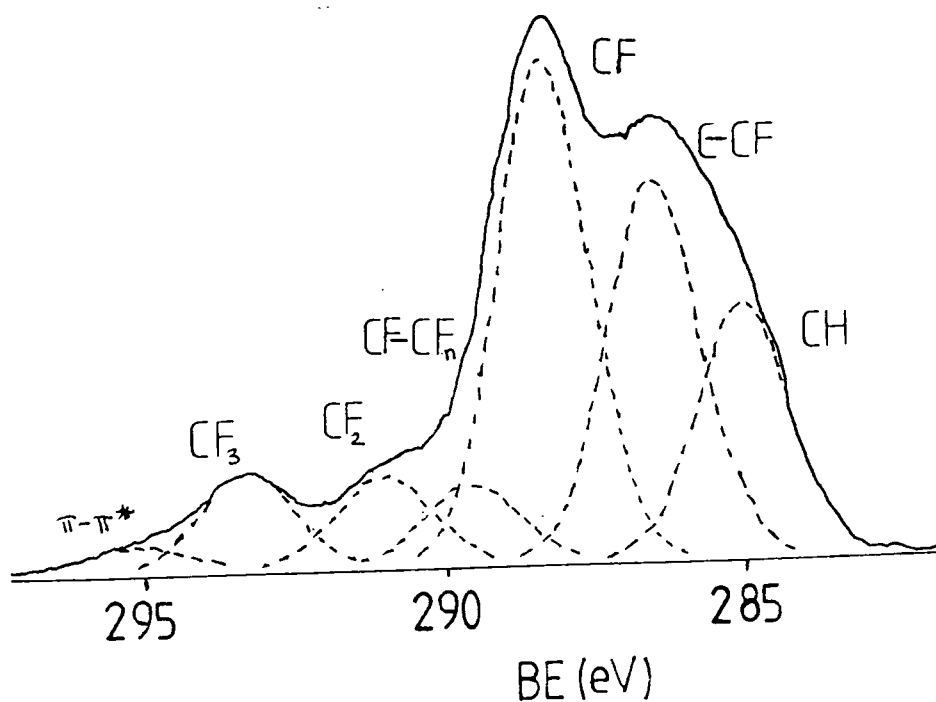
Figure 2.17 XPS C1s spectrum of a PFT photopolymer formed using an N_2 plasma with a CaF_2 window

Comparison of the C_{1s} spectrum of the PFT photopolymer with that of a low W/F plasma polymer (figure 2.5(a)) shows a great deal of similarity between the two. If the hydrocarbon contribution is ignored then the relative sizes of the component peaks in the plasma and photopolymers are as shown in table 2.5. The comparatively large size of the peak assigned to C-CF environments in the photopolymer may be due in part to a small amount of C-O, which occurs at about the same binding energy, arising from the contamination on the surface of the foil. If this were to be eliminated, then the spectra would be almost identical, with only slightly more of the more fluorinated environments present in the plasma polymer.

Table 2.5 Comparison of C_{1s} spectra of a low W/F plasma polymer and a surface photopolymer of PFT

Type of environment	% of C_{1s}	
	low W/F plasma polymer	surface photopolymer
C-CF	24	32
CF	44	43
CF-CF$_n$	8	6
CF$_2$	11	8
CF$_3$	9	8
π-π* shake up	3	2

The similarity between the photopolymer and the plasma polymer suggests that, at least under low power and high flow rate conditions, the plasma polymerisation proceeds via excited state chemistry. There is a considerable difference, however, in the deposition rates of the two polymers. The fact that the underlying substrate was still visible by XPS after 2 hours irradiation means that the surface photopolymer was only about 40Å thick. The low W/F plasma polymer was considerably thicker than this after only five minutes. One reason for this might be that the photon flux from the nitrogen plasma may be too low to produce the same concentration of excited species as are formed in the plasma by electron impact. This would also explain why the polymer formed was like a low W/F, rather than a high W/F plasma polymer. It is also possible however, that some ion chemistry is involved in the plasma polymerisation (e.g. the tropylium cation proposed by Kaplan and Dilks[6]), but does not significantly alter

the nature of the polymer formed.

In order to try to determine the nature of the excited state involved in the surface photopolymerisation, and hence the plasma polymerisation, of PFT, experiments were carried out using different combinations of light source and window. The vacuum UV absorption spectrum of PFT is similar to that of PFB[20] shown in figure 2.18, and contains S_2 and S_3 excited states centred at 198 and 178 nm, and a series of Rydberg states. The first ionisation potential occurs at 126 nm, and so it is just possible that a very small amount of ionising radiation could penetrate the calcium fluoride window, but a nitrogen plasma should produce very little radiation in the 120-126 nm range unless there is a hydrogen impurity.
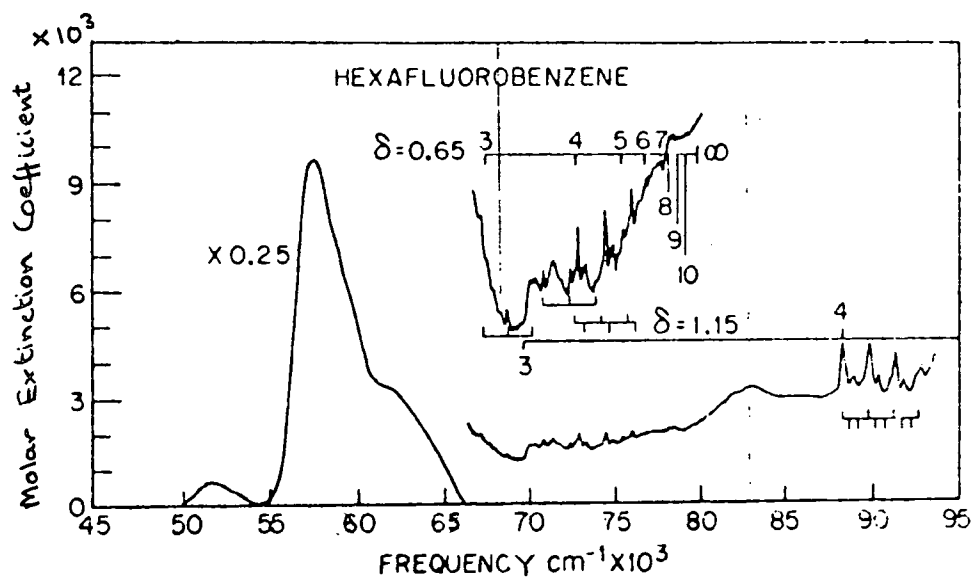
Figure 2.18 Vacuum UV absorption spectrum of Perfluorobenzene

Using a combination of a quartz window (cut off = 180 nm) and a nitrogen plasma no polymer could be produced. This is perhaps not very surprising as a nitrogen plasma emits little radiation in the 180-200 nm range, but since a considerable amount of radiation above 200 nm would be present, it does show that vacuum UV is required to form a PFT photopolymer.

Replacing the quartz window with one of suprasil (cut off = 160 nm), a very small amount of photopolymer was produced after 2 hours irradiation. This was only just detectable by XPS, its presence being shown by a small amount of CF_2 observable in the C_{1s} spectrum (figure 2.19). Other fluorocarbon environments present are also probably part of the polymer, but could also arise from adsorbed monomer. This polymer must have arisen from the radiation at 174 nm, and so from the S_3 state of PFT. The reason for the very low deposition rate is probably due to the fact that the transmission of light at this wavelength through the suprasil window is only partial, and so the UV intensity reaching the PFT must be very low.

Using a low pressure mercury arc lamp (emitting at 185 nm) in combination with suprasil produced a surface photopolymer at a deposition rate comparable to that with a nitrogen plasma and calcium fluoride window. The XPS C_{1s} spectrum of this polymer is shown in figure 2.20. The spectrum is similar to the photopolymer produced using the nitrogen plasma, but seems to contain more CF-CF_n and less CF environments which may indicate a decrease in the aromaticity of the polymer. The polymer at 185 nm must have been formed via the S_3 excited state, which probably then underwent a

81
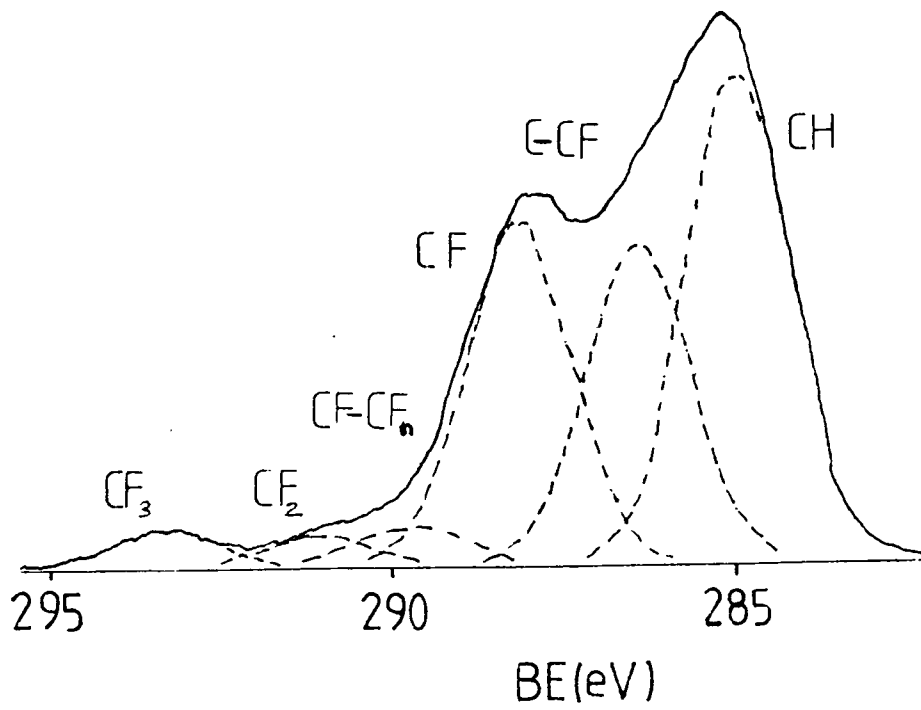
Figure 2.19 XPS C_{1s} spectrum of a PFT photopolymer formed using a nitrogen plasma and suprasil window
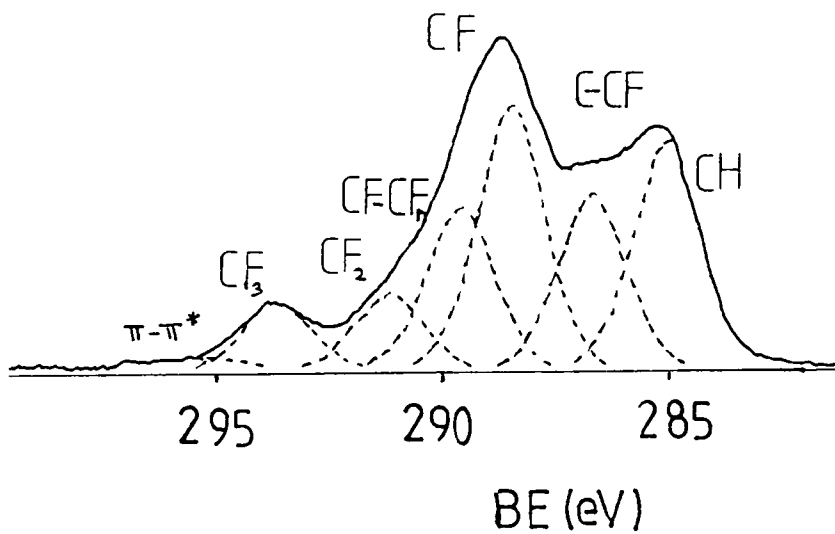
Figure 2.20 XPS C_{1s} spectrum of a PFT photopolymer formed at 185 nm

82

collapse to an S_0^v vibrationally excited ground state, as proposed by Ward and Wishnok[10] for benzene. The reason for the slight difference between this and the polymer formed with the nitrogen plasma could be due to the participation of a Rydberg state in the latter case, activated by the second nitrogen emission line at 149 nm. Polymer formation has been observed previously in the photolysis of benzene at 147 nm[21]. As the vacuum UV absorption spectrum of benzene is similar to that of perfluorobenzene and perfluorotoluene[20], this polymer must have been formed via a Rydberg state. The plasma polymerisation of PFT therefore probably proceeds via both the S_3 and Rydberg states.

2.4 SUMMARY

Plasma polymers of PFT and PFB are composed mainly of a perfluorinated alkyl benzene type structure, with benzene rings linked together by very short alkyl chains. The polymers also contain perfluoro naphthalene, cyclohexadiene, cyclohexene and cyclohexane rings, in a highly crosslinked network. SIMS analysis can detect no changes in the plasma polymers made under different conditions, but XPS shows that at low power and high flow rate the polymer contains a high percentage of aromatic type species, while at high power and low flow rate there are more aliphatic species (e.g. CF_2 groups) present.

Plasma polymers of perfluorocyclohexene and perfluorocyclohexane appear to contain similar alkyl benzene, naphthalene, cyclohexadiene, cyclohexene and cyclohexane type structures. These are however present omly in comparitively small

quantities, the bulk of these plasma polymers being made up of aliphatic fluorocarbon. The polymers are probably less crosslinked than the plasma polymers of PFB and PFT. Although not fully investigated, it appears that, unlike PFB and PFT, the perfluorocyclohexane plasma polymers made under different conditions may give different SIMS spectra. The plasma polymer of perfluorocyclohexene appears by XPS to contain slightly less aliphatic and more aromatic structure than that of perfluorocyclohexane.

Plasma polymerised benzene appears by SIMS to be the same as polystyrene, but the actual structure is more likely to be of the polyalkyl benzene type, similar to the PFB plasma polymer.

Like PFB, PFT can form a surface photopolymer similar to a plasma polymer from vacuum UV irradiation, indicating that the plasma polymerisation can proceed via excited states and that ion chemistry is not necessarily required. The photopolymer can be produced through initial excitation to the S_3 state, probably followed by collapse to a highly vibrationally excited ground state, but it is likely that Rydberg states also play a role in the plasma polymerisation.

REFERENCES

1a. H.Schuler and A.Michel, Z. Naturforsch, 10a, 495, (1955)

 b. H.Schuler, K.Prchal and E.Kloppenburg, Z. Naturforsch, 15a, 308, (1960)

2. A.Streitwieser and H.R.Ward, J. Am. Chem. Soc., 85, 539, (1963)

3a. D.T.Clark and D.Shuttleworth, J. Polym. Sci., Polym. Chem. Ed., 16, 1093, (1978)

 b. D.T.Clark and D.Shuttleworth, J. Polym. Sci., Polym. Chem. Ed., 17, 1317, (1979)

 c. D.T.Clark and D.Shuttleworth, J. Polym. Sci., Polym. Chem. Ed., 18, 27, (1980)

 d. D.T.Clark and D.Shuttleworth, J. Polym. Sci., Polym. Chem. Ed., 18, 407, (1980)

 e. D.T.Clark and M.Z.AbRahman, J. Polym. Sci., Polym. Chem. Ed., 19, 2129, (1981)

 f. D.T.Clark and M.Z.AbRahman, J. Polym. Sci., Polym. Chem. Ed., 19, 2689, (1981)

 g. D.T.Clark and M.Z.AbRahman, J. Polym. Sci., Polym. Chem. Ed., 20, 1717, (1982)

 h. D.T.Clark and M.Z.AbRahman, J. Polym. Sci., Polym. Chem. Ed., 20, 1729, (1982)

 i. D.T.Clark and M.Z.AbRahman, J. Polym. Sci., Polym. Chem. Ed., 21, 2907, (1983)

4. N.Inagaki, T.Nakanishi and K.Katsuura, Polym. Bull. (Berlin), 9, 10-11, 502-6, (1983)

5. A.B.Gil'man, R.R.Shifrina, V.M.Kolotyrkin, Platonov and K.V.Dvornikova, J. Fluorine Chem., 28, 1, 47-75, (1985)

6. S.Kaplan and A.Dilks, Org. Coat. Appl. Polym. Sci. Proc., 47, 212-16, (1982)

7. S.Kaplan and A.Dilks, J. Polym. Sci., Polym. Chem. Ed., 21, 1819-29, (1983)

8. H.S.Munro and C.Till, J. Polym. Sci., Polym. Chem. Ed., 26, 2873-79, (1988)

9a. J.E.Wilson and W.A.Noyes, J. Am. Chem. Soc., 63, 3025, (1941)

 b. K.Shindo and S.Lipsky, J. Chem. Phys., 45, 6, (1966)

85

c. J.K.Foote, M.H.Mallon and J.N.Pitts, J. Am. Chem. Soc., 88, 3698, (1966)

10. H.R.Ward and J.S.Wishnok, J. Am. Chem. Soc., 90, 5353, (1968)

11. J.K.Stille, R.L.Sung and J.Vanderkooi, J. Org. Chem., 30, 3116, (1965)

12. J.Amouroux and S.Thomas, ISPC-7, (Eindhoven), (1985), 1261.

13. M.Ross, Diss. Abstr. Int. B, 42, 6, 2357, (1981)

14. C.Till, Ph.D. Thesis, Durham, (1986)

15. J.R.Majer in "Advances in Fluorine Chemistry", Eds. M.Stacey, J.C.Tatlow and A.G.Sharpe, Butterworths, (1961)

16. J.C.Vickerman, A.Brown and D.Briggs, "Handbook of Static Secondary Ion Mass Spectroscopy", Wiley, Chichester, (1989)

17. D.Briggs and B.D.Ratner, Polym. Commun., 29, 6, (1988)

18. H.S.Munro and A.G.Shard, Unpublished Data.

19. H.Okabe, J. Opt. Soc. Amer., 54, 478, (1963)

20. M.B.Robin in "Higher Excited States of Polyatomic Molecules", Vol 2, Academic Press, London, (1975)

21. W.M.Jackson, J.L.Faris and B.Donn, J. Phys. Chem., 71, 3346, (1967)

CHAPTER 3

A MASS SPECTRAL ANALYSIS OF POLYMERISING BENZENE

AND PERFLUOROBENZENE PLASMAS

3.1 INTRODUCTION

A full understanding of the mechanisms involved in plasma polymerisation cannot be obtained without some analysis of the species present in the gas phase of the plasma. There are a variety of diagnostic techniques available which can provide information concerning the composition of a plasma; e.g. visible/UV optical emission spectroscopy[1], laser induced fluorescence[2], infra red absorption[3] and electron probe methods[4]. More information about these techniques can be found in chapter 1. The most useful diagnostic method however, is probably plasma mass spectroscopy. This involves the attachment of a mass spectrometer to the plasma chamber and the sampling of species from the plasma through a small hole. This can provide direct information about the ionic species present in the plasma, and if an ionisation chamber is used the neutral species from the plasma can also be investigated. From this a clear picture of the composition of a plasma can be obtained.

Mass spectroscopy has been used previously to examine the composition of polymerising plasmas of a number of compounds. In plasmas of methane hydrocarbon species containing up to seven carbon atoms have been observed in the plasma[5,6], indicating that considerable oligomerisation occurs in the gas phase, and that polymerisation reactions are not confined to the surface. Vasile and Smolinsky[6] correlated the abundances of certain gas phase species with the polymer deposition rate and concluded that ionic species such as $C_2H_3^+$, $C_2H_2^+$, CH_3^+, CH_2^+ and CH^+ had the greatest influence on the rate of polymer formation, while the neutral species such as CH_4, C_2H_2, C_2H_4 and C_2H_6 had the least influence.

It was also noted that the composition of the plasma varied depending on whether the sample was taken from close to the electrodes or close to the walls of the chamber. Mass spectroscopic studies of ethylene[7], acetylene[8,9] and tetrafluoroethylene[10] plasmas also showed the formation of oligomeric species in the gas phase, although that of a vinyltrimethylsilane plasma did not[11]. In contrast to the methane and other hydrocarbon systems, the formation of polymer in the case of tetrafluoroethylene appeared to be dominated by neutral species rather than positive ions. The ionic species observed were thought to derive from electron impact ionisation of neutral species in the plasma, or from sputtering of the polymer on the walls of the reactor, and to not be an integral part of the polymerisation process.

In this chapter the mass spectra of three plasma systems are examined: (a) benzene, (b) perfluorobenzene and (c) a benzene/perfluorobenzene mixture. Mass spectra of benzene plasmas have been examined previously[12,13] and have shown that there are a considerable number of dimeric products present in the positive ion spectrum, but at higher mass little was observed apart from a few very low intensity peaks up to a mass of about 400 a.m.u.[12]. The neutral mass spectrum was dominated by the C_6H_6 peak at 78 a.m.u., which led to speculation by Vasile and Smolinsky[13] that benzene might be polymerising via isomers such as fulvene formed through excited state chemistry. This is similar to the mechanism proposed by Munro and Till for perfluorobenzene[14] and also considered for perfluorotoluene in chapter 2.

A perfluorobenzene plasma has not been examined previously

by mass spectroscopy, but optical emission studies have shown the presence of CF_2 radicals and radical cations[15]. The species detected by mass spectroscopy are compared with those observed in the benzene plasma, and also with the SIMS analysis of a PFB plasma polymer discussed in chapter 2. This might show whether the species detected in the gas phase are incorporated into the polymer, or merely occur as volatile products.

Mixtures of benzene and perfluorobenzene have been found to copolymerise when subjected to a plasma[14]. The polymer formed is not simply a mixture of the plasma polymers of benzene and PFB, which would be the case if the two monomers were just co-depositing, but is different from both. This implies that there must be some sort of interaction between the two in the plasma. Mass spectroscopic analysis of the copolymerising plasma should show whether or not this is the case, and might give some indication as to the nature of any interactions. For further information about plasma copolymerisation see chapter 5.

3.2 EXPERIMENTAL

The experiments were carried out in a stainless steel vacuum chamber evacuated to a base pressure of approximately 10^{-6} torr by a diffusion pump. Monomer vapour was admitted to the chamber via a needle valve to the desired pressure, which was measured using a baratron pressure gauge. RF power was applied to an electrode in the plasma chamber and the plasma was balanced using a matching network. Species from the plasma were sampled through
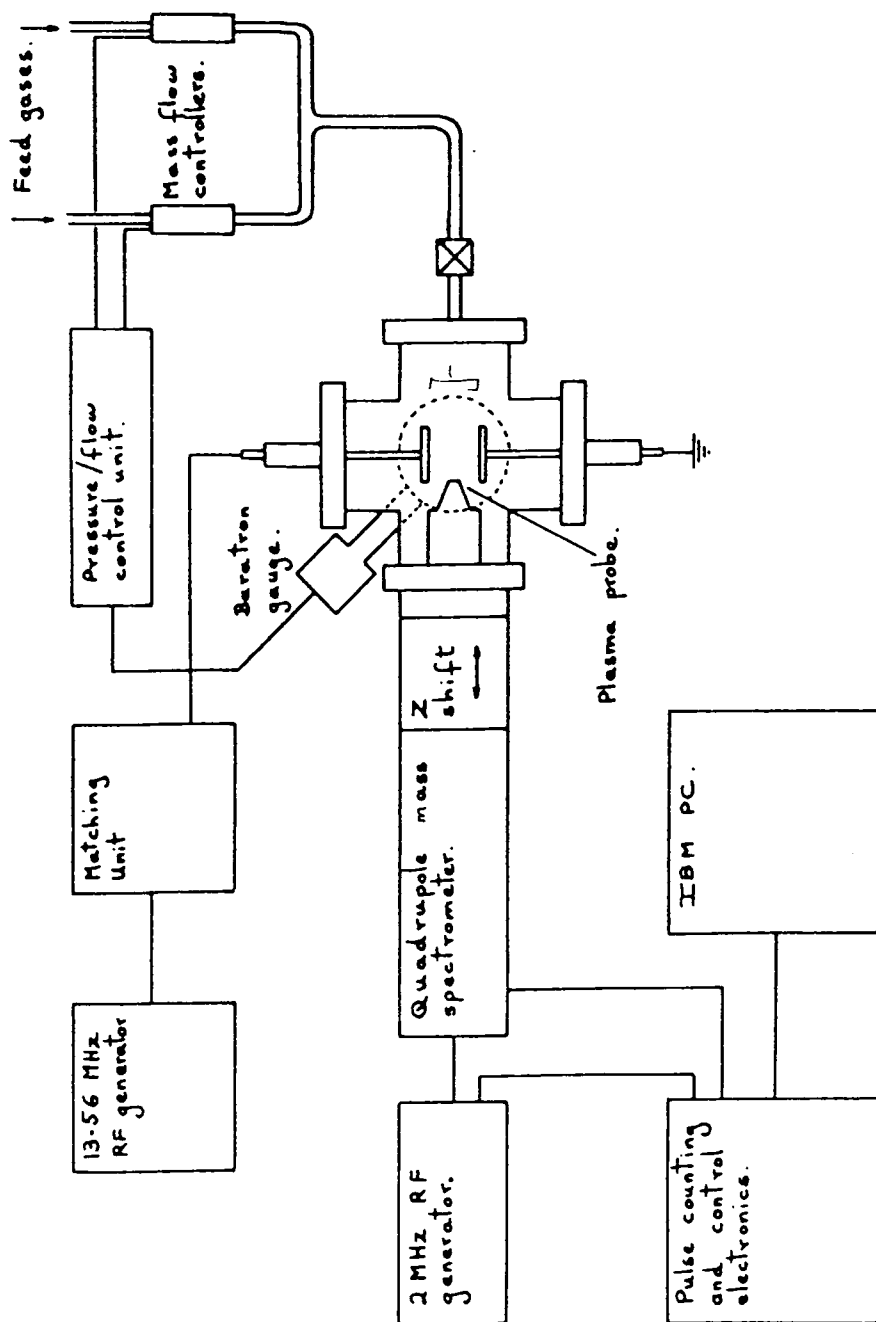
Figure 3.1 A schematic diagram of the plasma sampling quadrupole mass spectroscopy system

91

Labels: Electron multiplier | Quadrupole | CMA | Ion source | Einzel lens | Plasma probe

filament

To amplifier.

Typical ion trajectory.

Voltage	Ion Energy Analysis	Ion Mass Analysis	Neutrals Mass Analysis
V_{PB}	Ramped. E_I	Fixed. E_I	Fixed. $E_I \sim V_S$
V_1	Fixed. V_{pass}	Fixed. V_{pass}	Fixed. V_{pass}
V_{CMA}	Ramped. $E_I-\Delta$	Fixed. $E_I-\Delta$	Fixed. $E_I-\Delta$
$V_2\,V_B$	Ramped. E_I-V_{pass}	Fixed. E_I-V_{pass}	Fixed. E_I-V_{pass}
V_S	O	O	Fixed. 5-10 V
V_L	Ramped. $2E_I$	Fixed. $2E_I$	O
V_{PP}	Fixed. O-10V	Fixed. O-10V	O

E_I = Ion energy
V_{pass} = CMA pass energy.
V_{PB} = Pole bias voltage.
V_{CMA} = CMA retard voltage.
V_S = Ion source voltage.
V_L = Lens voltage.
V_{PP} = Plasma probe voltage
V_1, V_2, V_3. Lens voltages.

Figure 3.2 Internal structure of the SXP300/CMA mass spectrometer

a small hole in a probe which could be moved towards or away from the RF electrode, and could thus sample different regions of the plasma. This probe was attached to a 0-300 a.m.u. quadrupole mass spectrometer (figure 3.2) which was maintained at a pressure of about 10^{-6} torr by a turbomolecular pump. Ions from the plasma were focused through mass and energy analysers onto an electron multiplier, the signal from which was amplified and passed to an IBM PC computer where the results were displayed. Neutral species from the plasma could be analysed by using electron impact ionisation in an ion source chamber before the analyser to produce positive ions which could be detected by the electron multiplier. In order to avoid ions from the plasma also being detected, the ion focusing lens was earthed while analysing neutral species. Negative ions could unfortunately not be detected using this system.

For the copolymerisation experiment the two monomer vapours were mixed before they entered the plasma chamber. Unfortunately the ratio of the two in the monomer feed could not be determined accurately, but was approximately 1:1. Perfluorobenzene and benzene were supplied by Aldrich and degassed before use.

Deposition of polymer from the plasmas being analysed eventually led to the problem of the sampling hole becoming blocked. Some polymer could be removed by igniting an oxygen plasma in the chamber, but if there was a large amount of polymer to be removed, the apparatus had to be taken apart and cleaned. Partial blocking of the sampling hole affected some of the copolymerisation experiments restricting the number of ions which could be sampled.

3.3 RESULTS AND DISCUSSION

3.3.1 Benzene

a) Positive Ions

The positive ion mass spectrum of a benzene plasma with a power of 50 watts and a pressure of 0.04 torr is shown in figure 3.3. This spectrum was taken with the probe in an intermediate position between the edge of the plasma and the RF electrode, but since little variation was observed between different probe positions it can be taken to be representative of the plasma as a whole. The spectrum was taken of ions with an energy of 22 eV, since this is the point at which the ion energy distribution (observed for $C_6H_6^+$ ions) reached a maximum (figure 3.4). The ion energies measured are probably not the same as those of ions in the plasma, as there is probably some acceleration of the ions in the sheath between the plasma and the probe.

By far the most abundant ion observed was the molecular ion of benzene at 78 a.m.u.. Clusters of peaks were observed for fragments corresponding to $C_2H_n^+$ up to $C_{12}H_n^+$. The most prominent peaks are listed on table 3.1. The ions with masses of less than 78 a.m.u. could simply arise from electron impact on benzene or other molecules in the plasma, but the species detected with 7-12 carbon atoms are clearly the products of reactions in the plasma, and may represent initial stages of polymerisation. Among the major ions detected in this region were the molecular ions of toluene, naphthalene and biphenyl at 92, 128 and 154 a.m.u. respectively. These and most of the other ions detected have hydrogen to carbon ratios of 1 or slightly less, indicating a high level of unsaturation and suggesting that the aromatic
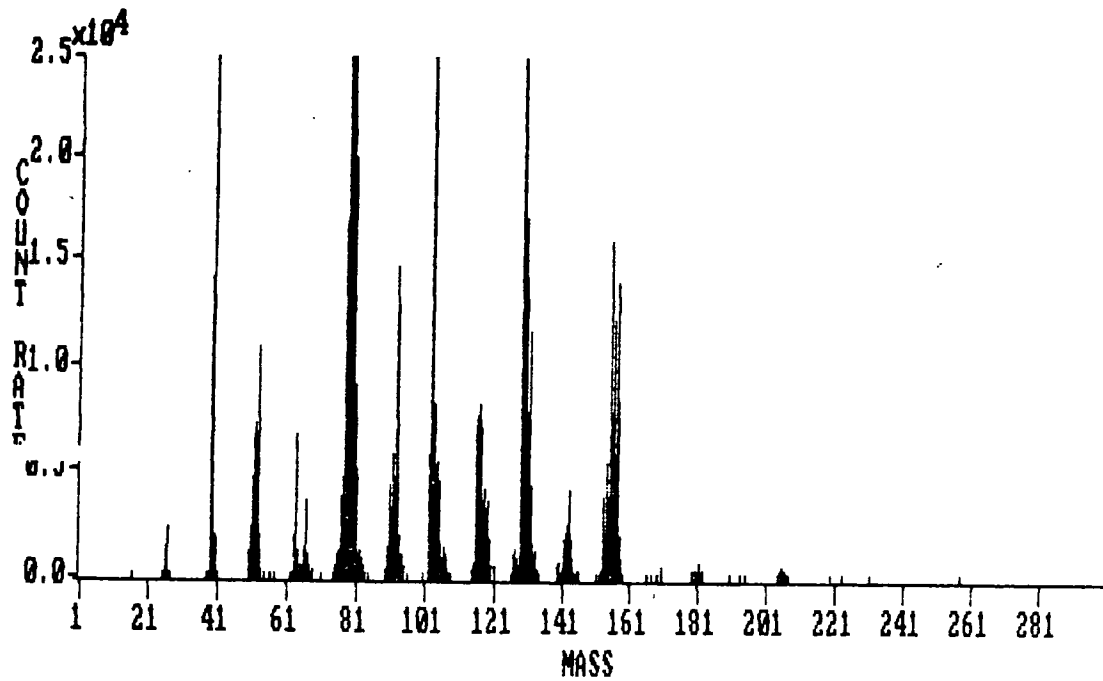
Figure 3.3 Positive Ion Mass Spectrum of a Benzene Plasma
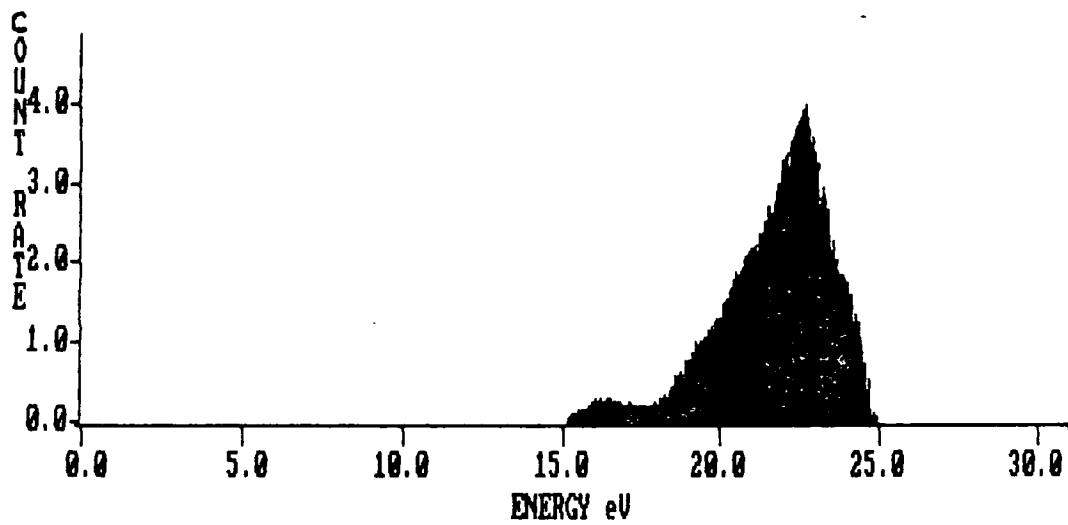
Figure 3.4 Ion energy distribution from a 50W benzene plasma

Table 3.1 Principal Ions in the Mass Spectrum of a Benzene Plasma

A.M.U.	Assignment	
39	$C_3H_3^+$	Benzene fragment
52	$C_4H_4^+$	
78	$C_6H_6^+$	Benzene molecular ion
92	$C_7H_8^+$	Toluene molecular ion
102	$C_8H_6^+$	
116	$C_9H_8^+$	
128	$C_{10}H_8^+$	Naphthalene molecular ion
154	$C_{12}H_{10}^+$	Biphenyl molecular ion
155	$C_{12}H_{11}^+$	
156	$C_{12}H_{12}^+$	

character of the monomer is being largely retained. Partial saturation of the aromatic rings is seen in some ions of low intensity, e.g. $C_{12}H_{14}^+$ at mass 158.

There are very few ions at masses of greater than 160 a.m.u., suggesting that little more than dimerisation takes place in the gas phase and that further polymerisation must occur mainly on the surface. There are some low intensity peaks at higher masses, e.g. in clusters around 167, 180, 193 and 205 a.m.u. corresponding to species with 13 to 16 carbon atoms. This shows that some further polymerisation is taking place in the gas phase via positive ions, but very little.

Reducing the plasma power to 20 watts produced very little

change in the positive ion spectrum, although no ions at masses of greater than 160 a.m.u. were observed in this case. This was probably because their intensities became too low, and suggests that less polymerisation takes place in the gas phase at low powers. A 50 watt plasma of benzene at 0.02 torr, showed the same peaks as the 50 watt, 0.04 torr plasma, but the intensities of the low mass fragments, especially C_4 species, were increased in relation to those of the higher mass fragments. The higher energies available per molecule appear to increase the amount of fragmentation in this case.

b) Neutral Species

The mass spectra taken of neutral species from a 50 watt, 0.02 torr plasma, using low electron impact ionisation energy (13 eV) showed only a C_6H_6 peak at 78 a.m.u.. If any other neutral species occur in the plasma it can only be in very small quantities, although isomers of benzene, such as fulvene, may be present. There does not therefore appear to be any significant amount of polymerisation in the gas phase via excited state or radical chemistry. This is in some disagreement with the observation that benzene can form a surface photopolymer[16,17], which must occur through excited states which can be accessed in the plasma. Therefore either the photopolymerisation must occur entirely on the surface and not in the gas phase, or neutral polymer forming species are present in the plasma, but in concentrations so small that they were not detected. The plasma polymerisation of benzene, or at least the part that takes place

in the gas phase, therefore appears to be dominated by ion chemistry, with radical and excited state chemistry playing little or no part.

The positive ion spectra are very similar to those observed previously for benzene[12,13], but the neutral spectra observed by Niinomi and Yanigahara[12] showed many peaks corresponding both to benzene fragments and oligomeric species. This is very different from the present observation, which could be due either to different plasma conditions used or the fact that the previous spectrum was of a mixed benzene/argon plasma, rather than of pure benzene. It may be therefore that under certain conditions neutral species do play a significant role in the initial gas phase reactions contributing to polymerisation.

3.3.2 Perfluorobenzene

a) Positive Ions

The positive ion mass spectrum of a 50 watt, 0.024 torr PFB plasma polymer is shown in figure 3.4. This spectrum was taken using ions of 27 eV energy, which at the maximum of the ion energy distribution for CF^+ ions (used as a guide since the molecular ion peak was of low intensity), shown in figure 3.5. The principal peaks in the mass spectrum are listed in table 3.2.

It can be seen that the degree of fragmentation occurring in the PFB plasma is much higher than for benzene. In the benzene plasma the molecular ion was the most intense peak observed, while for PFB it is only present in a fairly small peak at 186 a.m.u.. The most intense peaks in the spectrum are those at 31,
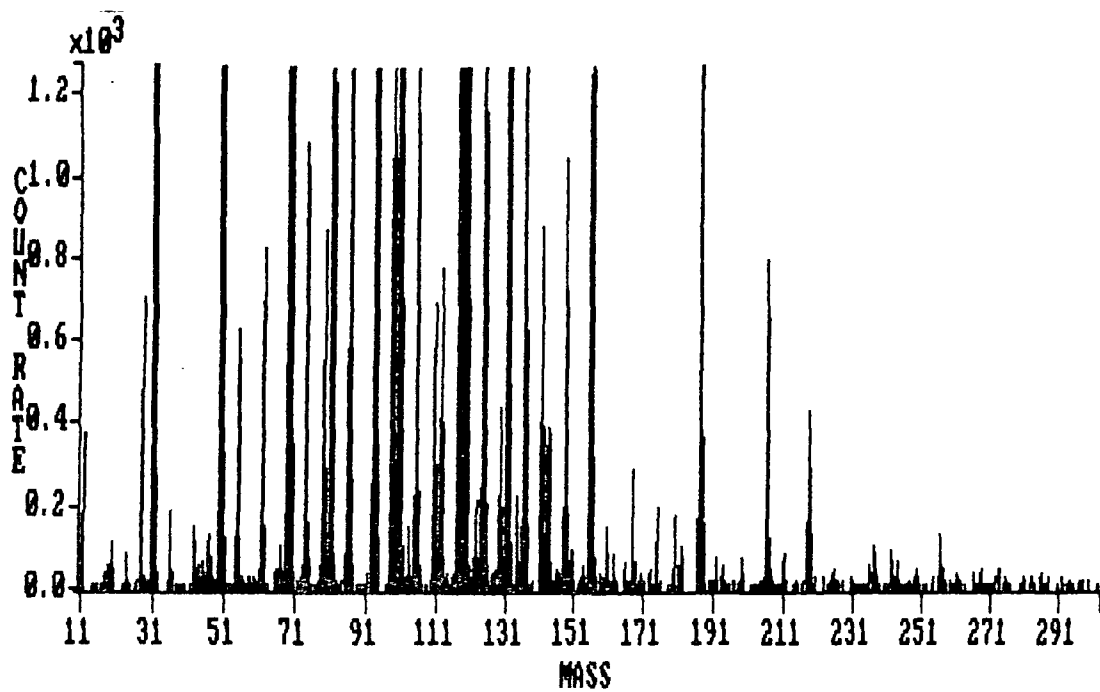
Figure 3.5 Positive Ion mass spectrum of a 50 watt, 0.024 torr
PFB plasma
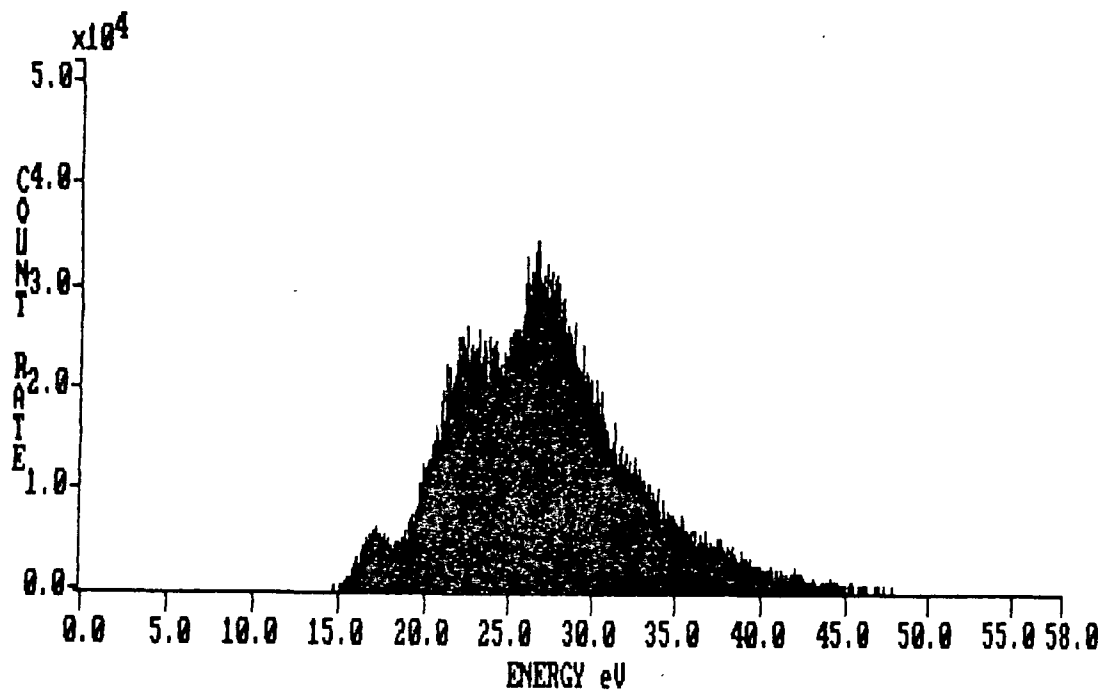
Figure 3.6 Energy distribution of CF+ ions from a 50 watt, 0.024
torr PFB plasma

Table 3.2 Principal peaks in the positive ion mass spectrum of a 50 watt PFB plasma

A.M.U.	Assignment	
31	CF^+	PFB fragment
50	CF_2^+	Fragment of larger fluorocarbons (not PFB)
69	CF_3^+	PFB fragment
93	$C_3F_3^+$	PFB fragment
100	$C_2F_4^+$	Tetrafluoroethylene molecular ion
117	$C_5F_3^+$	PFB fragment
124	$C_4F_4^+$	Perfluoroalkylbenzene fragment
136	$C_5F_4^+$	PFB fragment
155	$C_5F_5^+$	PFB fragment
186	$C_6F_6^+$	PFB molecular ion
205	$C_6F_7^+$	Possible precursor of perfluoro cyclohexene/diene structures
217	$C_7F_7^+$	Possible precursor of perfluoro alkylbenzene structures

50, 69, 93 and 117 a.m.u., which correspond to CF^+, CF_2^+, CF_3^+, $C_3F_3^+$ and $C_5F_3^+$, all of which are found on the electron impact mass spectrum of PFB[18], and are therefore probably formed in the plasma by electron impact fragmentation of PFB. The peaks at 136 and 155 a.m.u. are also fragments found in the mass spectrum of PFB. The CF_2^+ peak is not a major fragment of PFB, and so in this case probably arises from fragmentation of other perfluorocarbon species present. The peak at 217 a.m.u. ($C_7F_7^+$) probably arises

from reaction of a PFB molecule with CF^+, and may be a precursor to the perfluoroalkylbenzene structure of the polymer observed by SIMS in chapter 2. The $C_4F_4^+$ ion observed at 124 a.m.u. is found as a fragment in the electron impact mass spectra of some perfluoroalkylbenzenes, and in this case is possibly derived from the $C_7F_7^+$ ion. The $C_6F_7^+$ ion at 205 a.m.u. could arise from reaction of a fluorine atom with the molecular cation, and appears to represent the first stage of saturation of the benzene ring in forming the perfluorocyclohexene and perfluorocyclohexadiene structures observed in the polymer by SIMS. The $C_2F_4^+$ peak at 100 a.m.u. is the molecular ion of tetrafluoroethylene, and is not observed (except at very low intensity) in the SIMS spectrum of the polymer. With little olefinic or aliphatic structure present in the polymer it seems unlikely that the tetrafluoroethylene can make a direct contribution to polymer formation, but it may undergo further reaction in the gas phase to produce products which can be incorporated into the polymer. The $C_2F_4^+$ ion in the plasma probably arises from ionisation of tetrafluoroethylene formed by the reaction of two CF_2 radicals, or the $C_2F_4^+$ ion could be formed from the reaction of a CF_2 radical and a CF_2^+ ion.

When the plasma power was reduced to 20 watts and the pressure increased to 0.04 torr, most of the higher mass peaks seen in the previous spectrum disappeared. The principal peaks observed, listed on table 3.3, are all at 117 a.m.u. or less, and correspond to small fragments of PFB or other fluorocarbons, apart from the tetrafluoroethylene peak at 100 a.m.u. The peaks at 81 and 86 a.m.u. were both present in the previous spectrum,

101

Table 3.3 Principal Peaks in the Mass Spectrum of a 20 Watt, 0.04 torr PFB Plasma

A.M.U.	Assignment	A.M.U.	Assignment
31	CF^+	86	$C_4F_2^+$
50	CF_2^+	93	$C_3F_3^+$
69	CF_3^+	100	$C_2F_4^+$
81	$C_2F_3^+$	117	$C_5F_3^+$

but at low intensity, and so do not appear on table 3.2. No PFB molecular cation, or any potentially polymer forming species were observed.

When the plasma power was reduced further to 5 watts at 0.04 torr (very mild polymerising conditions), the mass spectrum, taken at an ion energy of 15 eV, was totally dominated by the CF^+ peak at 31 a.m.u., although very small peaks were also observed at 50, 69, 93 and 117 a.m.u..

It appears that as the power to flow rate ratio is decreased, so the average mass of the fragments observed decreases. Even in the high W/F, 50 watt, 0.024 torr plasma most of the ions observed were small fragments, unlikely to lead to the formation of the type of aromatic based polymer observed by SIMS analysis, and at lower powers and high flow rates no potentially polymer forming gas phase species were observed at all. It therefore seems that high energy ion chemistry plays little or no part in the formation of a PFB plasma polymer.

A closer examination of the ion energy distribution of CF^+

ions from the 5 watt plasma (figure 3.7) shows 2 separate maxima at about 8 eV and 15 eV. The previous mass spectrum was taken using 15 eV ions and showed little other than CF^+, but a spectrum taken at 8 eV was very different, (figure 3.8). In this case the number of small mass fragments was quite low and the spectrum was dominated by comparatively high mass species, including some larger than the molecular ion. The principal peaks are listed on table 3.4.

Table 3.4 <u>Principal peaks in the 8 eV positive ion mass spectrum</u>
<u>of a 5 watt, 0.04 torr PFB plasma</u>

A.M.U.	Assignment	A.M.U.	Assignment
31	CF^+	148	$C_6F_4^+$
50	CF_2^+	155	$C_5F_5^+$
69	CF_3^+	167	$C_6F_5^+$
93	$C_3F_3^+$	186	$C_6F_6^+$
98	$C_5F_2^+$	205	$C_6F_7^+$
117	$C_5F_3^+$	217	$C_7F_7^+$
136	$C_5F_4^+$	272	$C_{10}F_8^+$

The higher mass species appear to represent initial stages in the polymerisation process. The peaks at 205, 217 and 272 a.m.u. are all present in the SIMS analysis of a PFB plasma polymer and could be precursors of the perfluorohexadiene, perfluoroalkylbenzene and perfluoronaphthalene groups in the plasma polymer.

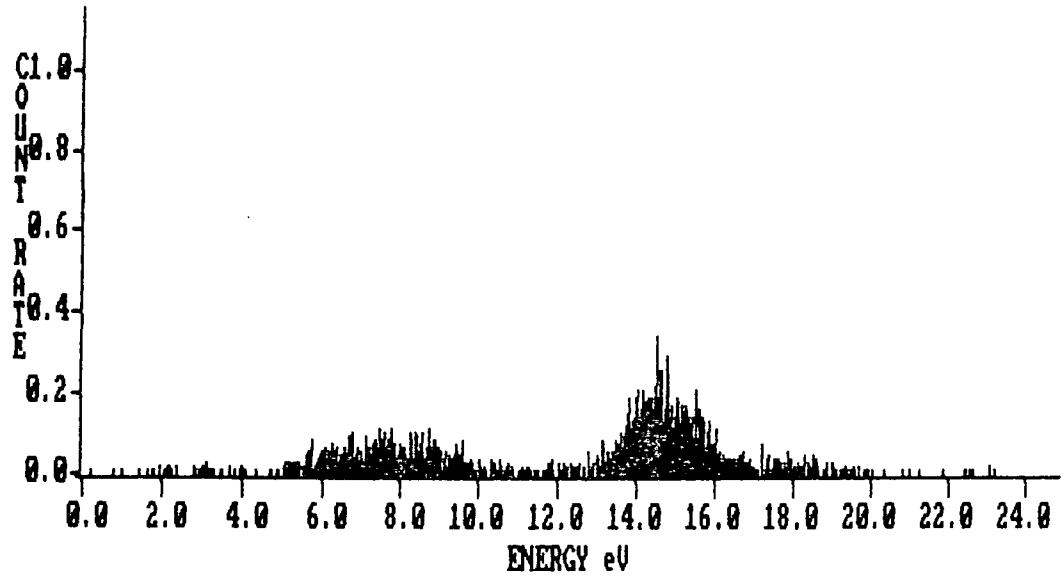This suggests that there are two separate ion energy regimes

Figure 3.7. Ion energy distribution of CF^+ ions from a 5 watt, 0.04 torr PFB plasma
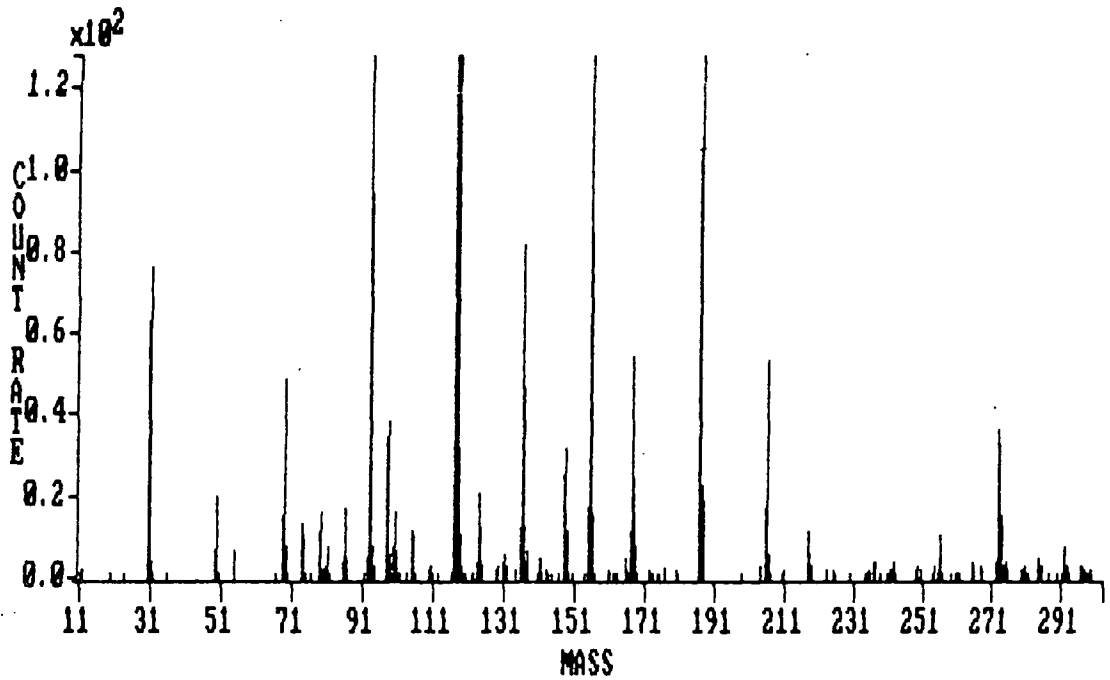
Figure 3.8 Mass spectrum of 8 eV positive ions from a 5 watt, 0.04 torr PFB plasma

104

in the plasma, high energy ions which are only small fragments of a PFB molecule (especially CF^+), and higher mass ions at low energy, which might be involved in plasma polymerisation.

As has been mentioned previously however, the ion energies measured in the analyser are not representative of those in the plasma. The reason for this is that ions are accelerated while moving between the plasma and the probe. Electrons in the plasma have higher average velocities than the heavier positive ions, and so diffuse out of the plasma at a greater rate, leaving a net positive charge. Since the probe is earthed there is a potential difference between it and the plasma, and so a zone, or sheath, forms around the probe in which positive ions from the plasma are

Figure 3.9 Diagram showing the sheath around the sampling probe

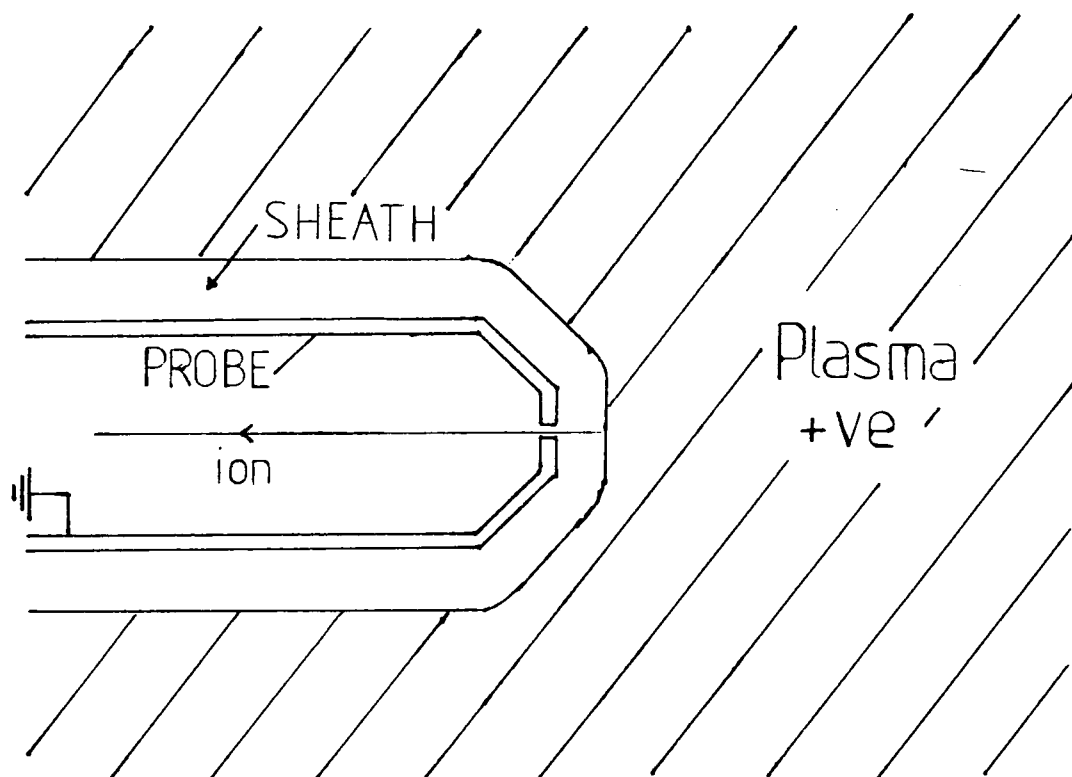accelerated towards the probe (see figure 3.9). This means that the ion energies measured in the analyser are higher than those present in the plasma. The situation might be further complicated however by the RF field. Although there is a net acceleration of the ions towards the probe, at any one instant in time the RF field will have a greater effect on any charged species, causing them to oscillate towards and away from the probe. It has been suggested by Wild and Koidl, in the case of an argon plasma, that this combination can cause a series of peaks to occur in the measured ion energy distribution[19]. The measured energy of an ion will depend on how long it has spent in the accelerating influence of the sheath, which will in turn depend on the initial position of the ion. An ion close to the probe may be sampled on the first RF cycle, when the RF field is in alignment with the sheath potential. An ion further away may not reach the probe before the RF field reverses and pulls the ion back towards the plasma. In this case however, the sheath potential opposes the RF field and the ion does not move so far away as it was originally. It is therefore closer after each successive cycle, and will eventually reach the probe and be analysed. Since the measured energy of the ion depends on how long it has spent in the sheath, and hence how many cycles it has gone through, the ion energy distribution will have a peak corresponding to ions analysed from each RF cycle (see figure 3.10).

If this process is occurring in the 5 watt PFB plasma it could explain the origin of the two peaks observed in the ion energy distribution, which would probably correspond to ions being analysed on the first and second RF cycles respectively.
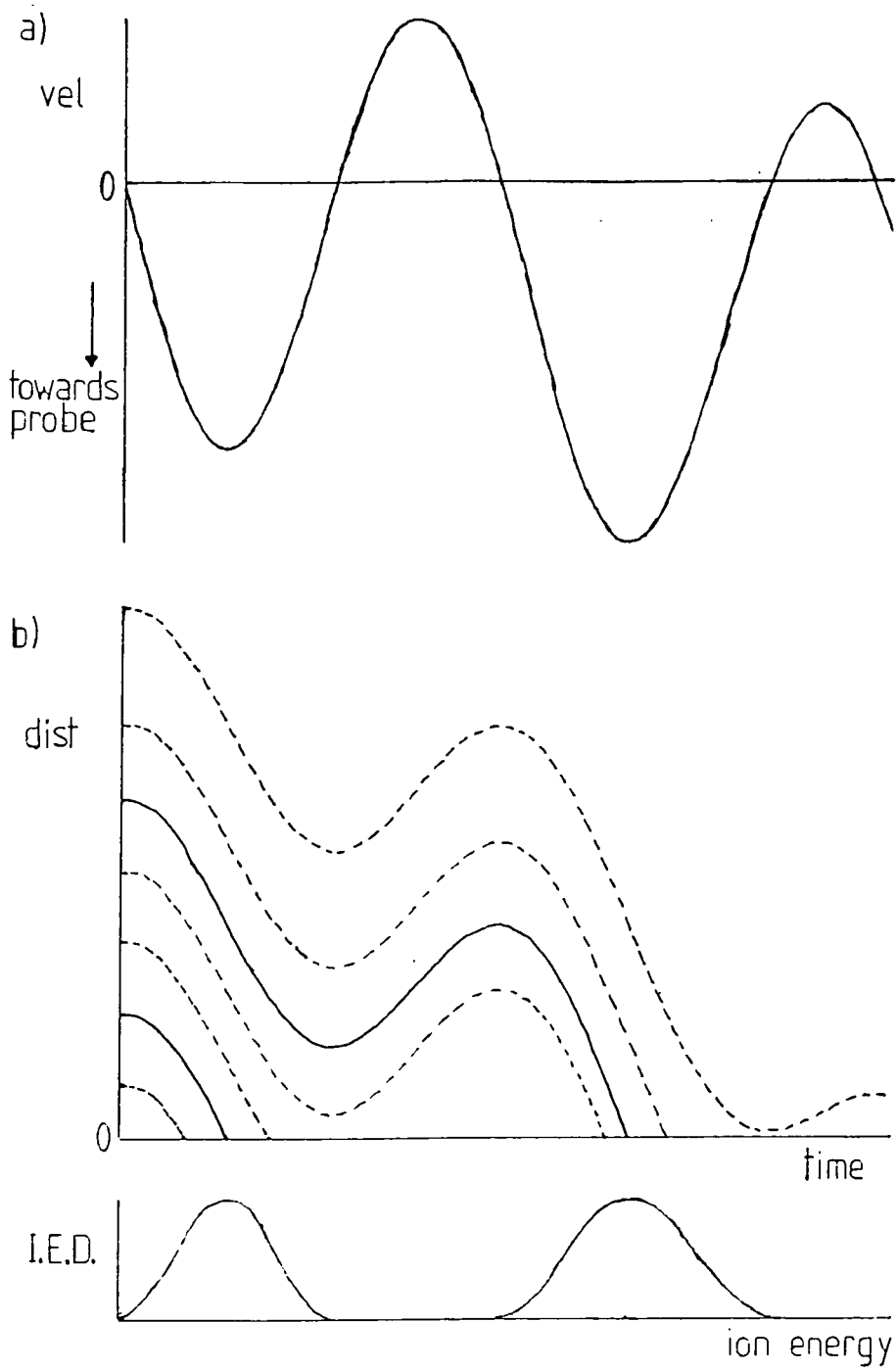
Figure 3.10 (a) Velocity and (b) Distance from the probe, of ions in the plasma sheath as a function of time, showing the origin of peaks in the ion energy distribution.

The peak at 8 eV would therefore be due to material close to the probe, while the 15 eV would be representative of material from further out in the plasma. In this case the plasma as a whole consists of very small ionic fragments such as CF^+, while close to the probe there are considerably more high mass ionic species. A possible explanation for the presence of this material close to the probe is that it could have been ablated from polymer already deposited. Any positive ions ablated would not be able to travel more than the distance corresponding to one RF cycle away from the probe as they would be pulled back by the electric field. Hence no high mass fragments are seen in the 15 eV peak. The spectrum obtained from the 8 eV peak bears some resemblance to the SIMS spectrum observed for a PFB plasma polymer (see chapter 2). Any differences between the two might be accounted for by the much lower energy ions impacting on the surface in the plasma than in the SIMS experiment, and also by the possibility of chemical etching by reactive fluorine species taking place in the plasma[20].

Series of peaks, often running into one another, were also observed in the ion energy distributions from other plasmas (e.g. figures 3.4 and 3.6), but separate mass spectra were not taken for each peak. It is likely that these peaks arise in the same way as for the 5 watt plasma.

It appears that positive ions in the gas phase of the 5 watt plasma do not contain structures similar to those observed in the plasma polymer. Only in very high power, low flow rate plasmas is any evidence seen of the build up of high mass positive ions. The milder the plasma conditions become, the

smaller the positive ion fragments observed are. It seems unlikely that ion chemistry is much involved in polymer formation except in very high power plasmas. Further supporting evidence for this comes from examination of the neutral species.

b) Neutral Species

The mass spectra of neutral species from a 20 watt, 0.047 torr PFB plasma, using electron impact energies of 11 eV and 27 eV, are shown in figures 3.11(a) and 3.11(b) respectively. The 11 eV electrons have sufficient energy to ionise most species but cause very little fragmentation, so the ions detected should correspond to the neutral species in the plasma. The count rate was very low however, so a second spectrum was taken using 27 eV electrons, which are likely to cause some fragmentation, in order to detect the low intensity peaks at high mass. Apart from some hydrocarbon contamination, particularly the peak at 58 a.m.u. (C_4H_{10}), the principal peaks from a combination of the two spectra are listed in table 3.5.

The most prominent peak in the mass spectrum is that at 186 a.m.u. corresponding to the PFB molecule. It is possible that isomers of PFB, such as perfluorofulvene and perfluorohexadienyne may also contribute to this peak. There are a large number of low mass peaks (e.g. CF_2 , CF_3, C_4F_2 and C_5F_3), many of which correspond to small fragments of PFB or other fluorocarbons. The most abundant low mass species however is tetrafluoroethylene, which occurs at 100 a.m.u., but the lack of any significant amount of aliphatic or olefinic material in a PFB plasma polymer
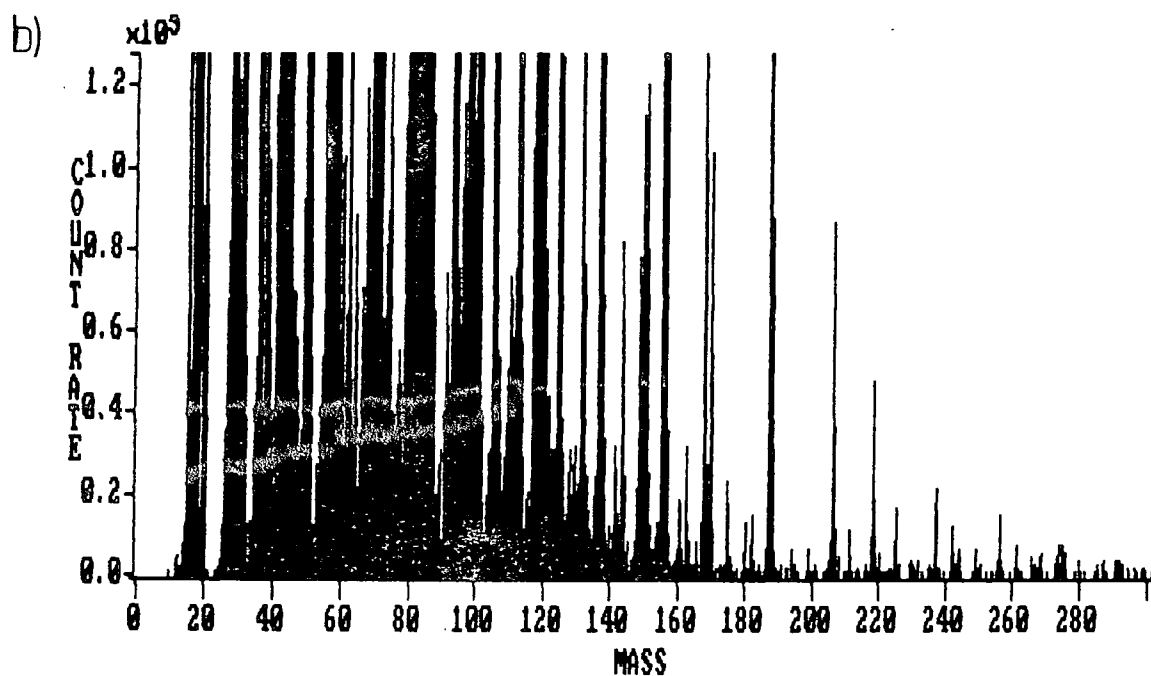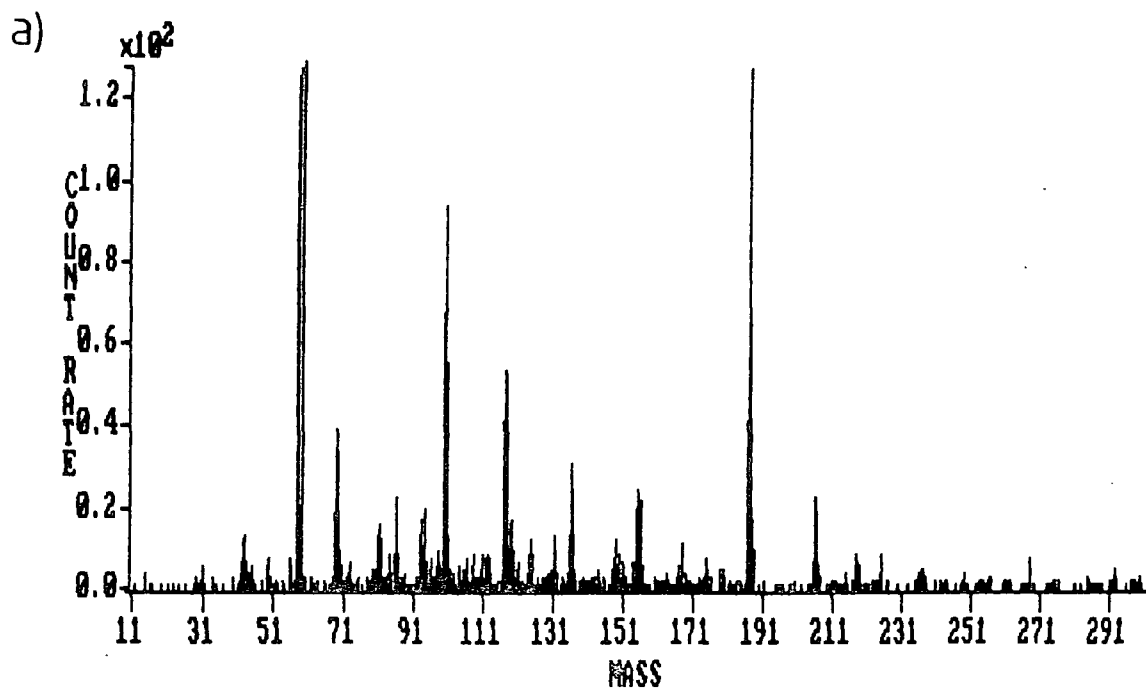
Figure 3.11 Mass spectra of neutral species from a 20 watt, 0.047
torr PFB plasma using (a) 11 eV and (b) 27 eV
electron impact ionisation

Table 3.5 Neutral species detected in the 20 watt, 0.047 torr PFB plasma

A.M.U.	Assignment	
50	CF_2	
69	CF_3	
86	C_4F_2	$CF{\equiv}C-C{\equiv}CF$
100	C_2F_4	Tetrafluoroethylene
117	C_5F_3	
119	C_2F_5	Perfluoroethyl radical
136	C_5F_4	
155	C_5F_5	
186	C_6F_6	PFB molecule, and also possibly isomers of PFB (e.g. fulvene)
205	C_6F_7	
217	C_7F_7	
224	C_6F_8	Perfluorocyclohexadiene
236	C_7F_8	Perfluorotoluene
255	C_7F_9	

suggests that this may not have a major role in the polymerisation. A number of species of higher mass than PFB are present including perfluorotoluene and perfluorocyclohexadiene, both of which are likely precursors to structural features in the plasma polymer. The perfluorohexadiene is probably formed by reaction of PFB with fluorine radicals, via the C_6F_7 radical. Perfluorotoluene and the C_7F_7 radical are likely to arise from attack of CF_3 or CF_2 radicals, on PFB, and the C_7F_9 radical could be produced by attack of fluorine on perfluorotoluene.

In a higher power plasma (50 watts) a peak was also observed at 267 a.m.u. corresponding to C_8F_9, which could be a perfluoroethylbenzene or perfluoroxylene radical. The high power plasma contained slightly more high mass material than the 20 watt or a 5 watt plasma, less PFB monomer and considerably more tetrafluoroethylene. It is possible that this could be connected to the fact that more CF_2 groups are observed by XPS in a high power PFB plasma polymer. Generally however, the neutral mass spectra of different power PFB plasmas were fairly similar.

Although species were found in the gas phase that could be precursors to perfluoroalkylbenzene and perfluorocyclohexadiene structures in the plasma polymer, no peak was observed for perfluoronaphthalene at 272 a.m.u., despite the fact that this type of structure was observed by SIMS analysis of PFB plasma polymers. It seems that this must therefore form on the surface of the polymer. A possible route to its formation could be the reaction of difluorodiacetylene, observed as a peak at 86 a.m.u., with aromatic rings in the surface of the polymer.

The lack of species with masses greater than 267 a.m.u. in the gas phase suggests that polymerisation takes place mainly on the surface. The polymer formation is probably based around PFB, perfluorotoluene, perfluorocyclohexadiene and others of the larger gas phase species adsorbed on the walls of the chamber. These probably react with much smaller fragments such as CF, CF_2 and CF_3 radicals or ions colliding with the surface. These would provide the short alkyl links between the aromatic and other rings suggested by the SIMS analysis. Perfluoronaphthalene rings

probably arise from reaction of difluorodiacetylene with aromatic rings on the surface of the polymer. The increased CF_2 content observed in polymers formed from high power polymers could arise from incorporation of tetrafluoroethylene, or from an increased number of the small fragments colliding with the surface.

3.3.3 Perfluorobenzene/Benzene
a) Positive Ions

The positive ion spectrum taken from a 0.04 torr, 50 watt plasma of mixed benzene and perfluorobenzene vapour is shown in figure 3.12. The precise ratio of the two monomers in the plasma was not known but was thought to be close to 1:1. The composition of the positive ions in the plasma however was mostly hydrocarbon
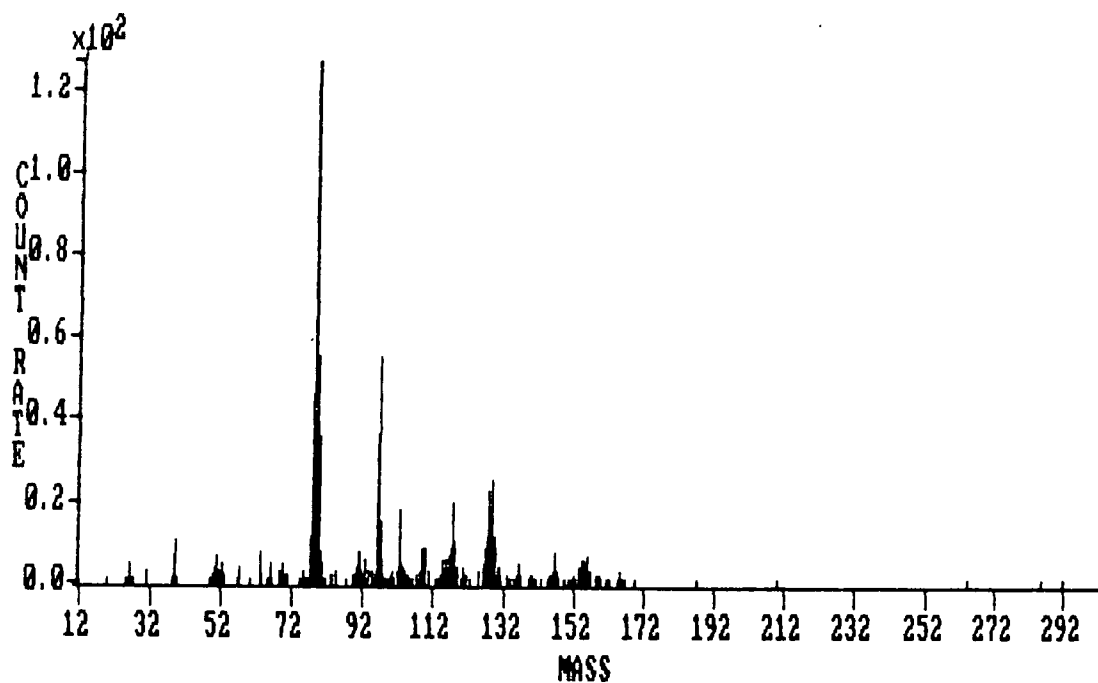

Figure 3.12 Positive ion mass spectrum of a PFB/Benzene plasma

Table 3.6 Principal peaks in the positive ion mass spectrum of a PFB/benzene plasma

A.M.U.	Assignment	
78	$C_6H_6^+$	Benzene molecular ion
96	$C_6H_5F^+$	Monofluorobenzene molecular ion
102	$C_8H_6^+$	Phenyl acetylene molecular ion
109	$C_7H_6F^+$	
117	$C_5F_3^+$	PFB fragment
127	$C_{10}H_7^+$	
128	$C_{10}H_8^+$	Naphthalene molecular ion
146	$C_7H_5F_3^+$ or	Trifluoromethyl benzene
	$C_{10}H_7F^+$	Monofluoronaphthalene
154	$C_{12}H_{10}^+$	Biphenyl molecular ion

(see table 3.6), possibly because hydrocarbons ionise more easily. The most prominent peak in the spectrum is that of the benzene molecular ion at 78 a.m.u., but no peak was observed for the PFB molecular ion at 186 a.m.u.. All the hydrocarbon species observed were also found in the benzene plasma, and the only fluorocarbon peak ($C_5F_3^+$) was also found in PFB plasmas. Peaks at 96, 109 and 146 a.m.u. represent mixed fluorocarbon and hydrocarbon species, showing that some interaction does occur in the gas phase. These generally contain only one fluorine atom (or a CF_3 group if the peak at 146 a.m.u. is trifluoromethyl benzene rather than monofluoronaphthalene) substituted for a hydrogen atom in a derivative of the benzene, and so represent only limited interaction between the fluorocarbon and hydrocarbon components of the plasma.

114

b) Neutral Species

The mass spectrum of neutral species from a 50 watt, 0.04 torr benzene/PFB plasma, taken using 12 eV electron impact ionisation, is shown in figure 3.13, and the main peaks are listed on table 3.7. As in the case of the positive ions the largest peak is that for benzene at 78 a.m.u., but in this case the peak for PFB at 186 a.m.u. was also observed. There are some other species that are either pure hydrocarbon (e.g. acetylene, methylacetylene, naphthalene and biphenyl at 26, 40, 128 and 154 a.m.u. respectively), or pure fluorocarbon (e.g. CF_2 and tetrafluoroethylene at 50 and 100 a.m.u.), but the majority are a mixture of the two. The series of substituted benzenes $C_6H_nF_{6-n}$ were all present except for trifluorobenzene, as were some partially fluorinated acetylenes and either fluoronaphthalene or
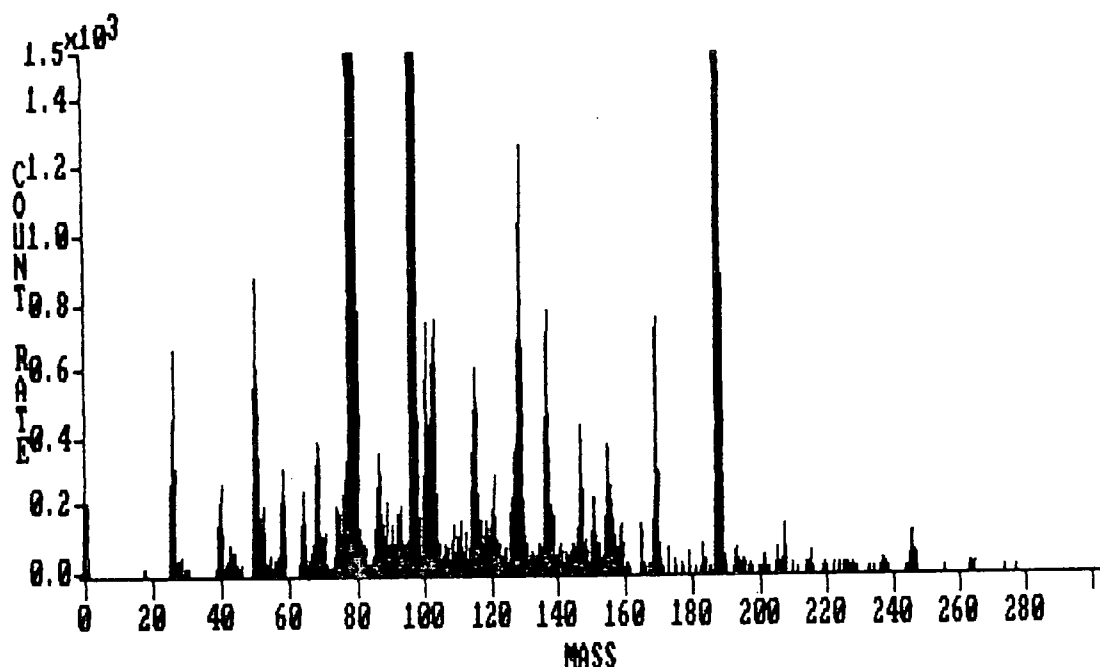

Figure 3.13 Mass spectrum of neutral species from a benzene/PFB plasma

Table 3.7 Principal peaks in the mass spectrum of neutral species from a benzene/PFB plasma

A.M.U.	Assignment*	
26	C_2H_2	Acetylene
40	C_3H_4	Methyl acetylene
50	CF_2	
58	C_3H_3F	$F-C\equiv C-CH_3$
64	$C_2H_2F_2$	Difluoroethylene
68	C_4HF	$F-C\equiv C-C\equiv C-H$
78	C_6H_6	Benzene
86	C_4F_2	Difluorodiacetylene
96	C_6H_5F	Monofluorobenzene
100	C_2F_4	Tetrafluoroethylene
102	C_8H_6	Phenylacetylene
114	$C_6H_4F_2$	Difluorobenzene
120	C_8H_5F	$Ph-C\equiv C-F$
128	$C_{10}H_8$	Naphthalene
136	C_5F_4	
146	$C_7H_5F_3$ or	Trifluoromethyl benzene
	$C_{10}H_7F$	Monofluoronaphthalene
150	$C_6F_4H_2$	Tetrafluorobenzene
154	$C_{12}H_{10}$	Biphenyl
168	C_6F_5H	Pentafluorobenzene
186	C_6F_6	Perfluorobenzene

* For many of the peaks there are several possible assignments. The ones listed are those thought to be most likely in view of the nature of the monomers.

trifluoromethylbenzene. A number of other peaks arising from mixed fluorocarbon/hydrocarbon species were observed at very low intensities, including a peak at 244 a.m.u. corresponding to either C_6F_9H or $C_9F_7H_3$, the highest mass peak observed. There is obviously a very considerable gas phase interaction between the hydrocarbon and fluorocarbon species, which would explain why a PFB/benzene plasma copolymer is not simply a mixture of the two homopolymers. The fact that most interaction seems to take place among the neutral species is consistent with the fact that a surface photo-copolymer of PFB and benzene, similar to the plasma polymer can also be made[14]. It is interesting to note that a considerably greater range of neutral hydrocarbon species were found in the copolymerising mixture, than in the plasma of pure benzene. There were also no CF_3 or C_5F_3 peaks detected in the mixture, both of which occurred fairly prominently in the plasmas of PFB. It seems therefore that the chemistry of the individual hydrocarbon and fluorocarbon components of the mixture is perturbed by the presence of the other component.

3.4 SUMMARY

In a benzene plasma positive ions with masses up to a mass of 156 a.m.u. ($C_{12}H_{12}^+$), including the molecular ions of toluene, phenyl acetylene, naphthalene and biphenyl, were present with high intensities, and some higher mass species were observed at low intensity. There seemed to be little change in the spectra as the plasma conditions were varied. The neutral spectra, showed

little other than the benzene molecule. This suggests that benzene plasma polymerisation proceeds mainly via an ionic mechanism, although since benzene is known to form a vacuum UV surface photopolymer it is likely than some polymerisation will occur from excited state chemistry of the neutral molecules, possibly taking place on the surface.

Perfluorobenzene plasmas, in contrast to those of benzene, showed little evidence of oligomer formation in the gas phase positive ion spectra, which were dominated by small fragments such as CF^+. The average size of the positive ions observed increased with increasing plasma power, suggesting that a limited amount of gas phase reaction leading to polymerisation may take place via positive ions in high power plasmas. The ion energy distributions obtained from many plasmas showed a series of peaks, and a positive ion mass spectrum taken from the lower energy peak of a 5 watt PFB plasma showed a considerable amount of high mass material. It is thought however that the peak structure was due to RF modulation of the plasma sheath potential, which means that this peak was probably due to ions from very close to the probe. The high mass material observed was probably ablated from polymer on the probe, and was therefore not representative of material in the plasma.

Neutral species with masses greater than that of PFB were observed, including possible precursors to the perfluoroalkylbenzene and perfluorocyclohexadiene structures seen in the SIMS analysis of PFB plasma polymers. No perfluoronaphthalene was observed in the gas phase, but this

118

could be formed by reaction of difluorodiacetylene with aromatic structures on the surface of the polymer. Tetrafluoroethylene was observed in the neutral mass spectra, particularly in high power PFB plasmas. It was proposed that the plasma polymer builds up around PFB monomer and the larger neutral species formed in the gas phase adsorbed onto the walls of the reactor, by reaction of these with small gas phase fluorocarbon fragments such as CF, CF_2 and CF_3 radicals or ions. This would account for the structure of aromatic and other ring systems linked by very short alkyl chains suggested by SIMS analysis. The increased CF_2 content of polymers formed from high power PFB plasmas could be due to incorporation of tetrafluoroethylene.

The positive ion spectrum from a mixed benzene/PFB plasma showed mainly hydrocarbon fragments, but there were some partially fluorinated species observed. The mass spectrum of the neutral species showed much more interaction between hydrocarbon and fluorocarbon, with many mixed hydrocarbon/fluorocarbon species present. The individual hydrocarbon and fluorocarbon fragments observed in the mixed plasma were also different from those found in the separate benzene and PFB plasmas. This high degree of gas phase interaction between the two monomers explains why they plasma copolymerise to form a material that is not simply a combination of the two homopolymers.

REFERENCES

1. R.A.Gottscho and T.A.Miller, Pure Appl. Chem., 56, 189, (1984)

2. P.J.Hargis Jr. and M.J.Kushner, Appl. Phys. Lett., 40, 779, (1982)

3. H.Sakai, P.Hansen, M.Esplin, R.Johansson, M.Petola and J.Strong, Appl. Opt., 21, 228, (1982)

4. P.Branson and F.J.M.J.Massen, Spectrochim. Acta., 29B, 203, (1974)

5. P.Marcus and I.Platzner, Int. J. Mass Spectrom. Ion Phys., 32, 77, (1979)

6. M.J.Vasile and G.Smolinsky, J. Macromol. Sci. Chem., A10, 473, (1976)

7. G.Smolinsky and M.J.Vasile, Int. J. Mass Spectrom. Ion Phys., 22, 171, (1976)

8. M.J.Vasile and G.Smolinsky, Int. J. Mass Spectrom. Ion Phys., 24, 11, (1977)

9. I.Platzner and P.Marcus, Int. J. Mass Spectrom. Ion Phys., 41, 241, (1982)

10. M.J.Vasile and G.Smolinsky, J. Phys. Chem., 81, 26, (1977)

11. M.J.Vasile and G.Smolinsky, Int. J. Mass Spectrom. Ion Phys., 13, 381, (1974)

12. M.Niinomi and K.Yanigahara, ACS Symp. Ser., 108 (Plasma Polymerisation), 87, (1978)

13. M.J.Vasile and G.Smolinsky, Int. J. Mass Spectrom. Ion Phys., 24, 311, (1977)

14. H.S.Munro and C.Till, J. Polym. Sci., Polym. Chem. Ed., 26, 2873, (1989)

15. C.Till, Ph.D. Thesis, Durham, (1986)

16. J.E.Wilson and W.A.Noyes Jr., J. Am. Chem. Soc., 63, 3025, (1941)

17. H.R.Ward and U.Wishnok, J. Am. Chem. Soc., 90, 5333, (1968)

18. J.R.Majer in "Advances in Fluorine Chemistry", Eds. M.Stacey, J.C.Tatlow and A.G.Sharpe, Butterworths (1961)

19. Ch.Wild and P.Koidl, Appl. Phys. Lett., 54, 505, (1989)

20. H.Yasuda and T.Hsu, J. Polym. Sci., Polym. Chem. Ed., 16, 415, (1978)

CHAPTER 4

RETENTION OF CARBOXYLATE FUNCTIONALITY IN THE PLASMA POLYMERISATION OF CARBOXYLIC ACIDS AND ESTERS

4.1 INTRODUCTION

Formation of a thin film containing a high concentration of carboxylic acid groups is of interest not only because of the highly wettable surface that would be obtained, but also because further reactions could be carried out to produce a wide range of surface functionalities, e.g. acid chlorides, amides, esters etc. Attachment of species such as proteins could be accomplished via acid chlorides[1] or by using a carbodiimide in aqueous solution[2]. Plasma polymerisation is a convenient way of forming thin films of controllable thickness, but retention of oxygen containing functional groups such as carboxlates is generally very poor[3,4]. This is due to elimination of water, carbon monoxide and carbon dioxide from oxygen containing compounds in a plasma[5]. Plasma polymers of acrylic acid and propionic acid have been found by Yasuda and Hsu[6] to give contact angles with water of about 60° under normal plasma conditions, indicating a considerable loss of oxygen, but if a pulsed plasma was used, the contact angles obtained were very low, indicating much less monomer fragmentation. This is probably caused by activation during the plasma pulse, followed by addition of monomer during the "off" period, to produce a material more like a conventional polymer.

Plasma polymers of some vinyl compounds which retain most of the functional groups of their starting monomers, have been made using low power and high flow rate conditions in a continuous plasma. Allyl alcohol and allyl amine plasma polymer formed under these conditions have been found to retain a high percentage of alcohol and amine groups respectively[7]. Plasma polymers of a series of unsaturated alcohols formed at low power were found to

123

be relatively hydrophilic, and to retain some of their -OH groups[8]. Plasma polymers with high carboxylic acid concentration have been produced by using a mixture of acrylic acid and carbon dioxide[9], and also by exposing a freshly made acrylic acid plasma polymer to the monomer at its saturated vapour pressure for 30 minutes[10]. In the latter case the monomer reacted with trapped free radical sites on the polymer to produce essentially a very thin layer of poly acrylic acid.

In this chapter the formation of plasma polymers of carboxylic acids is investigated, with respect to retention of functionality and the effect of chain length and unsaturation. Acrylic, vinyl acetic and allyl acetic acids are used to examine whether the separation between the acid group and the double bond affects the degree of retention (e.g. whether the allyl configuration is important), or whether simply the presence of both groups within the same molecule is all that is required. The results of these are compared with those obtained from acetic, propionic, butyric and valeric acids, in order to discover how important unsaturation is in the retention of acid groups. Methyl acrylate and methyl methacrylate are used to examine whether retention of carboxylate groups can be achieved for esters as well as for acids. Methacrylic acid was used for comparison with methyl methacrylate.

The surface photopolymerisations of methyl methacrylate and examples of saturated and unsaturated acids are also investigated in order to probe the mechanism of the plasma polymerisation.

Table 4.1 Monomers used in chapter 4

Propionic acid CH_3CH_2COOH

Butyric acid $CH_3CH_2CH_2COOH$

Valeric acid $CH_3CH_2CH_2CH_2COOH$

Acetic acid CH_3COOH

Methyl acrylate $CH_2=CHCOOCH_3$

Acrylic acid $CH_2=CHCOOH$

Vinyl acetic acid $CH_2=CHCH_2COOH$

Allyl acetic acid $CH_2=CHCH_2CH_2COOH$

Methacrylic acid $CH_2=C(CH_3)COOH$

Methyl methacrylate $CH_2=C(CH_3)COOCH_3$

Surface photopolymerisation of carboxylic acids has not previously been reported, but methyl methacrylate is known to form a polymer under UV irradiation from the vapour phase at pressures of 10 torr and above. In the presence of mercury, which can act as a triplet sensitiser, Melville[11] observed rapid polymer formation in the gas phase, and continued growth of polymer after illumination had stopped, indicating chain growth and the presence of long lived free radical sites. Tsao and Erlich[12] also obtained a polymer from the laser photolysis of methyl methacrylate vapour, in the absence of mercury, but did not observe polymer formation in the gas phase or, continued polymerisation after irradiation had ceased. They therefore concluded that these effects observed by Melville had been due to the formation of triplet states, which might be expected to be long lived. Deposition rate measurements of methyl methacrylate photopolymerisation at 10 torr are carried out in order to determine whether or not the effects observed by Melville could be reproduced without triplet sensitisation.

4.2 EXPERIMENTAL

Plasma polymerisations were carried out in the reactor shown in figure 4.1. The experimental procedure followed was the same as described in chapter 2. UV photopolymerisations were performed using the same procedure and apparatus as for vacuum UV surface photopolymerisation (see chapter 2), except that the plasma chamber to the right hand side of the calcium fluoride window was replaced by a 200W Oriel medium pressure mercury arc lamp. For deposition rate measurements of the photopolymerisation of methyl methacrylate, a Kronos QM 331 deposition monitor was used in the apparatus shown in figure 4.2. The monitor consisted of a vibrating quartz crystal, the frequency of which depended on the weight of material deposited on it. A 500W Hanovia medium pressure arc lamp was used as a UV source. The deposition monitor was affected by the heating caused by the UV lamp. This heating effect was measured in a separate experiment with no monomer present, but was found to be small compared with the rate of polymer deposition. Samples for XPS analysis were collected in separate runs on a piece of aluminium foil placed on top of the deposition monitor.

Samples were analysed by XPS using a Kratos ES200 spectrometer with a take off angle of 35°. Contact angles were measured using a small drop (3ul) of distilled water placed on the polymer surface. The width (d) and height (h) of the drop were measured using a microscope and the contact angle (θ) was calculated from equation 4.1.

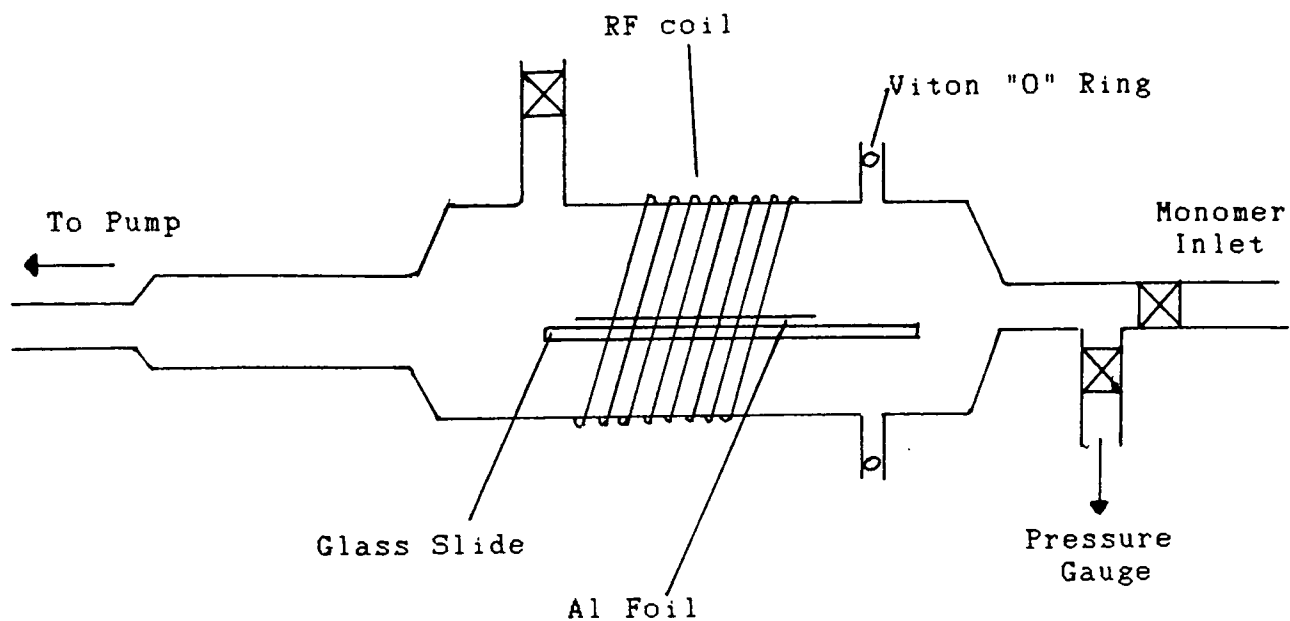$$\tan\left(\frac{\theta}{2}\right) = 2h/d \qquad\qquad 4.1$$
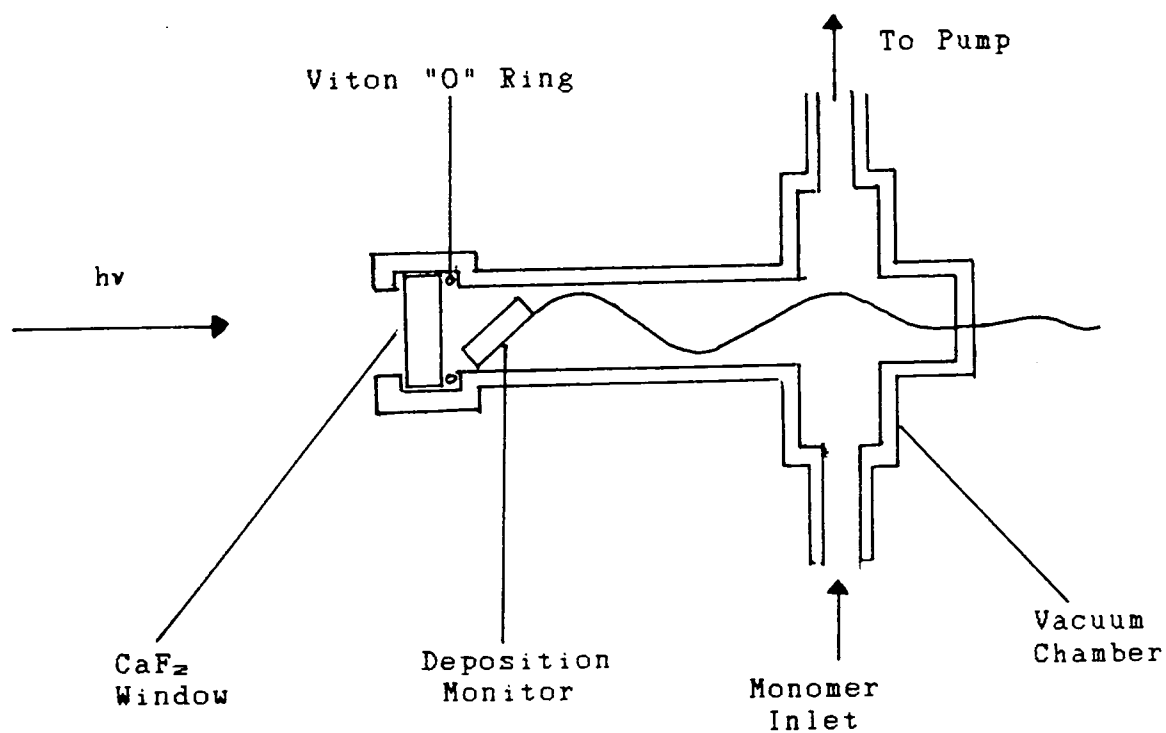
Figure 4.1 Plasma reactor used in chapter 4

Figure 4.2 Apparatus used for deposition rate measurements

Contact angles of less than $5°$ were too low to measure and are quoted as being zero.

4.3 RESULTS AND DISCUSSION

4.3.1 Unsaturated Carboxylic Acids

(a) Plasma Polymers

Plasma polymers of acrylic acid, vinyl acetic acid and allyl acetic acid were each made under three different sets of conditions:-

(i)   Power = 10W, pressure = 0.16 torr, flow rate $\simeq$ 4-5 cm^3/min

(ii)   Power = 2W, pressure = 0.16 torr, flow rate $\simeq$ 4-5 cm^3/min

(iii) Pulsed Plasma, average power = 1W, pressure = 0.2 torr,
flow rate $\simeq$ 10 cm^3/min

The allyl acetic acid had too low a vapour pressure to carry out the pulsed plasma under the conditions shown, so a pressure of 0.18 torr and a flow rate of 5 cm^3/min were used instead.

C_{1s} and O_{1s} XPS spectra of acrylic acid plasma polymers obtained under all three sets of conditions are shown in figure 4.3. The C_{1s} core levels were peak fitted using the following binding energies for the constituent peaks:-

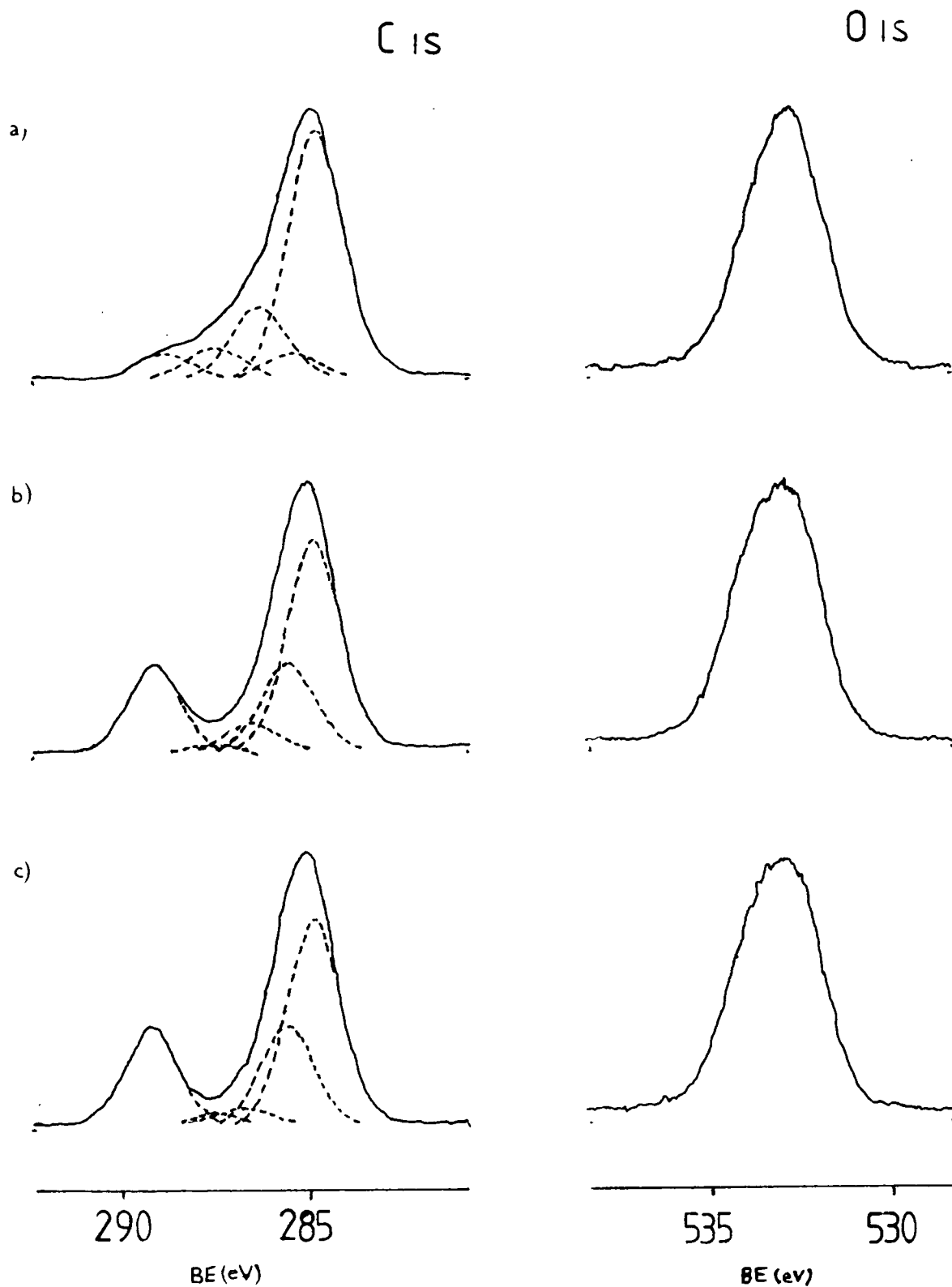|	
CH	285.0 eV
$\underline{C}$-CO_2	285.7 eV
C-O	286.7 eV
C=O	287.7 eV
O-C=O	289.1 eV

Figure 4.3 C1s and O1s XPS spectra of plasma polymerised acrylic
acid   (a) at 10W
              (b) at 2W
              (c) with pulsed plasma

The results of XPS analyses for each of the acids under each set of conditions are shown in table 4.2. The degrees of retention of oxygen and carboxylate groups were calculated by comparing the composition of the polymer with the monomer: the results are presented in table 4.3.

Table 4.2 Composition of unsaturated carboxylic acid plasma polymers as shown by XPS

Acid	Plasma Condition	O:C ratio	% of C_{1s}				
			CH	$C-CO_2$	C-O	C=O	O-C=O
Acrylic	10W	0.27	63	6	17	7	6
	2W	0.44	50	21	6	2	21
	pulsed	0.51	47	23	4	2	23
Vinyl Acetic	10W	0.17	72	3	15	5	3
	2W	0.36	61	16	4	2	16
	pulsed	0.42	55	20	2	1	21
Allyl Acetic	10W	0.19	72	3	15	5	3
	2W	0.36	63	16	3	2	16
	pulsed	0.36	64	16	3	1	16

It can be seen from table 4.2 that the polymers formed at 10W contain comparatively small amounts of oxygen, and have only low concentrations of $C-CO_2$ and O-C=O groups. A considerable number of C-O, and to a lesser extent C=O groups, not present in the original monomers, have been created during polymerisation. Table 4.3 shows that the degree of oxygen retention is fairly low

(34-47%) and the degree of carboxylate retention is only 13-18%.
The comparatively high level of C-O environments suggests that
some or all of the O-C=O groups could be esters rather than acid
groups. The number of acid groups on these surfaces must
therefore be very low indeed. This is confirmed by the high
contact angles (see table 4.4) of 56-72°. A surface containing a
high concentration of carboxylic acid groups would be expected to
be hydrophilic, and to have a very low contact angle with water.

Table 4.3 Retention of oxygen and carboxylate in plasma polymers
of unsaturated carboxylic acids

Acid	Plasma Condition	% Retention of oxygen	% Retention of carboxylate	% of oxygen present as carboxylate
Acrylic	10W	40	18	45
	2W	67	62	92
	pulsed	77	69	90
Vinyl Acetic	10W	34	13	40
	2W	72	64	89
	pulsed	84	82	96
Allyl Acetic	10W	47	17	36
	2W	90	82	91
	pulsed	90	79	88

At 2W and with the pulsed plasma the retention of
functionality was much higher, although some of the films were
rather oily, due to the low degree of polymerisation at low W/F.
Table 4.2 shows high O:C ratios, high concentrations of C-CO$_2$ and

131

O-C=O groups and only low concentrations of C-O and C=O groups for all the acids. Table 4.3 shows that the percentage retention of oxygen was high (67-90%) and that almost all (typically 90%) of this was in the form of O-C=O groups. The low levels of C-O mean that all or nearly all of the O-C=O observed must present as be acid groups, rather than as esters. For acrylic and vinyl acetic acids the 2W plasmas generally gave slightly lower levels of retention than the pulsed plasmas, but in all cases the composition of the polymer was essentially similar to that of the corresponding conventional polymer. The contact angles (table 4.4) with water were all too low to measure (<5°), as would be expected for surfaces with a high concentration of carboxylic acid groups.

Table 4.4 Contact angles of plasma polymers of unsaturated carboxylic acids

Acid	Contact angle of plasma polymer with water[*]		
	10W	2W	pulsed
Acrylic	56°	0	0
Vinyl acetic	72°	0	0
Allyl acetic	65°	0	0

[*]Contact angles too low to measure are quoted as zero

From these results it can be concluded that under low W/F conditions the plasma polymerisation of unsaturated carboxylic

acids proceeds mainly through the opening of the double bond, as in conventional polymerisation. The alternative type of reaction, involving elimination or rearrangement of the acid groups, does not occur to a large extent under these conditions, probably because the activation energy is too high. Under higher W/F conditions, when more energy is available per molecule, reactions involving the acid group dominate the polymerisation resulting in a plasma polymer with a low oxygen content and very little retention of monomer structure. In the pulsed plasma reactions involving the acid groups might occur to some extent during the pulse of RF power, but in the off period other monomer units may add on to the activated molecule via the double bond opening, producing small sections of conventional polymer. This type of mechanism may also occur in the low W/F continuous plasma if the power concentration is so low that activation of a molecule becomes very infrequent.

There seems to be little difference in behaviour of the different acids during polymerisation, suggesting that the ability to retain acid groups is not dependent on any particular position of the acid group with respect to the double bond. The highest level of carboxylate groups in a polymer (23% of carbon atoms) is in that formed from the acrylic acid, but this is simply due to the fact that acrylic acid possesses the highest percentage of acid groups of the monomers. There seems to be a tendancy for the percentage of carboxylate groups retained to increase as the hydrocarbon chain length increases. A possible explanation for this could that initial activation occurs at the double bond, and energy transfer to the acid group becomes more

difficult as their separation is increased.

(b) Photopolymers

Conventional UV photolyses (wavelength > 200 nm) of allyl acetic acid and acrylic acid were performed at monomer vapour pressures of 0.2 torr. The polymers were similar to the low W/F plasma polymers, except that there was a considerably higher level of hydrocarbon (see table 4.5). This could arise from contamination of the photopolymer by hydrocarbon present in the reaction chamber, or from elimination of carboxylate as carbon

Table 4.5 Photopolymers of acrylic and allyl acetic acids

		surface photopolymer of Acrylic acid	surface photopolymer of allyl acetic acid
O:C Ratio		0.39	0.29
	CH	59	68
%	C-CO2	18	13
of	C-O	3	4
C1s	C=O	3	2
	O-C=O	18	13
% retention of oxygen		59	72
% retention of carboxylate		54	66
% of oxygen as carboxylate		91	91
contact angle		0	not measured

dioxide. The former seems most likely, as a large amount of hydrocarbon was observed in the photopolymers of perfluorotoluene (see chapter 2). If this is the case then the surface photopolymers are essentially the same as the plasma polymers, and so the plasma polymerisation can be explained by excited state chemistry.

4.3.2 Saturated Carboxylic Acids
a) Acetic acid

If retention of acid functionality occursin the low W/F plasma polymerisation of unsaturated carboxylic acids, then it might be expected that saturated acids would not show the same behaviour. The plasma polymerisation of acetic acid appears to bear this out. The polymers formed under the three types of conditions used for the unsaturated acids all showed considerable loss of oxygen and rearrangement of the acid groups to form other oxygen functionalities. The results are presented in table 4.6 and the C_{1s} spectra for acetic acid plasma polymers formed at 10W and at 2W are shown in figure 4.4.

There is obviously some retention of structure at 2W and with the pulsed plasma as the percentage of carboxylate is still 50% of the monomer value, but there is also a considerable amount of C-O, suggesting that some of this is ester rather than acid. In the case of the 2W polymer the contact angle is not zero, also suggesting that the concentration of acid groups is not high. At 10W the polymer retains the monomer structure better than for the unsaturated acids, so the difference between high and low W/F plasma polymers of acetic acid is comparatively small.

135

Table 4.6. Plasma polymers of acetic acid

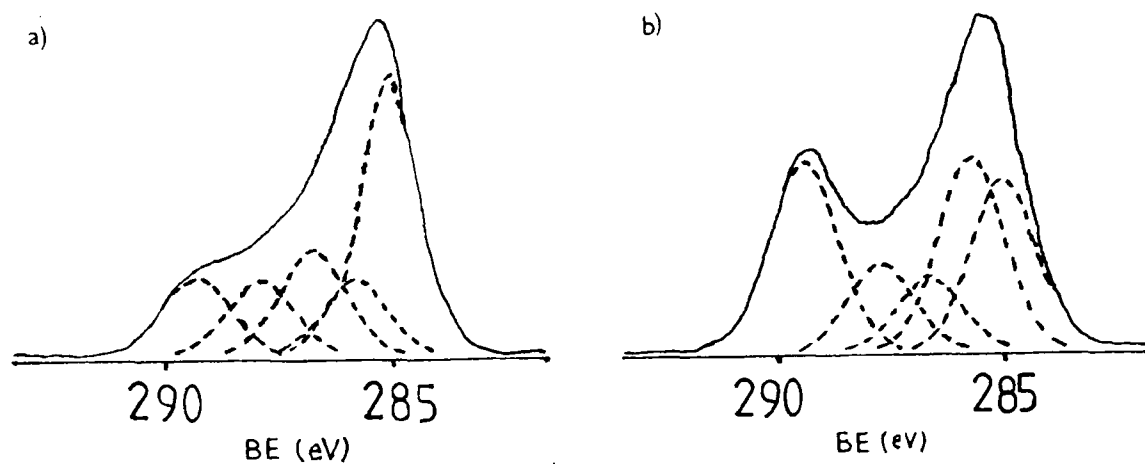|	Plasma Condition		
	10W	2W	pulsed
O:C ratio	0.46	0.64	0.59
CH	45	23	30
$C-CO_2$	12	26	25
C-O	18	10	9
C=O	12	12	11
O-C=O	12	26	25
% retention of oxygen	46	64	59
% retention of carboxylate	25	52	50
% of oxygen as carboxylate	25	81	83
contact angle	not measured	22°	0

Figure 4.4 C_{1s} XPS spectra of acetic acid plasma polymerised at (a) 10W , and (b) 2W

b) Propionic, Butyric and Valeric acids

These are the saturated analogues of the unsaturated acids studied, and should therefore provide the best comparison for investigating the effect of unsaturation in the plasma polymerisation of carboxylic acids. In the absence of a double bond, the degree of retention of monomer functionality might be expected to be comparatively low, as in the case of acetic acid. In fact, however, the plasma polymers of these acids were generally similar to those of the unsaturated acids. Using the same three sets of conditions as for the unsaturated acids, it was found that at 10W there was very little retention of structure, while at 2W and with a pulsed plasma high carboxylic acid levels were observed in the polymers formed. C_{1s} spectra of propionic acid plasma polymers formed at 10W and 2W are shown in figure 4.5. The results of all the plasma polymerisations of these acids are presented in tables 4.7, 4.8 and 4.9.
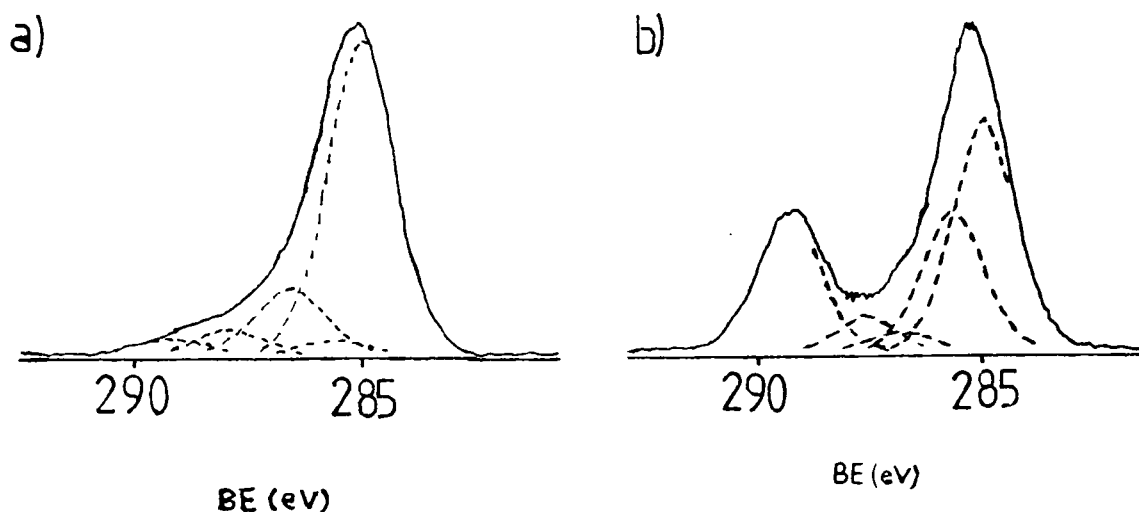

Figure 4.5 C1s XPS spectra of propionic acid plasma polymerised at (a) 10W and (b) 2W

137

Table 4.7 Composition of saturated acid plasma polymers as shown by XPS

Acid	Plasma condition	O:C ratio	% of C_{1s}				
			CH	$C-CO_2$	C-O	C=O	O-C=O
	10W	0.20	68	4	16	7	4
Propionic	2W	0.46	50	20	5	4	20
	pulsed	*	*	*	*	*	*
	10W	0.16	76	3	14	4	3
Butyric	2W	0.40	58	17	4	4	17
	pulsed	0.34	64	17	5	2	14
	10W	0.17	76	4	12	3	4
Valeric	2W	0.30	67	13	5	3	13
	pulsed	0.31	64	14	4	3	14

* The amount of polymer deposited in this case was so small that aluminium substrate, and hydrocarbon contamination on it was seen by XPS, and so accurate peak fitting was not possible. An accurate measurement of the contact angle was also not possible.

Table 4.8 Contact angles of saturated carboxylic acid plasma polymers

Acid	Contact angle with water		
	10W	2W	pulsed
Propionic	68°	0	*
Butyric	62°	0	0
Valeric	70°	26°	40°

Table 4.9 Retention of oxygen and carboxylate in plasma polymers of saturated carboxylic acids
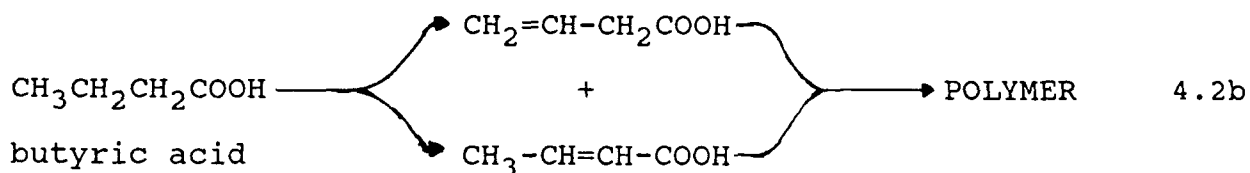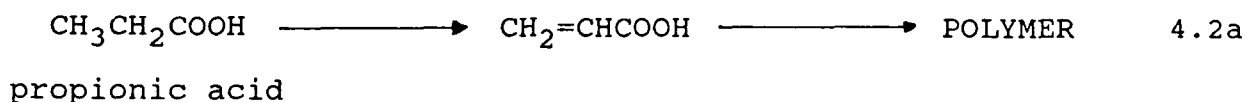
Acid	Plasma Condition	% Retention of oxygen	% Retention of carboxylate	% of oxygen present as carboxylate
Propionic	10W	30	11	25
	2W	82	75	91
	pulsed	*	*	*
Butyric	10W	32	13	41
	2W	79	69	87
	pulsed	68	58	85
Valeric	10W	34	20	59
	2W	75	65	86
	pulsed	78	71	91

The flow rate used for all three polymerisations of valeric acid was only 1.5 cm^3/min, due to its low vapour pressure. This may have caused its retention of monomer functionality to be slightly less good than it might otherwise have been. The contact angles for the 2W and pulsed plasma polymers of valeric acid were non-zero, despite the fact that the degree of retention of carboxylate was quite good. This must be due to the comparatively low percentage of acid groups in the monomer, and hence virtually all must be retained in order to give a wettable plasma polymer, as in the case of allyl acetic acid.

Generally the behaviour of these acids was very similar to that of the corresponding unsaturated acids. However, the

deposition rates of the plasma polymers were generally slower and the films were less oily. There was also no significant difference in the degree of retention of acid groups as the chain length varied; if anything the trend was opposite to that shown by the unsaturated acids.

The probable explanation of the retention of monomer structure at low W/F, is that hydrogen is eliminated from adjacent carbon atoms in the hydrocarbon chain to form an unsaturated acid, which then polymerises (equations 4.2a,b). Elimination of hydrogen is well known as a process which occurs during plasma polymerisation of hydrocarbons[13,14]. This would account for the slower rates of polymerisation observed, since only those acid molecules which had already undergone hydrogen elimination could take part in the polymerisation. For butyric and valeric acids there is more than one possible position for a double bond to form, and so the separation of the double bond and acid group will not necessarily increase as the chain length increases. This could explain why little difference was observed in the degrees of acid group retention between the saturated acids.

$$CH_3CH_2COOH \longrightarrow CH_2{=}CHCOOH \longrightarrow POLYMER \qquad 4.2a$$

propionic acid

$$CH_3CH_2CH_2COOH \longrightarrow \begin{array}{c} CH_2{=}CH{-}CH_2COOH \\ + \\ CH_3{-}CH{=}CH{-}COOH \end{array} \longrightarrow POLYMER \qquad 4.2b$$

butyric acid

Acetic acid cannot form a double bond by hydrogen elimination because it has only one carbon atom apart from the acid group. This therefore explains the poor degree of retention for acetic acid even under low W/F plasma conditions.

An attempt to produce a surface photopolymer of propionic acid, using conventional UV radiation and monomer pressure and flow rate of 0.2 torr and $3.5 cm^3$/min respectively, failed to produce any polymer after five hours irradiation time. This is consistent with the mechanism proposed for the plasma polymerisation, since it is unlikely that much loss of hydrogen will occur in the UV, to form acrylic acid.

4.3.3 Methyl Methacrylate

a) Plasma polymerisation

Having seen that carboxylic acids can be made to retain their acid groups upon plasma polymerisation, it might be possible for an unsaturated ester such as methyl methacrylate (MMA) to retain its ester groups, and form a material similar to poly methyl methacrylate (PMMA). The plasma polymerisation of MMA was therefore carried out under the following sets of conditions:
(i) power = 10W, pressure = 0.15 torr, flow rate = 0.5 cm^3/min,
(ii) power = 2W, pressure = 0.17 torr, flow rate = 10 cm^3/min,
(iii) pulsed plasma, average power = 1.5W, pressure = 0.19 torr, flow rate = $2cm^3$/min. The results of these experiments are shown in table 4.10, and XPS C_{1s} spectra of the plasma polymers formed at 10W and 2W are shown in figure 4.6.

As expected the 10W polymer retains very little ester, as shown by the low O-C=O peak. However, the 2W and pulsed plasmas

also produced polymers with fairly low degrees of carboxylate retention (54 and 57%), lower than for any of the carboxylic acids studied, except for acetic acid. Comparitively large numbers of C-O and C=O environments were created during polymerisation, showing considerable rearrangement of the ester group. It can be concluded therefore that the plasma polymerisation of methyl methacrylate does not provide good

Table 4.10 Polymers of Methyl Methacrylate

		Plasma condition		
		10W	2W	pulsed
	CH	67	46	50
%	$C-CO_2$	4	11	11
of	C-O	21	25	22
C_{1s}	C=O	4	7	5
	O-C=O	4	11	11
C-O not present as ester		18	14	11
% Retention of carboxylate		18	54	57
contact angle		70°	67°	68°
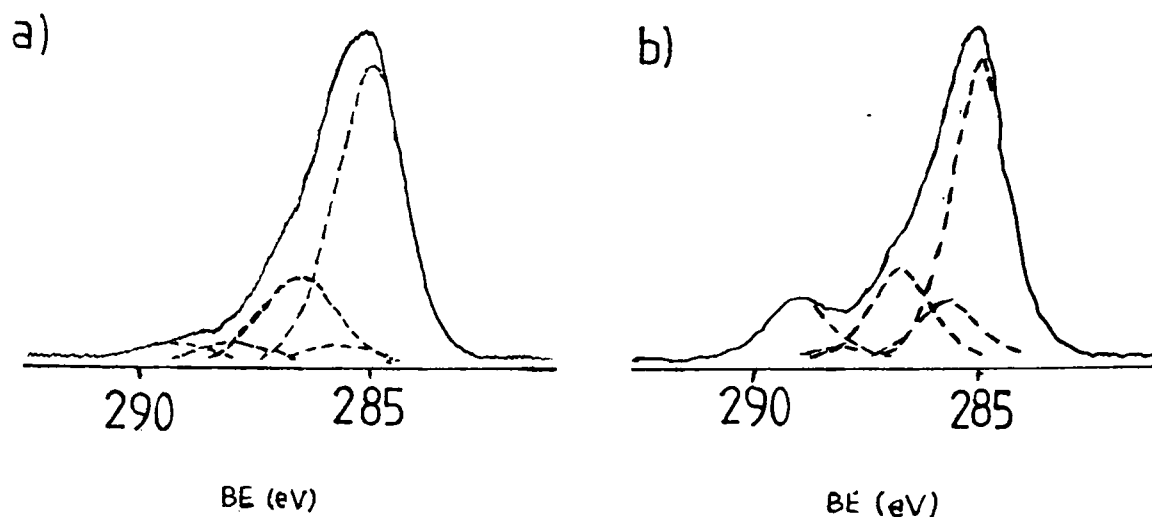
<u>Figure</u> <u>4.6</u> C_{1s} XPS spectra of MMA plasma polymerised at (a) 10W and (b) 2W

retention of monomer functionality, and so is different from that of the unsaturated carboxylic acids.

The structure of MMA differs from that of acrylic acid in two respects: (i) it is a methyl ester, rather than an acid, and (ii) it has a methyl group on the carbon atom next to the acid group. Which, if either, of these is responsible for the difference in behaviour during plasma polymerisation could be ascertained by comparing the low W/F plasma polymer of MMA with those of (i) methacrylic acid, and (ii) methyl acrylate. The results of the 2W plasma polymerisations of these compounds are shown in table 4.11.

Table 4.11 Comparison of 2W plasma polymers of methyl methacrylate, methyl acrylate and methacrylic acid.

		methyl methacrylate	methacrylic acid	methyl acrylate
	CH	47	57	50
%	$C-CO_2$	11	17	16
of	C-O	25	7	18
C_{1s}	C=O	7	2	0
	O-C=O	11	17	16
C-O not present as ester		15	*	2
% Retention of carboxylate		54	67	63

*   Not applicable

The degrees of carboxylate retention in the methacrylic acid and methyl acrylate plasma polymers are both higher than for that of MMA. More importantly, many fewer C-O and C=O environments have been created, showing much less rearrangement of the carboxylate group during plasma polymerisation. The methacrylic acid polymer had a contact angle with water too low to measure. Methacrylic acid and methyl acrylate therefore both behave like acrylic acid, retaining their functional groups, and not like MMA. The failure of MMA to retain its structure during low W/F plasma polymerisation cannot, therefore, be due to the fact that it is an ester or, due to its extra methyl group, but is a specific property of methyl methacrylate.

4.3.4 Photopolymerisation of Methyl Methacrylate

Further insight into the plasma polymerisation of MMA might be obtained from studying its surface photopolymerisation. If a polymer similar to the plasma polymer is produced, as in the case of the unsaturated acids, then the mechanism of plasma polymerisation is probably similar to that of the acids, with the efficiency of retention just being slightly worse. If a photopolymer similar to conventional PMMA is produced (ie much better retention of functionality than in the plasma polymer), then the plasma polymerisation is probably made up of two competing processes: (i) a "conventional" radical polymerisation type process, like that which dominates in the case of the acids, and (ii) another higher energy process which disrupts the ester group. If no photopolymer is formed then the mechanism must be completely different from that of the acids, involving a high energy pathway, and no conventional radical polymerisation.

The photolysis of MMA vapour at a pressure of 0.2 torr and a flow rate of 5 cm^3/min failed to produce any polymer after $3^1/_2$ hours. The mechanism of the plasma polymerisation must therefore be completely different from that of the acids. However, at a much higher vapour pressure (8 torr) a surface photopolymer was formed rapidly. XPS analysis of this polymer showed that it was not like any of the plasma polymers of MMA but was very similar to conventional PMMA (see table 4.12). The C_{1s} core level spectrum of this polymer is shown in figure 4.7. This is in agreement with Melville[11] and Tsao and Erlich[12], who both observed PMMA formation from photolysis of MMA at this sort of pressure. The small differences between the composition of the

polymer observed and that of PMMA could be due to UV wavelengths of less than 230 nm, which were observed by Melville to cause some decomposition of MMA.

Table 4.12 Comparison of C_{1s} core level spectra of plasma and photopolymers of MMA

	% of C_{1s}				
	CH	$C-CO_2$	C-O	C=O	O-C=O
Plasma Polymer (10W)	67	4	21	4	4
Plasma Polymer (2W)	46	11	25	6	11
Photopolymer (8 torr)	42	18	20	2	18
PMMA (theoretical)	40	20	20	0	20
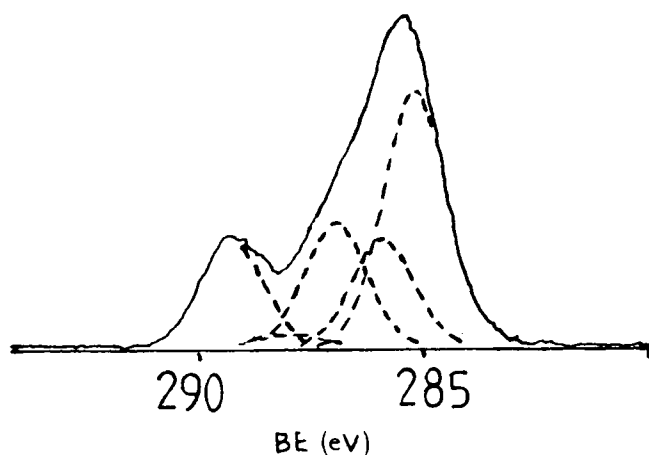
Figure 4.7 C1s XPS spectrum of MMA photopolymerised at 8 torr

To further examine the photopolymerisation of MMA deposition rate measurements were made during UV irradiation at 8 torr. Measurements were continued after irradiation had ceased in order to determine whether the polymer continued to grow in the dark as observed by Melville, or not as claimed by Tsao and Erlich. A plot of film thickness against time is shown in figure 4.8.

For the first five minutes after the light was switched on the film thickness decreased. This must correspond to depolymerisation of polymer already present on the thickness monitor from previous experiments. The UV lamp takes some time to "warm up" after switching on. During this time comparatively little UV radiation is emitted, but the lamp does give out infra red radiation. This must heat up the polymer on the thickness monitor, causing thermal depolymerisation. After about 10 minutes the UV output has reached a maximum value and causes rapid polymerisation. The polymerisation occurs much faster than any competing depolymerisation process, and so the monitor reading increases rapidly. After about 15 minutes the rate of polymerisation begins to decrease again. This is due to absorption of UV light by polymer building up on the calcium fluoride window, causing a reduction in the UV flux reaching the reaction chamber.

After 20 minutes the UV lamp was switched off. As can be seen from the graph, polymer growth continues at a slower but roughly constant rate. The rate of this growth decreased only gradually; the reading was observed to be still slowly increasing 2 days later. This observation is in agreement with that of
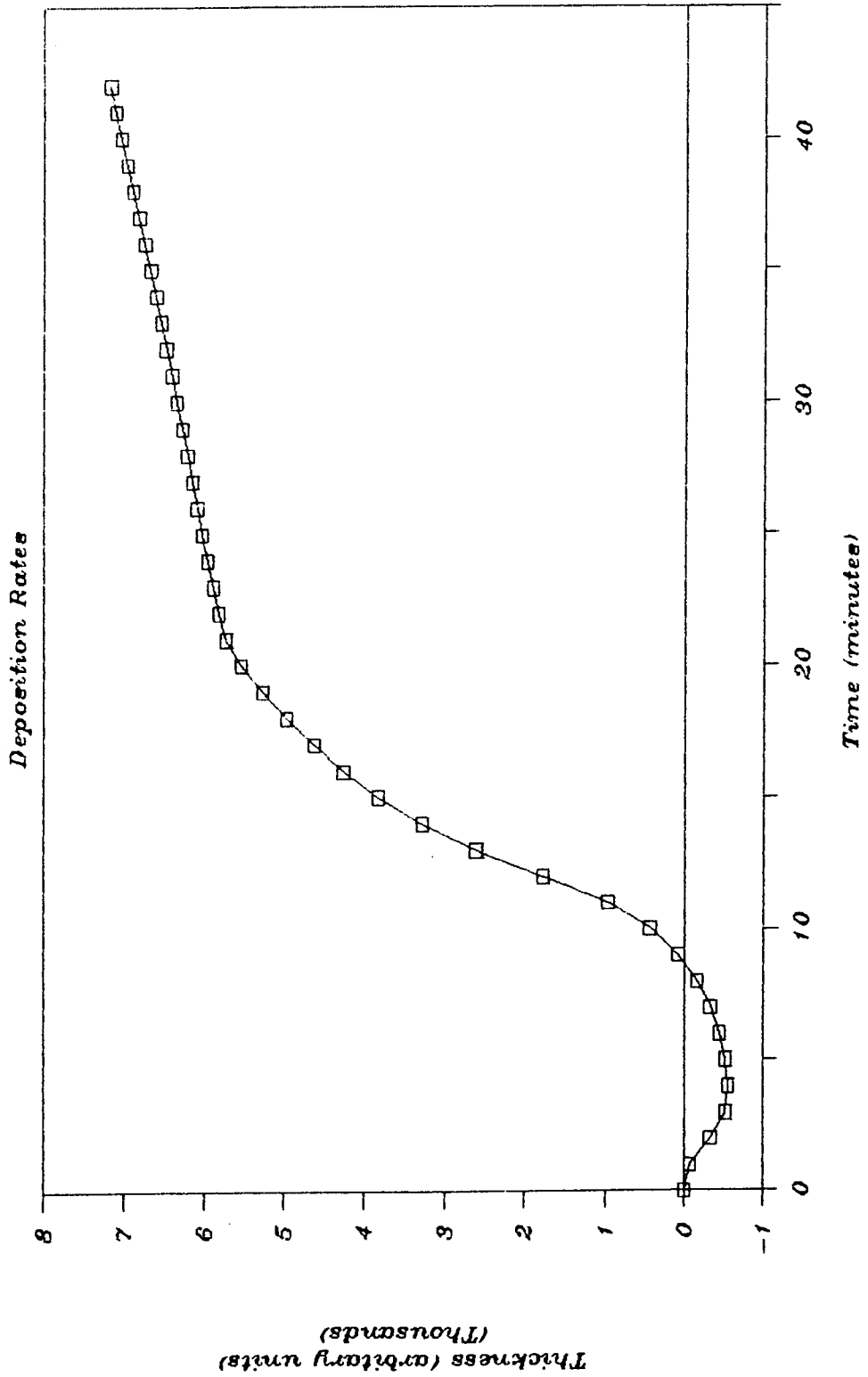
Figure 4.8 Deposition rates of an MMA photopolymer at 8 torr

148

Melville, despite the fact that no mercury was present to act as a triplet sensitiser. It is possible that Tsao and Erlich did not notice polymerisation in the dark because it is slow compared to that during UV irradiation. Unlike Melville's observations, however, no formation of polymer was observed in the gas phase.

This type of "living" polymerisation has also been observed for MMA in a plasma initiated reaction by Kuzuya et. al[15]. A plasma polymer was formed from one of a variety of monomers on the walls of a glass ampule. After the plasma was extinguished MMA, at its saturated vapour pressure, was introduced and the ampule sealed. Polymerisation of the MMA was found to occur on the plasma polymer, the trapped free radicals in the polymer acting as initiation sites, and to continue for several days. It would therefore appear that MMA vapour, at a pressure of a few torr or more, will polymerise in this way whenever it comes into contact with a surface containing free radical sites to act as initiators.

Continuing growth of polymer for a long period after irradiation had ceased must imply the presence on the surface of long lived free radicals at the end of growing polymer chains. This therefore shows that the photopolymerisation of MMA under these conditions proceeds via a radical chain growth mechanism.

The reason for the lack of polymer formation at lower pressures is probably due to the balance between the competing polymerisation and depolymerisation processes. At 8 torr the polymerisation occurred more rapidly than depolymerisation, so net polymer formation was observed. However the critical temperature for polymer formation, above which polymer formation

will not occur, is known to decrease as the pressure is lowered[15]. This is due to the entropy term becoming increasingly unfavourable. At 0.2 torr it is therefore likely that the critical temperature is exceeded at room temperature, and so depolymerisation will dominate and polymerisation will not occur. Measurements using the thickness monitor for the photolysis at 0.2 torr, show a negative slope, indicating that net depolymerisation is occuring. In the plasma the pressure is 0.2 torr or less, so the conventional type of polymerisation cannot occur, and so the monomer functionality is not retained. The reason why the other monomers can conventionally polymerise to some extent under plasma conditions, and so retain carboxylate groups in their plasma polymers, is thought to be due to greater thermal stability of their conventional polymers.

4.4 SUMMARY

Carboxylic acid monomers containing an olefinic double bond can be made to retain a high percentage of acid groups upon plasma polymerisation, producing a very hydrophilic surface. This can be achieved by using very low power and high flow rate conditions, in a continuous or pulsed plasma. Similar polymers can be produced photochemically, suggesting that conventional radical polymerisation is important in the plasma polymerisation mechanism under these conditions. Straight chain saturated carboxylic acids lose hydrogen in a plasma to form a double bond, and so polymerise in a similar way to the unsaturated acids. Acetic acid is an exception to this, as it is unable to form an olefinic double bond. Esters, such as methyl acrylate can also behave in a similar manner, but methyl methacrylate does not. This is probably due to the low thermal stability of polymethyl methacrylate in a vacuum. MMA does not photopolymerise at plasma polymerisation pressures, but at higher pressures produces a photopolymer similar to conventional PMMA. This forms via a chain growth mechanism and contains long lived active free radical chain ends. The difference in behaviour of MMA during photolysis at 8 torr and 0.2 torr shows the importance of using similar conditions when comparing plasma polymerisation with surface photopolymerisation.

<u>REFERENCES</u>

(1) B.Watkins, J.Behling, E.Kariv and L.Miller, J. Amer. Chem. Soc., 97, 354-9, (1975)

(2) J.Sheehan and G.Hess, J. Amer. Chem. Soc., 77, 1067, (1955)

(3) H.Yasuda and C.E.Lamaze, J. Appl. Polym. Sci., 17, 1519, (1973)

(4) H.Yasuda and C.E.Lamaze, J. Appl. Polym. Sci., 17, 1533, (1973)

(5a) H.Suhr and R.I.Weiss, Angew. Chem. 82, 295, (1970); Int. Ed. 9, 312, (1970)

(5b) H.Suhr in "Techniques and Applications of Plasma Chemistry", Eds. J.R.Hollahan and A.T.Bell, Wiley Interscience, New York, (1974)

(6) H.Yasuda and T.Hsu, J. Polym. Sci., Polym. Chem. Ed., 15, 81, (1977)

(7) W.R.Gombotz and A.S.Hoffman, Polym. Mater. Sci. Eng., 56, 720, (1987)

(8) K.Hozumi, Pure and Appl. Chem., 60, 697, (1988)

(9) N.Inagaki and M. Matsunaga, Polym. Bull. (Berlin), 13, 349, (1985)

(10) G.H.Heider Jr., M.B.Gelbert and A.M.Yacynych, Anal. Chem., 54 324, (1982)

(11) H.W.Melville, Proc. Roy. Soc. A, 163, 511, (1937)

(12) J.Y. Tsao and D.J. Erlich, Appl. Phys. Lett., 42, 997, (1983)

(13) H.Yasuda, M.O.Bumgarner and J.J.Hillman, J. Appl. Polym. Sci., 19, 531, (1975)

(14) H.Kobayashi, A.T.Bell and M.Shen, Macromolecules, 7, 277, (1974)

(15) M.Kuzuya, T.Kawaguchi, S.Mizutani and T.Okuda, J. Polym. Sci., Polym. Lett. Ed., 23, 69, (1985)

(16) H.Yasuda in "Plasma Polymerisation", Academic Press Inc., London, (1985), p.62

CHAPTER 5

PLASMA POLYMERS CONTAINING IODINE

5.1 INTRODUCTION

Polymers with a high degree of resistance to etching by oxygen plasmas are potentially useful as resist materials in the electronics industry. An example of a way in which this kind of property can be achieved is in the incorporation of iodine into polymers. Experiments with iodinated polystyrene[1] demonstrated that as the iodine content of the polymer was increased, the rate of etching in an oxygen plasma decreased correspondingly (see figure 5.1). The increased resistance to oxidation was ascribed to the formation of a surface layer of relatively involatile oxidised iodine species. This layer protected the hydrocarbon part of the polymer from oxidation, and hence being lost as carbon monoxide, carbon dioxide and water.

Munro and Beer[2] found that if iodine vapour was incorporated into an oxygen plasma, then the surface oxidation of a
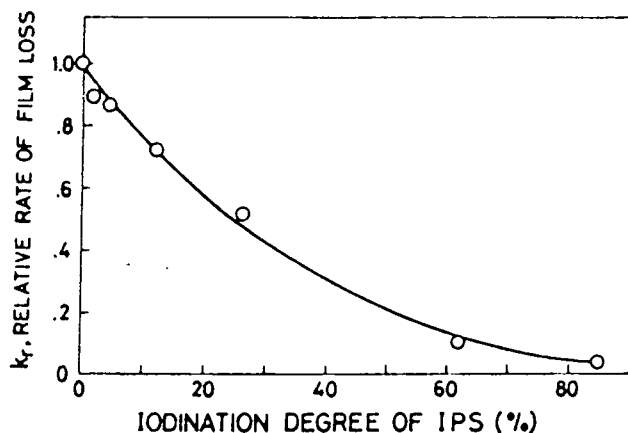
Figure 5.1 Dependence of the relative rates of iodinated polystyrene film loss on the degree of iodination

154

polyethylene substrate was considerably reduced. This was again explained by the formation of a protective layer of oxidised iodine on the surface of the polyethylene, originating from iodine species incorporated into the polymer from the plasma.

Plasma polymerisation represents a convenient one stage method for putting down a thin polymeric resist[3]. Unfortunately however, it is not easy to incorporate iodine into a plasma polymer, due to the weak nature of the carbon iodine bond which tends to break during the polymerisation process. An iodine containing plasma polymer derived from iodomethane has been reported[4] with an iodine to carbon elemental ratio of 1:11. This represents an elimination of over 90% of the iodine originally present in the starting monomer.

The aim of the work presented in this chapter is to discover methods of reducing the loss of iodine during the plasma polymerisation of iodo compounds. Two main approaches are considered:

(i) Plasma copolymerisation of iodobenzene with benzene,

(ii) Plasma polymerisation of allyl iodide.

The term "plasma copolymerisation" implies some sort of interaction between the two co-monomers in the gas phase, to produce a material that may be different from a linear combination of the plasma polymers of the individual monomers. An example of the difference between plasma copolymerisation and plasma codeposition can be found in deposition rate measurements in the following systems[5]. Mixtures of hexamethyldisiloxane and methyl methacrylate (figure 5.2a) show a linear relationship between deposition rate and vapour composition, indicating
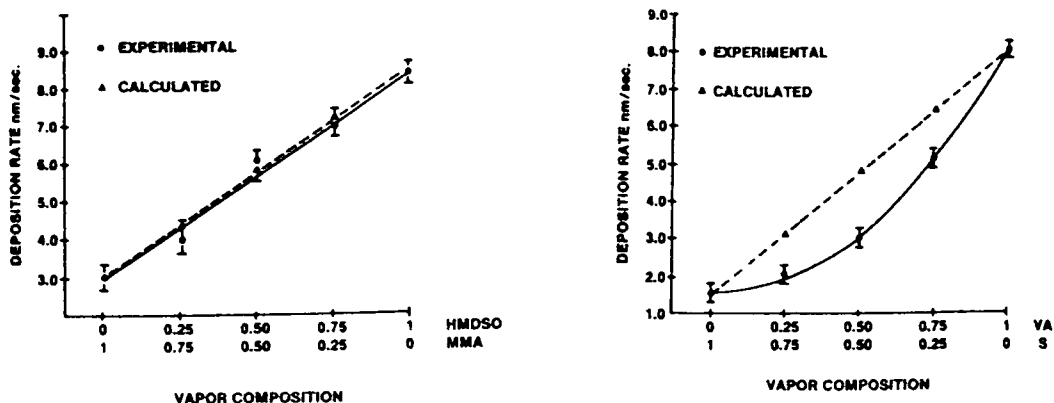
Figure 5.2 Deposition rates vs. vapour composition showing (a) codeposition and (b) copolymerisation
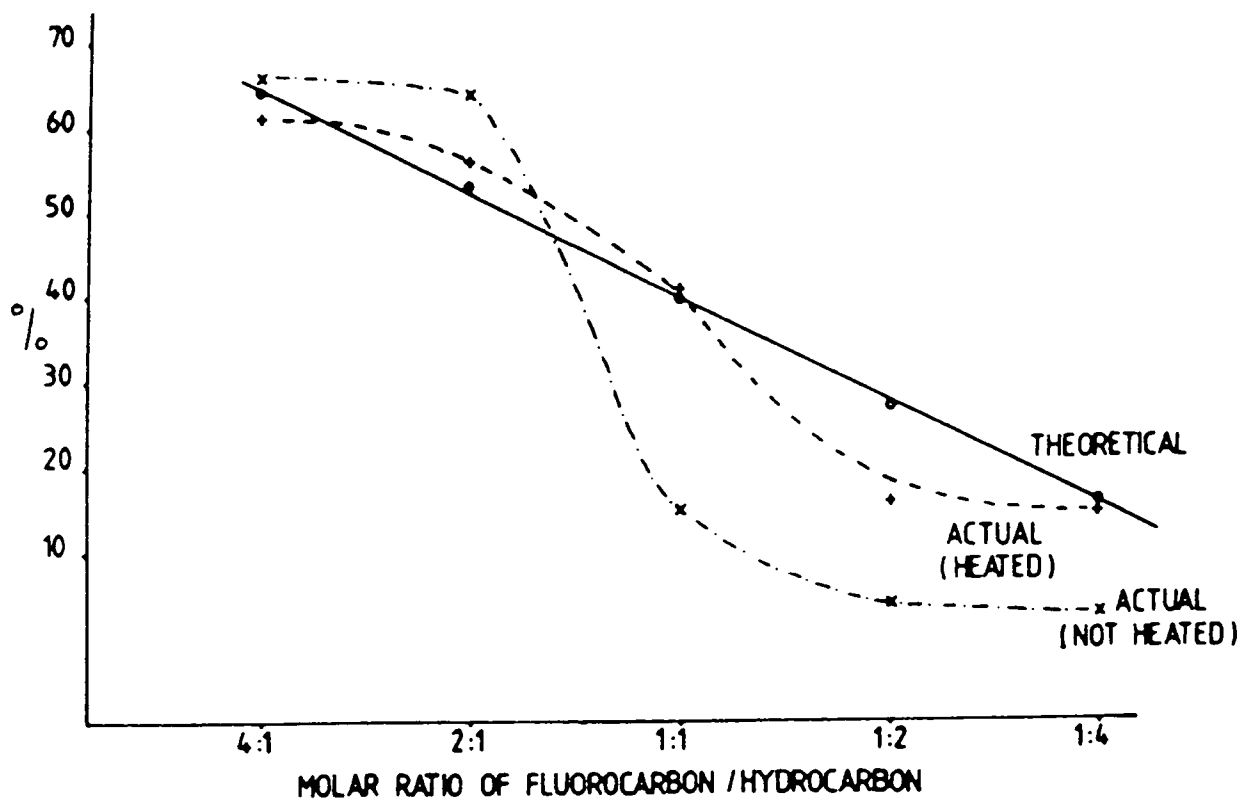

Figure 5.3 Percentage composition of fluorocarbon in plasma copolymers of naphthalene / perfluoronaphthalene vs. molar feed ratio to the plasma

codeposition, while styrene and vinyl acetate mixtures show a significant negative deviation, indicating that copolymerisation is occurring. An example of copolymerisation affecting the composition of a polymer is in the copolymerisation of naphthalene and perfluoronaphthalene[6], which shows considerable deviation from the theoretical composition (figure 5.3).

Results from mass spectral analysis of a benzene / perfluorobenzene plasma, presented in chapter 3, showed that there was considerable gas phase interaction between the two. If this is generally true for aromatic species, then copolymerisation may occur from a benzene / iodobenzene plasma. Interaction between the two monomers may lead to an alternative reaction route for the iodobenzene, suppressing the elimination of iodine. Although the stoichiometries of the starting mixtures mean that the amount of iodine expected in any polymer must be fairly small, the principle might also be applicable to monomers with higher iodine content to produce more heavily iodinated plasma polymers.

Allyl compounds plasma polymerised at low power and high flow rate have been found to retain a high percentage of their functional groups[7]. The data for the plasma polymerisation of carboxylic acids, in chapter 4, suggests that it is not the allyl group which is important, but the presence of, or ability to form, a double bond which could lead to addition polymerisation. Allyl iodide fulfils this requirement, and so might be expected to retain a high percentage of iodine in its plasma polymer.

The series of iodine containing plasma polymers formed by the copolymerisation method are treated with an oxygen plasma to

examine their resistance to oxidation. The surface compositions before and after treatment are analysed using XPS to gauge the oxidation level and iodine content of the polymer surfaces.

5.2 EXPERIMENTAL

Plasma polymerisations were carried out as described in chapter 2, using the reactor shown in chapter 4. For the copolymerisation experiments the two monomer vapours were fed into the reactor through a "T-piece" arrangement (figure 5.4), so that they would be mixed before entering the plasma. The flow rate of each monomer was controlled by a separate needle valve, and was measured separately by closing off the tap to the other monomer feed. The monomer ratios quoted in this chapter are the ratios of the flow rates.
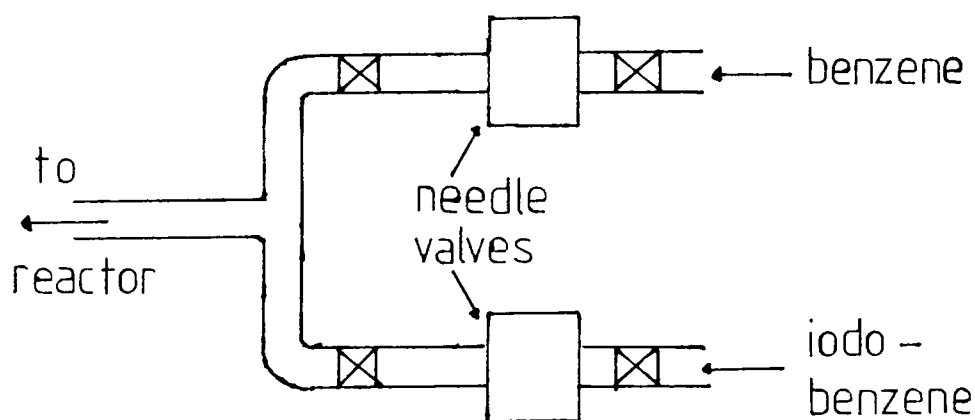
Figure 5.4 "T-piece" arrangement for plasma copolymerisation

Monomers were supplied by Aldrich and degassed before use using a succession of freeze thaw cycles. Iodobenzene and allyl iodide are light sensitive and so their monomer tubes were wrapped in aluminium foil. Allyl iodide is also heat sensitive, and so was kept in a refrigerator between runs.

Surface photopolymerisations were carried out as in chapter four.

Oxygen plasma treatments were carried out in a Polaron E2000 plasma asher/etcher pumped by an Alcatel rotary oil pump to a base pressure of 4×10^{-2} mbar. Oxygen, supplied by BOC, was introduced to the reaction chamber to a pressure of 0.2 mbar, and the polymer samples were subjected to a 20 watt plasma for one minute.

XPS analyses were carried out on a Kratos ES300 XPS spectrometer. UV spectra were taken of plasma polymers deposited onto quartz, using a Pye Unicam SP 8000 visible/UV spectrophotometer. Solid state NMR spectra were obtained from a CXP-200 NMR spectrometer using solid adamantane as a reference material. The carbon RF field strength was adjusted to allow for maximum transverse magnetism of the adamantane signal (^{13}C RF field strength = 62.5 kHz) and the Hartmann-Hahn match was then set by variation of the proton RF field strength until a maximum adamantane signal was observed. Slow spinning, a 1.5 ms contact time and a recycle delay of 5s were used. The shifts were converted to the TMS scale by using a shift of 38.4 ppm for the higher frequency adamantane resonance shift. After this procedure the spectrometer was ready to perform the cross-polarisation experiment on the sample. For the samples studied the spinning

frequency was varied to differentiate between the major resonances and the spinning sidebands. The peak intensities are not usually quantitative but depend on the contact time used. In this case however the relative intensities of the peaks was observed to remain constant as the contact time was varied, and so the peak areas can be taken to be approximately quantitative.

5.3 RESULTS AND DISCUSSION

5.3.1 Iodobenzene / Benzene Plasma Copolymers

Plasma copolymers of benzene and iodobenzene were prepared from monomer feed ratios of iodobenzene : benzene of 1:2, 1:1, 2:1, and 4:1. All were prepared using a total monomer pressure of about 10^{-1} torr and a plasma power of 18 watts. Individual plasma polymers of benzene and iodobenzene were also prepared under the same conditions. XPS analysis of these polymers shows the presence of carbon and (except for the benzene plasma polymer) iodine, in all cases. The $I_{3d}{}^{5/2}$ core level spectra showed a single peak at 620.5 eV consistent with iodine covalently bonded to carbon, or as I_2. There was generally also a small peak in the O_{1s} core level spectra at about 532.7 eV, indicating the presence of oxygen in all cases. XPS spectra for the iodobenzene plasma polymer are shown in figure 5.5, and the C:I and C:O elemental ratios are listed on table 5.1.
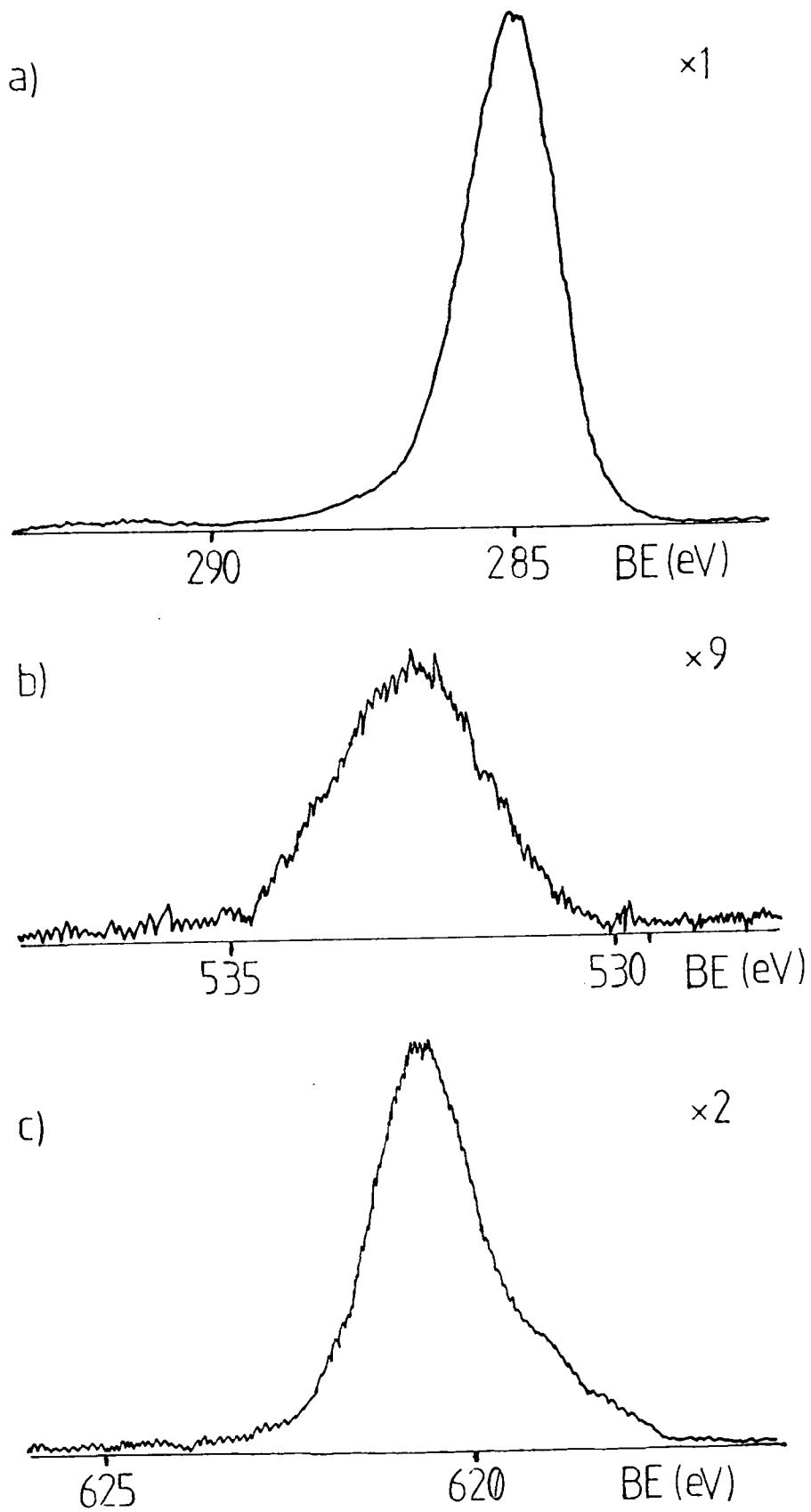
Figure 5.5 XPS core level spectra of an iodobenzene plasma polymer. (a) C_{1s}, (b) O_{1s} and (c) $I_{3d}^{5/2}$

161

Table 5.1 Elemental ratios for iodobenzene/benzene plasma polymers and copolymers

Plasma Polymer/Copolymer		I:C Ratio (polymer)	I:C Ratio (monomer)	O:C Ratio (polymer)
Benzene		0	0	1:16
Iodobenzene/benzene	1:2	1:39	1:18	1:82
Iodobenzene/benzene	1:1	1:29	1:12	1:58
Iodobenzene/benzene	2:1	1:22	1:9	1:52
Iodobenzene/benzene	4:1	1:21	1:7.5	1:50
Iodobenzene		1:26	1:6	1:39

The oxygen content of all the plasma polymers is so low as to be almost negligible in all cases except that of the benzene plasma polymer. This might indicate that the presence of iodine is inhibiting oxidation of the polymers, but could also be due to the benzene plasma polymer having been left in air longer before XPS analysis.

The results show that some iodine is lost during the formation of all the polymers. The highest level of iodine in any of the polymers was about 1 iodine per 20 carbon atoms. This occurred in the cases of the 2:1 and 4:1 iodobenzene/benzene copolymers. The iodine concentration found in the plasma polymer of pure iodobenzene corresponded to only 1 in 26 carbon atoms. Figure 5.6 shows a plot of the iodine content of the plasma polymers versus the percentage of iodobenzene in the monomer feed. It can be seen that there is a strong positive deviation from linearity, indicating that true plasma copolymerisation is

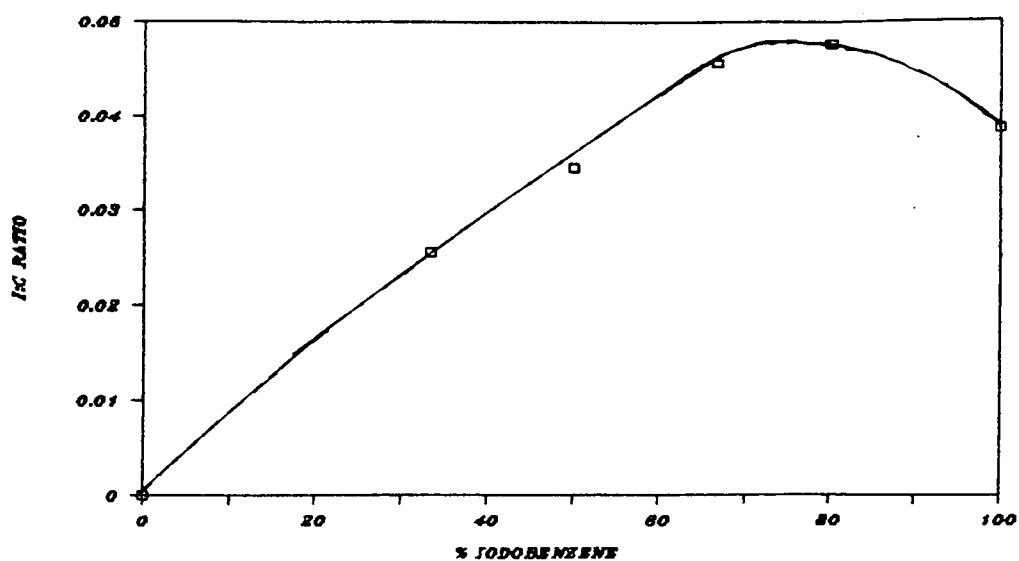## IODOBENZENE/BENZENE PLASMA COPOLYMERS

Figure 5.6 Variation of the iodine content of iodobenzene/benzene plasma copolymers with monomer feed ratio
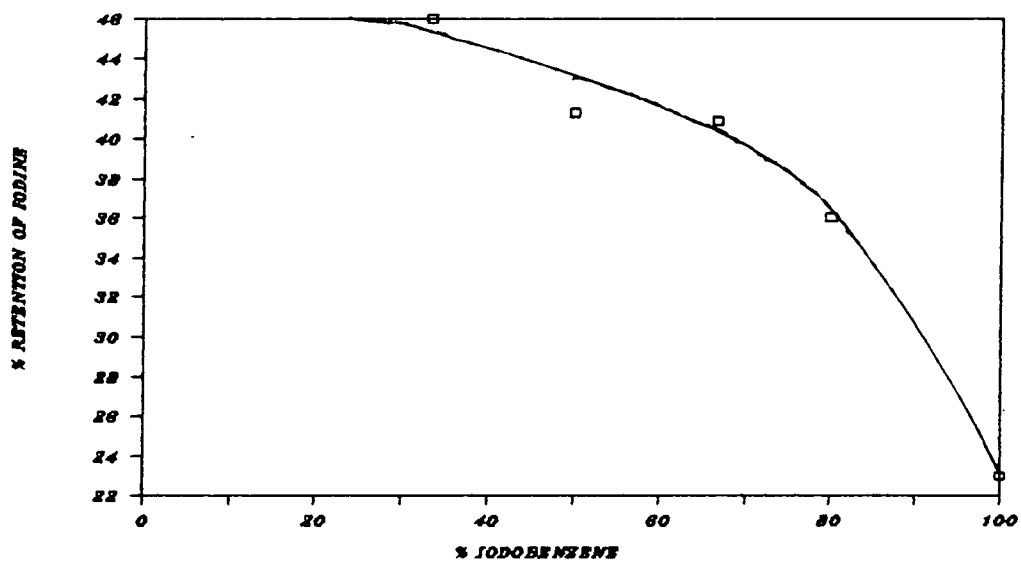
IODOBENZENE/BENZENE PLASMA COPOLYMERS

Figure 5.7 The percentage of iodine retained in iodobenzene / benzene plasma copolymers as a function of monomer feed ratio

163

taking place. The graph suggests that the optimum iodine content occurs with a monomer feed containing 70-80% iodobenzene. The percentage of iodine retained, however, is highest when the amount of iodobenzene in the monomer ratio is low, shown graphically by figure 5.7. In the case of pure iodobenzene only 23% of the iodine present in the monomer is retained, while copolymers from a 70-80% iodobenzene mixture retain about 37%. As the amount of iodobenzene in the monomer mixture is decreased, the percentage of iodine retained becomes even higher, reaching about 45% for low iodobenzene concentrations. The percentage of iodine found in the polymer is therefore a compromise between the amount of iodine originally present and the percentage retained upon plasma polymerisation, a compromise which leads to a maximum iodine content in the case of a copolymer from a 70-80% iodobenzene/benzene mixture.

The reason for the increased retention of iodine when benzene is present must be due to some interaction between the iodobenzene and benzene molecules, which provides an alternative reaction pathway to the iodine elimination which seems to be preferred by pure iodobenzene. What this interactive mechanism might be is not however known.

5.3.2. Plasma Oxidation

A sample of each of the plasma polymers and copolymers produced above was subjected to a 20 watt oxygen plasma for 1 minute. XPS spectra were obtained from the treated polymers and gave the elemental compositions shown in table 5.2.

164

Table 5.2 Elemental ratios for iodobenzene/benzene plasma polymers after oxygen plasma treatment

Plasma Polymer/Copolymer		I:C Ratio	O:C Ratio
Benzene		0	1:3.3
Iodobenzene/benzene	1:2	1:55	1:3.3
Iodobenzene/benzene	1:1	1:49	1:3.0
Iodobenzene/benzene	2:1	1:39	1:3.4
Iodobenzene/benzene	4:1	1:22	1:3.3
Iodobenzene[*]		1:52	1:4.0

[*]The iodobenzene plasma polymer was only subjected to a 10 watt oxygen plasma for 30 seconds

It is clear from table 5.2 that all of the plasma polymers were oxidised to a similar extent by the oxygen plasma (the iodobenzene plasma polymer was oxidised slightly less than the others, but this is because it was subjected to milder conditions). The XPS spectrum of an oxidised polymer (figure 5.8) shows a C_{1s} envelope containing $\underline{C}$-CO_2, C-O, C=O, O-C=O and CO_3 groups, indicating considerable oxidation of the carbon skeleton of the polymer. The $I_{3d}^{5/2}$ core level shows a second peak at 624 eV, corresponding to I_2O_5. This shows that oxidised iodine species do form, but far from protecting the surface by forming a protective layer, the surface concentration of iodine has actually decreased in all cases (although only slightly in the case of the 4:1 copolymer). The iodine in the plasma polymer therefore appears to be having no effect in preventing plasma oxidation, and no evidence for the formation of a protective layer is seen.
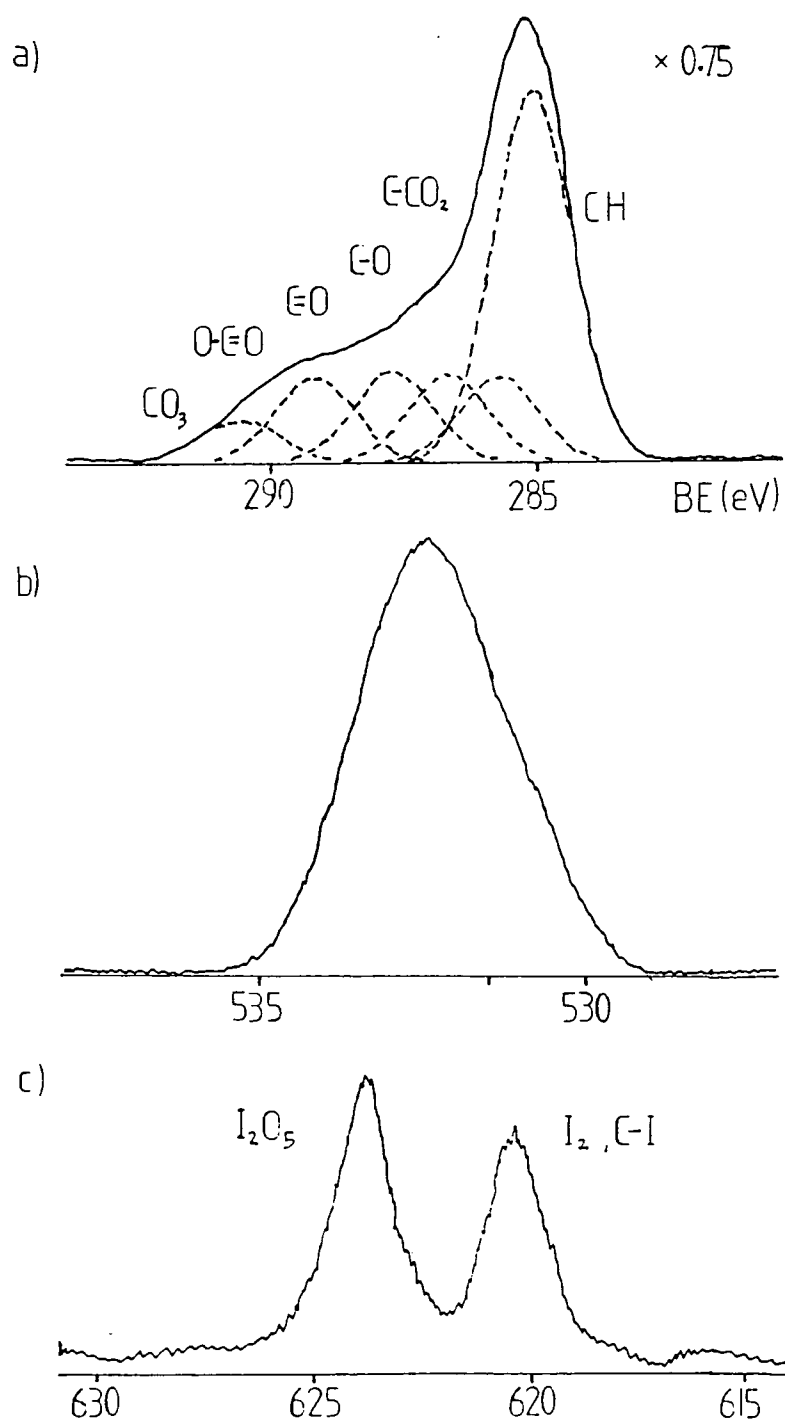
Figure 5.8 XPS spectra of a plasma oxidised iodobenzene plasma polymer. (a) C_{1s}, (b) O_{1s} and (c) $I_{3d}^{5/2}$

Even when left standing in air the surfaces of the plasma

polymers oxidise considerably (see table 5.3). After 1 week the

O:C ratios in the polymer surfaces were about 1:3. This must be

due to reaction of atmospheric oxygen with trapped free radicals

in the plasma polymers. Again also, the iodine concentration in

the surface is considerably lower than for the freshly made

polymers.

When these polymers are subjected to oxygen plasma

treatment for longer periods of time however, the iodine content

increases again. Figure 5.9 shows how the iodine content of an

iodobenzene plasma polymer increases with treatment time after

the initial drop. The changes in the $I_{3d}{}^{5/2}$ and O_{1s} XPS core

IODOBENZENE PLASMA POLYMERS
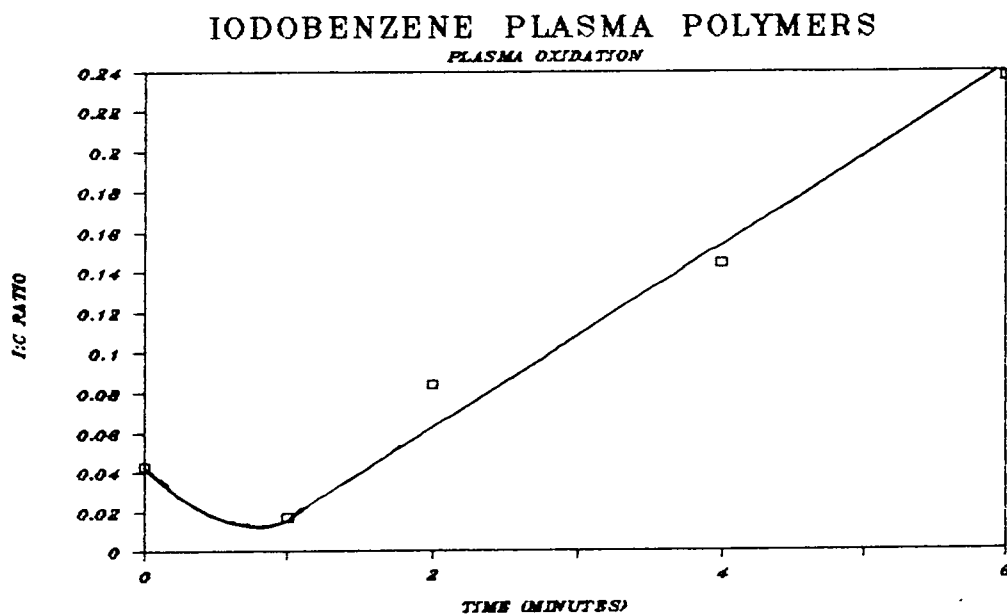
Figure 5.9 Iodine content of an iodobenzene plasma polymer as a
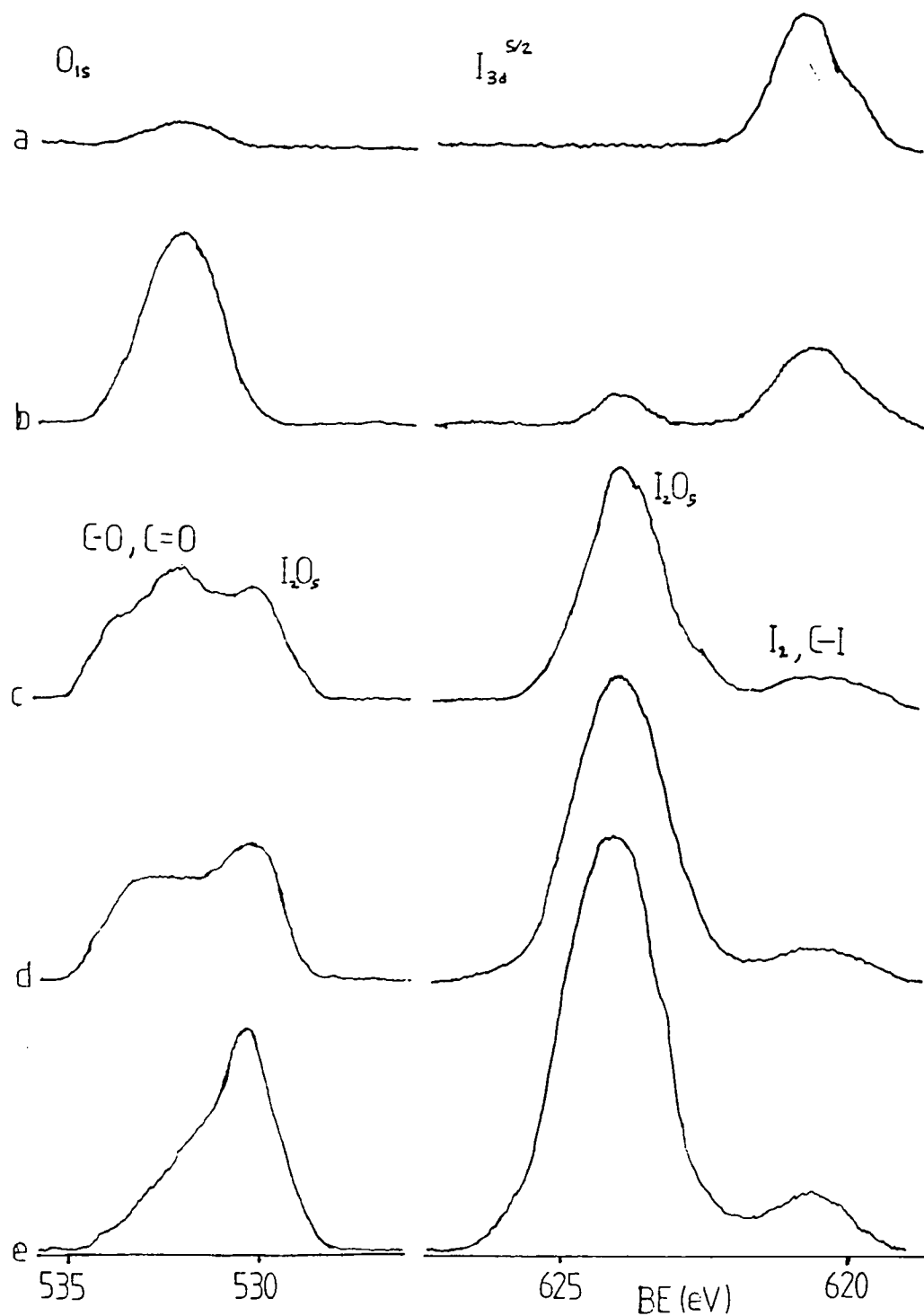function of oxygen plasma treatment time

Figure 5.10 XPS spectra of a plasma oxidised iodobenzene plasma
polymer as a function of treatment time
(a) 0 min, (b) 1 min, (c) 2 min, (d) 4 min, (e) 6 min

level spectra are shown in figure 5.10. After about 2 minutes almost all of the iodine is oxidised, with only about 10% left in the neutral form. Thereafter, although the amount of I_2O_5 increases, there is always some neutral iodine observed, probably present in the subsurface which has not yet been exposed to the plasma. The build up of I_2O_5 can also be observed in the O_{1s} spectra as a peak at 530.5 eV. After about 4 minutes this accounts for a greater percentage of the oxygen than do the oxidised carbon species at higher binding energy. The C_{1s} envelope does not change after the first minute, the oxidation of the polymer being balanced by loss of carbon monoxide and carbon dioxide.

The initial decrease in iodine content is probably due to loss of molecular iodine from the polymer. This would be lost in a vacuum (to which the polymer is subjected prior to and during plasma oxidation), and more slowly in air. The remaining iodine could then be plasma oxidised to I_2O_5, which being involatile would remain on the surface as the hydrocarbon of the polymer is lost. Although the etch rate may have been reduced by this, it was not stopped and all of the polymer had been etched away after 8 minutes. The iodine oxide layer had only built up to a level of 1 iodine per 4.3 carbon atoms after 6 minutes, and was therefore not a complete layer and could not completely prevent the oxidative etching process. If the starting level of iodine had been higher it is probable that a protective oxide coating would have been formed much more quickly, and the polymer would have been resistant to oxygen plasma etching. Incorporation of iodine into a plasma polymer could therefore provide resistance to an

oxygen plasma, but only if the initial iodine level was fairly high.

5.3.3 Allyl Iodide

A plasma polymer of allyl iodide produced at a power of 4 watts, a pressure of 0.16 torr and flow rate of 1.0 cm^3/min was found by XPS to have a C:I stoichiometry of 13:1. This is a higher iodine content than was found in any of the iodobenzene/benzene plasma copolymers, but since the C:I ratio in the starting material was 3:1, a large proportion of the iodine (76%) had been lost. Plasma polymers produced at higher powers (13 watts and 25 watts) had only slightly lower iodine contents, with C:I ratios of 16:1 and 17.5:1 respectively. The allyl group does not therefore appear to provide any protection against the loss of iodine from allyl iodide during low W/F plasma polymerisation. Attempts to form surface photopolymers of allyl iodide using both conventional and vacuum UV radiation failed, indicating that excited state chemistry is not responsible for the plasma polymerisation, and a radical addition mechanism like that proposed for acrylic acid does not occur.

At first sight therefore the plasma polymerisation of allyl iodide does not appear to be of great interest. Although the iodine content of the polymer is higher than in those produced from iodobenzene/benzene plasma copolymerisation it is unlikely to be sufficient to prevent oxygen plasma etching, and the percentage of iodine retention is rather low. Closer examination of the $I_{3d}^{5/2}$ XPS spectrum of an iodobenzene plasma polymer

however reveals that the iodine is present in two different type
of environments (figure 5.11a). Most of the iodine occurs at a
binding energy of 620.5 eV, corresponding to molecular iodine or
iodine covalently bonded to carbon, but there is a second peak at
about 619 eV accounting for about 25% of the iodine present. This
must be due to negatively charged iodine, and is thought to be
the first case of ionic species being found in a plasma polymer,
although the observation of negative ions has been claimed at the
interface between a perfluoropropane plasma polymer and the
substrate[8].

It can be seen from figure 5.11(b) that after being stored
for one day in air the polymer has lost a considerable amount of
iodine, as did the iodobenzene/benzene copolymers, and also that
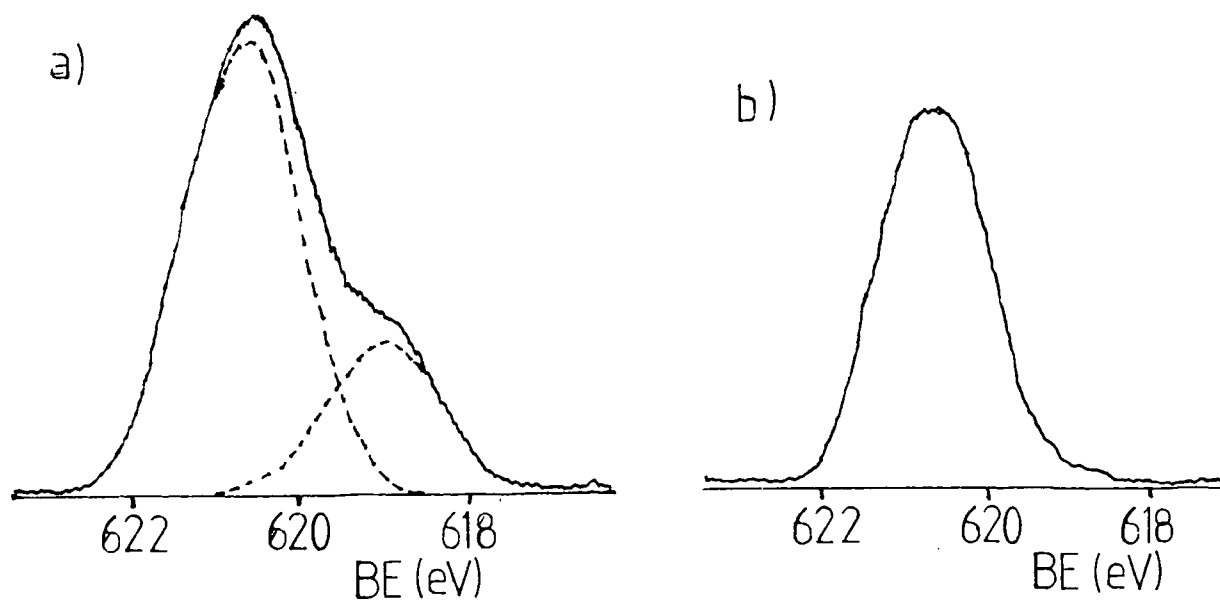
Figure 5.11 $I_{3d}^{5/2}$ XPS spectrum of an allyl iodide plasma polymer
(a) fresh, (b) after 1 day in air

the negative iodine has completely disappeared from the surface. Further evidence of the lack of long term stability of this species comes from UV absorption spectra of the plasma polymer (see figure 5.12). The spectrum of the freshly prepared polymer (figure 5.12a) shows a gradual increase in absorption as the wavelength decreases, probably due to trapped free radicals in the polymer, and also two distinct peaks at 295 and 375 nm with an intensity ratio of approximately 2:1 respectively. These peaks are characteristic of the I_3^- ion[9], which must therefore account for some, if not all, of the negative iodine observed by XPS.

It can be seen that most of the I_3^- had disappeared after 2 days and after 6 days there was hardly any left at all. This represents a somewhat longer lifetime than observed by XPS, probably due to the fact that the UV absorption examines the bulk of the polymer whereas XPS only examines the surface. If the decay is caused by contact with air, then it might be expected to occur more rapidly on the surface than in the bulk of the material.

The negative iodine peak in the XPS spectrum is in the position expected for an I^- ion[10] rather than I_3^-, which due to delocalisation of the negative charge might be expected to occur at slightly higher binding energy. This could indicate the presence of I^- in the polymer in addition to I_3^-, but could also be explained by decomposition of the I_3^- ion during analysis. When a sample of tetramethylammonium triiodide ($Me_4N^+I_3^-$) was examined by XPS a single iodine peak was observed at a binding energy of 619 eV, with only 1/3 of the intensity expected from
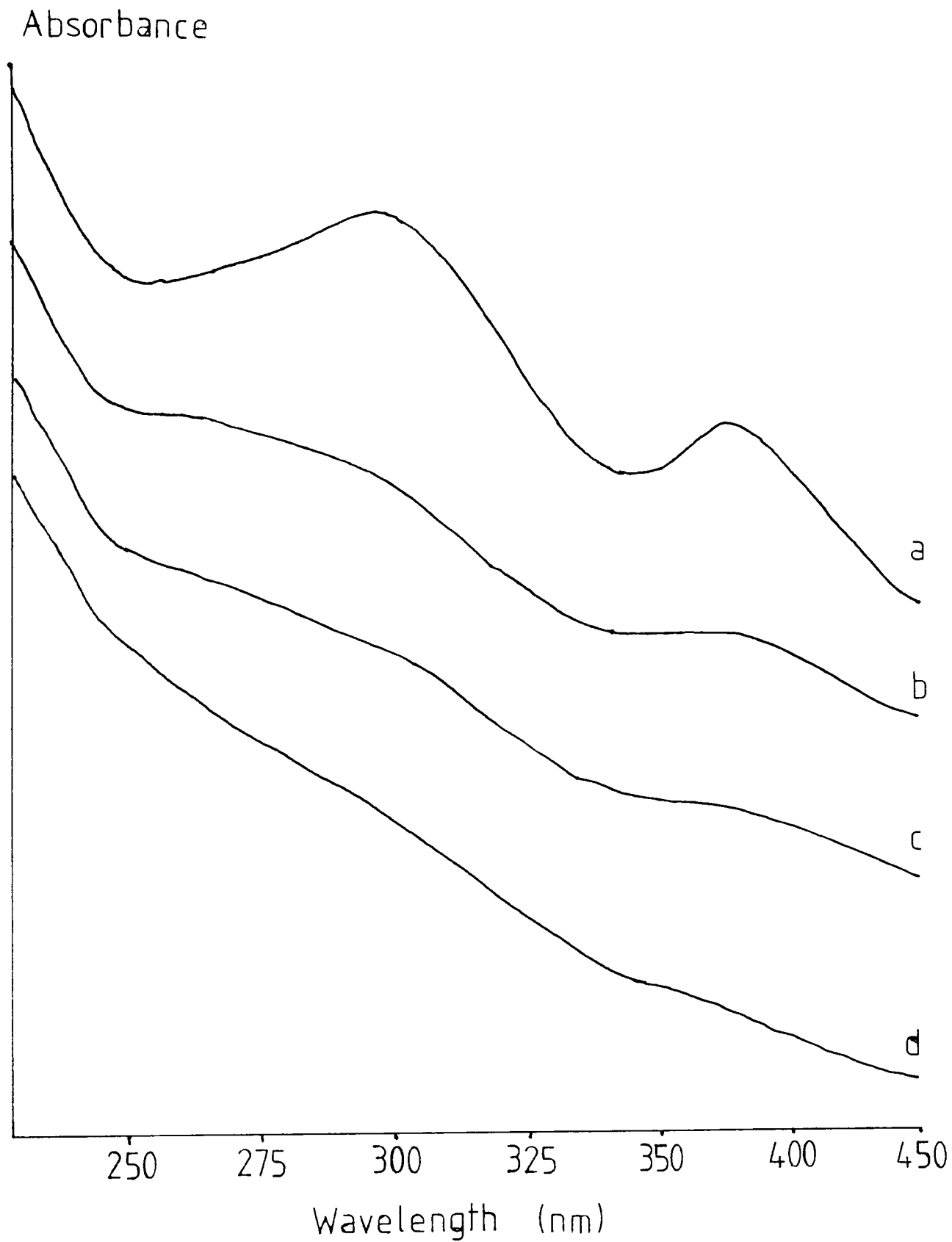
172

Figure 5.12 UV absorption spectra of an allyl iodide plasma
polymer. (a) fresh, (b) after 1 day in air,
(c) after 2 days , (d) after 6 days

the molecular stoichiometry. Clearly the I_3^- ion had decomposed to give I^- with loss of I_2 and so any I_3^- compound analysed by XPS would appear to be the iodide. Therefore, although the presence of I^- ions in the plasma polymer of allyl iodide cannot be ruled out, there is no evidence for them.

If there are negative ions present in the plasma polymer then there must also be positively charged counter-ions. XPS shows that there are no elements present in the polymer other than carbon, iodine a small trace of oxygen and presumably hydrogen (which cannot be detected by XPS). Hydrogen can be ruled out as a possible counter-ion since, although HI_3 is known, it is covalent and not ionic. The I_3^- ion must therefore be balanced by a carbocation. Given the nature of the monomer, the most likely candidate is an allylic cation with the positive charge delocalised over three carbon atoms. This delocalisation causes an allyl cation to be resonance stabilised, and so it might be expected to survive in the polymer for a few days (the lifetime indicated by the UV spectra for the ionic species), whereas most other carbocations are very unstable except in strongly acidic media.

There is no evidence in the C_{1s} XPS spectrum of the plasma polymer (figure 5.13) for any positively charged carbon species (expected to occur at higher binding energy than hydrocarbon), but an allylic cation, being delocalised, might only show a very small chemical shift which might not be noticeable. An allyl cation would give an absorption in its UV spectrum at about 300 nm[11], but unfortunately this coincides with one of the absorptions of the I_3^- ion, and so it is not possible to tell
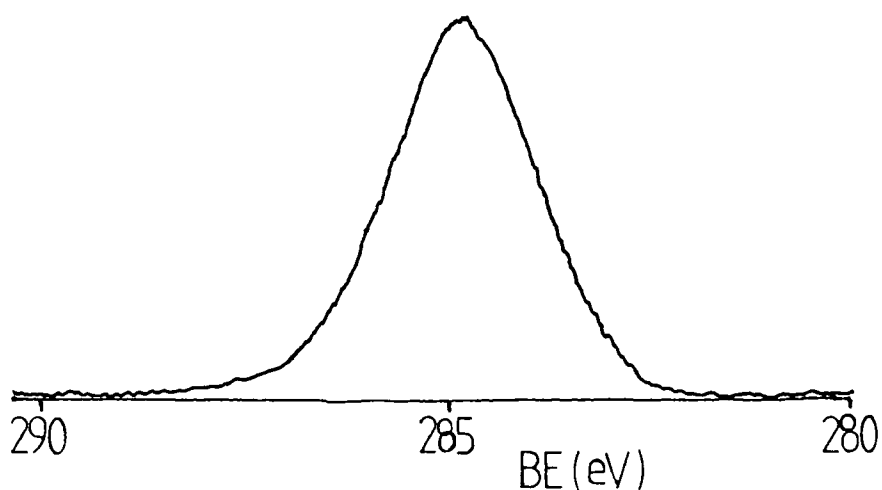
BE (eV)

Figure 5.13 C1s XPS spectrum of an allyl iodide plasma polymer

from this whether there is any allyl cation present.

A technique which might be able to confirm the presence of an allyl cation is solid state NMR. In ^{13}C NMR an allylic cation would give peaks in the 200 to 260 ppm range for the terminal carbon atoms, and a peak at about 140 to 160 ppm for the central carbon atom[12]. The chemical shift of the terminal carbon atoms is higher than for any other common type of carbon environment, apart from aldehydes and ketones. As there was shown by XPS to be only a small trace of oxygen on the surface of a freshly prepared allyl iodide plasma polymer, and as fresh samples were used for NMR analysis, there is unlikely to be any significant signal from these groups. Any peak observed at just over 200 ppm should therefore indicate the presence of an allyl cation.

The solid state ^{13}C NMR spectrum of an allyl iodide plasma polymer prepared using a power of 6 watts, a pressure of 0.16

torr and a flow rate of 1.0 cm^3/min is shown in figure 5.14(a). It shows two large, broad peaks centred at 40 ppm and 130 ppm corresponding to a wide range of aliphatic and olefinic environments respectively. There is also a peak centred at about 215 ppm which at first sight would appear to be due to an allyl cation, but this is in fact a spinning sideband of the alkene peak. If there is any signal from an allyl cation, then it is hidden under this peak.

The ^{13}C NMR spectrum of a second allyl iodide plasma polymer, made under the same pressure and flow rate conditions but at 10 watts, is shown in figure 5.14(b). It can be seen that there are considerable differences between this spectrum and the previous one. The alkene peak has virtually disappeared and instead there is a low, broad absorption between 150 ppm and 235 ppm. This is not a spinning sideband of the alkane peak, since it did not move when then spinning speed was changed. The part of this peak at high ppm is likely to be due to the terminal carbon atoms of allyl cations in a range of environments, while the low shift end is likely to be due to the central atom, and possibly some olefinic or aromatic environments at the upper end of their chemical shift range. Carbonyl groups could be responsible for a large proportion of the broad peak if a large amount of oxygen had somehow become incorporated into the polymer (and this was not seen in the XPS analysis of a second sample of the same polymer, run simultaneously with the NMR), but it would be very unusual for a carbonyl group to occur as high as 235 ppm, and so at least some of this peak must be due to an allyl cation.
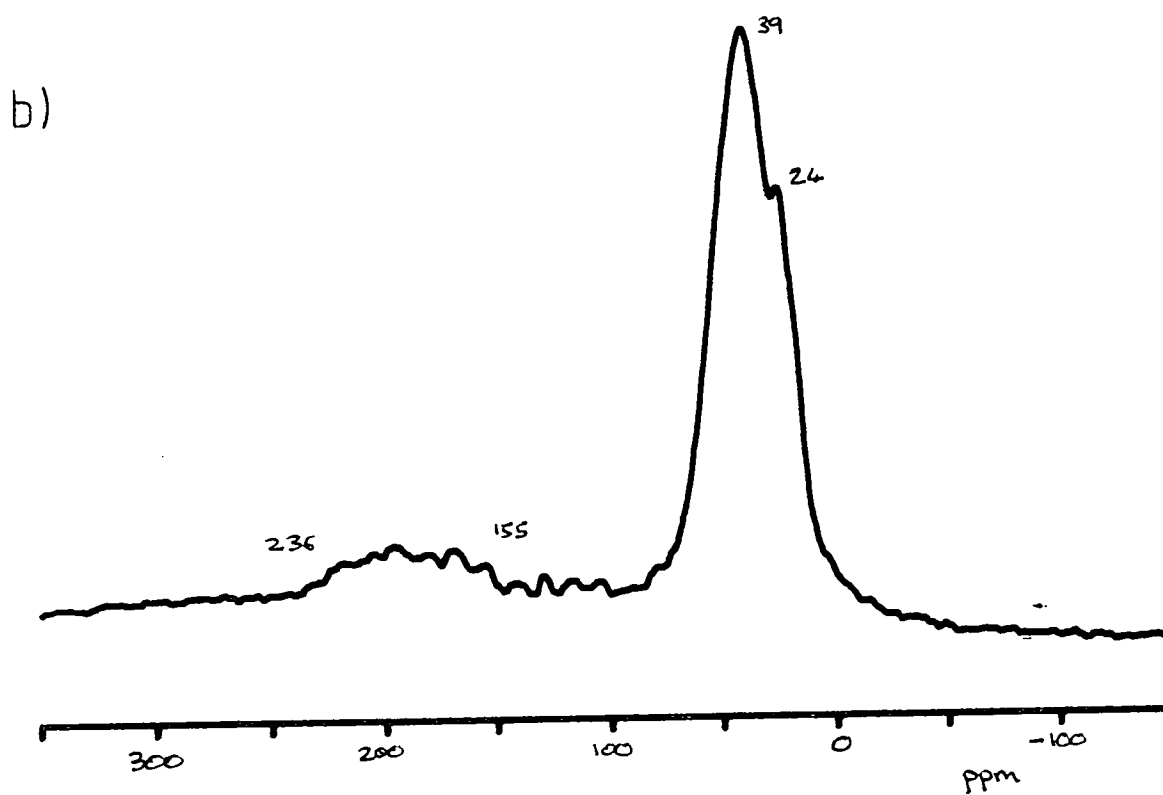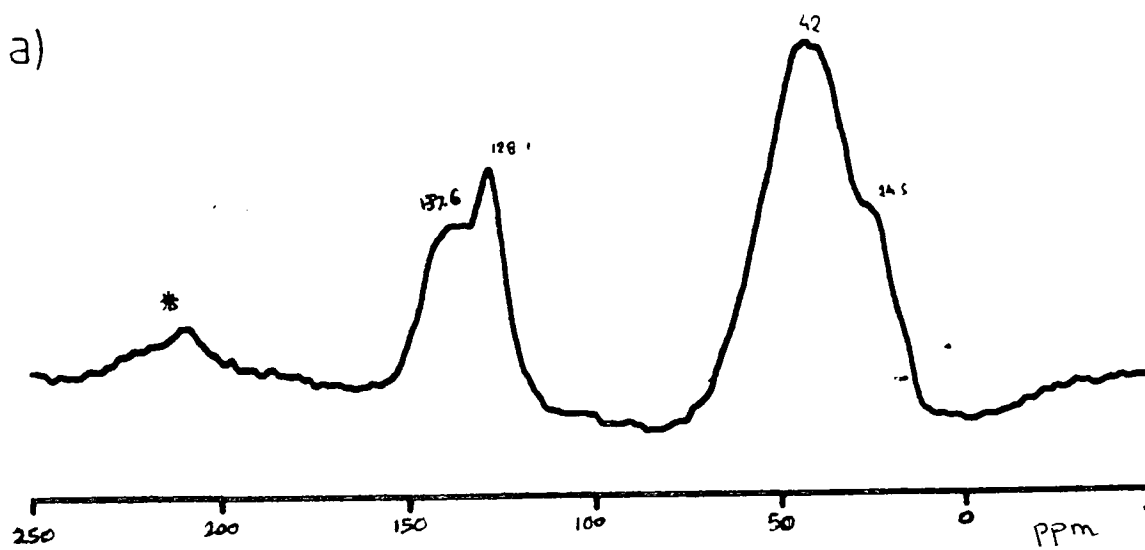
Figure 5.14 Solid state ^{13}C NMR spectra of allyl iodide plasma polymers (a) 6W , (b) 10W

5.4 SUMMARY

The plasma polymers formed from mixtures of iodobenzene and benzene vapours retain a higher percentage of iodine than does a plasma polymer of iodobenzene. This must be due to interaction between the benzene and iodobenzene molecules in the gas phase, which provides an alternative polymerisation pathway from that taken by iodobenzene alone, and involves less loss of iodine. The highest iodine content of any of the copolymers is about 1 iodine to 20 carbon atoms, and occurs when the monomer feed consists of 70-80% iodobenzene and 20-30% benzene.

All these polymers lose iodine, probably as I_2, when left standing in air, and the hydrocarbon on the surface is subject to considerable oxidation. When treated in an oxygen plasma for 1 minute there is a similar loss of iodine and hydrocarbon oxidation. When treated for longer periods of time the total iodine content increases as involatile I_2O_5 builds up on the surface. In order for this to become a complete layer and provide protection from oxygen plasma etching, the initial iodine content of the plasma polymer would have to be considerably higher.

Allyl iodide loses a high proportion of its iodine on plasma polymerisation, but it can still form a polymer with a concentration of 1 iodine per 13 carbon atoms. The most interesting feature of this polymer is that some of the iodine is present as I_3^-, probably balanced by an allylic cation. These species are stable for less than a day on the surface of the polymer, but can remain for several days in the bulk. This is thought to be the first case of ionic species being found in a plasma polymer.

REFERENCES

1. T.Ueno, H.Shiraishi, T.Iwayanagi and S.Nonogaki,
    J. Electrochem. Soc., 132, 1168-71, (1985)

2. H.S.Munro and H.Beer, Polym. Commun., 27, 79, (1986)

3. H.Yamada, T.Sato, S.Ito, S.Morita and S.Hattori, ACS Polym.
    Mater. Sci. Eng. 56, 424, (1987)

4. J.H.Dully, F.J.Wodarczyk and J.J.Ratto, J. Polym. Sci., Polym
    Chem. Ed., 25, 1187-90, (1987)

5. M.Sanchez, H.P.Schreiber and M.R.Wertheimer, ACS Polym.
    Mater. Sci. Eng., 56, 792, (1987)

6. H.S.Munro and C.Till, J. Polym. Sci., Polym. Chem. Ed., 25,
    1065, (1987)

7. W.R.Gombotz and A.S.Hoffman, ACS Polym. Mater. Sci. Eng., 56,
    720, (1987)

8. Y.Haque and B.D.Ratner, J. Polym. Sci., Polym. Phys. Ed., 26,
    1237, (1988)

9. A.I.Popov and R.F.Swenson, J. Am. Chem. Soc., 77, 3724,
    (1955)

10. "Handbook of X-Ray Photoelectron Spectroscopy", Ed.
    G.E.Muilenberg, Perkin Elmer Corporation, Minnesota, (1979)

11. N.C.Deno, J.Bollinger, N.Friedman, K.Hafer, J.D.Hodge and
    J.J.Houser, J. Am. Chem. Soc., 85, 2998 (1963)

12. H.O.Kalinowski, S.Berger and S.Braun, "Carbon-13 NMR
    Spectroscopy", Wiley, (1988)

CHAPTER 6

SURFACE PHOTOPOLYMERISATION AS A MODEL FOR THE PLASMA POLYMERISATION OF N-VINYL PYRROLIDINONE

180

6.1 INTRODUCTION

The work presented in earlier chapters has shown that there is often a similarity between the plasma polymers and surface photopolymers of a compound, and that the photopolymerisation may be used to help understand the plasma polymerisation. In this chapter the photopolymerisation of N-vinyl pyrrolidinone (NVP), is studied in order to gain some insight into the plasma polymerisation mechanism.

Plasma polymers of NVP have been prepared previously[1] and, along with the plasma polymers of other nitrogen containing compounds have been considered for use as reverse osmosis membranes[1b]. Their use has also been proposed in the surface treatment of silicone rubber contact lenses, as the hydrophilic surface provides greater comfort for the eye[2]. It has been shown that two different types of NVP plasma polymer can be formed depending on the plasma conditions used. Bieg and Ottesen[3] found that plasma polymers produced under low W/F gave infra-red spectra fairly similar to that of the conventional polymer, but the spectra of high W/F NVP plasma polymers were coniderably different. Munro and Till[4] showed that at low power and high flow rate a hydrophilic polymer was formed, with a contact angle with water of approximately zero, while under high power and low flow rate conditions a hydrophobic polymer (contact angle $\simeq$ 60°) was produced. They also found that polymers apparently identical to both these types of plasma polymer could be produced using surface photopolymerisation. It was therefore proposed that the plasma polymerisation of NVP proceeds via an excited state mechanism.

In this chapter the composition of polymers produced by plasma and photochemical means are examined in relation to the power, flow rate and photon flux conditions used, in order to obtain a clearer insight into how these factors influence the nature of the polymer formed. This can also show how closely the plasma polymers and surface photopolymers match, and so give an idea of the importance of excited state chemistry in the plasma polymerisation. The plasma and photopolymerisation of N-methyl pyrrolidinone (NMP) and N-ethyl pyrrolidinone (NEP) are investigated in order to determine whether the effects observed for NVP are due to the presence of the vinyl group. XPS and SIMS are used to characterise the polymers formed.
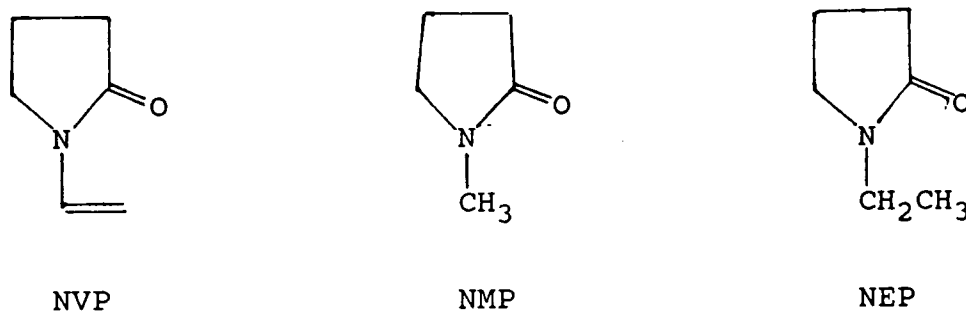

Figure 6.1 Monomers used in chapter 6

Further investigations are then carried out into some mechanistic aspects of the photopolymerisation. The dependence of the polymer deposition rate on ultra violet light intensity is examined to obtain an order of reaction with respect to photon flux for the polymer formation. The deposition rate is also monitored as a function of the angle of incidence of the UV light

182

on the thickness monitor, in order to determine whether the photochemical polymerisation reactions are occurring on the surface or in the gas phase.

Finally, the surface photopolymerisation is carried out using pulsed UV irradiation, and the polymer deposition rate monitored as a function of pulse frequency, in an attempt to determine the lifetime of reactive species involved in the polymerisation process. This is based on work by Melville[5] on methyl methacrylate. Melville found that using slow pulses of UV light (with equal periods of light and dark) gave a deposition rate of half that for continuous irradiation. This was because active species in the polymerisation, created in the light period, all decayed during the subsequent dark period, and so polymerisation only occurred for half the time. At high pulse frequencies however, species created during the light pulse did not have time to decay before the next pulse. This was therefore effectively the same as continuous irradiation but at half the light intensity. The rate of polymer formation was therefore equal to $(^1/_2)^n$ x the deposition rate under continuous irradiation, where n = the reaction order with respect to photon flux. The deposition rate at high frequency was therefore different from that at low frequency, unless the reaction order was exactly one. The frequency of change-over between these two cases corresponded to the lifetime of the active species in the polymerisation reaction.

The effect of frequency has also been investigated for plasma polymerisation. Morita, Bell and Shen[6] examined the

deposition rate of an ethane plasma polymer as a function of the frequency of an a.c. discharge, between 50 Hz and 13.56 MHz. They observed a complex relationship due to several different factors, as shown in figure 6.2.
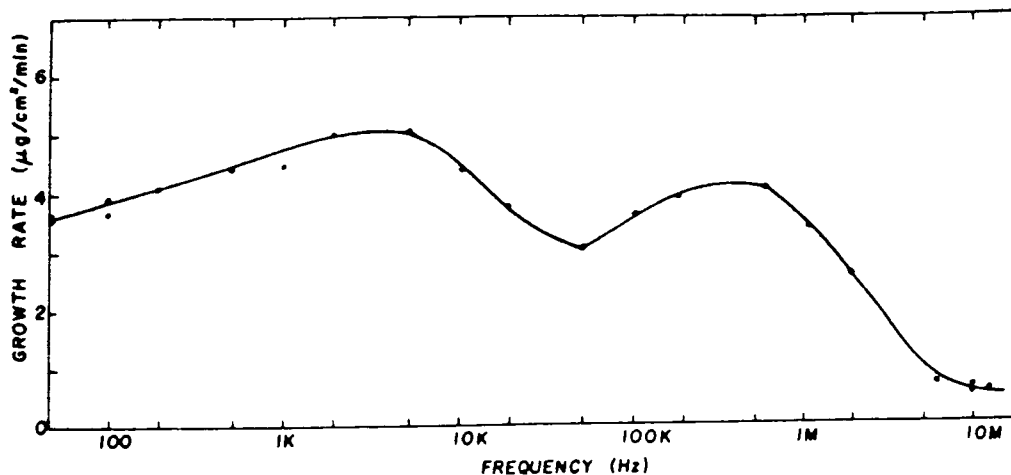

Figure 6.2 Effect of discharge frequency on the rate of polymer deposition from an ethane plasma

The initial increase in deposition rate was ascribed to an increase in concentration of the gas phase radicals, due to similar effects to those observed by Melville in the photopolymerisation of methyl methacrylate. The decreasing rate above 5 kHz was thought to be due to a decrease in the number of ions hitting the electrodes (on which the deposition rate was measured), as there was less time for migration before the electric field reversed. The increase above 50 kHz was put down to an increase in the energy of electrons striking the anode, and

the low deposition rates at about 10 MHz were thought to be due to poor charge transport to the electrode from the plasma. Similar results are not expected however in photopolymerisation as there are no electric fields, free ions, or free electrons, nor are they likely in an inductively coupled plasma where there are no electrodes.

6.2 EXPERIMENTAL

Plasma polymerisations were carried out using the procedure described in chapter 2 and the reactor shown in chapter 4 (figure 4.1). No needle valve was used for introducing the NVP into the reaction chamber, as its vapour pressure was very low. Instead, a Young's tap was used to control the flow rate.

Surface photopolymerisations were carried out in the conventional UV (wavelength > 200 nm) as in chapter 4. Deposition rates were measured using the quartz crystal thickness monitor in the apparatus described in chapter 4. The surface photopolymerisation of NVP was much slower than that for MMA, so the error caused by the heating effect was significant. Each deposition rate experiment was therefore repeated without monomer present to allow for this.

Photon flux was measured using an Applied photophysics digital voltmeter with photocell. This measured the total radiation of all wavelengths, so a second measurement was taken through a pyrex filter, which cut out all radiation below 290 nm. The difference in the two readings gave the intensity of UV radiation below 290 nm. Photon flux was varied by moving the lamp

towards or away from the apparatus. The photon flux at any lamp

position could then be calculated using equation 6.1.

$$I = k / d^2 \qquad\qquad 6.1$$

where I = UV intensity (mW/cm^2)
       d = distance between lamp and thickness monitor (cm)
       k = a constant (= 1420 mW)

Intensity readings were taken in different positions to

check that this equation was obeyed.

Angle of incidence variations were accomplished simply by
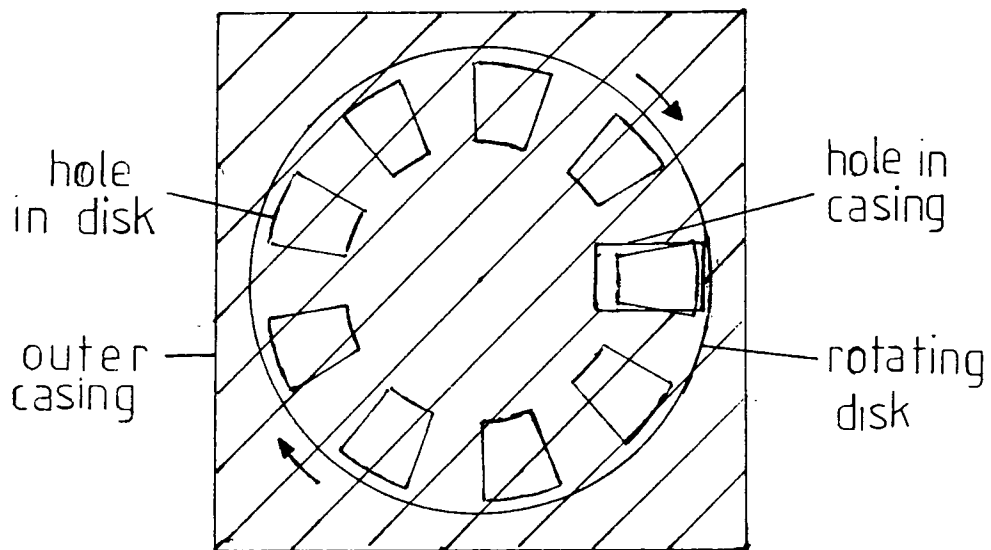
altering the angle of the thickness monitor with respect to the

incoming light.

Figure 6.3 Rotating sector used for producing pulsed irradiation

Pulsed irradiation was achieved by using a rotating disk placed between the UV source and the calcium fluoride window. The disk, shown in figure 6.3, was cut with a series regularly spaced sectors around the outside. The UV light was allowed to shine onto the disk through a hole in an outer casing, so that when the disk was rotated, pulsed irradiation was produced, with equal lengths of light and dark periods. Since the size of the sectors was the same as that of the hole through which the light was shining, the actual variation of UV light intensity with time was sinusoidal, rather than as distinct periods of light and dark.

XPS analyses of plasma and photopolymers were carried out in a Kratos ES 300 spectrometer. A Perkin Elmer PHI series 5000 combined XPS/SIMS spectrometer using xenon ions and a 0-250 a.m.u. quadrupole analyser, and a VG SIMSLAB spectrometer employing a 0-800 a.m.u. quadrupole analyser were used for SIMS analysis. Contact angles are with distilled water and were measured by the sessile drop technique as described in chapter 4.

NVP, NEP and NMP were supplied by Aldrich and degassed before use with a series of freeze thaw cycles.

6.3 RESULTS AND DISCUSSION

6.3.1 NVP Plasma polymers

A series of plasma polymers of NVP were produced at a constant flow rate of 2.6 cm^3/min and a pressure of 0.2 torr with powers ranging from 2.5 to 50 watts. Each of these was analysed using XPS and contact angle measurements. The results are displayed graphically on figures 6.4 and 6.5. The most remarkable change is that in contact angle. At low power (below about 8W) the contact angle with distilled water is zero, which is the same as that for conventionally polymerised NVP. By about 15W, however, the polymers formed become much more hydrophobic with contact angles of about 50°. As the power is increased further, the contact angle decreases slowly down to about 33° at 50W.

There is little change in the nitrogen to carbon ratio as shown by XPS (figure 6.5), apart from a slight decrease as the power increases, up to 20W. The values at 20W and above are close to that of the monomer and conventional polymer (0.16:1). The changes in the oxygen to carbon ratio mirror to some extent the changes in contact angle. At low power the oxygen to carbon ratio is fairly high at 0.14:1 (close to the value of 0.16:1 for the monomer or conventional polymer). At about 15W, where the contact angle is highest, the amount of oxygen in the polymer reaches a minimum (oxygen : carbon = 0.07:1). At higher powers, as the contact angle decreases, the relative proportion of oxygen increases again. At 50W the O:C ratio is 0.17:1, even higher than for polymers formed at very low powers, even though the contact angle does not decrease back down to zero. This suggests that the

oxygen in the polymers formed at high power tends to be in less polar environments.

Closer examination of the O_{1s} core level spectra (figure 6.6) reveal that there are changes in the type of oxygen environments for polymers produced at different powers. At low power almost all the oxygen is in a single type of environment with a binding energy of 531.2 eV. This is the same as for the conventional polymer, and so is likely to correspond to an N-C=O environment. There is also a shake up satellite centred at 539 eV from the C=O bond. The 15W and 50W polymers show much broader oxygen peaks centred at 532.5 eV. This represents a much greater range of oxygen environments probably including N-C=O, C=O and C-O groups. The shake up satellite is much smaller for these polymers. The C_{1s} spectra show little change throughout, and are similar to that of the conventional polymer. The N_{1s} spectra show a single peak at 399.7 eV in all cases, characteristic of amine, although for the polymers formed at high power the peak is fairly broad showing a range of different amine environments.
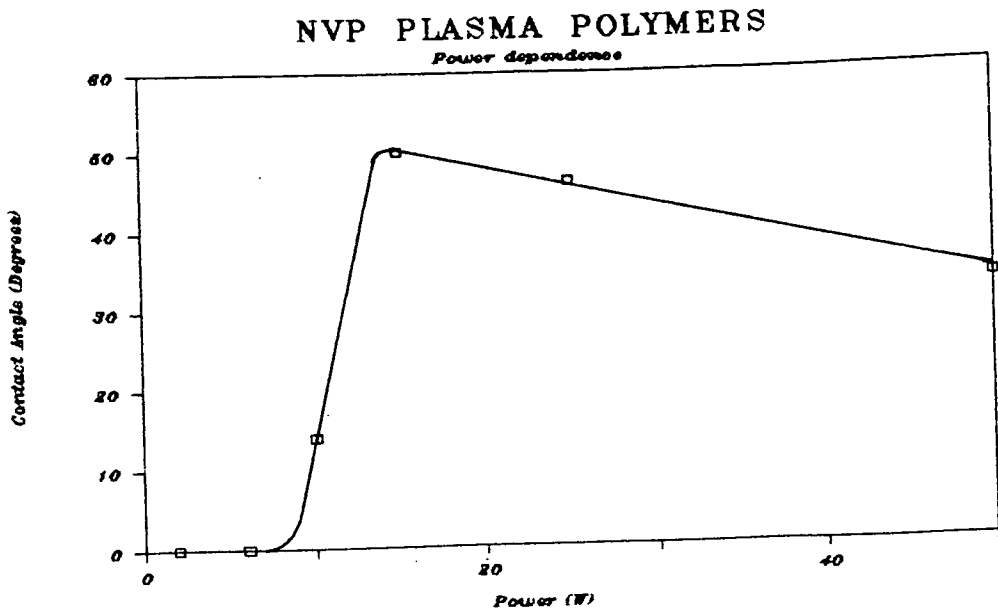
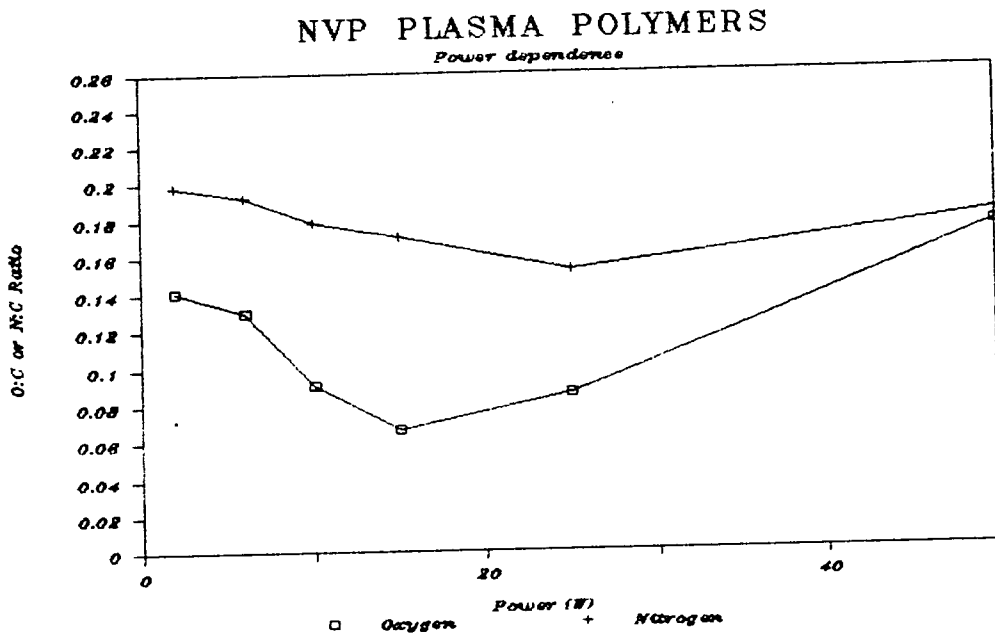Figure 6.4 Variation of contact angle with power for NVP plasma
polymers

Figure 6.5 Variation of N:C and O:C ratios with power for NVP
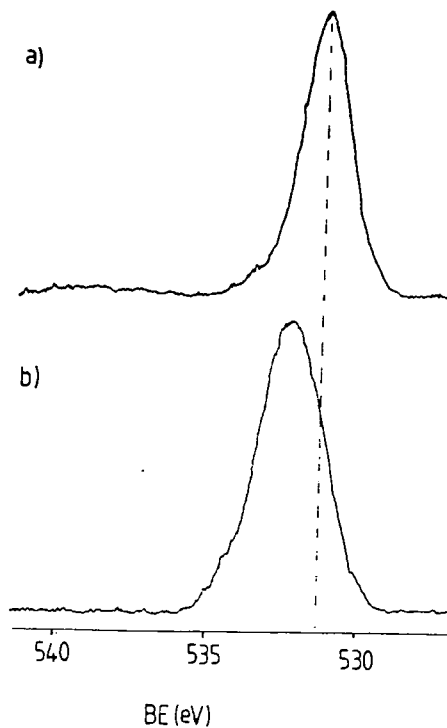plasma polymers

<u>Figure 6.6</u> XPS O_{1s} spectra of NVP plasma polymers formed at (a) 6W and (b) 50W

A second series of NVP plasma polymers were produced at a constant power of 6W with flow rates varying from 0.16 to 2.6 cm^3/min. The variations in contact angle and elemental composition, shown by XPS, are presented in figures 6.7 and 6.8, the flow rates being quoted in logarithmic form. The results are very similar to those for power variation at constant flow rate, low flow rate plasma polymers being the same as those formed at high power, and high flow rate polymers corresponding to those formed at low power. The variation in oxygen to carbon ratio is not quite so great, but shows the same trends.
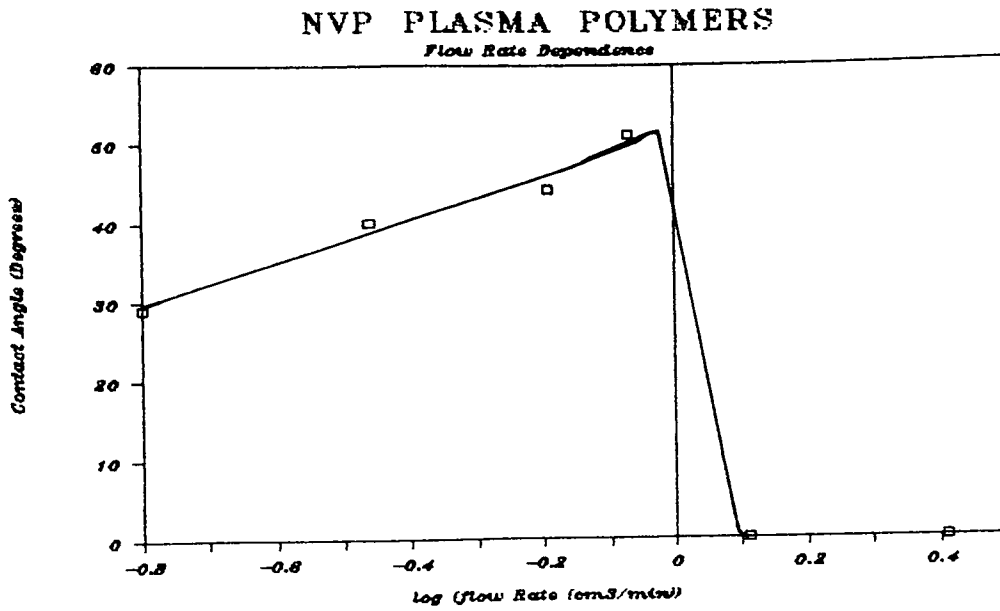
NVP PLASMA POLYMERS
Flow Rate Dependence

Figure 6.7 Variation of contact angle with flow rate for NVP plasma polymers

NVP PLASMA POLYMERS
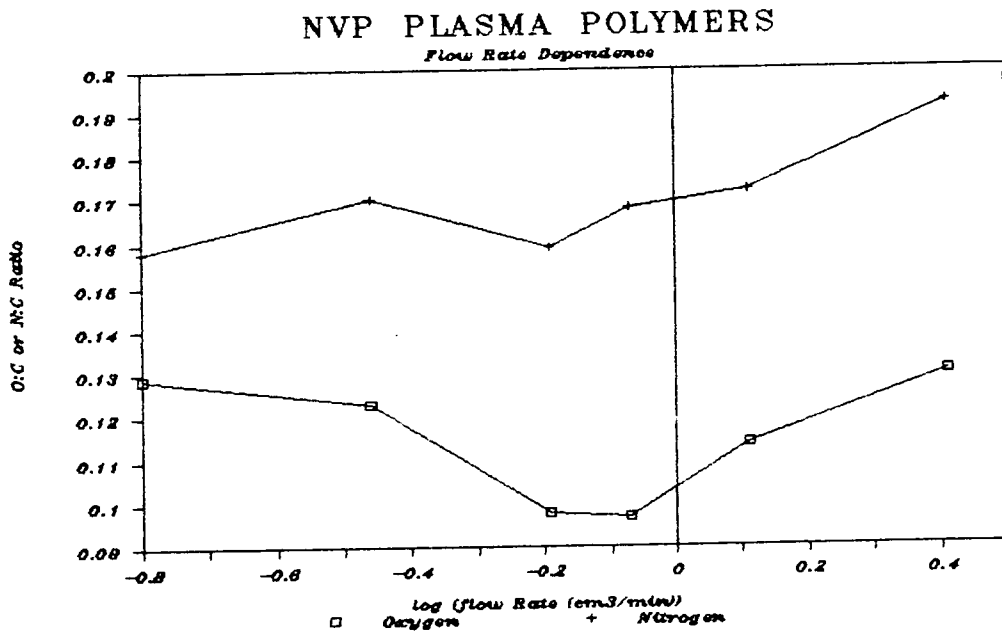### Flow Rate Dependence

Figure 6.8 Variation in N:C and O:C ratios with flow rate for NVP plasma polymers
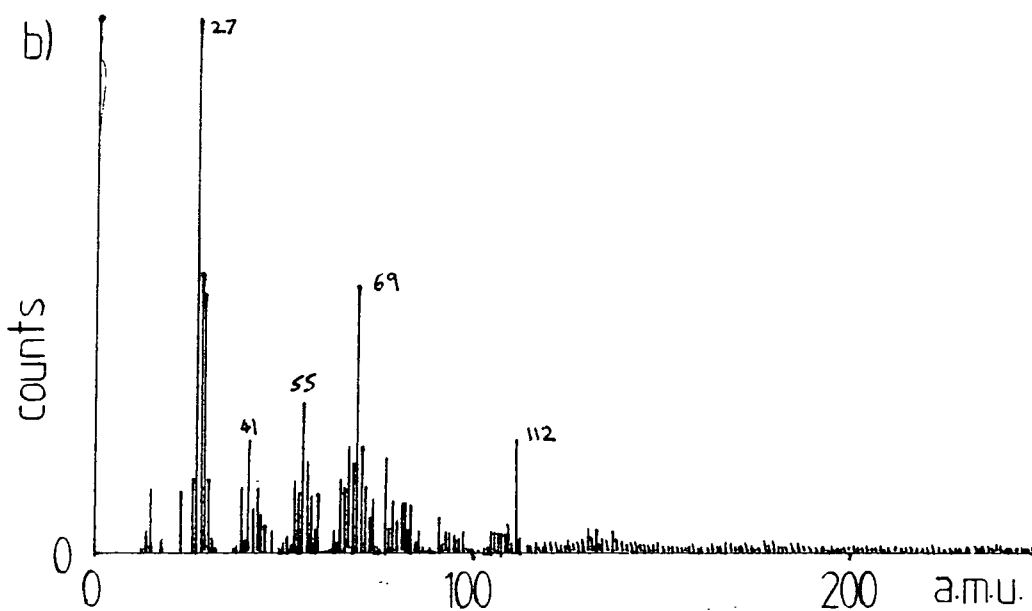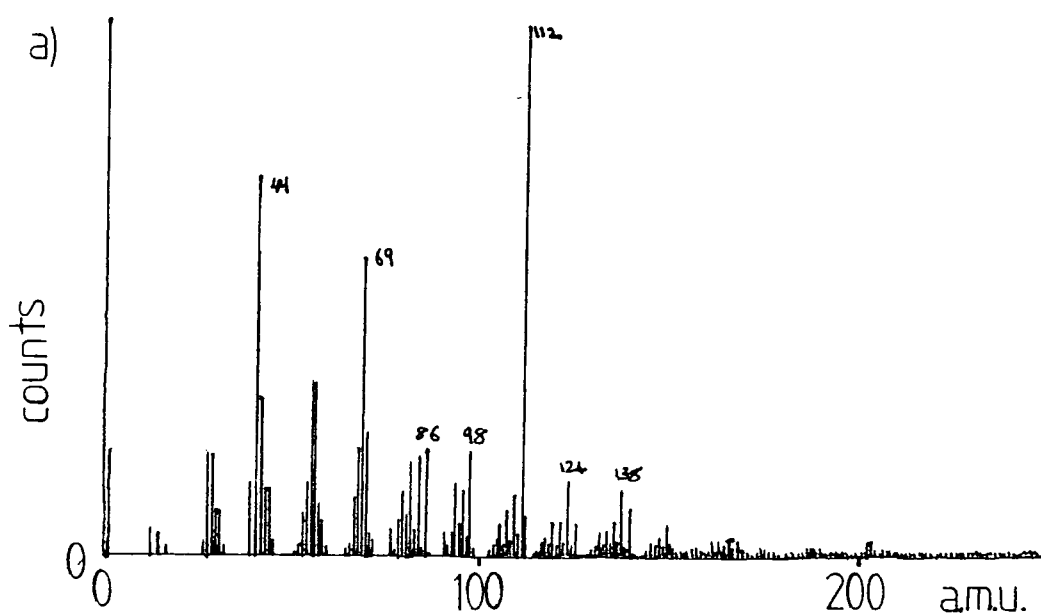
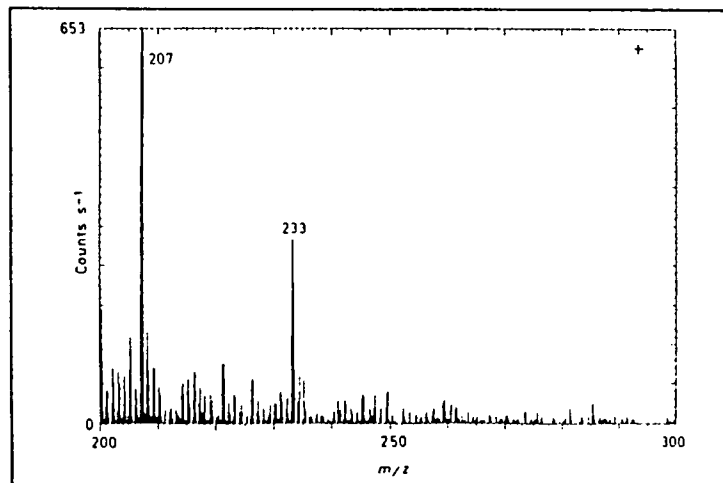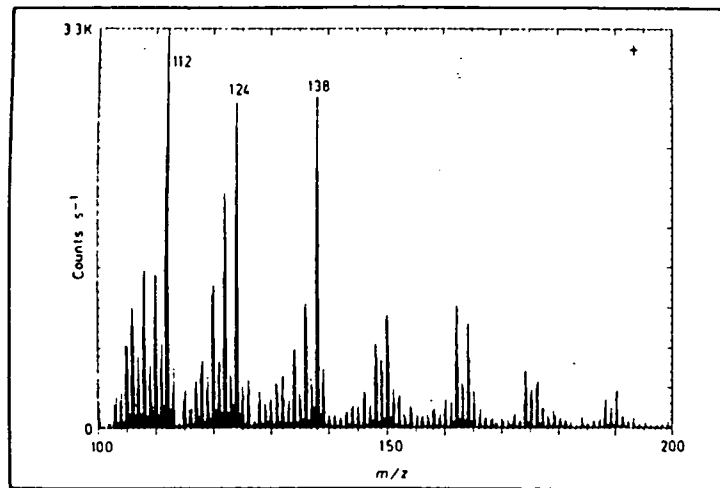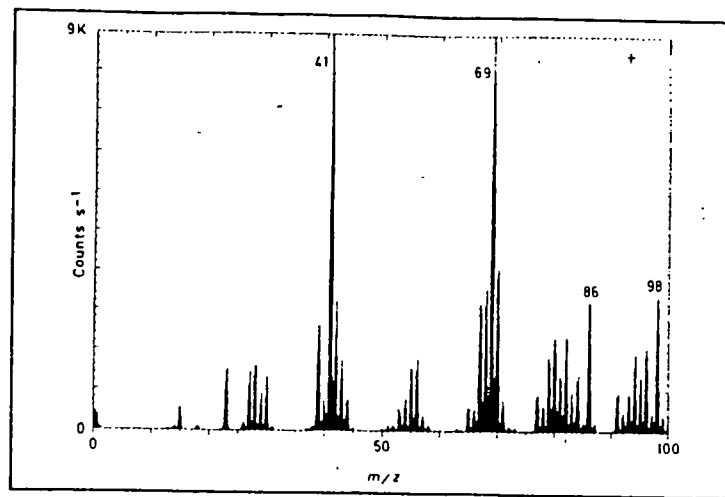**Figure 6.9** Positive Ion SIMS spectra of NVP plasma polymers (a) hydrophilic and (b) hydrophobic

193

Figure 6.10 Positive Ion SIMS spectrum of
poly (N-vinyl pyrrolidinone)

Positive ions

$CH_3-CH=CH^+$ (41D), $\qquad$ $CH_3-CH=CH-C\equiv O^+$ (69D)

86D $\qquad$ 98D $\qquad$ 112D

124D $\qquad$ 138D

207D $\qquad$ 233D
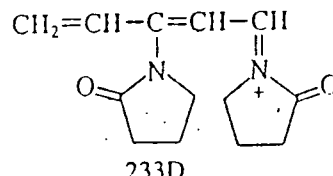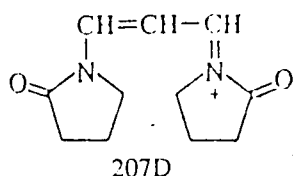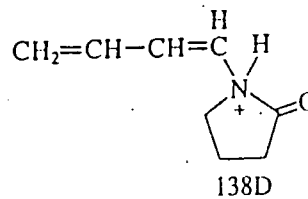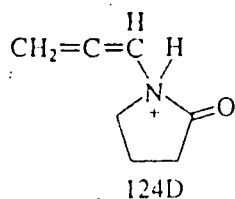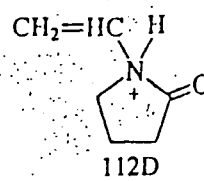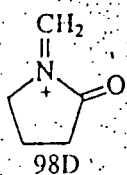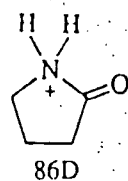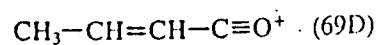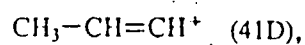
Figure 6.11 Structures of some ions present in the positive ion
SIMS spectrum of poly (N-vinyl pyrrolidinone)[7]

Samples of the hydrophilic and hydrophobic types of NVP

plasma polymer were analysed using static SIMS (figure 6.9 a,b),

and compared with that of the conventional polymer (figure 6.10).

It can be seen that the spectrum of the hydrophilic polymer is

very similar to the conventional polymer, with clusters of peaks

centred at 27, 41, 55, 69, 86, 98, 112, 124, 138, 150 and 175

a.m.u., the structures of some of which are shown in figure 6.11.

However, the peaks at 207 and 233 a.m.u. corresponding to dimeric

structures, are not present in the spectrum of the plasma

polymer, indicating that there is some difference between that

and the conventional polymer.

The SIMS spectrum of the hydrophobic plasma polymer shows similar clusters of peaks up to 112 a.m.u., corresponding to a protonated NVP molecular ion, but nothing above this. This may indicate considerable cross-linking and lack of any sort of regular structure between NVP units. The cluster of peaks around 27 a.m.u. ($C_2H_3^+$) is also much more intense, suggesting that there are more short chain hydrocarbon species, not characteristic of poly (N-vinyl pyrrolidinone).

It can be concluded from this study of NVP plasma polymerisation that there are two main types of polymer which can be formed. At low W/F the polymer is hydrophilic and similar to the conventional polymer (though not quite identical), while at high W/F the polymer formed is hydrophobic and considerably different from the conventional polymer. Increasing the W/F ratio further alters the nature of the polymer slightly, with an increase in the oxygen content and a small drop in the contact angle.

6.3.2 NMP and NEP Plasma Polymers

NMP and NEP have exactly the same monomeric structure as NVP, except that they possess a methyl or ethyl group instead of the vinyl group. They can therefore be used as a test for the importance of the vinyl group in the plasma polymerisation of NVP. If plasma polymers of NMP and NEP are the same as those of NVP, then the vinyl group would appear to be unimportant in the

NVP plasma polymerisation, but if they are different then it must play a major role.

Plasma polymers of NMP were formed under three sets of conditions. Under very low power (2.5W) and high flow rate (2.6cm^3/min) conditions the polymer formed was virtually the same as that formed from NVP under the same conditions, giving a contact angle with distilled water of zero. The XPS analysis showed a single oxygen environment at about 531 eV, the same as that for the corresponding NVP plasma polymer. The oxygen to carbon and nitrogen to carbon ratios were 0.17:1 and 0.22:1 respectively, similar to the monomer values of 0.2:1 for both. Using higher W/F conditions (7.5 W, 1.2 cm^3/min) a hydrophobic (contact angle = 44°) was formed. There was considerable loss of oxygen (the oxygen to carbon ratio was 0.11:1), and the O_{1s} core level spectrum showed a broad range of oxygen environments. This is basically similar to the NVP plasma polymer formed at 15 W and 2.6 cm^3/min. Under even higher W/F conditions (17 W, 0.35cm^3/min), the polymer formed was similar to a high W/F NVP plasma polymer, except that the oxygen to carbon ratio of the polymer was still comparatively low (0.13:1). NEP behaved similarly on plasma polymerisation, producing a hydrophilic plasma polymer at low W/F (2.5 watts, 2.0 cm^3/min), and a hydrophobic polymer at higher W/F.

From these results it can be concluded that the plasma polymerisation of NMP and NEP is essentially the same as that of NVP. It is therefore unlikely that the vinyl group plays a major role in the plasma polymerisation of NVP. This might be expected under high W/F conditions, but not for the low W/F polymers,

which are very similar to conventionally polymerised NVP, formed through the opening of the double bond. The results from chapter four on the low W/F plasma polymerisation of unsaturated acids would tend to suggest that polymerisation via the double bond is likely to be an important mechanism under mild conditions. NEP could lose hydrogen from neighbouring carbon atoms of its ethyl group to form NVP, which could then polymerise to form a material similar to conventional poly (vinyl pyrrolidinone) in a manner similar to that for propionic acid, but this could not occur in the case of NMP. It is possible that the NMP could form a similar plasma polymer to the NVP by another mechanism (e.g. by loss of hydrogen from neighbouring carbon atoms of the ring to form a double bond, which could then be involved in addition polymerisation without disrupting the structure of the NMP very much). Yasuda and Lamaze[8] found that the rate of plasma polymerisation of N-ethyl pyrrolidinone was only half that for NVP, suggesting that the vinyl group had a significant effect. They also showed that the pressure in the reactor increased during the plasma polymerisation of N-ethyl pyrrolidinone, which indicated monomer fragmentation, possibly hydrogen elimination, was dominant. In contrast, the pressure in an NVP plasma decreased, suggesting that polymerisation was dominating.

6.3.3 Photopolymerisation

Photopolymers of NVP were produced at a constant pressure and flow rate of 0.2 torr and 1.8 cm^3/min respectively, with a range of UV light intensities. The contact angles of the polymers obtained are plotted on figure 6.12. It can be seen that at low photon flux the polymer is completely wettable, while at greater light intensities the polymer becomes much more hydrophobic, having a contact angle of about 60°. Comparison with figure 6.7 shows that this behaviour is very similar to the variation in contact angle of the plasma polymer as the power used in its formation is varied. There is however no evidence for any decrease in contact angle at very high photon fluxes, as there is for very high W/F plasma polymers.

XPS analysis of these polymers shows O:C and N:C elemental ratios of about 0.15 : 1 in all cases. This is similar to the composition of plasma polymers formed at low power, but does not mirror the decrease in oxygen content at higher powers. The absence of this change in the level of oxygen makes the large difference in contact angles between the high and low photon flux materials more difficult to explain. However, a closer examination of the O_{1s} core level spectra shows some changes which might give a reason for the contact angle changes. The O_{1s} spectra of high and low photon flux materials are shown in figure 6.14. At low photon flux the spectrum is very similar to that of a hydrophilic NVP plasma polymer, with nearly all the oxygen in a single environment at 531.2 eV corresponding to the N-C=O type of environment found in the conventional polymer. As in the corresponding plasma polymer there is also a small shoulder at

CONTACT ANGLE VS. PHOTON FLUX
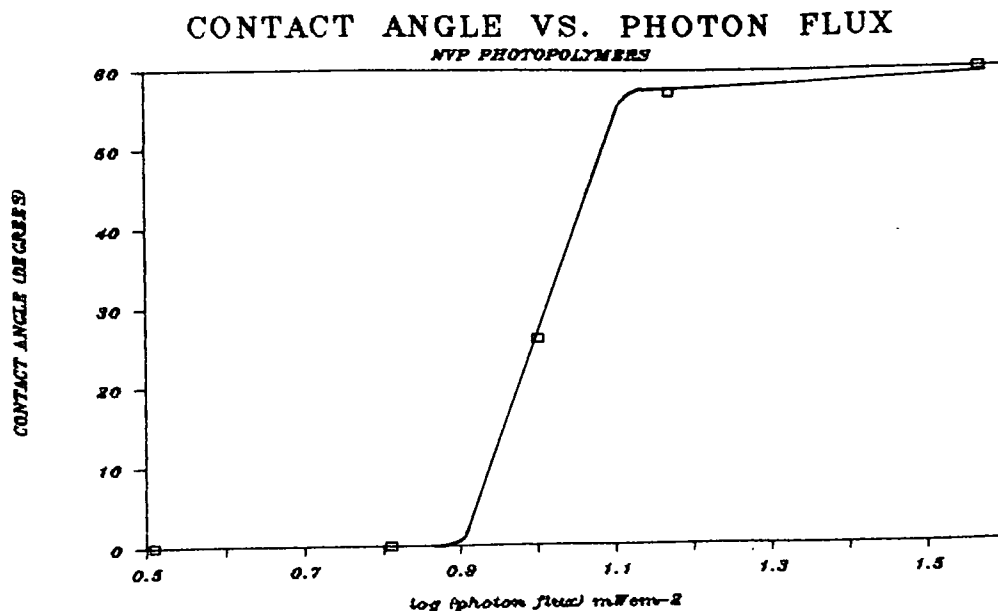
NVP PHOTOPOLYMERS

Figure 6.12 Variation of contact angle with photon flux for NVP photopolymers

NVP PHOTOPOLYMERS

PHOTON FLUX DEPENDENCE
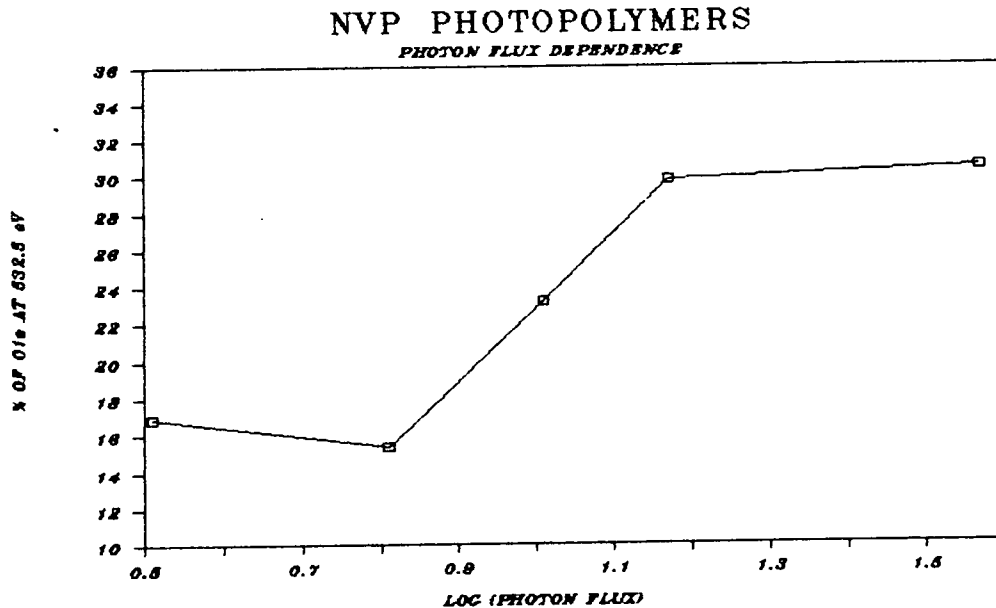
Figure 6.13 Variation in composition of the O1s core level with photon flux for NVP photopolymers
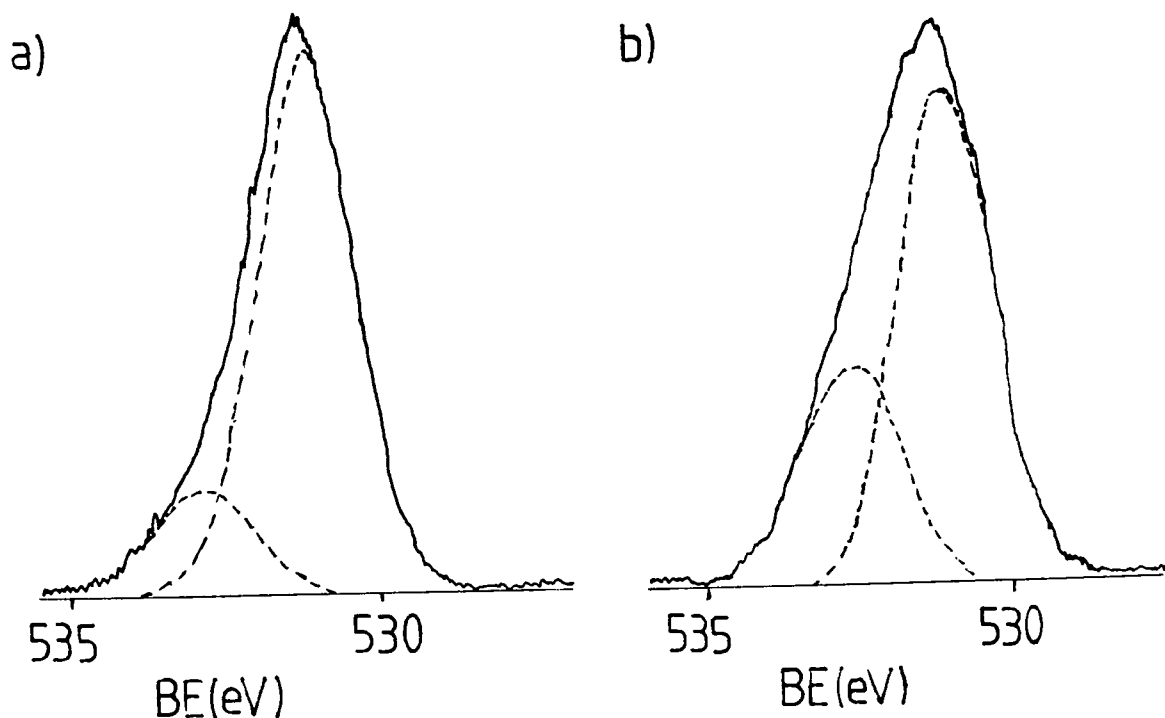
Figure 6.14 XPS O1s spectra of NVP photopolymers formed at
(a) low photon flux, (b) high photon flux

532.5 eV. The spectrum of the hydrophobic photopolymer is similar
to this but the peak corresponding to the second oxygen
environment is considerably larger in this case. A plot of the
changes in the ratios of these two peaks is shown in figure 6.13,
and can be compared with the differences in contact angle shown
in figure 6.12. The change in the O_{1s} occurs fairly suddenly and
at the same photon flux as for the sharp rise in contact angle.
The higher binding energy oxygen must therefore be in an
environment that does not enable it to significantly influence
the contact angle, unlike the oxygen in the pyrrolidinone ring,
which has a large hydrophilic effect. The change in the O_{1s}
between the high and low photon flux photopolymers is much less
than for the plasma polymers. Therefore, although at low power or

photon flux the plasma and photopolymers are very similar, the high photon flux photopolymer is not the same as a high power plasma polymer despite having some characteristics in common.

The photopolymer produced at low photon flux at a lower pressure and flow rate (0.13 torr and 0.6 cm^3/min) was found to be essentially the same as that formed at high photon flux and at 0.2 torr. It would therefore appear that a photon flux / flow rate relationship similar to the W/F relationship in plasma polymerisation applies.

Positive ion SIMS spectra of hydrophilic and hydrophobic photopolymers of NVP are shown in figure 6.15. Comparison with figure 6.10 shows that the spectrum for the hydrophilic photopolymer is virtually identical to that for the conventional polymer, including the peaks at 207 and 233 a.m.u. corresponding to dimeric structures. The implication of this is that under low photon flux conditions it is essentially a conventional polymer that is formed. The hydrophilic plasma polymer does not show the two peaks above 200 a.m.u., so there is a slight difference between the plasma and photopolymers.

The SIMS spectrum of the hydrophobic photopolymer is similar to that of the hydrophobic plasma polymer. The clusters of peaks up to 112 a.m.u. are essentially the same, but there is also a significant peak at 124 a.m.u. not present in the hydrophobic plasma polymer, but found in the conventional and hydrophilic polymers. It therefore appears that the hydrophobic photopolymer is intermediate in structure between the hydrophobic and hydrophilic plasma polymers, but closer to the hydrophobic type.
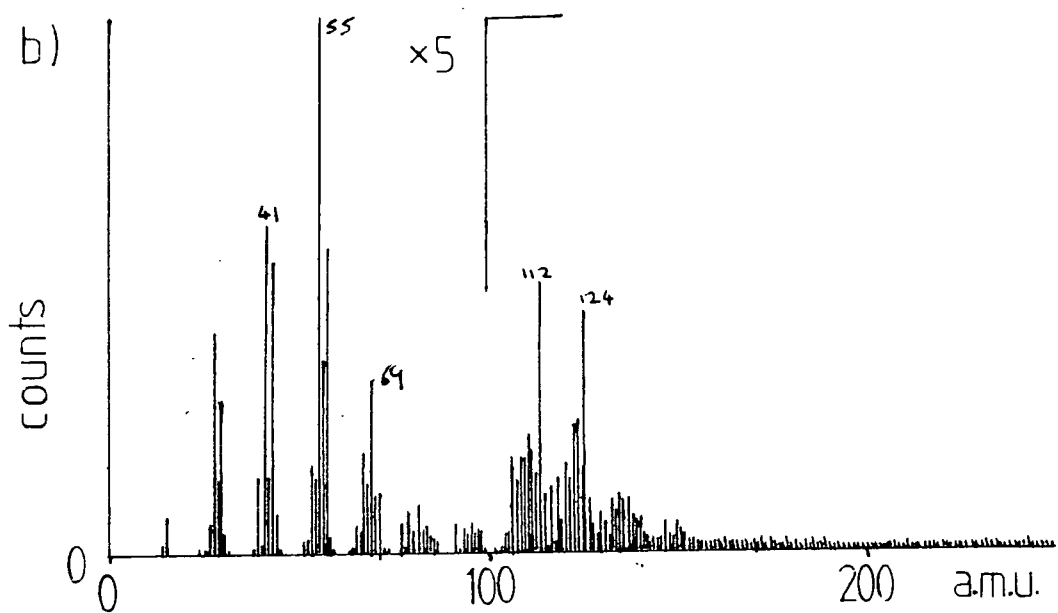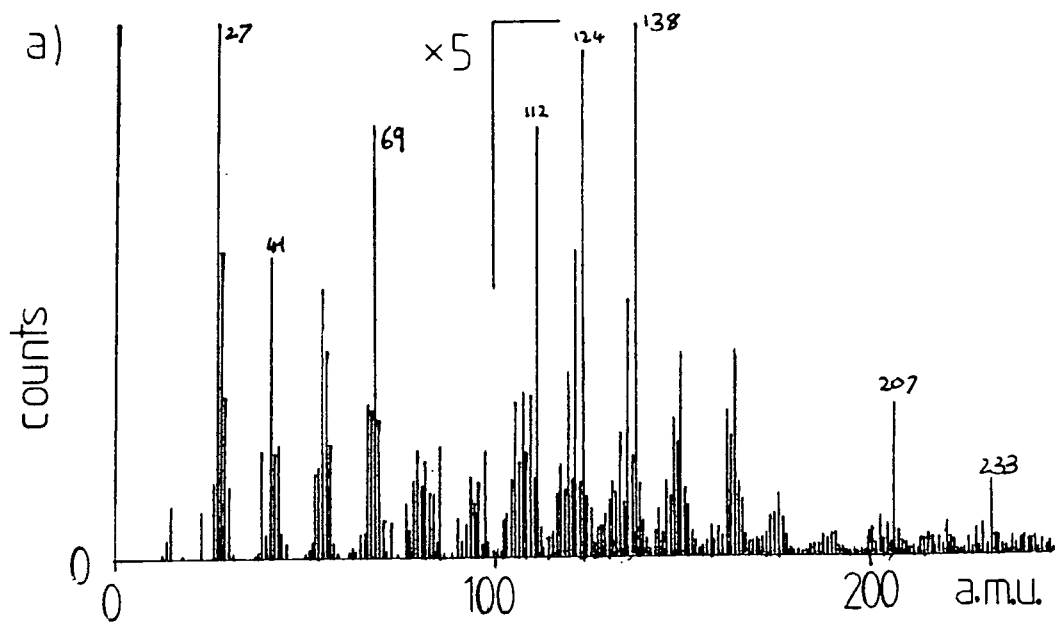
Figure 6.15 Positive ion SIMS spectra of NVP photopolymers
(a) hydrophilic, (b) hydrophobic

203

Photolyses of NMP and NEP for 5 hours at pressures of 0.19 torr both failed to show any polymer when the aluminium substrates were examined using XPS. This is clearly different from the NVP, suggesting that the vinyl group is important in the NVP photopolymerisation. As the photopolymerisation of NVP is similar to the low W/F plasma polymerisation it is therefore likely that the vinyl group is important in the plasma polymerisation also. The reason suggested earlier for the similarity between the plasma polymers of NMP, NEP and NVP (i.e. loss of hydrogen to form a double bond, followed by polymerisation), is consistent with the lack of photopolymer formed from NMP and NEP. As in the case of the saturated acids (see chapter 4), hydrogen loss does not occur so easily during UV photolysis as in a plasma, so formation of olefinic groups which can lead to polymerisation is very restricted, and little or no polymer is formed.

6.3.4 The Influence of Photon Flux on the Deposition Rate of NVP Photopolymers

The deposition rates of a series of NVP photopolymerisations were measured using a quartz crystal thickness monitor, under conditions of 0.2 torr pressure, an NVP flow rate of 1.8 cm^3/min and with a range of UV light intensities from 3 to 40 mW/cm^2 (the same sets of conditions as used for XPS and contact angle analysis). Allowance was made for the heating effect of the lamp on the monitor by repeating each experiment with no monomer present; the difference between the two values obtained being

Photon Flux (mW/cm^2)	Deposition* Rate	Contact Angle (degrees)	% of O_{1s} at 532.5 eV
3.2	2	0	17
6.4	6	0	15
10.0	11	26	23
14.8	15	57	30
37.0	28	60	30

* Arbitrary units

DEPOSITION RATE VS. PHOTON FLUX
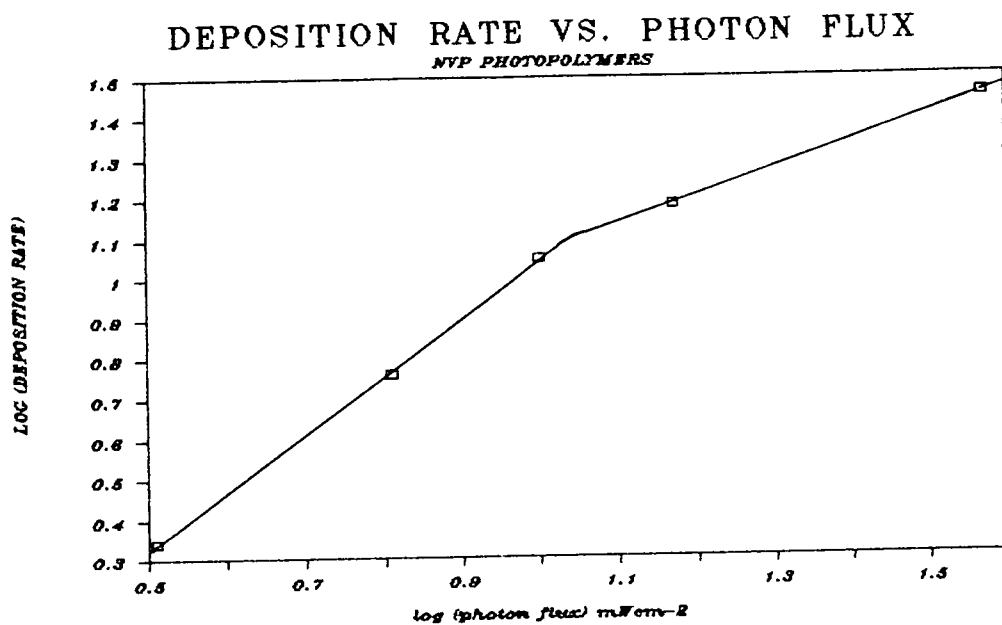
Figure 6.16 Logarithmic plot of deposition rates of NVP
         photopolymers as a function of photon flux

taken as the NVP polymerisation rate. The results are presented on table 6.1 and plotted in logarithmic form in figure 6.16.

The slope of the plot of log (deposition rate) against log (photon flux) shown on figure 6.16 should be equal to the order of the polymerisation reaction with respect to light intensity, since if,

$$\text{Rate} = k \text{ (Intensity)}^n \qquad\qquad 6.2$$

where k is a constant, then,

$$\log \text{ (Rate)} = \log k + n \log \text{ (Intensity)} \qquad 6.3$$

Examination of figure 6.16 will show that the slope is not constant, but undergoes a change at a photon flux of about 10 mW/cm^2. At low UV light intensities the slope of the graph is 1.45 (or within experimental error, 1.5), indicating a reaction order of 1.5. There must therefore be at least two photons of light involved in the reaction. At high UV light intensities the slope is less, giving a reaction order of about 0.7. There are unfortunately not enough data points to be able to tell whether there is a sudden change in the reaction order, or a gradual decrease with increasing photon flux. Comparison of figure 6.14 with figures 6.12 and 6.13 and the data in table 6.1 shows that this change in reaction order corresponds to the changes observed in the nature of the polymer formed. There appear to be two very distinct types of NVP photopolymer: the hydrophilic polymer, similar to the conventional polymer and the low W/F plasma polymer, formed at low light intensities with a photon flux

dependence of 1.5, and the hydrophobic polymer formed at high light intensities with a photon flux dependence of 0.7, which appears to be intermediate in nature between the high and low W/F plasma polymers.

At low UV intensities there is a light deficiency making the photon flux rate determining, while at high photon intensity there seems to be an excess of light so the dependence of the deposition rate on light intensity decreases. This is analogous to the dependence of deposition rate on W/F in plasma polymerisation shown by Yasuda[9]. The fact that the order is decreased by about a half suggests that only one of the two photon induced processes ceases to be rate determining, so the two steps involving UV light must be different. The reaction reaction orders of 0.7 and 1.5 instead of 1 and 2 are possibly due to the termination mechanisms. For a one photon reaction, termination of polymerisation by radical recombination would lead to a reaction order of 0.5, while termination by collision with the reactor walls would give a reaction order of 1.0[10]. It therefore appears that these two processes are occurring in roughly equal proportions.

As the low power plasma polymerisation is like the low photon flux photopolymerisation, it is likely that two activation steps are also involved in the formation of the plasma polymers. One reason for the difference between the two types of plasma polymer may be due to whether the power input is sufficient to saturate one of the two excitation processes. In the case of the high W/F plasma polymer however, the situation is further complicated by the high energy ion chemistry accessible. It is

probably this which causes the differences observed between the high W/F plasma polymers and the high photon flux surface photopolymers of NVP.

In the photolysis of butadiene, ascribed to a two photon process, it was found by Srinivasan[11], that there was an induction period caused by the requirement of a build up of gas phase products for polymerisation. No such induction period was observed in the photopolymerisation of NVP under any condition, so it appears that no such build up is necessary in this case.

6.3.5 The Influence of the Angle of Incidence of UV Light on the Deposition Rate of an NVP Surface Photopolymer

The deposition rates of NVP photopolymers were measured with the thickness monitor positioned so as to give incident angles of 90°, 45° and 0°. The conditions used (0.18 torr, low light intensity) were such as to produce the hydrophilic polymer, so the results should be relevant to low W/F plasma polymerisation. Each experiment was repeated with an aluminium foil substrate in place of the thickness monitor so that polymer could be collected and analysed by contact angle measurement to confirm that the polymer formed was of the hydrophilic type. The results of the three experiments are given in table 6.2.

Table 6.2 The effect of incident angle on deposition rate

Incident Angle (degrees)	Deposition Rate (arbitrary units)	Polymer Type
90	7.0	hydrophilic
45	5.5	hydrophilic
0	3.7	hydrophilic

When the incident angle was 0° the amount of UV radiation directly striking the surface of the thickness monitor was approximately zero. The formation of polymer in this case must therefore be a result of species activated in the gas phase. When the incident angle was 90° the deposition rate was approximately double that at 0°. This shows that photon activated reactions are also occurring on the surface of the monitor, and in this case accounts for approximately half of the polymer formation. When the incident angle was 45° the amount of light hitting the surface was less, and so the rate of polymer formation was intermediate between that at 0° and 90°. The intensity of the light incident on the surface is proportional to $\sin(\theta)$, where θ is the angle of incidence, so at 45° the light intensity is $1/\sqrt{2}$, or about 70% of that at 90°. Using this, it should be possible to obtain an order of reaction with respect to photon flux for the light induced process on the surface. Unfortunately the deposition rates quoted have an error of about ± 1, and so are too inaccurate for this to be done. More precise measurements are needed to obtain this information.

In a separate experiment half the calcium fluoride window

was covered by a mask so that part of the reaction chamber would receive no UV irradiation. The deposition monitor was placed in this part of the chamber in such a position as to be approximately 0.5cm from the nearest UV radiation. The deposition rate on the monitor in this case was found to be 3.0. The fact that polymer is formed on the monitor shows that the reactive species formed by the UV radiation are comparatively long lived. The length of time can be calculated from equation 6.4.

$$t = d^2/D \qquad\qquad 6.4$$

where t = the time to diffuse to the monitor
 d = distance over which diffusion occurs (0.5 cm)
 and D = diffusion coefficient

The diffusion coefficient is given by equation 6.5.

$$D = \bar{u}\lambda/3 \qquad\qquad 6.5$$

where $\bar{u}$ = the mean speed of the molecules
 and λ = the mean free path of the molecules

The molecular speed and mean free path can be calculated from equations 6.6 and 6.7.

$$\bar{u}^2 \approx \overline{u^2} = 3PV / Nm \qquad\qquad 6.6$$

where P = pressure
 V = volume
 N = number of molecules
 m = mass of each molecule

$$\lambda = 1/\sqrt{2}\ \pi n x^2 \qquad\qquad 6.7$$

where n = number of molecules per cubic centimetre
 x = diameter of a molecule

Taking the diameter of an NVP molecule to be approximately 4Å and the pressure as 0.18 torr, the values of u and λ are found to be 25000 cms^{-1} and 0.02 cm respectively. This leads to a value for the diffusion coefficient of 180 cm^{2}s^{-1}, and so to a value for the time taken to diffuse 0.5 cm of 1.4 x 10^{-3}, or 1/720 seconds.

The deposition rate was slightly less than for the experiment with the deposition monitor at 0°, suggesting that not all the activated molecules diffuse so far as 0.5 cm before deactivation. The value of 1/720 seconds is therefore probably of the same order of magnitude as the lifetime of the polymerising species in the gas phase: i.e. the mean lifetime is probably in the range from 1/100 to 1/1000 seconds.

The comparitively long life of the active species and their ability to diffuse over significant distances means that patterned deposition, characteristic of many surface photopolymers[12], can not be achieved for NVP.

6.3.6 NVP Photopolymerisation with Pulsed Irradiation

A more accurate method of determining the lifetime of the polymerising species is to use pulsed irradiation[5]. As described in the introduction to this chapter, irradiation at pulse frequencies slower than the lifetime of the active species should produce a deposition rate of half that for continuous irradiation, while pulse frequencies greater than the lifetime give rise to a deposition rate of $(1/2)^n$ of the value for continuous irradiation, where n is the order of reaction with

respect to photon flux. For the hydrophilic NVP photopolymer, where n = 1.5 plot of deposition rate versus pulse frequency should produce a graph similar to figure 6.17(a), with a value for the deposition rate at high frequencies of $(1/2)^{1.5}$, or about 35% of that for continuous irradiation.

A series of NVP photopolymerisations were carried out using pulsed irradiation of between 100 and 1000 Hz at 0.18 torr, using conditions suitable for producing the hydrophilic polymer and the deposition rate for the continuous irradiation was also measured. Each experiment was repeated with an aluminium foil substrate in place of the deposition monitor so that it could be confirmed that the hydrophilic polymer was being formed in each case. The results of the deposition rate measurements are plotted on figure 6.17(b).

It can be seen that at the lowest frequency measured the deposition rate is roughly 50% of that for continuous irradiation, as expected. It is possible however, that further variation may occur outside the frequency range investigated.

At 200 Hz the deposition rate had decreased to approximately 30% of the continuous value. This is not far different from the predicted 35%, suggesting that the lifetime of the active species is between 1/100 and 1/200 seconds (i.e. $7.5 \times 10^{-3} \pm 2.5 \times 10^{-3}$ seconds). At higher pulse frequencies however, there are large variations in deposition rate not predicted by the theory. It is possible that these changes correspond to the lifetimes of species involved in the polymerisation and other competitive reactions. This would suggest a very complex mechanism for the photopolymerisation involving many species.

THEORETICAL DEPOSITION RATES
PULSED IRRADIATION
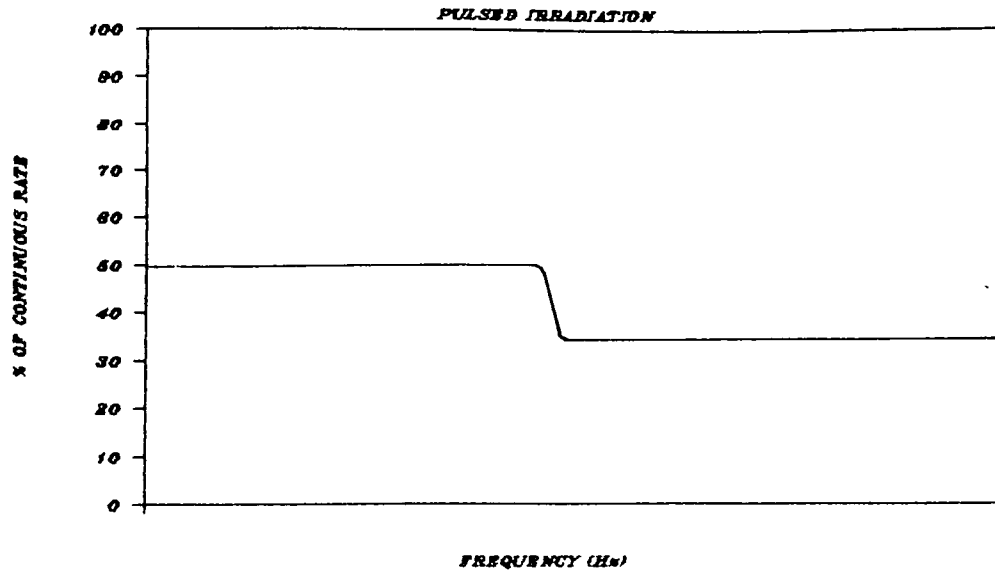
OBSERVED DEPOSITION RATES
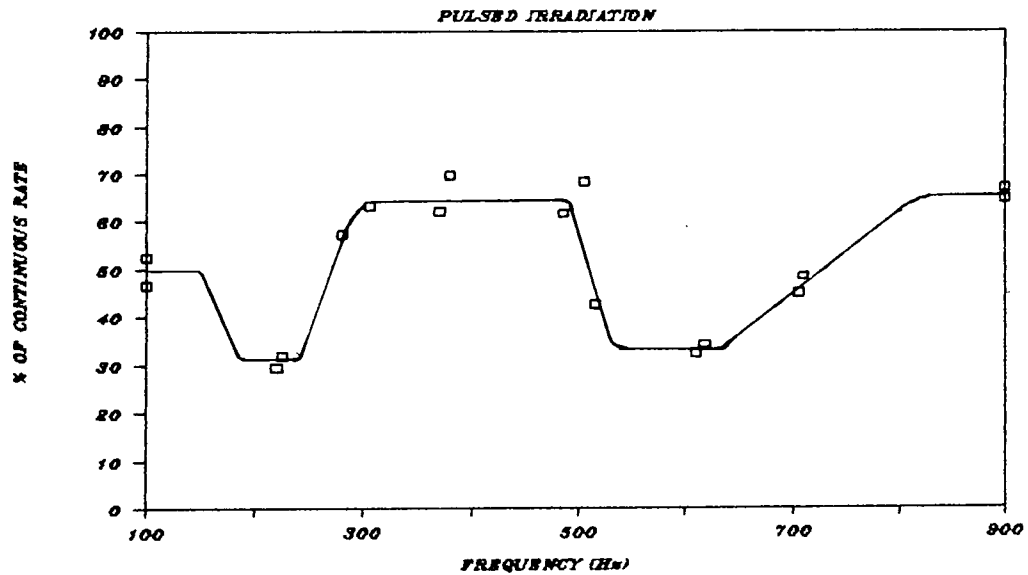## PULSED IRRADIATION

Figure 6.17 Deposition rates of NVP photopolymers as a function of the frequency of pulsed irradiation. (a) theoretical, (b) observed

213

Between 300 and 500 Hz and at 900 Hz the deposition rate is
about 65% of that for continuous irradiation and between 500 Hz
and 600 Hz the value is again at about 30% of the continuous
value. A one photon reaction giving a reaction order of 0.7 would
be expected, at high pulse frequency, to lead to a deposition
rate of $(1/2)^{0.7}$ or 62% of the continuous rate. This is fairly
close to the values obtained between 300 and 500 Hz and at 900
Hz. It is therefore possible that the reaction is switching
between a one photon and a two photon process as the pulse
frequency is increased. Why this should occur is not known, but
the process is obviously far from simple. The single photon
reaction occurring at certain frequencies of pulsed
irradiation (if this is the case) is not the same as the 0.7
order reaction taking place with high photon flux or low flow
rate and continuous irradiation. This is demonstrated by the fact
that the polymer produced in the former case is hydrophilic,
while that produced in the latter case is hydrophobic.

A similar series of experiments were attempted for the
hydrophobic photopolymer. In order to be able to obtain the
correct polymer type with pulsed irradiation the vapour pressure
of the NVP had to be reduced to 0.13 torr. Unfortunately this led
to a reduction in the polymer deposition rate which meant that
accurate readings could not be taken. Pulsed irradiations in the
range 50-500 Hz appeared to give consistent readings of about
half the rate for continuous irradiation, apart from a possible
slight dip at 275 Hz. This would seem to imply that the lifetime
of species in this case is probably less than 1/500 seconds, but
the inaccuracy of the data makes this very uncertain.

6.4 SUMMARY

Two distinct types of NVP plasma polymer can be produced. At low W/F the polymer has a zero contact angle with water and is similar to the conventional polymer. At high W/F a hydrophobic polymer is produced which is considerably different from the conventional polymer. The oxygen content an hydrophilicity of this second type increase slightly at very high W/F. Two types of surface photopolymer can also be produced by varying the photon flux/flow rate ratio. At low photon flux the polymer is very similar to the hydrophilic plasma polymer, but there are some differences between the high W/F plasma polymer and the high photon flux photopolymer, (which seems in some respects to be intermediate between the high and low W/F plasma polymers). A possible reason for these differences is that high energy ion chemistry, not available photochemically, may play an important role in the high W/F plasma polymerisation.

NMP and NEP plasma polymerise very similarly to NVP, but do not form surface photopolymers. The vinyl group is therefore important in the photopolymerisation of NVP, and so probably also in the low W/F plasma polymerisation. The plasma polymerisation of NMP and NEP probably proceeds through the loss of hydrogen to form a double bond, in a similar manner to the saturated acids in chapter 4.

Further study of the NVP photopolymerisation shows that the reaction orders with respect to photon flux for the hydrophilic and hydrophobic polymers are 1.5 and 0.7 respectively, suggesting a two photon process, one part of which ceases to be rate determining at high photon flux. No induction period was

observed, suggesting that a build up of activated gas phase species is not required. Under hydrophilic conditions the photon induced reactions occur both in the gas phase and on the surface. Polymerising species in the gas phase are able to travel a considerable distance before deactivation, indicating that their lifetime is of the order of 10^{-2} to 10^{-3} seconds. Experiments with pulsed irradiation suggest that the lifetime may be between 1/100 and 1/200 seconds, and that the reaction is complex and may switch between one and two photon processes at different pulse frequencies. This mechanistic information about the hydrophilic photopolymer probably also applies to the hydrophilic plasma polymer.

REFERENCES

1a. A.B.Gil'man, L.S.Tuzov, V.M.Kolotyrkin and V.K.Polapov, Vyshokomol Soedin Ser. B, 24, 4, 315-317, (1982). (Chem. Abs. 96 200703a)

b. H.Yasuda, Appl. Polym. Symp., 22, 241-53, (1973)

2. M.Kuriaki, M.Hasebe, Y.Miwa and Y.Mizutani, Kobunshi Ronbunshu, 42, 11, 841-7, (1985). (Chem. Abs. 104 155917u)

3. K.W.Bieg and D.K.Ottesen in "Plasma Polymerisation", Eds. M.Shen and A.T.Bell, ACS Symp. Ser. 108, Am. Chem. Soc., Washington D.C., (1979)

4a. H.S.Munro, Polym. Mater. Sci. Eng., 56, 318, (1987)

b. C.Till, Ph.D. Thesis, (1986)

5. H.W.Melville, Proc. Roy. Soc. A, 163, 511, (1937)

6. M.Shen and A.T.Bell in "Plasma Polymerisation", ACS Symp. Series 108, Washington D.C., (1979), Chap 1.

7. J.C.Vickerman, A.Brown and D.Briggs, "Handbook of Static Secondary Ion Mass Spectroscopy", Wiley, Chichester, (1989)

8. H.Yasuda and C.E.Lamaze, J. Appl. Polym. Sci., 17, 1533-44, (1973)

9. H.Yasuda and T.Hirotsu, J. Polym. Sci., Polym. Chem. Ed., 16, 743, (1978)

10. G.M.Burnett, "Mechanism of Polymer Reactions", Interscience, New York, (1954)

11. I.Haller and R.Srinivasan, J. Chem. Phys., 40, 7, 1992, (1964)

12. A.N.Wright in "Polymer Surfaces", Eds. D.T.Clark and W.J.Feast, Wiley (1978)

APPENDIX

COLLOQUIA, LECTURES AND SEMINARS GIVEN BY INVITED SPEAKERS

IN DURHAM UNIVERSITY CHEMISTRY DEPARTMENT

OCTOBER 1986 - JULY 1989

(Lectures attended are marked with an asterisk)

ALLEN, Prof. Sir G. (Unilever Research)   13th November 1986
    Biotechnology and the Future of the Chemical Industry

BARTSCH, Dr. R. (University of Sussex)   6th May 1987
    Low Co-ordinated Phosphorus Compounds

BLACKBURN, Dr. M. (University of Sheffield)   27th May 1987
    Phosphonates as Analogues of Biological Phosphate
    Esters

BORDWELL, Prof. F.G. (Northeastern University, U.S.A.)   9th March 1987
    Carbon Anions, Radicals, Radical Anions and
    Radical Cations

✻ CANNING, Dr. N.D.S. (University of Durham)   26th November 1986
    Surface Adsorption Studies of Relevance to
    Heterogeneous Ammonia Synthesis

CANNON, Dr. R.D. (University of East Anglia)   11th March 1987
    Electron Transfer in Polynuclear Complexes

CLEGG, Dr. W. (University of Newcastle-upon-Tyne)   28th January 1987
    Carboxylate Complexes of Zinc; Charting a
    Structural Jungle

DÖPP, Prof. D. (University of Duisburg)   5th November 1986
    Cyclo-additions and Cyclo-reversions Involving
    Captodative Alkenes

✻ DORFMÜLLER, Prof. T. (University of Bielefeld)   8th December 1986
    Rotational Dynamics in Liquids and Polymers

GOODGER, Dr. E.M. (Cranfield Institute of Technology)   12th March 1987
    Alternative Fuels for Transport

GREENWOOD, Prof. N.N. (University of Leeds)   16th October 1986
    Glorious Gaffes in Chemistry

HARMER, Dr. M. (I.C.I. Chemicals & Polymer Group)   7th May 1987
    The Role of Organometallics in Advanced Materials

HUBBERSTEY, Dr. P. (University of Nottingham)   5th February 1987
    Demonstration Lecture on Various Aspects of
    Alkali Metal Chemistry

HUDSON, Prof. R.F. (University of Kent)   17th March 1987
    Aspects of Organophosphorus Chemistry

✻ HUDSON, Prof. R.F. (University of Kent)   18th March 1987
    Homolytic Rearrangements of Free Radical Stability

* JARMAN, Dr. M. (Institute of Cancer Research)   19th February 1987
        The Design of Anti Cancer Drugs

    KRESPAN, Dr. C. (E.I. Dupont de Nemours)   26th June 1987
        Nickel(O) and Iron(O) as Reagents in Organofluorine
        Chemistry

* KROTO, Prof. H.W. (University of Sussex)   23rd October 1986
        Chemistry in Stars, between Stars and in the Laboratory

    LEY, Prof. S.V. (Imperial College)   5th March 1987
        Fact and Fantasy in Organic Synthesis

    MILLER, Dr. J. (Dupont Central Research, U.S.A.)   3rd December 1986
        Molecular Ferromagnets; Chemistry and Physical
        Properties

* MILNE/CHRISTIE, Dr. A./Mr. S. (International Paints)   20th November 1986
        Chemical Serendipity - A Real Life Case Study

    NEWMAN, Dr. R. (University of Oxford)   4th March 1987
        Change and Decay: A Carbon-13 CP/MAS NMR Study of
        Humification and Coalification Processes

* OTTEWILL, Prof. R.H. (University of Bristol)   22nd January 1987
        Colloid Science a Challenging Subject

    PASYNKIEWICZ, Prof. S. (Technical University, Warsaw)   11th May 1987
        Thermal Decomposition of Methyl Copper and its
        Reactions with Trialkylaluminium

    ROBERTS, Prof. S.M. (University of Exeter)   24th June 1987
        Synthesis of Novel Antiviral Agents

* RODGERS, Dr. P.J. (I.C.I. Billingham)   12th February 1987
        Industrial Polymers from Bacteria

    SCROWSTON, Dr. R.M. (University of Hull)   6th November 1986
        From Myth and Magic to Modern Medicine

    SHEPHERD, Dr. T. (University of Durham)   11th February 1987
        Pteridine Natural Products; Synthesis and Use in
        Chemotherapy

    THOMSON, Prof. A. (University of East Anglia)   4th February 1987
        Metalloproteins and Magnetooptics

    WILLIAMS, Prof. R.L. (Metropolitan Police Forensic Science) 27th November 1987
        Science and Crime

    WONG, Prof. E.H. (University of New Hampshire, U.S.A.)   29th October 1986
        Coordination Chemistry of P-O-P Ligands

* WONG, Prof. E.H. (University of New Hampshire, U.S.A.)   17th February 1987
        Symmetrical Shapes from Molecules to Art and Nature

UNIVERSITY OF DURHAM

Board of Studies in Chemistry

COLLOQUIA, LECTURES AND SEMINARS GIVEN BY INVITED SPEAKERS
1ST AUGUST 1987 to 31st JULY 1988

* BIRCHALL, Prof. D. (I.C.I. Advanced Materials)   25th April 1988
    Environmental Chemistry of Aluminium

* BORER, Dr. K. (University of Durham Industrial Research Labs.) 18th February 1988
    The Brighton Bomb - A Forensic Science View

BOSSONS, L. (Durham Chemistry Teachers' Centre)   16th March 1988
    GCSE Practical Assessment

* BUTLER, Dr. A.R. (University of St. Andrews)   5th November 1987
    Chinese Alchemy

* CAIRNS-SMITH, Dr. A. (Glasgow University)   28th January 1988
    Clay Minerals and the Origin of Life

DAVIDSON, Dr. J. (Herriot-Watt University)   November 1987
    Metal Promoted Oligomerisation Reactions of Alkynes

* GRADUATE CHEMISTS (Northeast Polytechnics and Universities)   19th April 1988
    R.S.C. Graduate Symposium

GRAHAM, Prof. W.A.G. (University of Alberta, Canada)   3rd March 1988
    Rhodium and Iridium Complexes in the Activation of
    Carbon-Hydrogen Bonds

* GRAY, Prof. G.W. (University of Hull)   22nd October 1987
    Liquid Crystals and their Applications

HARTSHORN, Prof. M.P. (University of Canterbury, New Zealand)   7th April 1988
    Aspects of Ipso-Nitration

* HOWARD, Dr. J. (I.C.I. Wilton)   3rd December 1987
    Chemistry of Non-Equilibrium Processes

* LUDMAN, Dr. C.J. (Durham University)   10th December 1987
    Explosives

* McDONALD, Dr. W.A. (I.C.I. Wilton)   11th May 1988
    Liquid Crystal Polymers

MAJORAL, Prof. J.-P. (Université Paul Sabatier)   8th June 1988
    Stabilisation by Complexation of Short-Lived
    Phosphorus Species

MAPLETOFT, Mrs. M. (Durham Chemistry Teachers' Centre)   4th November 1987
    Salters' Chemistry

NIETO DE CASTRO, Prof. C.A. (University of Lisbon   18th April 1988
    and Imperial College)
    Transport Properties of Non-Polar Fluids

* OLAH, Prof. G.A. (University of Southern California)   29th June, 1988
    New Aspects of Hydrocarbon Chemistry)

* PALMER, Dr. F. (University of Nottingham)   21st January 1988
    Luminescence (Demonstration Lecture)

PINES, Prof. A. (University of California, Berkeley, U.S.A.) 28th April 1988
    Some Magnetic Moments

RICHARDSON, Dr. R. (University of Bristol)   27th April 1988
    X-Ray Diffraction from Spread Monolayers

ROBERTS, Mrs. E. (SATRO Officer for Sunderland)   13th April 1988
    Talk - Durham Chemistry Teachers' Centre - "Links
    Between Industry and Schools"

ROBINSON, Dr. J.A. (University of Southampton)   27th April 1988
    Aspects of Antibiotic Biosynthesis

* ROSE van Mrs. S. (Geological Museum)   29th October 1987
    Chemistry of Volcanoes

SAMMES, Prof. P.G. (Smith, Kline and French)   19th December 1987
    Chemical Aspects of Drug Development

SEEBACH, Prof. D. (E.T.H. Zurich)   12th November 1987
    From Synthetic Methods to Mechanistic Insight

SODEAU, Dr. J. (University of East Anglia)   11th May 1988
    Durham Chemistry Teachers' Centre Lecture: "Spray
    Cans, Smog and Society"

SWART, Mr. R.M. (I.C.I.)   16th December 1987
    The Interaction of Chemicals with Lipid Bilayers

TURNER, Prof. J.J. (University of Nottingham)   11th February 1988
    Catching Organometallic Intermediates

* UNDERHILL, Prof. A. (University of Bangor)   25th February 1988
    Molecular Electronics

WILLIAMS, Dr. D.H. (University of Cambridge)   26th November 1987
    Molecular Recognition

* WINTER, Dr. M.J. (University of Sheffield)   15th October 1987
    Pyrotechnics (Demonstration Lecture)

COLLOQUIA, LECTURES AND SEMINARS GIVEN BY INVITED SPEAKERS
1ST AUGUST 1988 to 31st JULY 1989

ASHMAN, Mr. A. (Durham Chemistry Teachers' Centre)　　3rd May, 1989
    The Chemical Aspects of the National Curriculum

＊ AVEYARD, Dr. R. (University of Hull)　　　　　　　15th March, 1989
    Surfactants at your Surface

AYLETT, Prof. B.J. (Queen Mary College. London)　　16th February, 1989
    Silicon-Based Chips:- The Chemist's Contribution

BALDWIN, Prof. J.E. (Oxford University)　　　　　　9th February, 1989
    Recent Advances in the Bioorganic Chemistry of
    Penicillin Biosynthesis

＊ BALDWIN & WALKER, Drs. R.R. & R.W. (Hull University)　24th November, 1988
    Combustion: Some Burning Problems

BOLLEN, Mr. F. (Durham Chemistry Teachers' Centre)　18th October, 1988
    Lecture about the use of SATIS in the classroom

BUTLER, Dr. A.R. (St. Andrews University)　　　　　15th February, 1989
    Cancer in Linxiam: The Chemical Dimension

＊ CADOGAN, Prof. J.I.G. (British Petroleum)　　　　10th November, 1988
    From Pure Science to Profit

CASEY, Dr. M. (University of Salford)　　　　　　　20th April, 1989
    Sulphoxides in Stereoselective Synthesis

WATERS & CRESSEY, Mr. D. & T. (Durham Chemistry Teachers'　1st February, 1989
                             Centre)
    GCSE Chemistry 1988: "A Coroner's Report"

CRICH, Dr. D. (University College London)　　　　　27th April, 1989
    Some Novel Uses of Free Radicals in Organic
    Synthesis

DINGWALL, Dr. J. (Ciba Geigy)　　　　　　　　　　18th October, 1988
    Phosphorus-containing Amino Acids: Biologically
    Active Natural and Unnatural Products

ERRINGTON, Dr. R.J. (University of Newcastle-upon-Tyne)　1st March, 1989
    Polymetalate Assembly in Organic Solvents

FREY, Dr. J. (Southampton University)　　　　　　　11th May, 1989
    Spectroscopy of the Reaction Path: Photodissociation
    Raman Spectra of NOCl

* HALL, Prof. L.D. (Addenbrooke's Hospital, Cambridge)   2nd February, 1989
      NMR - A Window to the Human Body

HARDGROVE, Dr. G. (St. Olaf College, U.S.A.)   December, 1988
      Polymers in the Physical Chemistry Laboratory

HARWOOD, Dr. L. (Oxford University)   25th January, 1988
      Synthetic Approaches to Phorbols Via Intramolecular
      Furan Diels-Alder Reactions: Chemistry under Pressure

JÄGER, Dr. C. (Friedrich-Schiller University GDR)   9th December, 1988
      NMR Investigations of Fast Ion Conductors of the
      NASICON Type

* JENNINGS, Prof. R.R. (Warwick University)   26th January, 1989
      Chemistry of the Masses

JOHNSON, Dr. B.F.G. (Cambridge University)   23rd February, 1989
      The Binary Carbonyls

JONES, Dr. M.E. (Durham Chemistry Teachers' Centre)   14th June, 1989
      Discussion Session on the National Curriculum

JONES, Dr. M.E. (Durham Chemistry Teachers' Centre)   28th June, 1989
      GCSE and A Level Chemistry 1989

* LUDMAN, Dr. C.J. (Durham University)   18th October, 1988
      The Energetics of Explosives

MACDOUGALL, Dr. G. (Edinburgh University)   22nd February, 1989
      Vibrational Spectroscopy of Model Catalytic Systems

MARKO, Dr. I. (Sheffield University)   9th March, 1989
      Catalytic Asymmetric Osmylation of Olefins

McLAUCHLAN, Dr. K.A. (University of Oxford)   16th November, 1988
      The Effect of Magnetic Fields on Chemical Reactions

MOODY, Dr. C.J. (Imperial College)   17th May, 1989
      Reactive Intermediates in Heterocyclic Synthesis

MORTIMER, Dr. C. (Durham Chemistry Teachers' Centre)   14th December, 1988
      The Hindenberg Disaster - an Excuse for Some Experiments

NICHOLLS, Dr. D. (Durham Chemistry Teachers' Centre)   11th July, 1989
      Demo. "Liquid Air"

PAETZOLD, Prof. P. (Aachen)   23rd May, 1989
      Iminoboranes XB≡NR: Inorganic Acetylenes?

PAGE, Dr. P.C.B. (University of Liverpool)   3rd May, 1989
      Stereocontrol of Organic Reactions Using 1,3-dithiane-
      1-oxides

*POLA, Prof. J. (Czechoslovak Academy of Sciences)   15th June, 1989
    Carbon Dioxide Laser Induced Chemical Reactions -
New Pathways in Gas-Phase Chemistry

REES, Prof. C.W. (Imperial College London)   27th October, 1988
    Some Very Heterocyclic Compounds

REVELL, Mr. P. (Durham Chemistry Teachers' Centre)   14th March, 1989
    Implementing Broad and Balanced Science 11-16

SCHMUTZLER, Prof. R. (Technische Universitat Braunschweig) 6th October, 1988
    Fluorophosphines Revisited - New Contributions to an
Old Theme

* SCHROCK, Prof. R.R. (M.I.T.)   13th February, 1989
    Recent Advances in Living Metathesis

SINGH, Dr. G. (Teesside Polytechnic)   9th November, 1988
    Towards Third Generation Anti-Leukaemics

* SNAITH, Dr. R. (Cambridge University)   1st December, 1988
    Egyptian Mummies: What, Where, Why and How?

STIBR, Dr. R. (Czechoslovak Academy of Sciences)   16th May, 1989
    Recent Developments in the Chemistry of Intermediate-
Sited Carboranes

VON RAGUE SCHLEYER, Prof. P. (Universitat Erlangen Nurnberg) 21st October, 1988
    The Fruitful Interplay Between Calculational and
Experimental Chemistry

WELLS, Prof. P.B. (Hull University)   10th May, 1989
    Catalyst Characterisation and Activity